A FLUME STUDY OF BED FORMS IN A MEDIUM SAND AS A FUNCTION OF FLOW VELOCITY

by

MARY JANE W. GOETTEL

SUBMITTED TO THE DEPARTMENT OF EARTH, ATMOSPHERIC, AND PLANETARY SCIENCES IN PARTIAL FULLFILLMENT OF THE REQUIREMENTS FOR THE DEGREE OF

DOCTOR OF PHILOSOPHY
in Geology

at the

MASSACHUSETTS INSTITUTE OF TECHNOLOGY

February 1991

Signature of Author _____
Department of Earth, Atmospheric and Planetary Sciences
January 24, 1991

Certified by _____
John B. Southard
Thesis Supervisor

Accepted by _____
Thomas H. Jordan
Chairman, Department Committee

A FLUME STUDY OF BED FORMS IN A MEDIUM SAND AS A FUNCTION OF FLOW VELOCITY

by

MARY JANE W. GOETTEL

Submitted to the Department of Earth, Atmospheric, and Planetary Sciences in February 1991 in partial fulfillment of the requirements for the degree of Doctor of Philosophy in Geology

ABSTRACT

Flume experiments were conducted to examine both quantitatively and observationally the similarities and differences between the different kinds of flow-transverse bed forms: ripples, two-dimensional dunes, and three-dimensional dunes. A series of experiments was conducted as a function of mean flow velocity using a medium sand (0.51 mm) and a constant flow depth (15 cm).

The bed forms over the entire range of these experiments appeared to be governed by basically the same kinematics and dynamics, and the geometric properties of the bed forms changed smoothly and systematically as functions of mean flow velocity. No abrupt changes in bed-form kinematics, bed-form dynamics, or bed-form size were observed with changes in mean flow velocity. These experiments suggest that ripples and dunes may not be two dynamically different kinds of bed forms.

A single model for the generation and continued existence of bed forms is presented. The proposed model is based on the hypothesis that the nonconstant sediment transport rate caused by the phenomenon of fluid bursting at the base of the turbulent boundary layer results in both the development and continued existence (lack of attenuation) of the bed forms. In this model, the size of the bed forms is determined by the dynamics of the continual generation of new slipfaces and the evolution from small scales to larger scales. The size of individual bed forms is continally changing.

Thesis Supervisor: Dr. John B. Southard
Title: Professor of Geology

TABLE OF CONTENTS

LIST OF SYMBOLS

d	Mean flow depth
g	Acceleration of gravity
H	Height of a slipface (subcategories: H_m and H_r)
H_m	Height of a major slipface (subcategories: H_{m-m} and H_{m-r})
H_{m-m}	Height of a major slipface immediately upstream from another major slipface
H_{m-r}	Height of a major slipface immediately upstream from a ripplet slipface
H_r	Height of a ripplet
L_c	Length from a major slipface immediately upstream from a ripplet to the next major slipface downstream (composite with ripplets: the length between two major slipfaces with one or more ripplet slipfaces in between)
L_c/H_u	Length from a major slipface immediately upstream from a ripplet to the next major slipface downstream divided by the height of the slipface upstream (composite with ripplets divided by the height of the slipface upstream: the length between two major slipfaces with one or more ripplet slipfaces in between divided by the height of the slipface upstream)
L_m	Length from a major slipface to an immediately adjacent major slipface downstream
L_m/H_u	Length from a major slipface to an immediately adjacent major slipface downstream divided by the height of the slipface upstream
L_{m-a}	Length downstream from a major slipface to the next slipface regardless of the height of the slipface downstream (subcategories: L_m and L_r)

L_{m-a}/H_u	Length downstream from a major slipface to the next slipface regardless of the height of the slipface downstream divided by the height of the slipface upstream (subcategories: L_m/H_u and L_r/H_u)
L_{m-m}	Length between major slipfaces - set of lengths most commonly used (subcategories: L_m and L_c)
L_{m-m}/H_u	Length between major slipfaces divided by the height of the slipface upstream (subcategories: L_m/H_u and L_c/H_u)
L_r	Length from a major slipface to an immediately adjacent ripplet slipface downstream
L_r/H_u	Length from a major slipface to an immediately adjacent ripplet slipface downstream divided by the height of the slipface upstream
M_b	Bed-surface slope
M_{b-r}	Bed-surface slope relative to the flume rails
M_r	Slope of the flume rails
$dM_r/turn$	Change in the slope of the rails per crank turn
M_w	Water-surface slope
M_{w-r}	Water-surface slope relative to the flume rails
n	Sample size
S	Water-surface slope
V	Flow velocity
$Y_b(750)$	Least-squares fit to a straight line of the bed-surface profile evaluated at 750 cm
$Y_w(750)$	Least-squares fit to a straight line of the water-surface profile evaluated at 750 cm
ρ_w	Density of water
$\tau = \rho_w gdS$	Boundary shear stress

LIST OF TABLES

LIST OF FIGURES

Fig. 6-19 Comparison of bed-form length divided by upstream height: L_c/H_u, L_r/H_u, L_m/H_u, and L_{m-a}/H_u vs. mean flow velocity. 436

ACKNOWLEDGMENTS

I would like to thank my advisor, Professor John B. Southard, for his help and suggestions.

I would also like to thank the many people who have provided invaluable support and help, each in their own special way, during the time that I have been working on this thesis. I would especially like to thank Dr. Henry Hoey, Dr. Kenneth Goettel, and my brother, Dr. Robert Westervelt. I would most especially like to thank to my mother, Dr. Marie Westervelt.

I would also like to thank my friends, Bill Bonacci, Sue Ann Shoemaker, Paula Johnson, Eva Garcia, Mike Pogodzinski, Bob Woerner, and Stu Inglis, who have always expressed confidence in me.

CHAPTER 1

HISTORICAL BACKGROUND AND STATEMENT OF PURPOSE

Section 1-1

Introduction

Over a certain range of flow conditions, water flowing over unconsolidated sediment results in the formation of sediment waves or bed forms in the sediment bed oriented transverse to the mean flow with gentle upstream slopes and steep downstream slopes. Transverse bed forms have been observed to be ubiquituous in a wide variety of natural environments where the flow velocity is sufficient to transport the sediment, including streams, rivers, tidal environments, the continental shelf, and canyons on the continental slope (Ashley et al., 1990). Flow-transverse bed forms which develop from unidirectional flows have been observed to range in spacing from centimeters to over 1,000 meters. The smallest bed forms are usually referred to as ripples, while the larger bed forms have been referred to by a variety of names including dunes, megaripples, sandwaves, and bars. Ripples are commonly superimposed on larger bed forms. Also, different scales of larger bed forms have been observed superimposed on one another, resulting in the idea of a hierarchy of bed forms each governed by different dynamics.

Section 1-2

Background

Various approaches have been used in the study of bed forms developed by unidirectional flows, including (1) systematic flume experiments, (2) empirical data analysis, (3) theoretical modeling, and (4) observational studies. Systematic flume experiments have delineated changes in the bed configuration as a function of changing hydraulic conditions. A characteristic sequence of bed forms has been generally recognized as a function of mean flow velocity for a constant mean flow depth. The sequence of bed forms depends on sediment size. For very fine sands with mean diameters less than about 0.18 mm, the sequence with increasing mean flow velocity is ripples then upper plane bed with sediment movement. Dunes (i.e., large-scale bed forms) do not develop in very fine sands. For fine to medium sands, the sequence with increasing velocity becomes ripples, two-dimensional dunes, three-dimensional dunes, then upper plane bed. For coarse sands with mean diameters greater than about 0.8 mm, the sequence is lower plane bed with sediment movement, two-dimensional dunes, three-dimensional dunes, then upper plane bed. Ripples (i.e., the smallest bed forms) do not develop in coarse sands. When the Froude number approaches 1.0 another type of bed form, antidunes, develop regardless of the preceding type of bed form.

Ripples and dunes are produced by flows with Froude numbers less than 1.0, for which the water-surface waves are out of phase with the bed forms. The development of these bed forms does not depend on the existence of a free surface; these bed forms develop even if the water surface is replaced by a planar solid upper boundary, so that the experiment is conducted in a closed conduit (Middleton and Southard, 1984). When the Froude number approaches 1.0 (i.e., becomes greater than about 0.8) antidunes develop regardless of the preceding type of bed form. The development of antidunes is dependent on the free-water surface: antidunes are in phase with the water surface waves and interact strongly with the surface waves. This study is restricted to the examination of bed forms that develop independently of the existence of a free surface: ripples, two-dimensional dunes, and three-dimensional dunes.

The purpose of the present study is to examine both quantitatively and observationally the similarities and differences between ripples, two-dimensional dunes, and three-dimensional dunes. A series of flume experiments was conducted as a function of mean flow velocity using a medium sand and a constant flow depth. The papers most relevant to the present study, from each of the different approaches of studying bed forms mentioned above, are briefly summarized in the following sections.

Section 1-3

Flume Experiments

Systematic flume experiments have delineated the sequence of bed forms described above. Gilbert (1914) described changes in the bed configuration as a function of mean flow conditions. In the 1950's and 1960's Simons and Richardson delineated the broad outline of the characteristic sequence of bed forms that is generally recognized today. They carried out an extensive series of flume experiments in which the bed configuration was examined for a wide variety of sediment sizes and flow conditions. A summary of their experiments is described by Guy et al. (1966). They outline two flow regimes with increasing discharge: (1) the lower flow regime for fine to medium sediment is plane bed with no sediment movement, ripples, ripples superimposed on dunes, dunes, and transition from dunes to rapid-flow forms and (2) the upper flow regime is upper plane bed with sediment movement and antidunes. They note that the change in appearance of the sediment bed from a ripple pattern to a dune pattern is "abrupt". They distinguish ripples from dunes primarily by the "abrupt" change in size scale of the bed forms with changing flow conditions. For medium sand (0.45 mm), "the height of ripples was less than 0.10 foot (3.0 cm) and their longitudinal spacing was less than 2.0 feet (61 cm)", while the average height of dunes was greater than 0.15

feet (4.6 cm) and the spacing was greater than 4.0 feet (122 cm) (Simons et al, 1961). They note that "along with the dunes, potholes formed that had a depth equal to the height of the dunes."

Pratt (1972) conducted a series of flume experiments in narrowly graded, medium sand (0.49 mm). Pratt divides his observations into phases based on visual classification of the bed forms and measurement of bed form dimensions. The phases with increasing mean flow velocity defined by Pratt are as follows:

phase 1 - flat bed with no grain movement;

phase 2A - ripples whose "wavelengths are independent of flow depth and velocity;"

phase 2B - an unstable region where ripple crests become less orderly;

phase 3 - initial dunes usually with superimposed ripples;

phase 4A - dunes which increase in size as the phase 4B boundary is approached; and

phase 4B - dunes degenerating towards flat bed.

Costello and Southard (1981) conducted a series of flume experiments using four sand sizes from medium to coarse sand and a flow depth of about 15 cm. In medium sand with increasing mean flow velocity they observed ripples then dunes, while in coarser sand they observed

lower flat bed with sediment transport, then dunes. They divide dunes into two subphases with increasing mean flow velocity. "Two-dimensional dunes (2D dunes), with fairly straight, continuous, even crests and no strong localized scour in troughs, are formed at relatively low flow velocities; three-dimensional dunes (3D dunes), with strongly sinuous, discontinuous, uneven crests and strong, localized scour pits in troughs, are formed at relatively high flow velocities. 3D dunes tend to be higher than 2D dunes, have larger height/spacing ratios, and show less variability in height, spacing, and migration rate." They suggest that "dunes can be viewed as kinematic shock waves; the differences between 2D dunes and 3D dunes lie in the differing importance of shock-wave coupling and of sand transport in bed-form troughs."

Allen (1982) provides a comprehensive review of the bed-form literature. Allen cites the frequency distributions of the wavelength and height of transverse bed forms shaped by one-way water streams as evidence that these bed forms do not form a continuous population and are divided into at least two morphologically distinct classes: ripples and dunes. He states: "The reality of a morphologically distinct class of ripples, and the validity of the proposed quantitative limits, is amply proved by the frequency distributions of wavelength and height prepared by Allen (1963, 1968) and G.E. Williams (1971) from the

laboratory and field." The distributions appear to be strongly bimodal. Allen indicates that ripples have heights less than 0.04 m (4.0 cm) and lengths less than 0.6 m (60 cm). He also notes that ripples sometimes occur superimposed on the upstream slope of dunes while secondary ripples do not occur superimposed on ripples.

Section 1-4

Empirical Data Analysis

The empirical relationships between the different kinds of bed forms have been examined by using dimensional analysis and presenting the data on bed forms in dimensionless diagrams. Allen (1982) gives a comprehensive review of dimensionless diagrams presenting data on bed forms. Most authors have presented data on bed forms in two-dimensional diagrams using various combinations of two dimensionless variables. In these diagrams there tends to be some overlapping of stability fields of the different kinds of bed forms. Southard (1971) presents data on bed forms of Guy et al. (1966) in a three-dimensional diagram using dimensionless variables which are particularly useful in sedimentology. In this diagram the stability fields of the different kinds of bed forms do not tend to overlap. Southard and Boguchwal (1990) have comprehensively redone this diagram, using data from 39 flume studies, explicitly including the effect of water temperature.

Section 1-5

Theoretical Modeling

Because of the complexity of the problem, there have not been as many attempts at analytical models as other approaches. Exner (1920) derived the sediment conservation equation and combined it with the assumption that the sediment discharge is a function of the mean flow velocity. He obtained the result that with time a sinusoidal mound on the sediment bed will become flattened and elongated, and develop a longitudinal profile like a bed form: as the mound is elongated, the solution eventually becomes double-valued at the downstream end, thereby developing a slipface. The sediment on the top of the mound is eroded and deposited on the downstream slope, eventually resulting in the development of a slipface at the downstream end of the mound. However, with time the slipface migrates downstream and the mound becomes longer and lower until it is ultimately levelled.

Analytically, the assumption that the sediment discharge is directly proportional to the mean flow velocity results in bed forms being unstable. Where the bed elevation is highest, the mean flow velocity is greatest, and therefore the sediment erosion is greatest. As a result, the bed form is ultimately levelled.

Since then a number of stability analyses have been performed; for example, Kennedy (1963, 1969), Reynolds

(1965), Smith (1970), Engelund (1970), Engelund and Fredsoe (1974), and Richards (1980). However, the complexity of the problem limits the usefulness of analytical approaches. For example, in many stability analyses an artificial lag distance between the sediment discharge and mean flow velocity must be used in order for a disturbance on the planar bed to grow. The need for an artificial lag distance suggests that an essential element of the process of bed form development has not been included in the analysis.

Section 1-6

Observational Studies

Because of the complexitiy of the problem and the present limitations of analytical approaches, observational studies of bed forms have provided the most useful information about the mechanics of bed forms. Raudkivi (1963) observed the formation of ripples from a plane sediment bed when the flow was only slightly beyond the threshold of particle movement. He notes that the location of the initial deformation of the plane bed appeared to be "by chance" at one or more points and gradually "spread out" downstream. He observes "the tendency for the particles to 'pile up' and move intermittently when the flow was only slightly beyond the treshold of particle movement." One of the suggested explanations for the

chance pile-up of grains is the intermittent system of strong eddies in the boundary region of a turbulent flow. Raudkivi describes the mechanism of ripple formation as follows: "When the threshold conditions of sediment transport are exceeded, a disturbance in the plane surface is created by a chance piling-up. This surface disturbance establishes an interface or surface of discontinuity in the flow, similar to that with flow past a negative step. Where the core of this interface meets the sand boundary it excavates more material because of increased turbulent agitation in the interface between the wake and main stream. This extra material entrained cannot be supported by flow over a plane boundary. The turbulent agitation is a maximum where the core of the interface meets the boundary and decreases with distance downstream. The additional entrained material settles out as it passes downstream, away from the stronger agitation of the core region, leading to a new ripple face."

Southard and Dingler (1971) studied "the propagation of sediment ripples behind mounds of sediment in uniform flows of water over flat beds of fine sand." They interpret propagation vs. nonpropagation "in terms of the tentative hypothesis that ripple development is governed by the relationship between minimum height of bed irregularity necessary to generate ripples on an otherwise flat bed and the maximum height of bed irregularity that can be built up

by flow over an originally flat bed. Minimum mound height for propagation of ripples was found to be non-zero even when there was some sediment movement on the surrounding flat bed, but there was no sign of spontaneous development of ripples on the flat bed under these conditions."

Williams and Kemp (1971) extended Raudkivi's work and examined how small bed irregularities are formed on an initially flat bed and how these irregularities develop into ripples. They cite research on the structure of the viscous sublayer indicating that despite the layer being dominated by viscosity, there are large, three-dimensional, unsteady velocities present within the layer. They note that the flow pattern takes the form of high and low velocity streaks, laterally spaced. The high-velocity streaks result from high-velocity fluid spiralling in from outside the viscous sublayer. The high-velocity fluid interacts with low-velocity fluid at the boundary which is then ejected away from the boundary as a turbulent "burst". (The sequence of a high-velocity streak or "sweep" and the subsequent ejection of fluid away from the boundary as a turbulent burst is referred to as "bursting" or the burst-sweep cycle.) Also, when high velocity fluid reaches the bed it spreads out and causes instantaneous lateral velocities up to 30% of the longitudinal velocities. Williams and Kemp observed that as the flow exceeds the conditions for grain movement, the bed texture develops a

random streaky pattern in the direction of flow and that ripples tend to develop where the streaks appear to run together to form rough diagonal edges at various positions on the bed. Ripples develop when discontinuities occur on the downstream slope of the diagonal edges. Williams and Kemp summarize the stages in the initiation of ripples from a flat bed as follows: "(1) the formation of an initial disturbance; (2) flow separation occurring from the disturbance; amd (3) the separation eddy arresting grains so as to amplify the disturbance and the separation eddy."

Section 1-7

Statement of Purpose

Despite the large number of studies of bed forms, there is very little detailed, quantitative data on the size and shape of bed forms or on the kinematics of the bed forms. In most studies, only estimates of the mean size are available and the sediment bed is subjectively categorized to be a certain kind of bed form. Bed forms are frequently treated as if the size and shape of the bed forms for a given set of flow conditions are approximately uniform throughout the sediment bed (i.e., on average, the bed forms are represented by one size and shape). For example, for the extensive series of flume experiments by Simons, Richardson, and Albertson (1961), the wavelength of the bed forms was "computed by dividing the overall flume

length, from crest to crest or trough to trough, over which the bed configuration had been measured by the number of dunes or ripples in that length". As a result, there is no information about the size distributions of the bed forms or the shape of the bed forms. However, the implicit assumption that the size and shape of the bed forms for a given set of flow conditions are approximately uniform may not be justified. Pratt (1972) notes with respect to the complexity of dune beds, the "definition of individual dunes involved personal decisions in particular cases." Also, although at least ripples and dunes have been generally recognized to be morphologically distinct and dynamically different, there are no generally accepted models to explain the differences.

The purpose of the present study is to examine both quantitatively and observationally the similarities and differences between the different kinds of flow-transverse bed forms previously delineated by other authors in flume studies: ripples, two-dimensional dunes, and three-dimensional dunes. The present study was designed to obtain detailed, quantitative data on the bed geometry and to make concurrent observations of the kinematics and dynamics of the different kinds of bed forms. A series of flume experiments was conducted as a function of mean flow velocity using a medium sand and a constant flow depth: the experiments were conducted at closely spaced velocity

intervals over the range of mean flow velocities in which the transitions between these three different kinds of bed forms occur in order to document and examine these transitions. Because of the complexity of the problem, the observational approach supported by detailed quantitative data on the bed geometry appeared to be potentially the most useful approach.

CHAPTER 2

EXPERIMENTAL EQUIPMENT AND PROCEDURES

Section 2-1.0

Experimental Equipment

The experiments were conducted in a tilting, recirculating flume with a channel made of transparent acrylic plastic. The dimensions of the flume are 11.5 m long, 0.92 m wide and 0.56 m deep. The flume is the same as that used by Costello and Southard (1981) with some modifications to the arrangement of the return flow; more details on the flume equipment and a diagram of the flume are given by Costello (1974). A vertical propeller pump recirculated both the sediment and water from the tailbox to the headbox through two 6-inch (15.2 cm) return pipes beneath the channel. The discharge was controlled by a gate valve in each of the return pipes; also, any percentage of the flow could be pumped directly from the pump outlet back into the tailbox by means of a bypass pipe with a gate valve, thereby bypassing the return pipes and flume channel. The discharge was measured with a Venturi meter in each return pipe connected to a mercury-water manometer. The steel truss that supports the flume channel has a pivot support near the downstream end. The slope of the flume channel was adjusted by a hand crank. To estimate the slope of the flume channel, the change in the

slope of the channel per "crank turn up from level" was determined using the still water surface as a reference level.

An arrangement of baffles at the head of the channel was used to make the flow more uniform across the channel. A plywood sheet 0.61 m long and the same width as the channel was suspended on the water surface just downstream from the baffles to damp surface waves generated at the inlet. The first section of the channel downstream from the baffles was covered with a wooden false bottom 1.17 m long and the same width as the channel to minimize scour by the developing boundary layer.

An auxiliary system was used to pump water from the tailbox to a settling barrel to obtain sediment-free water to flush the bearings of the main pump. When water from the settling barrel overflowed back into the tailbox it passed through a fiberglass filter in the tailbox to remove algae and fines to maintain water clarity. Algicide was also regularly used. A cooling coil with an adjustable volume of cold tap water was immersed in the settling barrel to help control the water temperature. Water lost from the flume by evaporation was continually replaced by a drip device. The drip device consisted of a large plastic filter flask in which a constant water level was maintained by means of an overflow; the flask had a tap near the bottom with a stopcock which could be adjusted to the

desired drip rate.

A steel rod was mounted along the top of each of the upper sidewall supports parallel to the flume bottom. These two rods acted as rails for an instrument carriage and are referred to as the flume rails. A point gage attached to the instrument carriage was used to measure the elevations of the water surface and the bed surface. The vernier scale on the point gage could be read to the nearest 0.1 mm. A tape measure was attached along the top of one of the sidewall supports starting at the downstream end of the head box and extending to the entrance of the tailbox; the tape is 1115.5 cm long. This tape was used to locate the position at which measurements and photography were taken; these positions are referred to in the text. Quantitative data on the size and shape of the bed forms was taken in the downstream section of the flume from 500 cm to 1000 cm; this section of the flume is referred to as the test section.

The sediment bed was leveled using a beveled board attached at right angles to two pieces of angle steel. This bed-leveling device could be clamped to the instrument carriage and adjusted to the desired elevation to produce a planar bed. The sediment discharge was measured using a wire-mesh trap that could be installed in the tailbox at the end of the flume channel level with the channel bottom. The trap design is given by Costello (1974).

The sand used for these experiments was a well-sorted medium sand with a mean size of 0.51 mm and a geometric standard deviation of 1.08. This sand is the same sand as the 0.51 mm sand used by Costello and Southard (1981). The sand came from a composite of commercially available glacial outwash sands composed mostly of subangular quartz with about 10% fine-grained rock fragments. More information about the sand and sand preparation is given by Costello (1974).

Section 2-2.0

Experimental Procedures

All of the experiments were conducted at a constant mean flow depth of 15 cm, using the 0.51 mm sand described above. Twelve flume runs were conducted, each at a constant mean flow velocity; the mean flow velocity was systematically varied from 28.6 cm/s to 47.4 cm/s. Variations in the sediment bed configuration and water-surface slope were examined as functions of mean flow velocity.

Section 2-2.1

Runs 1 through 9

For the primary set of experiments, Runs 1 through 9, the mean flow velocity was increased for successive runs in increments of 1.4 cm/s to 3.6 cm/s from 28.6 cm/s to 47.4

cm/s. Each flume run lasted from 6 to 11 days, with most being six days long. During each experiment the mean flow depth, mean flow velocity, and water temperature were regularly monitored and adjusted to maintain approximately constant mean flow conditions. The water-surface slope was also regularly determined and the slope of the flume channel was adjusted to equal the water slope. The sediment bed was regularly observed and the bed configuration was systematically documented using still photography, real-time and time-lapse movie photography, and longitudinal, centerline bed-surface profiles. The procedure used for a standard data set for Runs 1 through 9 is outlined below. During an experiment, after the initial data set, two data sets were usually taken each day; the total number of data sets for each run varied from 10 to 18. For the initial and final data sets, the procedure was modified as indicated below. The date and time were recorded when all data and photography were taken and when adjustments were made to the flow conditions.

A) Procedure: Initial Data Set

The sand formed a sediment bed about 8 cm thick on the bottom of the flume channel. After the flume was filled with water to a flow depth greater than 15 cm, the sediment bed was carefully leveled from the edge of the exposed false bottom downstream to the tailbox, to form a planar

bed. The slope of the flume channel was preset to an approximate value, estimated from data for experiments conducted at similar flow conditions using the same sand (Costello, 1974). A longitudinal bed-surface profile was taken by measuring the bed-surface elevation with the point gage along the centerline of the flume from 500 cm to 1000 cm at 50-cm intervals. After correcting the bed-surface elevations for irregularities in the flume rails, the least-squares fit to a straight line was calculated for the bed-surface profile. The value of the straight line at the midpoint of the profile, 750 cm, was used to estimate the bed-surface elevation.

Before each experiment was started, the flume was run very briefly at a velocity of about 22 cm/s in order to preset the depth approximately; at this velocity there was no sediment movement on the bed. The point gage was positioned at 750 cm at the desired water elevation; water was removed or added until the point gage just touched the water surface. Before the depth was preset, the drip was preset to compensate approximately for water evaporation. The discharge was increased to a value slightly less than the desired discharge and then carefully increased to the desired value. While the discharge was being adjusted, the point gage, positioned at 750 cm at the desired water elevation, was used to monitor the depth. As the discharge was increased, the depth was readjusted to approximately

15 cm, as described above. The term "start-up" is used in the descriptions of the bed forms to refer to the time when the flow velocity was first adjusted upward from 22 cm/s.

For Runs 1 through 9, time-lapse movie photography of the sediment bed was taken through the sidewall during the entire experiment except when real-time movie photography was being taken. The field of view of the movie camera was centered at about 860 cm. A small clock and reference scales were attached to the sidewall in the field of view. The trigger for the movie camera was started before bed forms developed in the field of view, and the trigger was normally turned off after the flume pump was turned off at the end of the experiment. The time interval for the trigger of the movie camera was chosen so that major crests were photographed many times as they migrated across the field of view of the movie camera. As the flow velocity was increased, the time interval was shortened; the range of time intervals for Runs 1 through 9 was 111 seconds to 65 seconds.

The sediment bed was carefully observed as bed forms developed from the planar bed; observations were documented with still photography. For Runs 1 through 4, a longitudinal bed-surface profile was taken of the bed forms propagating downstream from the false bottom after the bed forms had propagated more than half the length of the sediment bed. The profile was taken by measuring the bed-

surface elevation with the point gage from the bed-form front upstream to the false bottom. The farthest downstream section of the profile, where the bed forms were relatively small, was taken at one-cm intervals; upstream, two-cm intervals were used.

A water-surface profile was taken as described below for a standard data set to determine the flow depth and the water-surface slope; the depth was evaluated using the bed elevation estimated from the leveled bed. Adjustments were made in the depth and channel slope as described for a standard data set. The room and water temperatures, flow velocity, and movie camera were also monitored as described for a standard data set.

B) Procedure: Standard Data Set

The procedure outlined below was the standard procedure used to monitor the mean flow conditions and to document the sediment bed configuration during the course of an experiment after the initial data set was taken. The steps of the procedure are listed in chronological order.

1) Measurements and documentation

a) The room temperature and water temperature were recorded to the nearest 0.1 ^{o}C.

b) The manometer readings for each of the Venturi meters were recorded to the nearest 0.005 inches (0.127 mm) of mercury.

c) A sequence of overlapping, plan-view color slides was taken from above with the wide-angle lens of the full width of the sediment bed from 500 cm to 1000 cm; for most of the runs these slides were centered at 100-cm intervals starting at 550 cm. Immediately following the above sequence, slides of downstream and upstream views of the entire sediment bed in the test section were also taken with the wide-angle lens. Once during each experiment, a parallel sequence of plan-view slides was taken with the regular lens concurrently with the standard sequence described above. These slides were centered at 50-cm intervals starting at 525 cm and were taken in pairs alternately with the corresponding slides of the standard sequence. Also during each experiment, slides were taken of both representative and unusual features, using the wide-angle lens, the regular lens, and/or the micro lens.

For the later runs, additional still photography was included: at least once during Runs 7, 8, and 9, the standard sequence of slides of the sediment bed in the test section (as described above) was repeated up to five times at 20-minute to 100-minute intervals in order to document changes in the bed configuration over relatively short time periods. Also, for Runs 8 and 9, at least one sequence of overlapping, plan-view color slides was taken with the wide-angle lens of the entire width of the sediment bed for the full length of the sediment bed instead of just the

test section, to document variations in the bed forms along the length of the sediment bed. These slides were centered at approximately 100-cm intervals starting at about 230 cm.

d) A longitudinal, bed-surface profile was taken by measuring the bed elevation with the point gage along the centerline of the flume from 1000 cm to 500 cm at two-cm intervals. The longitudinal positions of crests were recorded to the nearest centimeter and the bed elevations of all crests were measured.

e) A longitudinal water-surface profile was taken by measuring the water-surface elevation with the point gage along the centerline of the flume from 500 cm to 1000 cm at 10-cm intervals. For each longitudinal position, three consecutive water-surface measurements were made; the mean of the three measurements was recorded.

f) The room temperature and water temperature were recorded as in Step a.

g) The manometer readings for the Venturi meters were recorded as in Step b.

h) Visual observations were made of the sediment bed.

i) For Runs 7 and 9, close-up, real-time movie photography of representative features of the sediment bed was taken, both from above through a plexiglass sheet suspended on the water surface and from the side through the sidewall. The real-time movie photography was taken in the middle of the run when it was necessary to change film

for the time-lapse photography and/or during the final data set. For these runs the time-lapse movie photography was terminated near the beginning of the final data set.

2) Calculations

a) After correcting the bed-surface and water-surface profiles for irregularities in the rails, the least-squares fit to a straight line was calculated for each profile; for the bed-surface profile 6-cm intervals were used and for the water-surface profile 10-cm intervals were used. The bed-surface and water-surface slopes relative to the slope of the flume rails were estimated by the slopes of these straight lines. The mean flow depth was estimated by the difference of these lines evaluated at the midpoint of the lines, 750 cm.

b) The average evaporation rate for the time period between the two most recent water-surface profiles was determined using the preset drip rate and the change in water-surface level between the starting times of these two water-surface profiles. The water-surface level was estimated by the least-squares fit to a straight line of the water-surface profile, evaluated at the midpoint of the line, 750 cm.

c) The mean flow velocity was calculated for the two sets of manometer readings. The average of the two values was used to estimate the mean flow velocity for the data set.

3) Adjustment of flow conditions and flume maintenance

a) The slope of the flume channel (i.e. the slope of the rails) was adjusted to be approximately equal to the water-surface slope. The channel slope was recorded in terms of the number of "crank turns up from level"; adjustments were made to the nearest half turn.

b) The mean flow depth was adjusted to 15 cm by adding or removing measured quantities of water to the flume.

c) The drip rate was adjusted to compensate for the newly calculated evaporation rate.

d) The input to the cooling coil was adjusted to maintain approximately constant water temperature.

e) Occasionally, minor adjustments were made to the discharge to maintain the desired velocity.

f) To maintain good water clarity, algicide was added periodically to the water in the flume, and the filter in the tailbox was changed periodically.

g) The movie camera and the clock in the field of view of the movie camera were wound, and the time, footage, and frame-counter reading were recorded to check whether the camera was advancing properly.

C) Procedure: Final Data Set

The data taken during the final data set were the same as for a standard data set with the addition of a sediment discharge measurement; however, the order in which the data

were taken was changed. The following order was used: temperature and manometer reading, water-surface profile, visual observations, still photography, bed-surface profile, and temperature and manometer readings.

The sediment discharge measurement was taken near the end of an experiment to minimize the effect of the interruption of sediment supply to the upstream end of the flume on the sediment bed in the test section during the experiment. The sediment discharge measurement was started at different times during the experiment for different runs, depending primarily on the apparent sediment transport rate. For Runs 8 and 9, the sediment trap was inserted in the tailbox after the final water-surface profile was taken so that the calculated water-surface slope would not be affected by changes in the water surface due to the presence of the trap. For most of the lower velocity runs, however, the sediment trap was inserted in the tailbox at the end of the preceding data set in order to allow sufficient time for a moderate-sized sediment sample to accumulate in the trap before the end of the experiment. When the sediment trap was inserted, an equivalent volume of water was removed from the flume. Similarly, when the trap was removed, a volume of water roughly equivalent to the volume of the trap plus sediment was added to the flume. The weight of the sediment samples ranged from 3.2 to 8.5 kilograms, and the measurement

periods ranged from 50 minutes to about 46 hours.

The still photography, bed-surface profile and final temperature and manometer reading were taken immediately before the flume pump was turned off, so that the final bed-surface profile with the flume on could be directly compared to an analagous bed-surface profile with the flume off. Differences in these profiles indicate changes in the bed configuration that occurred on the time scale of taking a bed-surface profile (about 60 to 70 minutes). Comparison of these profiles also gives an indication of how much the profiles of individual bed forms were distorted by taking bed-surface profiles with the flume on.

At the end of a run, the discharge in the flume channel was gradually decreased and stopped before the flume pump was turned off to minimize water-surface waves in the channel and disturbance of the sediment bed. The gate valve for the bypass pipe was opened, allowing part of the water to recirculate directly through the tailbox (bypassing the flume channel), and then the gate valves for the return pipes were gradually closed. After the flume pump was turned off, all of the auxiliary systems were turned off, including the movie camera, the cooling coil and the drip.

D) Procedure: Follow-Up

The procedure at the end of an experiment, after the flume pump was turned off, is outlined below.

1) The sediment sample in the sediment trap was dried and weighed to the nearest gram to determine the sediment discharge.

2) At least three longitudinal water-surface profiles were taken of the still water surface by measuring the elevation of the water surface with the point gage from 500 cm to 1000 cm at 20-cm intervals. As for a standard data set, each recorded water-surface elevation was the mean of three consecutive measurements. To allow time for water-surface waves to dissipate, these profiles were taken more than ten hours after the flume pump was turned off. The profiles were spaced over a time period from a few hours to more than two days. After correcting the water-surface elevations for irregularities in the rails, the least-squares fit to a straight line was calculated for each of the profiles. The average of the slopes of the lines was used to estimate the slope of the flume channel (i.e., the slope of the flume rails) at the end of the experiment. The value was compared to the channel slope estimated from the recorded number of "crank turns up from level" at the end of the experiment.

3) A sequence of plan-view slides of the sediment bed in the test section and slides of downstream and upstream

views of the sediment bed in the test section were taken as described for a standard data set.

4) A bed-surface profile was taken as described for a standard data set.

5) The flume was slowly drained. As bed forms began to emerge above the water surface, slides of downstream and upstream views of the entire length of the sediment bed were taken with the wide-angle lens to examine qualitatively lateral variations in the height of bed forms and to check for possible meandering patterns in the bed configuration.

6) After the flume had drained, another set of slides was taken as described in Step c. In addition, using the wide-angle lens, slides of downstream and upstream views of the entire length of the sediment bed were taken, and slides of the sidewall profile of the bed configuration were taken through the sidewall.

Section 2-2.2

Runs 10, 11 and 12

Runs 10, 11 and 12 were supplementary runs, carried out primarily to obtain plan-view, time-lapse movie photography of both developing and fully developed bed forms for flow velocities within the ripple, two-dimensional dune, and three-dimensional dune stability fields, described by Costello (1974). These runs also

provided an opportunity to observe and compare directly bed forms in these three different stability fields within a relatively short time period and to obtain additional still photography and real-time movie photography. The mean flow velocities for Runs 10, 11, and 12 were approximately 32.3 cm/s, 38.4 cm/s, and 47.4 cm/s, respectively. Each flume run lasted three days. In general, the mean flow conditions were monitored and adjusted as for Runs 1 through 9. The procedure used for these runs is outlined below.

A) Procedure: First Day

The procedure for the first day of each experiment was the same as that described for the inital data set of Runs 1 through 9, except for the modifications noted below. The procedure for monitoring and adjusting the flow depth was modified because of the presence of a plexiglass sheet suspended on the water surface in the test section when plan-view, time-lapse movie photography was being taken. The water-surface profile to determine and adjust the depth was taken at the beginning of each experiment before the plexiglass sheet was positioned in the flume instead of near the end of the initial data set. Before each experiment was started, the depth was roughly preset as described for Runs 1 through 9, using the point gage positioned at 750 cm at the desired water elevation with

the flume running at a velocity of about 22 cm/s. For Run 10, a water-surface profile was taken and the depth was adjusted to 15 cm, immediately after the discharge was set and before the plexiglass sheet was positioned in the flume. However, for Runs 11 and 12, a water-surface profile was taken, final adjustments were made in the depth, and the plexiglass sheet was positioned in the flume before the discharge was set in order to document the initial stages of the development of bed forms with time-lapse movie photography. To compensate for the drawdown of the water surface when the velocity was increased from 22 cm/s to the desired velocity, the depth was preset too deep by the amount of the drawdown, which was determined before the experiment.

For Runs 10 and 11, plan-view, time-lapse movie photography of the full width of the sediment bed was taken from above through a plexiglass sheet suspended on the water surface from before bed forms developed in the field of view until the middle of the third day of the experiment. The field of view of the movie camera was centered at 700 cm. A small clock and a reference scale were attached to the plexiglass sheet in the field of view. For Run 12, the time-lapse movie photography was not taken continuously, but during two separate time periods; an eleven-second time interval was used, necessitating that the movie camera be wound every two hours. The time

periods were chosen to document both developing and fully developed bed forms: (1) four hours, starting immediately before the discharge was set, and (2) six hours during the second day, starting about 28 hours after the discharge was set. For all three runs, a shorter time interval for the trigger of the movie camera was used than for the previous run at approximately the same mean flow velocity in order to obtain more detail of the kinematics of the bed forms; the range of the time intervals was 65 to 11 seconds.

The development of bed forms as a function of time was carefully observed and was documented using still photography over the full length of the sediment bed. The still photography was more extensive than for most of the initial data sets of Runs 1 through 9. For both Runs 10 and 11, six sequences of overlapping, plan-view color slides were taken at 28-minute to 146-minute intervals with the wide-angle lens over the length of the sediment bed where bed forms were developing. For Run 12, repeated slides centered at 700 cm were taken with the regular lens at about 13-second intervals during the first five minutes of the experiment to document the initial stages of development of bed forms. Later, a sequence of overlapping, plan-view color slides was taken with the wide-angle lens of the full length of the sediment bed. For all three runs, a variety of additional still

photography was taken with the wide-angle lens, the regular lens, and the micro lens.

B) Procedure: Second Day

During the second day of each experiment, one data set was taken which was the same as a standard data set of Runs 1 through 9, except for the modifications noted below.

More extensive still photography was taken than for a standard data set. The still photography included:

1) a sequence of overlapping, plan-view color slides of the entire length of the sediment bed, taken with the wide-angle lens,

2) a parallel sequence of slides of the sediment bed in the test section only, taken with the regular lens concurrently with the above sequence,

3) slides of downstream and upstream views of the sediment bed in the test section, taken with the wide-angle lens, and

4) additional slides of representative or unusual feature, taken with the wide-angle lens, regular lens, and micro lens.

Before the bed-surface and water-surface profiles were taken, the movie camera was turned off and the plexiglass sheet was removed from the flume. After these profiles were taken, the plexiglass sheet was repositioned in the flume and the movie camera was restarted. In lieu of a

second data set, additional temperature and manometer readings were taken periodically during the day, as described for a standard data set.

C) Procedure: Third Day

During the third day of each experiment, additional still photography and real-time movie photography were taken. For Runs 10 and 11, four sequences of overlapping, plan-view color slides of the entire length of the sediment bed were taken at 21-minute to 30-minute intervals with the wide-angle lens. For all three runs, a variety of additional still photography was taken. Also, for each run, close-up, real-time movie photography of representative features of the sediment bed was taken, both from above through the plexiglass sheet and from the side through the sidewalls.

Temperature and manometer readings were taken periodically during the day, as described for a standard data set, but no bed-surface or water-surface profiles were taken. After the photography was completed and the final temperature and manometer reading were taken, the flume pump and all auxiliary systems were turned off, as described for Runs 1 through 9.

D) Procedure: Follow-up

After Run 12, three longitudinal water-surface profiles were taken of the still water surface, and the slope of the flume channel (i.e., the slope of the flume rails) was determined as described for Runs 1 through 9. After these profiles were taken, the channel slope was rezeroed by turning the crank down the recorded number of "crank turns up from level" at the end of Run 12. Ten hours later, two more longitudinal, water-surface profiles were taken of the still water surface and the slope of the flume channel was determined.

CHAPTER 3

FLOW VARIABLES

Section 3-1

Mean Flow Depth

Description

The mean flow depth for a data set was estimated from the longitudinal bed-surface and water-surface profiles taken along the centerline of the flume. The least-squares fit to a straight line was calculated for each profile, and the average flow depth was estimated by the difference in elevation of these two lines evaluated at the midpoint of the lines, 750 cm (i.e., mean flow depth = $Y_w(750) - Y_b(750)$, where $Y_w(750)$ and $Y_b(750)$ are the least-squares fit to straight lines of the water-surface and bed-surface profiles, respectively, evaluated at a longitudinal position of 750 cm). This estimate of the mean flow depth is a good approximation of the flow depth averaged over the length of the test section along the centerline of the flume and is thus a good approximation of the mean flow depth associated with the bed-surface profile. (The quantitative data on the geometric properties of bed forms were derived from the bed-surface profiles.) Using the least-squares fit to a straight line for each profile effectively averages local variations in depth due to highs and lows in the bed-surface profile and due to

corresponding depressions and rises in the water-surface profile.

Measurement Errors

The errors in determining $Y_b(750)$ and $Y_w(750)$ were estimated by examining the propagation of the errors in individual bed-surface and water-surface elevations to $Y_b(750)$ and $Y_w(750)$, respectively (Bevington, 1969). In addition, the effects of the longitudinal spacing of data points and of the length of the profile on $Y_b(750)$ and $Y_w(750)$, the effect of the location of the end points of the profile relative to the crests and troughs of bed forms on $Y_b(750)$, and the reproducibility of $Y_b(750)$ were examined to determine whether any of these factors resulted in errors in $Y_b(750)$ or $Y_w(750)$ larger than the errors estimated by the propagation of the errors in individual bed-surface and water-surface elevations. The error in determining the mean flow depth for a data set was evaluated by the propagation of the errors in $Y_b(750)$ and $Y_w(750)$ to the mean flow depth.

A) Errors in $Y_b(750)$

1) Estimated standard deviation of individual bed-surface elevations.

To estimate the error in measuring individual bed-surface elevations with the point gage, one meter of a bed-surface profile, taken with the flume not running, was

repeated after the initial profile was completed, and the difference in the two point-gage readings for each longitudinal position was calculated. The mean of the ranges is 0.036 cm; the standard deviation of an individual bed-surface elevation estimated from this range is 0.032 cm.

2) Estimated standard deviation of $Y_b(750)$

The error in determining $Y_b(750)$ for a bed-surface profile was estimated by applying propagation-of-errors formulas to the equation for determining $Y_b(750)$ from the least-squares fit to a straight line for a sample bed-surface profile. Assuming that the point gage was positioned longitudinally with a standard deviation of 0.1 cm and using the estimated standard deviation of individual bed-surface elevations, 0.032 cm, the standard deviation of $Y_b(750)$ for the sample profile was calculated to be 0.189 cm.

3) Longitudinal spacing of individual bed-surface elevations

To examine the effect of the longitudinal spacing of individual bed-surface elevations, $Y_b(750)$ was calculated using both 5-cm and 10-cm spacing for six bed-surface profiles taken at 5-cm intervals. The mean of the absolute values of the difference in $Y_b(750)$ for 5-cm and 10-cm spacing is 0.017 cm. This value is less than the estimated standard deviation of $Y_b(750)$ for the sample profile using

6-cm spacing, 0.189 cm, and suggests that the use of 10-cm spacing would not significantly increase the error in $Y_b(750)$. Therefore, 6-cm spacing is sufficiently small to determine $Y_b(750)$ within the estimated standard deviation.

4) Length of profile

To examine the effect of the profile length, $Y_b(750)$ was calculated for each length between four and six meters at 6-cm intervals for two bed-surface profiles. The mean of the ranges of $Y_b(750)$ for lengths from four to five meters is 0.148 cm. This value is less than the estimated standard deviation of $Y_b(750)$, 0.189 cm, for the sample profile, which is five meters long, and suggests that a five-meter profile is sufficiently long to define a stable value of $Y_b(750)$ within the estimated standard deviation. This result also suggests that the exact location of the beginning and end points of a bed-surface profile relative to the crests and troughs of bed forms does not strongly affect the value of $Y_b(750)$.

5) Choice of end points

The effect of the location of the end points of a profile relative to crests and troughs of bed forms was directly examined by calculating $Y_b(750)$ for two extreme cases for two bed-surface profiles: 1) starting the profile at a crest and ending at the low point in a trough, and 2) starting at the low point in a trough and ending at a crest. The difference in $Y_b(750)$ for the two cases was

calculated for each profile; the mean of the absolute values of the difference for the two profiles is 0.053 cm. This value is less than the estimated standard deviation of $Y_b(750)$ for the sample profile, 0.189 cm, and suggests that the location of the end points of a profile relative to the crests and troughs of bed forms does not significantly affect the value of $Y_b(750)$.

6) Reproducibility

To examine the reproducibility of $Y_b(750)$ on the time scale of taking a profile, five pairs of consecutive bed-surface profiles were taken. The mean of the absolute values of the difference in $Y_b(750)$ for the consecutive profiles is 0.078 cm. This value is less than the estimated standard deviation of $Y_b(750)$ for the sample profile, 0.189, and suggests that the value of $Y_b(750)$ remained stable, within the estimated standard deviation, sufficiently long to take a bed-surface profile (about 60 to 70 minutes).

B) Errors in $Y_w(750)$

1) Estimated standard deviation of individual water-surface elevations

To examine the error in measuring individual water-surface elevations with the point gage, the range of three consecutive water-surface measurements for each longitudinal position of a sample water-surface profile was recorded when the profile was being taken. The mean of the

ranges is 0.027 cm; the standard deviation of a single water-surface measurement estimated from this range is 0.016 cm. Each water-surface elevation recorded during the experiments was the mean of three consecutive measurements; therefore, by the propagation of the error in single measurements, the estimated standard deviation of an individual water-surface elevation recorded during the experiments is 0.0092 cm.

2) Estimated standard deviation of $Y_w(750)$

The error in determining $Y_w(750)$ was estimated by applying propagation-of-errors formulas to the equation determining $Y_w(750)$ from the least-squares fit to a straight line for a sample water-surface profile. Assuming that the point gage was positioned longitudinally with a standard deviation of 0.1 cm and using the estimated standard deviation of individual water-surface elevations recorded during the experiments, 0.0092 cm, the standard deviation of $Y_w(750)$ for the sample profile, was calculated to be 0.082 cm.

3) Longitudinal spacing of individual water-surface elevations

To examine the effect of the longitudinal spacing of individual water-surface elevations, $Y_w(750)$ was calculated using both 10-cm and 20-cm spacing for five water-surface profiles taken at 10-cm intervals. The mean of the absolute values of the difference in $Y_w(750)$ for 10-cm and

20-cm spacing is 0.006 cm. This value is less than the estimated standard deviation of $Y_w(750)$ for the sample profile using 10-cm spacing, 0.082 cm, and suggests that the use of 20-cm spacing would not significantly increase the error in $Y_w(750)$. Therefore, 10-cm spacing is sufficiently small to determine $Y_w(750)$ within the estimated standard deviation.

4) Length of profile

To examine the effect of the length of the profile, $Y_w(750)$ was calculated for each length between four and five meters at 5 cm intervals for a sample water-surface profile. The range in $Y_w(750)$ for lengths from four to five meters is 0.002 cm. This value is less than the estimated standard deviation of $Y_w(750)$ for the sample profile which is five meters long, 0.082 cm, and suggests that a five-meter profile is sufficiently long to define a stable value of Yw(750) within the estimated standard deviation.

C) Error in mean flow depth

The error in determining the mean flow depth for a data set was estimated by applying propagation-of-errors formulas to the equation for the mean flow depth. Using the estimated standard deviations of $Y_w(750)$ and $Y_b(750)$ for the sample water-surface and bed-surface profiles (0.082 cm and 0.189 cm, respectively), the standard

deviation of the mean flow depth was calculated to be 0.206 cm.

Results

For Runs 1 through 9, the mean flow depth for a run was estimated by the average of the mean flow depths for all of the data sets of the run, excluding the initial data set, which was taken when bed forms were developing from a planar bed. The mean flow depth and sample standard deviation for each run are listed in Table 3-1. The mean flow depths with 90% confidence intervals are plotted as a function of mean flow velocity in Figure 3-1; the confidence intervals for the means were determined from the sample standard deviation for each run.

For Runs 10 through 12, the mean flow depth for a run was estimated by the mean flow depth for the data set taken on the second day of the experiment, the mean flow depth for each run is listed in Table 3-1.

The mean of the sample standard deviations of the mean flow depth for Runs 1 through 9 is 0.277 cm. This value is 34% larger than the estimated error in determining the mean flow depth, 0.206 cm. The sample standard deviation for a run is a measure of the variation in the values of the mean flow depth during a run; this variation results from the error in determining the mean flow depth at a given time and may also result from real variations in the mean flow

depth as a function of time during a run. If the mean flow depth remained constant during a run, the sample standard deviation would be an estimate of the error in determining the mean flow depth at a given time; therefore, the sample standard deviation for a run is probably an upper limit on the real error in determining the mean flow depth for a data set. Comparison of the mean of the sample standard deviations and of the estimated error suggests that the mean flow depth varied slightly as a function of time during individual flume runs and/or that the real error in determining the mean flow depth was slightly greater than the estimated error. The relatively large sample standard deviations for Runs 1 and 2 are probably at least partly due to real variations in the mean flow depth as a function of time during the runs. Refinements in equipment and procedures during the first two runs resulted in better depth control and thus in smaller sample standard deviations for the later runs.

All of the experiments were conducted at an approximately constant mean flow depth of 15 cm. The average of the mean flow depths for Runs 1 through 9 is 14.986 cm; this value is within 0.1% of 15 cm. The sample standard deviations for the individual runs indicate that the mean flow depth remained relatively constant as a function of time during individual flume runs. Statistical tests were used to determine whether the mean flow depths

for all of the experiments were approximately the same and also to determine a probable upper bound on how much the mean flow depths for the experiments differed from 15 cm.

To examine whether the mean flow depths for Runs 1 through 9 were significantly different from one another, the significance of the difference between the mean flow depth for each run and the mean flow depth for each of the other runs was calculated. The mean flow depth for Run 1 is significantly different from the mean flow depth for each run, 2 through 9, at the 0.10 level of significance (i.e., the probability of rejecting the hypothesis that the means are the same, when the hypothesis is true, is less than or equal to 0.10). For Runs 2 through 9, the mean flow depth for each run is not significantly different from the mean flow depth or each of the other runs, 2 through 9, at the 0.10 level of significance (i.e., the data are insufficient to indicate that the means are different at the 0.10 level of significance).

To determine a probable upper bound on the magnitude of the difference between the mean flow depths for Runs 1 through 9, the 90% confidence interval for the difference between the mean flow depth for each run and the mean flow depth for each of the other runs was calculated. For Runs 1 through 9, the absolute magnitude of the difference between the mean flow depth for each run and that for each of the other runs is less than 0.656 cm at the 0.10 level

of significance. Excluding Run 1, the absolute magnitude of the difference between the mean flow depth for each run and that for each of the other runs is less than 0.373 cm at the 0.10 level of significance. Therefore, for Runs 2 through 9, the mean flow depth for each run is different by no more than 2.5% from the mean flow depth for any of the other runs, 2 through 9, at the 0.10 level of significance; the mean flow depth for Run 1 is different by no more than 4.4% from the mean flow depth for any of the other runs, 2 through 9, at the 0.10 level of significance.

To determine a probable upper bound on the difference between the mean flow depth for each run, 1 through 9, and 15 cm, the 90% confidence interval for the mean flow depth for each run was examined. For Runs 1 through 9, the mean flow depth for each run is within $\pm$0.490 cm or 3.3% of 15.000 cm at the 0.10 level of significance. The data on the mean depth indicate not only that the mean flow depth was maintained at a relatively constant value as a function of time during individual flume experiments, but also that the mean flow depth was approximately the same for all of the experiments.

Section 3-2

Mean Flow Velocity

Description

The mean flow velocity for a data set was estimated by the average of the flow velocities determined from the two sets of manometer readings taken during the data set. The mean flow velocity was calculated using Bernoulli's equation for steady, frictionless, incompressible flow with the inclusion of a discharge coefficient to account for the effects of viscosity and turbulence (Li and Lamb, 1964). For the range of return-pipe Reynolds numbers in the experiments, the discharge coefficient ranges from 0.983 to 0.984 (ASME, 1959). The following values were used in the velocity calculations: the mean flow depth for the data set, the standard value of the acceleration of gravity (980.665 cm/s^2), and the densities of water (0.99707 g/cm^3) and mercury (13.5340 g/cm^3) at 25 ^oC (Weast, 1974).

Measurement Errors

The error in determining the mean flow velocity was estimated by applying propagation-of-errors formulas to the equation for the velocity. The error in the mean flow velocity is due primarily to the errors in the mean flow depth, the manometer readings, and the discharge coefficient; the errors in the other variables are negligible. The error in reading the manometer was

estimated by noting the range of the readings over a time period of a few minutes; for the range of flow velocities of the experiments, the standard deviation of the manometer reading estimated from this range varied from 0.010 to 0.015 inches of mercury. Using the estimated standard deviation of the mean flow depth (0.206 cm), the above estimates of the standard deviation of the manometer reading, and the standard deviation of the discharge coefficient estimated from the published tolerance limits (0.004; ASME, 1950), the standard deviation of the mean flow velocity ranges from 0.42 cm/s to 0.68 cm/s for the range of flow velocities of the experiments.

Results

For Runs 1 through 9, the mean flow velocity for a run was estimated by the average of the mean flow velocities for all of the data sets of the run, excluding the initial data set taken when bed forms were developing from a planar bed. The mean flow velocity and sample standard deviation for each run are listed in Table 3-2. The mean flow velocities with 90% confidence intervals are plotted as a function of run number in Figure 3-2; the confidence intervals for the means were determined from the sample standard deviation for each run.

For Runs 10 through 12, the mean flow velocity for a run was estimated by the mean flow velocity for the data

set taken on the second day of the experiment; the mean flow velocity for each run is listed in Table 3-2.

The sample standard deviations of the mean flow velocity for Runs 1 through 9 range from 0.26 cm/s to 1.11 cm/s. The relatively large values of the sample standard deviation for Runs 1 and 2 are due primarily to variations in the mean flow depth. The sample standard deviations for Runs 3 through 9 range from 0.26 cm/s to 0.82 cm/s. These values are similar to the estimated errors in determining the mean flow velocity for the range of flow velocities of the experiments, 0.42 cm/s to 0.68 cm/s. The sample standard deviations that are larger than the estimated errors suggest that the mean flow velocity varied slightly as a function of time during these flume runs and/or that the real error in determining the mean flow velocity was slightly larger than the estimated error.

For Runs 1 through 9, the mean flow velocity was systematically increased in increments of 1.4 cm/s to 3.6 cm/s in order to examine the sediment bed configuration as a function of mean flow velocity. To determine whether the mean flow velocities for Runs 1 through 9 were significantly different from one another, the significance of the difference between the mean flow velocities for successive runs was calculated. For Runs 1 through 9, the mean flow velocity for each run is significantly different from the mean flow velocity for each of the other runs at

the 0.0005 level of significance (i.e., the probability of rejecting the hypothesis that the means are the same, when the the hypothesis is true, is less than or equal to 0.0005). Therefore, even though the mean flow velocities for successive runs were closely spaced, the data on the sediment bed configurations for Runs 1 through 9 represent data for distinctly different mean flow velocities.

Section 3-3

Water Surface Slope

Description

The water-surface slope for a data set was estimated by the sum of the slope of the flume rails and the water-surface slope relative to the flume rails (i.e., $M_w = M_r + M_{w-r}$, where M_w is the water-surface slope, M_r is the slope of the flume rails, and M_{w-r} is the water-surface slope relative to the flume rails). This estimate is based on the trigonometric approximation that the tangent of the sum of two angles is equal to the tangents of the two angles when the absolute value of the product of the tangents of the two angles is much less than 1; for the largest water-surface slope (M_w) measured during the experiments, the product of the slope of the rails (M_r) and the water-surface slope relative to the rails (M_{w-r}) is 5.41×10^{-7}.

The slope of the flume rails (M_r) for a data set was estimated by the product of the change in the slope of the

rails per crank turn (dM_r/turn) and the recorded number of "crank turns up from level" at the time the water-surface profile was taken. Before the experiments, an approximate value of dM_r/turn was determined; after the experiments, a more accurate value was determined. The change in the slope of the rails per crank turn (dM_r/turn) was calculated using the rail slope measured at the end of Run 12 and was also calculated using the difference between this slope and the rail slope measured after the channel slope was reset to zero; the mean of these two values, -8.48×10^{-5}, was used to estimate dM_r/turn. The rail slope at the end of Run 12 was the largest rail slope measured during the experiments; the flume channel was tilted 19.5 "crank turns up from level", corresponding to a rail slope of -1.65×10^{-3}. The water-surface slope relative to the flume rails (M_w_r) was estimated by the slope of the least-squares fit to a straight line of the water-surface profile.

Measurement Errors

The error in determining the rail slope directly from a still-water-surface profile was estimated by the mean of the sample standard deviations of the rail slopes measured at the end of each run. The effects of the longitudinal spacing of data points and of the length of the profile on the measured rail slope were also examined to determine

whether either of these factors resulted in an error in the measured rail slope larger than the error estimated from the sample standard deviations. The error in determining the rail slope (M_r) for a data set, calculated as described above, was evaluated by the propagation of the error in the measured rail slope and the error in positioning the crank to the calculated rail slope (M_r).

The error in determining the water-surface slope relative to the rails (M_{w-r}) was estimated by the propagation of the error in individual water-surface elevations to M_{w-r}. In addition, the effects of the longitudinal spacing of data points and of the length of the profile on M_{w-r} and the reproducibility of M_{w-r} were examined to determine whether any of these factors resulted in an error in M_{w-r} larger than the error estimated by the propagation of the error in individual water-surface elevations. The error in determining the water-surface slope (M_w) for a data set was evaluated by the propagation of the error in the calculated rail slope (M_r) and the error in the water-surface slope relative to the rails (M_{w-r}) to the water-surface slope (M_w).

A) Errors in rail slope

1) Estimated standard deviation of measured rail slope

To estimate the error in determining the rail slope directly from a still-water-surface profile, the sample

standard deviation of the rail slopes measured at the end of each run was calculated for each run. The mean of these sample standard deviations is 9.60×10^{-6}. This value was used to estimate the standard deviation of the measured rail slope, estimated directly by the slope of the least-squares fit to a straight line of a still-water-surface profile.

2) Longitudinal spacing of individual water-surface elevations

To examine the effect of the longitudinal spacing of individual water-surface elevations on the measure rail slope, the rail slope was calculated using both 10-cm and 20-cm spacing for three still-water-surface profiles taken at 10-cm intervals. The mean of the absolute values of the difference in the rail slope for 10-cm and 20-cm spacing is 3.80×10^{-6}. This value is less than the sample standard deviation of the rail slope for the three profiles using 10-cm spacing, 1.26×10^{-5}, and suggests that the use of 10-cm spacing instead of 20-cm spacing would not increase the accuracy of the measure rail slope.

3) Length of profile

To examine the effect of the length of the profile on the measured rail slope, the rail slope was calculated for each length between four and five meters at 20-cm intervals for the five still-water-surface profiles used to calculate M_r/turn. For each of these profiles, the standard

deviation of the rail slope was estimated from the range of the rail slopes for profile lengths from four to five meters; the mean of these standard deviations is 7.28×10^{-6}. This value is less than the standard deviation of the measured rail slope estimated using five-meter profiles, 9.60×10^{-6}, and suggests that a five-meter profile is sufficiently long to define a stable value of the measured rail slope within the estimated standard deviation.

4) Estimated standard deviation of calculated rail slope (M_r)

The error in determining the rail slope (M_r) for a data set, calculated as described above, was estimated by applying propagation-of-errors formulas to the equations for the rail slope (M_r), for the range of rail slopes of the experiments. Using the estimated standard deviation of the measured rail slope, 9.60×10^{-6}, as the standard deviation of each of the individual rail slopes measured at the end of Run 12 and of each of the rail slopes measured after the channel slope was reset to zero, and assuming that the crank was positioned with a standard deviation of 5^{o}, the standard deviation of the calculated rail slope (M_r) ranges from 1.44×10^{-6} to 6.60×10^{-6} for 2.5 to 19.5 "crank turns up from level", respectively.

B) Errors in water-surface slope relative to the rails (M_{w-r})

1) Estimated standard deviation of water-surface slope relative to the rails (M_{w-r})

The error in determining the water-surface slope relative to the rails (M_{w-r}) was estimated by applying propagation-of-errors formulas to the equation for the slope of the least-squares fit to a straight line for a sample water-surface profile. Assuming that the point gage positioned longitudinally with a standard deviation of 0.1 cm and using the estimated standard deviation of individual water-surface elevations recorded during the experiments, 0.0092 cm, the standard deviation of the water-surface slope relative to the rails (M_{w-r}) for the sample profile was calculated to be 7.71×10^{-5}.

2) Longitudinal spacing of individual water-surface elevations

To examine the effect of the longitudinal spacing of individual water-surface elevations, the water-surface slope relative to the rails (M_{w-r}) was calculated using both 10 cm and 20 cm spacing for five water-surface profiles taken at 10 cm intervals. The mean of the absolute values of the difference in M_{w-r} for 10-cm and 20-cm spacing is 2.28×10^{-5}. This value is less than the estimated standard deviation of M_{w-r} for the sample profile using 10-cm spacing, 7.71×10^{-5}, and suggests that the use

of 20-cm spacing would not significantly increase the error in M_{w-r}. Therefore, 10-cm spacing is sufficiently small to determine the water-surface slope relative to the rails (M_{w-r}) within the estimated standard deviation.

3) Length of profile

To examine the effect of the length of the profile, the water-surface slope relative to the rails (M_{w-r}) was calculated for each length between four and five meters at 5-cm intervals for a sample water-surface profile. The range in M_{w-r} for lengths from four to five meters is 3.38×10^{-5}. This value is less than the estimated standard deviation of M_{w-r} for the sample profile which is five meters long, 7.71×10^{-5}, and suggests that a five-meter profile is sufficiently long to define a stable value of the water-surface slope relative to the rails (M_{w-r}) within the estimated standard deviation.

4) Reproducibility

To examine the reproducibility of the water-surface slope relative to the rails (M_{w-r}) on the time scale of taking a profile, five pairs of consecutive water-surface profiles were taken. The mean of the absolute values of the difference in M_{w-r} for the consecutive profiles is 4.36×10^{-5}. This value is less than the estimated standard deviation of M_{w-r} for the sample profile, 7.71×10^{-5}, and suggests that the value of the water-surface slope relative to the rails (M_{w-r}) remained stable,

within the estimated standard deviation, for time periods sufficiently long to take a water-surface profile (about 20 to 30 minutes).

C) Error in water-surface slope (M_w)

The error in determining the water-surface slope (M_w) for a data set was estimated by applying propagation-of-errors formulas to the equation for the water-surface slope (M_w) for the sample water-surface profile used to estimate the standard deviation of the water-surface slope relative to the rails (M_{w-r}). Using the appropriate estimate of the standard deviation of the calculated rail slope (M_r) for the recorded number of "crank turns up from level" for the sample profile, 2.04×10^{-6}, and the estimated standard deviation of the water-surface slope relative to the rails (M_{w-r}) for the sample profile, 7.71×10^{-5}, the standard deviation of the water-surface slope (M_w) was calculated to be 7.71×10^{-5}. This result indicates that the error in determining the water-surface slope (M_w) is due primarily to the error in the water-surface slope relative to the rails (M_{w-r}); the error in determining the rail slope (M_r) is negligible.

To examine the water-surface profiles for possible backwater effects, the water-surface slope of the upstream half of the water-surface profile was compared to the slope of the full profile for each water-surface profile of Runs 1 through 9, except those taken during the initial data set

and those taken while the sediment trap was in the tailbox. For each run, the significance of the difference between the mean water-surface slope of the upstream half of the profile and that of the full profile was calculated using two different methods as recommended by Johnson (1940): 1) assuming that the two samples are independent and 2) assuming that paired members of the two samples are correlated; the more sensitive test indicates the significance level. For Runs 1 and 2, the mean water-surface slope of the upstream half of the profile is significantly different from that of the full profile at the 0.10 level of significance. For both Runs 1 and 2, the mean water-surface slope of the upstream half of the profile is more negative (i.e., steeper) than that of the full profile; this difference may be due to backwater effects. For Runs 3 through 9, the means are not significantly different at the 0.10 level of significance.

Results

For Runs 1 through 9, the mean water-surface slope for a run was estimated by the average of the water-surface slopes for all of the data sets of the run, excluding the initial data set and data sets taken while the sediment trap was in the tailbox. The mean water-surface slope and sample standard deviation for each run are listed in Table 3-3. The mean water-surface slopes with 90% confidence

intervals are plotted as a function of mean flow velocity in Figure 3-3; the confidence intervals for the means were determined from the sample standard deviation for each run. The negative sign of the mean water-surface slopes is retained to facilitate comparison with the mean bed-surface slopes which are both positive and negative. It is not standard to include the negative sign: the negative sign is usually assumed.

For Runs 10 through 12, the mean water-surface slope for a run was estimated by the water-surface slope for the data set taken on the second day of the experiment; the mean water-surface slope for each run is listed in Table 3-3.

The mean of the sample standard deviations of the mean water-surface slope for Runs 1 through 9 is 1.30×10^{-4}. This value is 69% larger than the estimated error in determining the water-surface slope, 7.71×10^{-5}. and suggests that the water-surface slope probably varied somewhat as a function of time during individual flume runs. However, this result may also suggest that the real error in determining the water-surface slope was larger than the estimated error.

To examine the trends in the mean water-surface slope as a function of mean flow velocity, the significance of the difference between the mean water-surface slopes for successive runs was calculated. At the 0.05 level of

significance, the mean water-surface slopes for Run 2 and 3 are significantly more negative than the mean water-surface slope for Run 1; the mean water-surface slopes for Runs 1, 2, 3, 7, 8, and 9 are all significantly more negative than those for runs 4, 5, and 6; and the mean water-surface slope for Run 9 is significantly more negative than those for all of the other runs, 1 through 8. Therefore, the following trends in the mean water-surface slope as a function of mean flow velocity are significant at the 0.05 level of significance: the mean water-surface slope becomes steeper (i.e., more negative) with the increase in mean flow velocity from Run 1 (28.6 cm/s) to Run 2 (30.0 cm/s), becomes less steep from Run 3 (32.1 cm/s) to Run 4 (34.1 cm/s), and becomes progressively steeper with the increases in velocity from Run 6 (38.0 cm/s) to Run 7 (40.9 cm/s) and from Run 8 (43.8 cm/s) to Run 9 (47.4 cm/s).

Section 3-4

Bed Surface Slope

Description

The bed-surface slope for a data set was estimated by the sum of the slope of the flume rails and the bed-surface slope relative to the flume rails (i.e., $M_b = M_r + M_{b-r}$, where M_b is the bed-surface slope, M_r is the slope of the flume rails, and M_{b-r} is the bed-surface slope relative

to the flume rails). As noted in Section 3.3, this trigonometric approximation is valid when the absolute value of the product of the slope of the rails (M_r) and the bed-surface slope relative to the rails (M_{b-r}) is much less than 1; for the largest bed-surface slope measured during the experiments, this product is 8.59×10^{-6}. The slope of the flume rails (M_r) was estimated, as described in Section 3.3, by the product of the change in the slope of the rails per crank turn (dM_r/turn), -8.48×10^{-5}, and of the recorded number of "crank turns up from level" at the time the bed-surface profile was taken. The bed-surface slope relative to the flume rails (M_{b-r}) was estimated by the slope of the least-squares fit to a straight line of the bed-surface profile.

Measurement Errors

The error in determining the bed-surface slope relative to the flume rails (M_{b-r}) was estimated by the propagation of the error in individual bed-surface elevations to M_{b-r}. In addition, the effects of the longitudinal spacing of data points, of the length of the profile, and of the location of the end points of the profile relative to the crests and troughs of bed forms on M_{b-r} and the reproducibility of M_{b-r} were examined. The error in determining the bed-surface slope (M_b) for a data set was evaluated by the propagation of the error in the

bed-surface slope relative to the rails (M_{b-r}) and the error in the calculated rail slope (M_r) to the bed-surface slope (M_b).

A) Errors in bed-surface slope relative to the rails (M_{b-r})

1) Estimated standard deviation of bed-surface slope relative to the rails (M_{b-r})

The error in determining the bed-surface slope relative to the rails (M_{b-r}) was estimated by applying propagation-of-errors formulas to the equation for the slope of the least-squares fit to a straight line for a sample bed-surface profile. Assuming that the point gage was positioned longitudinally with a standard deviation of 0.1 cm and using the estimated standard deviation of individual bed-surface elevations, 0.032 cm, the standard deviation of the bed-surface slope relative to the rails (M_{b-r}) for the sample profile was calculated to be 1.78×10^{-4}.

2) Longitudinal spacing of individual bed-surface elevations

To examine the effect of the longitudinal spacing of individual bed-surface elevations, the bed-surface slope relative to the rails (M_{b-r}) was calculated using both 5-cm and 10-cm spacing for six bed-surface profiles taken at 5-cm intervals. The mean of the absolute values of the difference in M_{b-r} for 5-cm and 10-cm spacing is

1.26×10^{-4} . This value is less than the estimated standard deviation of M_{b-r} for the sample profile using 6-cm spacing, 1.78×10^{-4}, and suggests that the use of 10-cm spacing would not significantly increase the error in M_{b-r}. Therefore, 6-cm spacing is sufficiently small to determine the bed-surface slope relative to the rails (M_{b-r}) within the estimated standard deviation.

3) Length of profile

To examine the effect of the length of the profile, the bed-surface slope relative to the rails (M_{b-r}) was calculated for each length between four and five meters at 6-cm intervals for a sample bed-surface profile. The range in M_{b-r} for lengths from four to five meters is 2.08×10^{-3}; the standard deviation of M_{b-r} estimated from this range is 5.82×10^{-4}. This value is more than three times larger than the standard deviation of M_{b-r} estimated by the propagation of the error in individual bed-surface elevations for the sample profile which is five meters long, 1.78×10^{-4}. On the average, the variation in M_{b-r} for the sample profile decreases as the length of the profile approaches five meters, however, even for lengths of almost five meters, the variation remains larger than the standard deviation estimated by the propagation of the error in individual bed-surface elevations. For lengths of 4.92 and 4.98 meters of the sample profile, the difference in M_{b-r} is 3.56×10^{-4}; this value is twice as large as the

standard deviation estimated by the propagation of the error in individual bed-surface elevations.

The variation in the bed-surface slope relative to the rails (M_{b-r}) for lengths from four to five meters suggests that a longer bed-surface profile would be necessary for a more accurate determination of M_{b-r}; the accuracy is limited by the length of the profile (i.e., the length of the flume), not by the precision of individual bed-surface measurements. Minimization of entrance and exit effects precluded the use of a significantly longer bed-surface profile. Consequently, the standard deviation of M_{b-r} estimated from the range of M_{b-r} for lengths from four to five meters is a better estimate of the error in determining M_{b-r} than the standard deviation estimated by the propagation of the error in individual bed-surface elevations and thus is used to estimate the error in the bed-surface slope relative to the rails (M_{b-r}) in the following sections.

4) Choice of end points

The effect of the location of the end points of a profile relative to the crests and troughs of bed forms was examined by calculating the bed-surface slope relative to the rails (M_{b-r}) for two extreme cases for a sample profile: 1) starting the profile at a crest and ending at the low point in a trough and 2) starting at the low point in a trough and ending at a crest. The difference in M_{b-r}

for the two cases is 7.30×10^{-4}. This value is less than the range of M_{b-r} for lengths from four to five meters for the same profile, 2.08×10^{-3}. Examination of the variation in M_{b-r} for lengths from four to five meters in conjunction with the plot of the bed-surface profile indicates that the range of M_{b-r} corresponds to variations in the bed elevation with wavelengths longer than the average spacing of major bed forms. These results suggest that the location of the end points of a profile at crests or troughs does not affect the value of the bed-surface slope relative to the rails (M_{b-r}) as strongly as does the limited length of the profile.

5) Reproducibility

To examine the reproducibility of the bed-surface slope relative to the rails (M_{b-r}) on the time scale of taking a profile, five pairs of consecutive bed-surface profiles were taken. The mean of the absolute values of the difference in M_{b-r} for the consecutive profiles is 5.08×10^{-4}. This value is slightly less than the standard deviation of M_{b-r} estimated from the range of M_{b-r} for lengths from four and five meters, 5.82×10^{-4}, and suggests that the value of the bed-surface slope relative to the rails (M_{b-r}) remained stable, within the error due to the limited length of the profile, for time periods sufficiently long to take a bed-surface profile (about 60 to 70 minutes).

B) Error in bed-surface slope (M_b)

The error in determining the bed-surface slope (M_b) for a data set was estimated by applying propagation-of-errors formulas to the equation for the bed-surface slope (M_b) for the sample bed-surface profile used to estimate the standard deviation of the bed-surface relative to the rails (M_{b-r}) for lengths from four to five meters. Using the appropriate estimate of the standard deviation of the calculated rail slope (M_r) for the recorded number of "crank turns up from level" for the sample profile, 2.32×10^{-6}, and the standard deviation of the bed-surface slope relative to the rails (M_{b-r}) estimated from the range of M_{b-r} for lengths from four to five meters for the sample profile, 5.82×10^{-4}, the standard deviation of the bed surface slope (M_b) was calculated to be 5.82×10^{-4}. This result indicates that the error in determining the bed-surface slope (M_b) is due primarily to the error in determining the bed-surface slope relative to the rails (M_{b-r}); the error in determining the rail slope (M_r) is negligible. Thus, the error in the rail slope is negligible for both the water-surface and the bed-surface slopes.

Results

For Runs 1 through 9, the mean bed-surface slope for a

run was estimated by the average of the bed-surface slopes for all of the data sets of the run, excluding the initial data set and data sets taken while the sediment trap was in the tailbox. The mean bed-surface slope and sample standard deviation for each run are listed in Table 3-4. The mean bed-surface slopes with 90% confidence intervals are plotted as a function of mean flow velocity in Figure 3-4; the confidence intervals for the means were determined from the sample standard deviation for each run. For Runs 10 through 12, the mean bed-surface slope for a run was estimated by the bed-surface slope taken on the second day of the experiment; the mean bed-surface slope for each run is listed in Table 3-4.

The mean of the sample standard deviations of the mean bed-surface slope for Runs 1 through 9 is 1.57×10^{-3}. This value is 169% larger than the estimated error in determining the bed-surface slope, 5.82×10^{-4}. This result suggests that the bed-surface slope varied as a function of time during individual flume runs, but may also indicate that the real error in determining the bed-surface slope was larger than the estimated error.

To examine the trends in the mean bed-surface slope as a function of mean flow velocity, the significance of the difference between the mean bed-surface slopes for successive runs was calculated. At the 0.10 level of significance, the mean bed-surface slope for Run 2 is

significantly more positive than those for Runs 1 and 3; the mean bed-surface slopes for Runs 4 and 5 are significantly more negative than that for Run 3; the mean bed-surface slope for Run 6 is significantly more negative than those for Runs 4 and 5; and the mean bed-surface slopes for Runs 8 and 9 are significantly more negative than those for all of the other runs, 1 through 7. For Runs 1 and 3, the 90% confidence intervals for the means include both positive and negative values. Therefore, the following trends in the mean bed-surface slope as a function of mean flow velocity are significant at the 0.10 level of significance: the mean bed-surface slope becomes positive or more positive with the increase in mean flow velocity from Run 1 (28.6 cm/s) to Run 2 (30.0 cm/s); becomes less positive or negative from Run 2 (30.0 cm/s) to Run 3 (32.1 cm/s); and becomes progressively more negative with the increases in velocity from Run 3 (32.1 cm/s) to Run 4 (34.1 cm/s), from Run 5 (36.1 cm/s) to Run 6 (38.0 cm/s) and from Run 6 (38.0 cm/s) to Run 8 (43.8 cm/s).

Section 3-5

Flow Variables Derived from the Water-Surface or Bed-Surface Slope

When the mean flow is steady and uniform, both the energy slope (i.e., the downstream gradient of total head)

and the boundary shear stress can be determined from the water-surface (or bed-surface) slope. Under these conditions, the energy slope is approximately equal to the water-surface (or bed-surface) slope and the boundary shear stress is approximately equal to $\rho_w gdS$, where ρ_w is the density of the water, g is the acceleration of gravity, d is the mean flow depth, and S is equal to the water-surface (or bed-surface) slope. However, when the mean flow is not steady and uniform, the energy slope and boundary shear stress vary as functions of longitudinal position and are not accurately estimated from the water-surface slope as described above. In flume experiments, the mean flow over an erodible sediment bed is commonly assumed to produce uniform flow; differences in the mean flow depth are assumed to be gradually eliminated by erosion where the mean flow is relatively shallow and rapid, and by deposition where the mean flow is relatively deep and slow.

To examine whether the mean flow in the test section of the flume was uniform, the significance of the difference between the mean water-surface slope and mean bed-surface slope was calculated for each run, 1 through 9. For Runs 2 through 9, the means are significantly different at the 0.01 level of significance. For Runs 2 and 3, the mean water-surface slope is negative, while the mean bed-surface slope is positive; the mean flow depth decreases slightly downstream. However, for Runs 4 through 9, the

mean bed-surface slope is more negative than the mean water-surface slope; the mean flow depth increases slightly downstream. For Run 1, the means are not significantly different at the 0.10 level of significance. Therefore, for Runs 2 through 9, the mean flow in the test section of the flume was not uniform at the 0.01 level of significance. The general trends in the difference between the mean water-surface slope and mean bed-surface slope as a function of mean flow velocity are evident in Figure 3-5; in this figure, the mean water-surface slopes and mean bed-surface slopes are plotted on the same scale for direct comparison.

To determine whether the mean flow in the test section of the flume was tending to approach uniform flow during the flume runs, the difference between the water-surface slope and bed-surface slope was examined as a function of time for each run. The experiments were started with uniform flow over a leveled sediment bed; during the experiments the channel slope was regularly adjusted to equal the water-surface slope to facilitate readjustment of the mean flow to uniform flow. Nonetheless, examination of the water-surface and bed-surface slopes indicates that the flow redistributed the sediment longitudinally in the flume, producing non-uniform flow, and tended to maintain longitudinal differences in mean flow depth. The difference between the water-surface slope and bed-surface

slope fluctuated about nonzero values; the difference did not tend to decrease during the experiments. The apparent lack of a tendency for the mean flow to approach uniform flow during the relatively long running times of the experiments (i.e., 6 to 11 days) suggests that the equilibrium or steady-state flow in the test section of the flume is not uniform. The longitudinal differences in mean flow depth and mean flow velocity may reflect adjustments of the flow toward an equilibrium or steady-state flow in which the mean sediment transport rate for each longitudinal section along the length of the flume is approximately constant.

The nonuniformity of the mean flow in the test section of the flume is probably due to inherent longitudinal variations in the flow conditions resulting from the limited length of the flume. The observed trends both in the initial, longitudinal redistribution of sediment in the flume and in the longitudinal variation in the mean flow depth as function of mean flow velocity might be at least partially explained by the relative importance of the developing boundary layer, possible backwater effects, and longitudinal variations in bed-form size. For the lower velocity runs, the average size of the equilibrium bed forms appeared to be similar throughout the length of the flume; however, for the higher velocity runs, the average size of the bed forms increased downstream, and the maximum

size of the bed forms was larger.

For the lower velocity runs, the mean water-surface slope was negative, while the mean bed-surface slope was positive; the mean flow depth decreased slightly downstream. For these runs, the relatively large boundary shear stress at the beginning of the developing boundary layer and possible backwater effects may have initially resulted in net erosion upstream and deposition downstream, producing positive bed-surface slopes. If the decrease in the mean flow depth downstream for each of these runs represents an approximately equilibrium flow, then the slightly deeper, slower flow upstream may have roughly balanced the effect on the mean sediment transport rate of the relatively large boundary shear stress in the developing boundary layer, thereby approximately equalizing the mean sediment transport rate along the length of the flume.

For the higher velocity runs, the mean bed-surface slope was more negative (i.e., steeper) than the mean water-surface slope; the mean flow depth increased slightly downstream. For these runs, the increase in bed-form size downstream may have had a more important effect on the mean flow than the developing boundary layer. The increase in bed-form size downstream may have resulted in increased turbulence and boundary shear stress downstream and thus in net erosion downstream and deposition upstream, producing

negative bed-surface slopes relative to the channel slope. If the increase in the mean flow depth downstream for each of these runs represents an approximately equilibrium flow, then the slightly deeper, slower flow downstream may have roughly balanced the effect on the mean sediment transport rate of the increased turbulence and boundary shear stress associated with the larger bed forms downstream, thereby approximately equalizing the mean sediment transport rate along the length of the flume.

The mean boundary shear stress for each run was calculated using the mean water-surface slope, the mean water density, and the mean flow depth for the run. The mean boundary shear stress for each run is listed in Table 3-5. Since the flow in the test section was not uniform, these values are only approximations of the mean boundary shear stress.

Section 3-6

Water Temperature

The water temperature for a data set was estimated by the average of the two water temperatures recorded during the data set. For Runs 1 through 9, the mean water temperature for a run was estimated by the average of the water temperatures for all of the data sets of the run, excluding the initial data set. The mean water temperature and sample standard deviation for each run are listed in

Table 3-6. For Runs 10 through 12, the mean water temperature for a run was estimated by the water temperature for the data set taken on the second day of the experiment; the mean water temperature for each run is listed in Table 3-6. The mean of the sample standard deviations for Runs 1 through 9 is 0.45 ^{o}C. This value is larger than the accuracy to which the thermometer could be read, 0.1 ^{o}C, and therefore is predominantly a measure of the variation of the water temperature as a function of time during individual flume runs.

The average of the mean water temperatures for Runs 1 through 9 is 27.45 ^{o}C. To determine a probable upper bound on the difference between the mean water temperature for each run, 1 through 9, and 27.45 ^{o}C, the 90% confidence interval for the mean water temperature for each run was calculated. For Runs 1 through 9, the mean water temperature for each run is within $\pm$1.62 ^{o}C of 27.45 ^{o}C at the 0.10 level of significance.

Section 3-7

Water Density, Viscosity, and Kinematic Viscosity

For Runs 1 through 12, the mean water density, viscosity, and kinematic viscosity for a run were determined from the mean water temperature for the run, using the data given by Weast (1974); the results are presented in Table 3-7. The averages of the mean water

density, viscosity, and kinematic viscosity for Runs 1 through 9 are also presented in Table 3-7. For each of these variables, the 90% confidence intervals for the mean water temperatures for Runs 1 through 9 were used to determine a probable upper bound on how much the mean for each run, 1 through 9, differed from the average of the means for Runs 1 through 9. The average of the mean water densities for Runs 1 through 9 is 0.9964 g/cm^3; the mean water density for each run, 1 through 9, is within $\pm$0.0005 g/cm^3 or 0.05% of the average value at the 0.10 level of significance. The average of the mean viscosities for Runs 1 through 9 is 0.008432 g/s cm; the mean viscosity for each run, 1 through 9, is within $\pm$0.000296 g/s cm or 3.5% of the average value at the 0.10 level of significance. The average of the mean kinematic viscosities for Runs 1 through 9 is 0.008462 cm^2/s; the mean kinematic viscosity for each run, 1 through 9, is within $\pm$0.000293 cm^2/s or 3.5% of the average value at the 0.10 level of significance.

Section 3-8

Reynolds Number and Froude Number

For Runs 1 through 12, the Reynolds number and Froude number for a run were calculated using the mean flow variables for the run; the results are presented in Table 3-8.

Section 3-9

Sediment Discharge

For Runs 1 through 9, the mean sediment discharge for a run, per unit width of the flume, was calculated using the dry weight of the sediment sample taken during the sediment-discharge measurement and the time period of the measurement; the results are listed in Table 3-9. The sediment discharges per unit width are plotted as a function of mean flow velocity in Figure 3-6. The errors associated with the sediment-discharge measurements were not examined quantitatively. Qualitatively, these measurements were assumed to provide rough estimates of the mean sediment discharge. For relatively large bed forms in a closed system, the sediment discharge for experimentally feasible measurement periods tends to vary substantially (Costello, 1974). Even for long measurement times, large sediment samples, and a bed configuration of ripples, Rathbun and Guy (1967) reported up to 100% variability in bed-load measurements.

On the average, the mean sediment discharge increased with mean flow velocity. For Runs 6 and 9, relatively low areas of the sediment bed were approaching the tailbox when the sediment trap was inserted. Consequently, for these runs, the measured sediment discharges may be lower than the actual mean sediment discharges. For the higher velocity runs, 7 through 9, not all of the sediment

entering the tailbox was caught by the sediment trap; some sediment was observed to be swept over the trap by the flow. Therefore, for these runs, the measured sediment discharges are probably also lower than the actual mean sediment discharges.

CHAPTER 4

OBSERVATIONS ON THE DEVELOPMENT OF BED FORMS

Section 4-1

Introduction

This chapter consists of descriptions of observations of the sediment bed during the initial data set of each flume experiment. These descriptions include observations of the sediment movement, the initial development of bed forms from a planar bed, and the evolution of the bed configuration toward equilibrium.

The observations of the bed forms were critical to the development of the qualitative model for the bed forms presented in Chapter 7. In addition, the observations resulted in the examination of some new quantitative measures of the bed-form geometry.

The initial development of bed forms from a planar bed provides important insights into the general process of bed-form development and stability. The development of bed forms from a planar bed is the least complex setting for observing fundamental similarities and differences between the different kinds of bed forms. Contrary to expectations, the process of the initial development of bed forms appeared to be basically the same over the entire range of flow conditions of these experiments. In particular, both the size and appearance of the very first

bed forms that developed from a planar bed were strikingly similar for all of the experiments, despite the large differences in the maximum size of the bed forms that developed later in the experiments. For all of the experiments, the initial bed forms were small and relatively two-dimensional; with time, the average size of the bed forms initially increased and the bed forms became more three-dimensional. However, as the mean flow velocity increased, the maximum size of the bed forms also increased. As a result the appearance and average size of the fully developed or equilibrium bed forms for the different flow velocities depended on the flow velocity.

The differences in the evolution of the bed configurations from a planar bed to fully developed bed forms for the different flow velocities, appeared to result from differences in the relative rates at which bed forms developed, propagated, and increased in size in addition to differences in the maximum size the bed forms could attain. However, the basic process of bed form development appeared to be the same over the entire range of flow conditions.

An important phenomenon observed for all of the experiments is the strong dependence of the local sediment transport rates, bed-form growth rates, and bed-form size on the bed configuration immediately upstream. This dependence was most evident while bed forms were first developing and increasing in size. Examples of this

phenomenon occur throughout the descriptions. For a given flow velocity, as the average size of the bed forms increased, the local sediment transport rates on the stoss sides of the bed forms also appeared to increase. For example the increase in the average size of the bed forms during the first five minutes of Run 12 was sufficient to result in an noticeable increase in the local sediment transport rates.

Another important phenomenon observed for all the experiments is the overtaking phenomenon. Slipfaces migrated at different rates and consequently began overtaking the adjacent slipface downstream or being overtaken almost immediately after they developed. In addition, both the size and shape of individual bed forms continually changed.

The observations are presented as a function of flow velocity: the initial development of the bed forms from a planar bed and the evolution of the bed configuration toward equilibrium are described for each run. Descriptive observations are presented separately for each run so that the data can be more easily interpreted independently by other researchers. No judgements about the type of bed form are included in the observations; however, the stability field as previously delineated by other authors is noted.

The observations in this chapter are very detailed.

The interpretation and analysis of the most important observations are presented in Chapter 7. However, all of the observations are consistent with the model proposed in Chapter 7.

Because of the similarity in the development of the bed forms over the entire range of flow conditions, the descriptions are somewhat repetitive. However, whereever possible only differences from the previously described runs, such as changes in the relative rates of processes, are described in detail. Parallel organization is used for all of the runs to facilitate locating data.

As the flow velocity was increased, the changes in the relative rates of processes were smooth and gradational. Therefore, it is possible to get an overview of the development of bed forms for the range of flow velocities by reading the descriptions selectively. More extensive photography was taken during the later runs. Therefore, some more unusual sequences of photographs are included with the descriptions of these runs.

In addition, Runs 10, 11, and 12 are supplementary runs carried out to observe and compare directly within a relatively short time period bed forms in the three different stability fields observed in Runs 1 through 9: ripples, two-dimensional dunes, and three-dimensional dunes. Therefore, the descriptions of these runs also provide an overview of the experiments. The development of

bed forms directly from the planar bed was particularly well documented for these runs. In addition, the effects of the water-surface plate in these runs provide some interesting examples of the dependence of the local sediment transport rates, rate of the development of bed forms, bed-form growth rates, and bed-form size on the bed configuration immediately upstream.

The location of the more complete descriptions of some of the observations and the location of some of the more unusual photography are listed below:

1) Run 1 - the propagation of bed forms downstream from the exposed false bottom and the nature of the sediment movement on the planar bed,

2) Run 2 - the propagation of highly three-dimensional bed forms,

3) Run 6 - the development of slipfaces directly from features of the planar-bed micro-topography,

4) Run 9 - a sequence of photographs illustrating typical changes in the appearance of the bed configuration as the average size of the bed forms increased at the beginning of a run,

5) Run 9 - a sequence of photographs showing the longitudinal variation in the average size and appearance of the bed forms before the false bottom was covered with sediment and while the average size of the bed forms was still increasing from upstream,

6) Run 9 - a particularly good example of the dependence of both the growth rate and the size of the bed forms on the bed configuration upstream,

7) Run 10 - sediment movement on the planar bed and the development of bed forms directly from the planar bed,

8) Run 10 - the decay of newly developed bed forms from upstream,

9) Run 11 - the development of bed forms directly from the hummocky planar-bed micro-topography,

10) Run 11 - a sequence of photographs illustrating the dependence of the local growth rate and size of bed forms on the bed configuration immediately upstream,

11) Run 12 - a sequence of photographs showing the rapid initial development of bed forms directly from the planar bed,

12) Run 12 - the overtaking phenomenon and a sequence of photographs illustrating overtaking with small, newly developed bed forms.

Section 4-2

Run 1

In Run 1 the mean flow velocity was gradually increased from approximately 22 cm/s to 28 cm/s during the first 40 minutes of the run. The mean flow conditions during this run were in the ripple stability field as

delineated by Costello (1974) and Costello and Southard (1981).

The first bed forms to develop propagated from the false bottom. Sediment movement on the leveled bed exposed the downstream edge of the false bottom, forming a small negative step. After the downstream edge of the the false bottom was exposed, increased erosion occurred a short distance downstream on the sediment bed; sediment was eroded in intermittent bursts of sediment movement that rapidly propagated a short distance downstream and then subsided. (The phrase "burst of sediment movement" is used to describe a sudden spurt of noticeably more intense sediment movement. The term burst in this context is used as a descriptive term and is not referring to fluid "bursts" of the burst-sweep cycle.) The deposited sediment gradually developed into a relatively straight-crested, two-dimensional bed form across the width of the flume. As this bed form developed, increased erosion similarly occurred a short distance downstream from its slipface; the subsequent deposition of the eroded sediment resulted in the development of another relatively straight-crested, two-dimensional bed form downstream from the original bed form. This process of bed-form propagation was repeated downstream. Values of the rate of propagation of the bed-form front, measured along the centerline of the flume after the mean flow velocity had been adjusted to 28 cm/s,

varied from 9 cm/hr to 24 cm/hr. Figure 4-1 is a close-up plan view (centered at about 470 cm) of the propagating bed-form front about 13 hours after start-up, i.e., starting to adjust the flow velocity upward (the ruler in this figure is approximately 15 cm long). This figure shows a new bed form developing downstream from the front and also shows the beginnings of an even newer disturbance on the planar bed immediately downstream from this newly developing bed form.

As the bed-form front propagated downstream, it became slightly convex downstream, because it propagated slightly faster in the center of the flume than near the sidewalls. The first few bed forms immediately upstream from the bed-form front (i.e., the most recently developed bed forms) were small and relatively straight-crested and two-dimensional. Upstream from these bed forms, the crests were more sinuous and the bed forms were more three-dimensional; three-dimensional scour pits occurred locally at various locations downstream from slipfaces. At a given longitudinal position in the flume, the bed forms initially became more three-dimensional with time. Figure 4-2 is an oblique view of the propagating bed-form front about 13 hours after start-up (the channel is about 91 cm wide). This figure shows the shape of the bed-form front and the more three-dimensional bed forms upstream from the front.

On average, the bed forms increased in both height and

spacing upstream from the propagating bed-form front. At a given longitudinal position, the average size of the bed forms initially increased with time. Before sediment covered the false bottom, the average size of the bed forms at the extreme upstream end of the flume, immediately downstream from the false bottom, became larger than the average size of the equilibrium bed forms that developed later in the test section of the flume.

The centerline bed profile of the bed forms propagating from the false bottom shows clearly that the bed forms were not migrating in a single plane; the low points at the base of adjacent slipfaces are not in a single plane. Slipfaces appear to be migrating at different rates, and the size and shape of the longitudinal profiles of individual bed forms are not uniform. Some slipfaces appear to be migrating up the stoss side of the adjacent bed form downstream and overtaking the slipface downstream. The centerline bed profile indicates that slipfaces began overtaking very shortly after they developed: the first four slipfaces upstream from the propagating front appear to be migrating in approximately a single plane; however, the fifth slipface upstream from the front is being overtaken.

The side-view, time-lapse movie photography of newly developed bed forms illustrates unambiguously that slipfaces were migrating at different rates and began

overtaking adjacent slipfaces downstream very shortly after they developed. The time-lapse movie photography also shows that both the size and shape of individual bed forms were continually changing.

Downstream from the propagating bed-form front the sediment bed initially remained a planar bed. At a given location on the planar bed, sediment movement was not continuous but occurred in intermittent, apparently random bursts of motion. A number of grains moved in each burst; grains moved downstream, parallel or at acute angles to the mean flow direction. The bursts of sediment movement propagated rapidly a short distance downstream and then subsided. As the bursts propagated downstream, they tended to spread laterally somewhat, resulting in narrow, fan-shaped streaks of grain motion, roughly parallel to the mean flow direction. The subparallel, fan-shaped bursts of sediment movement produced a characteristic, slightly streaky or hummocky, planar-bed micro-topography a few grain diameters in relief. This textured micro-topography consisted of low, short ridges or elongated mounds that were commonly lenticular in plan and shallow, narrow depressions. These micro-features were oriented with their long axes roughly parallel to the mean flow direction, at small angles to one another. The nature of the sediment movement on the planar bed and the resulting streaky or hummocky planar-bed micro-topography were similar to those

described by Williams and Kemp (1971).

By the time the bed-form front had propagated almost three meters downstream from the false bottom (about 13 hours after start-up), bed forms had also developed immediately downstream from a seam in the lefthand (facing downstream) sidewall about halfway down the flume. Initially these bed forms were relatively two-dimensional and propagated downstream in a narrow patch along the sidewall. Later, however, highly three-dimensional bed forms developed from the side of this patch of bed forms and propagated relatively rapidly, diagonally downstream across the flume, at about a 20^{o} angle to the mean flow direction.

The bed forms propagating from the false bottom and from the sidewall seam eventually covered the entire sediment bed. No bed forms developed directly from the hummocky, planar-bed micro-topography, away from the false bottom or sidewalls. At a given longitudinal position in the test section of the flume, the average size of the bed forms increased until the equilibrium value for that position was reached.

Section 4-3

Run 2

In Run 2 the mean flow velocity was gradually increased from approximately 26 cm/s to 30 cm/s during the

first 30 minutes of the run. The mean flow conditions during this run were in the ripple stability field as delineated by Costello (1974) and Costello and Southard (1981).

The first bed forms to develop propagated from the false bottom in basically the same manner as bed forms propagated from the false bottom in Run 1, but at a somewhat greater rate; the one value of the propagation rate, measured after the mean flow velocity had been adjusted to 30 cm/s, was 39 cm/hr. In general, the shape of the propagating bed-form front and the bed forms appeared similar to those in Run 1. As the bed-form front propagated downstream, it became slightly convex downstream. The first few bed forms immediately upstream from the front were small and relatively straight-crested and two-dimensional. The bed forms upstream were more three-dimensional with sinuous crests and three-dimensional scour pits at various locations. In general, at a given longitudinal position, the bed forms initially became more three-dimensional with time; however, as long as the false bottom was exposed, the bed forms immediately downstream from the false bottom remained relatively two-dimensional.

As in Run 1, the average size of the bed forms increased upstream from the propagating bed-form front, and, at a given longitudinal position, the average size of the bed forms initially increased with time. In addition,

before sediment covered the false bottom, the average size of the bed forms immediately downstream from the false bottom became larger than the average size of the equilibrium bed forms that developed later in the test section.

As in Run 1, the centerline profile of the bed forms propagating from the false bottom shows that the slipfaces were not migrating in a single plane but began overtaking almost immediately after they developed. The first few slipfaces immediately upstream from the propagating bed-form front appear to be migrating in approximately a single plane; however, the eighth slipface upstream from the front is being overtaken.

The side-view, time-lapse movie photography of newly developed bed forms also illustrates that the slipfaces were migrating at different rates and began overtaking adjacent slipfaces downstream or being overtaken almost immediately after they developed. As in Run 1, the time-lapse movie photography also shows that both the size and shape of individual bed forms were continually changing.

The sediment bed downstream from the propagating bed-form front initially remained a planar bed. Sediment movement on the planar bed was very similar to that in Run 1 and likewise resulted in a slightly streaky or hummockly planar-bed micro-topography.

When the bed-form front had propagated less than

halfway down the flume, bed forms developed downstream from seams in the sidewalls on both sides of the flume about halfway down the flume. Initially the bed forms on both sides were relatively two-dimensional and propagated downstream in narrow patches along the sidewalls. Later, however, as in Run 1, highly three-dimensional bed forms developed from the side of the patch of bed forms on the left-hand (facing downstream) side of the flume. These three-dimensional bed forms propagated relatively rapidly in a narrow spur diagonally downstream across the flume, at about a 20^{o} angle to the mean flow direction. As these bed forms propagated diagonally downstream toward the right-hand sidewall, two more spurs of three-dimensional bed forms developed from the lefthand side of this original spur of three-dimensional bed forms and propagated diagonally downstream toward the lefthand sidewall. Figure 4-3 is an oblique view (downstream from about 640 cm) of the resulting bed configuration about nine hours and 15 minutes after start-up.

The newly formed three-dimensional bed forms that propagated diagonally across the planar bed had a characteristic geometry. The crests of the slipfaces were short, concave downstream, and oriented at about a 45^{o} angle to the mean flow direction. The downstream angle between the crests and the direction of propagation was about 65^{o}. The diagonal propagation of these bed forms

resulted in the bed forms being arranged "en echelon" diagonally downstream in the direction of propagation. While the bed forms were propagating, there were very active three-dimensional scour pits downstream from their slipfaces: the sediment movement in the scour pits was markedly greater and more continuous than at other locations on the sediment bed.

The apparent mode of propagation of the three-dimensional bed forms was somewhat different from that described for relatively two-dimensional bed forms propagating downstream from the false bottom. Figure 4-4 is a schematic of the approximate geometric relationships that characterized the propagation of these three-dimensional bed forms. The three-dimensional bed forms appeared to propagate from the side of an existing bed form which did not extend across the full width of the flume and whose slipface curved obliquely upstream along the side of the bed form, at about a 45^{o} angle to the mean flow direction. The flow appeared to curl around the upstream end of the slipface on the side of this bed form and then to spiral diagonally downstream along this slipface, resulting in a relatively strong local separation vortex oriented at about a 45^{o} angle to the mean flow direction. Sediment in the trough along the side of this bed form was transported fairly continuously back up the slipface by the separation vortex and deposited on the slipface, forming a

ridge part way up the slipface. This ridge extended downstream beyond the slipface onto the planar bed.

Immediately downstream from the separation vortex, sediment was actively eroded in continual sweeping bursts of sediment movement that rapidly propagated a short distance diagonally downstream in the direction of propagation of the three-dimensional bed forms (at about a 65^{o} angle to the side of the original bed form and at about a 20^{o} angle to the mean flow direction) and then subsided. The deposited sediment developed into a new three-dimensional bed form. The crest of the new bed form was roughly parallel to the side of the original bed form, oriented at about a 45^{o} angle to the mean flow direction and was laterally offset from the side of the original bed form. As the new bed form developed, the downstream extension of the ridge on the original upstream slipface became a longitudinal ridge on the stoss side of the new bed form.

As the new three-dimensional bed form increased in height, the flow spiraled diagonally downstream along its slipface, resulting in another strong local separation vortex oriented at about a 45^{o} angle to the mean flow direction. The consequent scour and deposition resulted in the development of another three-dimensional bed form diagonally downstream from this bed form. Once a characteristic three-dimensional bed form developed from

the side of an existing bed form on the planar bed, the above mode of bed-form propagation was usually repeated downstream until the three-dimensional bed forms reached a sidewall.

One of the most striking differences between the propagation of highly three-dimensional bed forms and the propagation of relatively two-dimensional bed forms was that the local sediment transport rates associated with the propagation of three-dimensional bed forms were markedly greater than those associated with the propagation of two-dimensional bed forms for the same mean flow conditions. The greater transport rates associated with the propagation of three-dimensional bed forms appeared to be due to the strong local separation vortices oriented at about a 45^{o} angle to the mean flow direction. As a result of this difference in the local sediment transport rates, newly formed three-dimensional bed forms increased in size much more rapidly than newly formed two-dimensional bed forms. Also, the rate of propagation of three-dimensional bed forms was much greater than that of two-dimensional bed forms.

With time, the characteristic three-dimensional bed forms became relatively two-dimensional: the crests became oriented more nearly perpendicular to the mean flow direction; the active, diagonal vortices associated with the propagation of three-dimensional bed forms subsided;

and the longitudinal ridges gradually blended into the stoss sides of the bed forms.

As in Run 1, the bed forms propagating from the false bottom and from the sidewall seams eventually covered the entire sediment bed. No bed forms developed directly from the hummocky planar-bed micro-topography. At a given longitudinal position in the test section of the flume, the average size of the bed forms increased until the equilibrium value for that position was reached.

Section 4-4

Run 3

In Run 3 the mean flow velocity was gradually increased from approximately 30 cm/s to 32 cm/s during the first 15 minutes of the run. The mean flow conditions during this run were in the ripple stability field as delineated by Costello (1974) and Costello and Southard (1981).

The first bed forms to develop propagated from the false bottom in basically the same manner as bed forms propagated from the false bottom in Runs 1 and 2, but at a faster rate. The values of the propagation rate, measured after the mean flow velocity had been adjusted to 32 cm/s, were 53 cm/hr and 60 cm/hr. In general, the shape of the propagating bed-form front and the bed forms appeared similar to those in Runs 1 and 2. The bed-form front was

slightly convex downstream. The first few bed forms immediately upstream from the front were small and relatively straight-crested and two-dimensional. Upstream, the bed forms were more three-dimensional, with sinuous crests and local three-dimensional scour pits. At a given longitudinal position, the bed forms initially became more three-dimensional with time.

As in Runs 1 and 2, the average size of the bed forms increased upstream from the propagating bed-form front and at a given longitudinal position the average size of the bed forms initially increased with time. Before sediment covered the false bottom, the average spacing of the bed forms immediately downstream from the false bottom became larger than the average spacing of the equilibrium bed forms that developed later in the test section. Figure 4-5 is a plan view (centered at 460 cm) of the propagating bed-form front about five hours and ten minutes after start-up; this figure shows the relatively small, straight-crested, two-dimensional bed forms near the bed-form front and the larger, more three-dimensional bed forms upstream.

As in the lower velocity runs, the centerline bed profile of the bed forms propagating from the false bottom shows that the slipfaces were not migrating in a single plane but began overtaking almost immediately after they developed. Only the first few slipfaces immediately upstream from the propagating bed-form front appear to be

migrating in approximately a single plane; the fourth slipface upstream is being overtaken.

The side-view, time-lapse movie photography of newly developed bed forms also illustrates that slipfaces were migrating at different rates and began overtaking adjacent slipfaces downstream or being overtaken almost immediately after they developed. In addition, the side-view, time-lapse movie photography shows that both the size and shape of individual bed forms were continually changing.

The sediment bed downstream from the propagating bed-form front initially remained a planar bed. Sediment movement on the planar bed was similar to that in Runs 1 and 2; however, the bursts of sediment movement appeared to be more frequent, and on the average more grains appeared to move in each burst. A similar streaky or hummocky, planar-bed micro-topography resulted; however, the longitudinal mounds and depressions on the planar bed appeared more pronounced than in the lower velocity runs. Figure 4-6 is a plan view (centered at 920 cm) of the hummocky planar-bed micro-topography about 5 hours and 20 minutes after start-up.

By the time the bed-form front had propagated almost three meters downstream from the false bottom (almost four hours after start-up), bed forms had also developed downstream from seams in the sidewalls on both sides of the flume about halfway down the flume. Initially these bed

forms were relatively two-dimensional and propagated downstream in narrow patches along the sidewalls. However, about an hour later, highly three-dimensional bed forms developed from the side of the patch of bed forms on the left-hand (facing downstream) side of the flume. These three-dimensional bed forms propagated rapidly in a narrow spur diagonally downstream across the flume at about a 20^{o} angle to the mean flow direction. The geometry and apparent mode of propagation of these three-dimensional bed forms were basically the same as those of the three-dimensional bed forms that propagated diagonally across the planar bed in Runs 1 and 2. Figure 4-7 is a close-up plan view (centered at about 750 cm) of newly developed three-dimensional bed forms propagating diagonally downstream, about 5 hours and 30 minutes after start-up (the field of view is approximately 64 cm long). Figure 4-7 shows the characteristic geometry of these three-dimensional bed forms and also shows a newly developing scour pit and the beginnings of the associated longitudinal ridge, extending from the upstream slipface downstream onto the planar bed.

As in Runs 1 and 2, the bed forms propagating from the false bottom and from the sidewall seams eventually covered the entire sediment bed. No bed forms developed directly from the hummocky planar-bed micro-topography. At a given longitudinal position in the test section of the flume, the

average size of the bed forms increased until the equilibrium value for that position was reached.

Section 4-5

Run 4

In Run 4 the mean flow velocity was gradually increased from approximately 32 cm/s to 33 cm/s during the first 15 minutes of the run. About 2 hours and 15 minutes later, the mean flow depth was adjusted to 15 cm, increasing the mean flow velocity to approximately 34 cm/s. After the first few minutes of this run, the mean flow conditions were near the boundary between the ripple and the two-dimensional dune stability fields as delineated by Costello (1974) and Costello and Southard (1981). After the depth was adjusted to 15 cm, the mean flow conditions were at the low-velocity end of the two-dimensional dune stability field.

The first bed forms to develop propagated from the false bottom in basically the same manner as bed forms propagated from the false bottom in the lower velocity runs, but at a faster rate. Values of the propagation rate, measured after the mean flow velocity had been adjusted to 34 cm/s, varied from 74 cm/hr to 87 cm/hr. In general, the propagating bed-form front and the bed forms appeared similar to those in the lower velocity runs. The first few bed forms immediately upstream from the front

were small and relatively two-dimensional; the bed forms upstream were more three-dimensional. In general, at a given longitudinal position, the bed forms initially became more three-dimensional with time; however, as long as the false bottom was exposed, the bed forms immediately downstream from the false bottom remained relatively two-dimensional.

As in the lower velocity runs, the average size of the bed forms increased upstream from the propagating bed-form front, and, at a given longitudinal position, the average size of the bed forms initially increased with time. While the false bottom was exposed, the average size of the bed forms immediately downstream from the false bottom increased more rapidly in the center of the flume than near the sidewalls. By the time the bed-form front had propagated about four meters downstream from the false bottom, the bed forms in about the first three meters downstream from the false bottom were larger in the center of the flume than near the sidewalls. Downstream from the false bottom, the relatively larger bed forms extended across a decreasing percentage of the width of the flume, forming a "tongue" of relatively larger bed forms down the center of the flume. Downstream from the "tongue" of relatively larger bed forms, the bed forms were approximately the same size across the full width of the flume. Before sediment covered the false bottom, the

average spacing of the bed forms immediately downstream from the false bottom became larger in the center of the flume than the average spacing of the equilibrium bed forms that developed later in the test section.

As in the lower velocity runs, the centerline bed profile of the bed forms propagating from the false bottom shows that the slipfaces were not migrating in a single plane but began overtaking almost immediately after they developed. Only the first few slipfaces immediately upstream from the propagating bed-form front appear to be migrating in approximately a single plane; the fourth slipface upstream from the front is being overtaken.

The side-view, time-lapse movie photography of newly developed bed forms also illustrates that the slipfaces were migrating at different rates and began overtaking or being overtaken almost immediately after they developed. In addition, both the size and shape of individual bed forms were continually changing.

The sediment bed downstream from the propagating bed-form front initially remained a planar bed. Sediment movement on the planar bed was similar to that in Run 3 and likewise resulted in a markedly hummocky planar-bed micro-topography. The sides of diagonally offset, lenticular mounds which were closely spaced or had coalesced formed diagonal and zigzag lineations and diamond-shaped patterns on the planar bed.

By the time the bed-form front had propagated about 3.3 meters downstream from the false bottom (about three hours and ten minutes after start-up), a three-dimensional bed form had developed from the left-hand (facing downstream) side of the bed-form front not far from the left-hand sidewall. Three-dimensional bed forms propagated rapidly diagonally downstream from this bed form to the left-hand sidewall in basically the same manner as three-dimensional bed forms propagated diagonally across the planar bed in the lower velocity runs. However, within 35 minutes, these three-dimensional bed forms had become relatively straight-crested and two-dimensional and were propagating downstream in a narrow patch along the left-hand sidewall in basically the same manner described for relatively two-dimensional bed forms propagating downstream from the false bottom.

By the time the bed-form front had propagated about 3.3 meters downstream from the false botton, bed forms had also developed along the right-hand sidewall at about 980 cm. These bed forms were relatively two-dimensional and propagated downstream in a narrow patch along the sidewall to the tailbox. Later, when the bed-form front had propagated about another meter downstream (about 4 hours and 30 minutes after start-up), bed forms also developed downstream from a seam in the right-hand sidewall at about 800 cm. These bed forms also were relatively two-

dimensional and propagated downstream along the sidewall. No spurs of highly three-dimensional bed forms developed from either patch of two-dimensional bed forms.

The bed forms propagating from the false bottom and from the sidewall eventually covered the entire sediment bed. No bed forms developed directly from the hummocky planar-bed micro-topography. At a given longitudinal position in the test section of the flume, the average size of the bed forms increased until the equilibrium value for that position was reached.

Section 4-6

Run 5

In Run 5 the mean flow velocity was gradually increased from approximately 33 cm/s to 34 cm/s during the first 20 minutes of the run. About an hour later, the mean flow depth was roughly adjusted, increasing the mean flow velocity to approxiately 35 cm/s. The mean flow conditions during this run were in the two-dimensional dune stability field as delineated by Costello (1974) and Costello and Southard (1981).

The first bed forms to develop propagated from the false bottom in basically the same manner as bed forms propagated from the false bottom in the lower velocity runs, but at a faster rate. The two values of the propagation rate, measured after the mean flow velocity had

been adjusted to 35 cm/s, were 124 cm/hr and 129 cm/hr. However, the shape of the propagating bed-form front was somewhat different from that in the lower velocity runs: bed forms propagated downstream much more rapidly in the center of the flume than near the sidewalls, resulting in a pointed train of bed forms propagating down the center of the flume with planar bed on either side at the downstream end. In general, the bed forms appeared similar to those in the lower velocity runs. The most recently developed bed forms near the bed-form front were small and relatively straight-crested and two-dimensional, and the bed forms upstream were more three-dimensional. At a given longitudinal position, the bed forms initially became more three-dimensional with time.

As in the lower velocity runs, the average size of the bed forms increased upstream from the propagating bed-form front, and at a given longitudinal position the average size of the bed forms initially increased with time. As in Run 4, while the false bottom was exposed, the average size of the bed forms immediately downstream from the false bottom increased more rapidly in the center of the flume than near the sidewalls, likewise resulting in a "tongue" of relatively larger bed forms down the center of the flume. Before sediment covered the false bottom, the average spacing of the bed forms immediately downstream from the false bottom became larger in the center of the

flume than the average spacing of the equilibrium bed forms that developed later in the test section; the spacing of the first bed form immediately downstream from the false bottom became paricularly large. As the spacing of this bed form increased, relatively small, short-crested bed forms developed on the stoss side and the crest of this bed form became irregular and discontinuous.

As in the lower velocity runs, the side-view, time-lapse movie photography of newly developed bed forms illustrates that the slipfaces were migrating at different rates and began overtaking or being overtaken almost immediately after they developed. In addition, both the size and shape of individual bed forms were continually changing.

By the time the bed forms in the center of the flume had propagated about 3.3 meters downstream from the false bottom, three-dimensional bed forms had developed from the righthand (facing downstream) side of the bed-form front and propagated diagonally downstream to the right-hand sidewall, in basically the same manner as three-dimensional bed forms propagated across the planar bed in the lower velocity runs. Figure 4-8 is a plan view (centered at 460 cm) of the propagating bed-form front one hour and 48 minutes after start-up. This figure shows the spur of three-dimensional bed forms after these bed forms had propagated to the right-hand sidewall and also shows the

pointed shape of the front of relatively two-dimensional bed forms propagating down the center of the flume. Later, when the bed forms in the center of the flume had propagated almost five meters downstream from the false bottom (about three hours after start-up), three-dimensional bed forms also developed from the left-hand side of the bed-form front and likewise propagated diagonally downstream to the left-hand sidewall. The development of three-dimensional bed forms from both sides of the propagating bed-form front resulted in the bed-form front becoming less pointed as the front propagated downstream.

The sediment bed downstream from the propagating bed-form front initially remained a planar bed. Sediment movement on the planar bed was similar to that in the lower velocity runs, but stronger; the bursts of sediment movement occurred in long, subparallel streaks of movement that were laterally spaced a few centimeters apart. The resulting hummocky planar-bed micro-topography was similar to that in Run 4. The sides of hummocks formed distinct, diagonal and zigzag lineations and diamond-shaped patterns on the planar bed.

The bed forms propagating from the false bottom eventually covered the entire sediment bed. No bed forms developed from the sidewalls or directly from the hummocky planar-bed micro-topography. At a given longitudinal

position in the test section of the flume, the average size of the bed forms increased until the equilibrium value for that position was reached.

Section 4-7

Run 6

In Run 6 the mean flow velocity was gradually increased from approximately 33 cm/s to 35 cm/s during the first 20 minutes of the run. About an hour later, the mean flow depth was roughly adjusted, increasing the mean flow velocity to approximately 37 cm/s. After the first few minutes of this run, the mean flow conditions were in the two-dimensional dune stability field as delineated by Costello (1974) and Costello and Southard (1981).

The first bed forms to develop propagated from the false bottom in basically the same manner as bed forms propagated from the false bottom in the lower velocity runs, but at a faster rate; the one value of the propagation rate, measured after the mean flow velocity had been adjusted to 37 cm/s, was 308 cm/hr. As in Run 5, bed forms propagated downstream much more rapidly in the center of the flume than near the sidewalls, likewise resulting in a pointed train of bed forms propagating down the center of the flume with planar bed on either side at the downstream end. However, the difference in the rate of propagation of

the bed forms in the center of the flume and that of the bed forms near the sidewalls was greater than in Run 5; consequently, the train of bed forms became more pointed (longer and narrower) than that in Run 5. Figure 4-9 is a plan view (centered at 450 cm) of the propagating bed-form front one hour and ten minutes after start-up. The bed-form front became increasingly pointed as the bed forms propagated farther downstream. In general, the bed forms appeared similar to those in the lower velocity runs. The most recently developed bed forms in the downstream section of the train were small and relatively straight-crested and two-dimensional; the bed forms upstream were more three-dimensional. At a given longitudinal position, the bed forms initially became more three-dimensional with time.

As in the lower velocity runs, the average size of the bed forms increased upstream from the propagating bed-form front, and, at a given longitudianl position, the average size of the bed forms initially increased with time. However, the increase in velocity from Run 5 to Run 6 resulted in a larger increase in the rate of propagation of the bed forms than in the rate of growth of the bed forms. Consequently, in Run 6, when the bed-form front had propagated a given distance downstream from the false bottom, the difference in size between the bed forms near the bed-form front and the bed forms upstream near the false bottom was not as great as that in Run 5: the newly

developed bed forms near the bed-form front were approximately the same size as those in Run 5; however, the bed forms upstream near the false bottom were not as large as those in Run 5. As in Runs 4 and 5, while the false bottom was exposed, the average size of the bed forms immediately downstream from the false bottom increased more rapidly in the center of the flume than near the sidewalls; consequently, upstream where bed forms covered the full width of the flume, there was a "tongue" of relatively larger bed forms down the center of the flume with smaller bed forms near the sidewalls.

Before sediment covered the false bottom, the spacing of the first bed form immediately downstream from the false bottom became significantly larger than the average spacing of the equilibrium bed forms that developed later in the test section. As the spacing of this bed form increased, relatively small, short-crested slipfaces developed on the stoss side of the bed form and migrated downstream, overtaking previously formed small slipfaces and the crest of this bed form; as a result, the crest of this bed form became irregular and poorly defined.

As in the lower velocity runs, the side-view, time-lapse movie photography of newly developed bed forms illustrates that the slipfaces were migrating at different rates and began overtaking or being overtaken almost immediately after they developed. In addition, both the

size and shape of individual bed forms were continually changing.

The sediment bed downstream from the propagating bed-form front initially remained a planar bed. Sediment movement on the planar bed was similar to that in Run 5 and resulted in a similar hummocky planar-bed micro-topography with diagonal and zigzag lineations and diamond-shaped patterns. In places the features of the planar-bed micro-topography became more pronounced than in any of the lower velocity runs. By the time the bed forms in the center of the flume had propagated almost 5.4 meters downstream from the false bottom to about 720 cm (about two hours after start-up), a V-shaped lineation (open end facing downstream), located at about 780 cm near the centerline of the flume, had developed into a small, well defined slipface with a V-shaped crest. A second, small bed form with a V-shaped crest propagated downstream from this slipface. Figure 4-10, a plan view (centered at 780 cm) of those two newly developed bed forms, also shows the surrounding hummocky planar-bed micro-topography with some distinct, diagonal and zigzag lineations. Later, the pronounced zigzag lineation downstream from the two small bed forms in Figure 4-10 also developed into a well defined slipface; small bed forms propagated downstream from this slipface. Before bed forms covered the entire sediment bed, a couple of other small slipfaces with V-shaped crests

developed directly from lineations on the planar bed near the centerline of the flume. This run was the first in which features of the hummocky planar-bed micro-topography developed directly into distinct bed forms which then propagated downstream.

Also, by the time the bed forms in the center of the flume had propagated almost 5.4 meters downstream from the false bottom, a three-dimensional bed form had developed from the left-hand side of the pointed bed-form front at about 620 cm. Three-dimensional bed forms propagated diagonally downstream from this bed form toward the left-hand sidewall, in basically the same way the three-dimensional bed forms propagated across the planar bed in the lower velocity runs. As these bed forms propagated diagonally downstream in a spur, a second spur of three-dimensional bed forms also developed from the lefthand side of the bed-form front a short distance downstream from where the first spur of three-dimensional bed forms originated; the bed forms in the second spur propagated diagonally downstream parallel to the original spur. Figure 4-11 is a plan view (centered at 600 cm) of the first spur of three-dimensional bed forms propagating diagonally downstream about two hours and 20 minutes after start-up. This figure also shows the side of the bed form from which the second spur developed (indicated by the arrow); a three-dimensional scour pit is just beginning to

develop downstream from the diagonal slipface along the side of this bed form. Figure 4-12 is an oblique view (downstream from 600 cm) of the two parallel spurs of three-dimensional bed forms about 20 minutes after Figure 4-11 was taken.

The bed forms propagating from the false bottom and the bed forms that developed directly from the hummocky planar-bed micro-topography gradually merged with one another and formed a continuous train of bed forms down the center of the flume from the false bottom to the tailbox with planar bed on either side at the downstream end. This train of bed forms gradually became wider from upstream until the entire sediment bed was covered with bed forms. At a given longitudinal position in the test section of the flume, the average size of the bed forms increased until the equilibrium value for that position was reached.

Section 4-8

Run 7

In Run 7 the mean flow velocity was gradually increased from approximately 35 cm/s to 39 cm/s during the first 25 minutes of the run. The mean flow conditions during this run were in the two-dimensional dune stability field as delineated by Costello (1974) and Costello and Southard (1981).

The first bed forms to develop propagated from the

false bottom in basically the same way bed forms propagated from the false bottom in the lower velocity runs, but much faster; the one value of the propagation rate, measured after the mean flow velocity had been adjusted to 39 cm/s, was 1640 cm/hr. As in Runs 5 and 6, the bed forms propagated downstream much more rapidly near the center of the flume than near the sidewalls, likewise resulting in a train of bed forms down the center of the flume with planar bed on either side at the downstream end. However, the shape of the bed-form front was somewhat different from that in Runs 5 and 6: in Run 7, bed forms initially propagated downstream most rapidly in two narrow, pointed trains on either side of the centerline of the flume instead of in a single, pointed train. These two trains of bed forms merged upstream, forming a double-pointed or forked train of bed forms down the center of the flume. The bed forms in the left-hand fork propagated downstream more rapidly than those in the righthand fork. As the left-hand fork became longer than the right-hand fork, the bed forms in the righthand fork merged laterally with the bed forms in the upstream part of the left-hand fork. By 40 minutes after start-up the right-hand fork had become indistinguishable and there was a single-pointed train of bed forms downstream from the false bottom with the downstream end of the train centered on the left-hand side of the flume (i.e., the former left-hand fork).

In general, the bed forms appeared similar to those in the lower velocity runs. However, the bed forms propagated downstream so rapidly compared to their rate of growth that, when the bed-form front had propagated almost all of the way to the tailbox, the bed forms in more than the downstream half of the flume were still similar in size and appearance to the most recently developed bed forms near the bed-form front. These bed forms were relatively small in height and spacing with relatively long, straight crests: very similar in size and appearance to newly formed, two-dimensional bed forms near the propagating bed-form fronts in all of the lower velocity runs. Figure 4-13 is a plan view (centered at 650 cm) of relatively small, two-dimensional bed forms 48 minutes after start-up. Upstream from these small two-dimensional bed forms, the bed forms became more three-dimensional, and the average size of the bed forms gradually increased.

As in the lower velocity runs, the side-view, time-lapse movie photography of newly developed bed forms shows that slipfaces were migrating at different rates and began overtaking or being overtaken almost immediately after they developed. In addition, both the size and shape of individual bed forms were continually changing.

As in the lower velocity runs, at a given longitudinal position, the average size of the bed forms initially increased with time. As in Runs 4, 5, and 6, while the

false bottom was exposed, the average size of the bed forms immediately downstream from the false bottom increased more rapidly in the center of the flume than near the sidewalls; consequently, upstream, where bed forms covered the full width of the flume, there was a "tongue" of relatively larger bed forms down the center of the flume with smaller bed forms near the sidewalls. However, in Run 7 the "tongue" of relatively larger bed forms did not become as pronounced as in the lower velocity runs; the "tongue" did not become as long and pointed. As in Runs 5 and 6, as the spacing of the first bed form immediately downstream from the false bottom increased, relatively small, short-crested slipfaces developed on the stoss side of this bed form, and the crest of this bed form became irregular and poorly defined.

The sediment bed downstream from the propagating bed-form front initially remained a planar bed. Sediment movement on the planar bed was similar to that in Run 6 and resulted in a similar hummocky planar-bed micro-topography with pronounced diagonal and zigzag lineations and diamond-shaped patterns. The lineations formed by the micro-relief on the planar bed became more pronounced with time. By the time the bed forms on the left-hand side of the flume had propagated about 6.5 meters downstream from the false bottom (about 37 minutes after start-up), a few small individual bed forms with V-shaped crests (open end facing

downstream) had developed directly from features of the planar-bed micro-topography downstream from the bed-form front in basically the same way that bed forms developed directly from the planar-bed micro-topography in Run 6. As the bed-form front continued to propagate downstream, more small slipfaces developed directly from lineations on the planar bed both downstream and to the side of the bed-form front. Most of the bed forms that developed directly from the planar-bed micro-topography initially had diagonal, V-shaped (open end facing downstream), or zigzag crests.

As the bed-form front propagated downstream, it merged with the bed forms that developed directly from the planar bed, and likewise the bed forms that developed directly from the planar bed merged with one another both longitudinally and laterally. By about 50 minutes after start-up, there was a continuous train of bed forms from the false bottom to the tailbox with the downstream end centered on the lefthand side of the flume. As the bed forms merged with one another, the short, diagonal, V-shaped, and zigzag crests became longer, straighter, and oriented more nearly perpendicular to the mean flow direction. As in Run 6, the train of bed forms gradually became wider from upstream until the entire sediment bed was covered with bed forms. While the bed-form front was propagating downstream from the false bottom onto the planar bed, no spurs of highly three-dimensional bed forms

developed either from the bed-form front or from the bed forms that developed directly from the planar bed.

Once the bed forms covered the entire sediment bed, the average size of the bed forms at a given longitudinal position in the test section of the flume continued to increase until the equilibrium value for that position was reached. At a given position in the test section, bed forms initially were relatively small, straight-crested, and two-dimensional. With time, the average size of the bed forms increased, and the bed forms gradually became more three-dimensional. Once the bed forms reached a certain critical size, very small slipfaces (compared to the slipfaces of the larger bed forms) began to develop on the stoss sides of the larger bed forms just upstream from the crests of the larger bed forms. These small slipfaces migrated downstream very rapidly compared to the larger slipfaces, overtaking the larger slipfaces. As the average spacing of the larger bed forms continued to increase, the small slipfaces developed progressively farther upstream from the crests of the larger bed forms, and, consequently, progressively longer trains of small bed forms developed on the stoss sides of the larger bed forms. As the small slipfaces migrated downstream, new small slipfaces continally developed on the stoss sides of the larger bed forms, upstream from the existing, small slipfaces and likewise migrated downstream relatively rapidly, thereby

forming trains of small bed forms on the stoss sides of the larger bed forms.

By the time the false bottom was covered with sediment and the average size of the bed forms at a given longitudinal position had reached the equilibrium value for that position, the longitudinal variation in the average size of the bed forms had become inverted. The average size of the bed forms increased downstream from the flume inlet instead of decreasing downstream from the false bottom.

Section 4-9

Run 8

In Run 8 the mean flow velocity was gradually increased from approximately 39 cm/s to 42 cm/s during the first two hours of the run. The mean flow conditions during this run were in the two-dimensional dune stability field as delineated by Costello (1974) and Costello and Southard (1981).

The first bed forms to develop propagated from the false bottom in basically the same way as in the lower velocity runs, but faster; similarly, the newly developed bed forms were relatively small, straight-crested and two-dimensional. However, very soon after the bed forms began to propagate from the false bottom, the sediment movement on the planar bed downstream resulted in the development of

small bed forms directly from the planar bed. Sediment movement on the planar bed was similar to that in Run 7, but stronger, and rapidly resulted in a similar hummocky planar-bed micro-topography with pronounced diagonal and zigzag lineations and diamond-shaped patterns. The lineations formed by the micro-relief on the planar bed first became pronounced in two parallel, longitudinal strips, which extended the full length of the flume and were centered slightly toward the left-hand side of the flume. Within 10 to 15 minutes after start-up, small slipfaces developed directly from the pronounced lineations at many points throughout the length of the flume and small bed forms were propagating downstream. These bed forms formed two discontinous strips of bed forms extending from the propagating bed-form front to the tailbox. As in Run 7, most of the bed forms that developed directly from the planar-bed micro-topography initially had diagonal, V-shaped (open end facing downstream), or zigzag crests. Figure 4-14, a plan view (centered at 700 cm) of the sediment bed 15 minutes after start-up, shows segments of the two discontinous strips of bed forms that developed directly from the planar-bed micro-topography.

Almost immediately after bed forms began to develop directly from the planar-bed micro-topography, the bed forms propagating from the false bottom began to merge with bed forms that developed directly from the planar bed a

short distance downstream from the bed-form front, and similarly bed forms that developed directly from the planar bed began to merge with one another both longitudinally and laterally. By 23 minutes after start-up, there was a single, continuous train of bed forms from the false bottom to the tailbox, centered slightly toward the left-hand side of the flume with planar bed on either side. As in Run 7, as the bed forms merged with one another, the short, diagonal, V-shaped, and zigzag crests became longer, straighter, and oriented more nearly perpendicular to the mean flow direction. The train of bed forms widened from the upstream end of the flume until the entire sediment bed was covered with bed forms. No spurs of highly three-dimensional bed forms developed on the planar bed.

In general, the bed forms appeared similar to those in the lower velocity runs. However, bed forms developed directly from the planar bed, propagated downstream from the false bottom, and merged with one another so rapidly compared to their rate of growth that, when bed forms first extended continuously throughout the full length of the flume, the bed forms in approximately the downstream two-thirds of the flume were still similar in size and appearance to newly developed bed forms near the propagating bed-form fronts in the lower velocity runs. These bed forms were relatively small in height and spacing with relatively long, straight crests. Figure 4-15 is a

plan view (centered at 650 cm) of relatively small, two-dimensional bed forms 32 minutes after start-up (the downstream two-thirds of this figure shows the same section of the sediment bed as the upstream two-thirds of Figure 4-14, 17 minutes after Figure 4-14 was taken). Upstream from the small two-dimensional bed forms, the bed forms became more three-dimensional, and the average size of the bed forms gradually increased.

As in the lower velocity runs, the side-view, time-lapse movie photography of newly developed bed forms indicates that slipfaces were migrating at different rates and began overtaking or being overtaken almost immediately after they developed. In addition, the size and shape of individual bed forms were continually changing.

As in the lower velocity runs, at a given longitudinal position, the average size of the bed forms initially increased with time. As in Runs 4 through 7, as long as the false bottom was exposed, the average size of the bed forms immediately downstream from the false bottom increased more rapidly in the center of the flume than near the sidewalls. However, the resulting "tongue" of relatively large bed forms did not become as pronounced as that in Run 7. Before sediment covered the false bottom, the spacing of the first bed form immediately downstream from the false bottom became larger than the average spacing of the equilibrium bed forms that develop later in

the test section. As the spacing of this bed form increased, relatively small slipfaces developed on the stoss side of this bed form and migrated downstream, overtaking previously formed small slipfaces and the crest of this bed form; as a result, the crest of this bed form became irregular and poorly defined.

Once bed forms covered the entire sediment bed, the average size of the bed forms at a given longitudinal position in the test section of the flume continued to increase until the equilibrium value for that position was reached. The bed forms initially were relatively small, straight-crested and two-dimensional. With time, the average size of the bed forms increased, and the bed forms gradually became more three-dimensional. As in Run 7, once the bed forms reached a certain critical size, relatively small slipfaces began to develop on the stoss sides of the larger bed forms just upstream from the crests of the larger bed forms. As the average spacing of the larger bed forms continued to increase, the small slipfaces developed progressively farther upstream from the crests of the larger bed forms, and, consequently, progressively longer trains of small bed forms developed on the stoss sides of the larger bed forms in the same manner as in Run 7.

As in Run 7, by the time the false bottom was covered with sediment and the average size of the bed forms at a given longitudinal position had reached the equilibrium

value for that position, the longitudinal variation in the average size of the bed forms had become inverted. The average size of the bed forms increased downstream from the flume inlet instead of decreasing downstream from the false bottom.

Section 4-10

Run 9

In Run 9 the mean flow velocity was increased to 47.6 cm/s during the first three minutes of the run. The mean flow conditions during this run were in the three-dimensional dune stability field as delineated by Costello (1974) and Costello and Southard (1981).

The initial development of bed forms throughout the full length of the flume occurred much more rapidly in Run 9 than in any of the lower velocity runs. By three minutes after start-up the entire sediment bed was covered with relatively small, straight-crested, two-dimensional bed forms, which were similar in size and appearance to newly developed bed forms near the propagating bed-form fronts in the lower velocity runs. The sequence of bed-form development during the first three minutes of this run was not directly observed, because completely opening the gate valves of the flume at the beginning of this run required about three minutes. However, consecutive time-lapse movie frames taken at 65-second intervals show that the entire

sediment bed in the field of view of the camera changed from a planar bed to small bed forms in less than 65 seconds, within about two minutes of start-up. Figure 4-16 is an upstream view of the entire sediment bed seven minutes after start-up.

As in the lower velocity runs, the side-view, time-lapse movie photography indicates that slipfaces were migrating at different rates and began overtaking or being overtaken almost immediately after they developed. In addition, both the size and shape of individual bed forms were continually changing.

As in the lower velocity runs, at a given longitudinal position, the average size of the bed forms initially increased with time; at a given longitudinal position in the test section of the flume, the average size of the bed forms increased until the equilibrium value for that position was reached. In general, the sequence of changes in the average size and appearance of the bed forms at a given longitudinal position as a function of time was similar to that described for Runs 7 and 8. This characteristic sequence of the development of bed forms is illustrated by Figures 4-17 through 4-21. These figures are plan views (centered at 850 cm) of the sediment bed, taken at 18-minute to 38-minute intervals during the first two hours of Run 9. In Figure 4-17, taken five minutes after start-up, the bed forms are small in height and

spacing with relatively long, straight crests. In Figures 4-18 and 4-19, taken 23 and 41 minutes after start-up, respectively, the bed forms are progressively larger in successive figures and are more three-dimensional than in Figure 4-17; the crests are less continuous and more sinuous than in Figure 4-17, and a number of three-dimensional scour pits are present downstream from slipfaces. In Figure 4-20, taken 77 minutes after start-up, the bed forms are larger than in the preceding figures and small slipfaces are present on the stoss sides of some of the larger bed forms, just upstream from the slipfaces of the larger bed forms. In Figure 4-21, taken 111 minutes after start-up, the bed forms are even larger than in Figure 4-20, and longer trains of small bed forms are present on the stoss sides of the larger bed forms; the small slipfaces that are farthest downstream in the trains appear to have the largest heights and appear to have larger heights than those in Figure 4-20. A three-dimensional scour pit in the upper righthand corner of Figure 4-21 is particularly obvious because the channel bottom is exposed in this scour pit. Figure 4-22 is a plan view (centered at 850 cm) of the bed configuration about 16 hours and 20 minutes after the run was started; on the average, the bed forms appear similar in size to those in Figure 4-21. The difference in appearance of the bed forms in Figures 4-21 and 4-22 is similar to differences observed

at a given longitudinal position for different data sets once the average size of the bed forms had reached the equilibrium value.

Although the bed forms were initially very similar in size throughout the full length of the flume, the average size of the bed forms immediately downstream from the false bottom initially increased much more rapidly than the average size of the bed forms downstream. However, unlike in Runs 4 through 8, the average size of the bed forms immediately downstream from the false bottom did not increase more rapidly in the center of the flume than near the sidewalls: at a given longitudinal position, the growth rate of the bed forms was relatively uniform across the width of the flume. Fifteen minutes after start-up, the bed forms in more than the downstream half of the flume were very similar in size and appearance to one another and the growth rate of the bed forms was relatively uniform throughout this section of the flume; however, upstream from these more uniform bed forms, both the average size and the growth rate of the bed forms increased upstream. As the bed forms upstream became larger than those downstream, the bed forms immediately downstream from the larger bed forms increased in size more rapidly than the bed forms farther downstream and consequently became larger than the bed forms farther downstream. In this way, progressively larger bed forms and growth rates propagated

downstream with time. By 45 minutes after start-up, the average size and the growth rate of the bed forms were relatively uniform in only the downstream third of the flume; upstream, the average size of the bed forms gradually increased to the false bottom. The dependence of both the growth rate and the size of the bed forms on the bed configuration upstream was particularly apparent in Run 9 because the bed forms were initially so similar in size throughout the full length of the flume.

Before the false bottom was covered with sediment and while the average size of the bed forms was still increasing from upstream, the longitudinal variation in the average size and appearance of the bed forms upstream at a given time was similar to the variation at a given longitudinal position as a function of time. This longitudinal variation in the average size and appearance of the bed forms upstream is illustrated by the bed configuration at about 45 minutes after start-up. By 45 minutes after start-up, the average size of the relatively uniform bed forms downstream had already increased several-fold and these bed forms had already become moderately three-dimensional. These bed forms are shown in Figure 4-19. Upstream, the average size of the bed forms increased, and the bed forms became more three-dimensional. As the average size increased upstream, small slipfaces began to develop on the stoss sides of the larger

bed forms just upstream from the slipfaces of the larger bed forms; farther upstream, trains of small bed forms were present on the stoss sides of the larger bed forms. By 45 minutes after start-up, the spacing of the first bed form immediately downstream from the false bottom was already larger than the average spacing of the equilibrium bed forms that developed later in the test section and was much larger than the average spacing of the other bed forms. This bed form had more small slipfaces on its stoss side than the other relatively large bed forms. The development of small slipfaces on the stoss side of this bed form had already resulted in the crest of this bed form becoming irregular and poorly defined in the same way as in Runs 5 through 8.

As in Runs 7 and 8, by the time the false bottom was covered with sediment and the average size of the bed forms at a given longitudinal position had reached the equilibrium value for that position, the longitudinal variation in both the average size and appearance of the bed form had become inverted: the average size of the bed forms increased downstream from the flume inlet, instead of decreasing downstream from the false bottom. The contrast in the appearance of the sediment bed immediately downstream from the false bottom before and after the false bottom was covered with sediment is illustrated by Figures 4-23 and 4-24. These figures are plan views (centered at

about 250 cm) of the sediment bed, 36 minutes and about 39 hours and 15 minutes after start-up, respectively. Figure 4-23 shows the first bed form immediately downstream from the false bottom, with small slipfaces on its stoss side. The small slipfaces that are farthest downstream have become so large that they appear to be breaking up the downstream end of this bed form into separate bed forms. In contrast, Figure 4-24 shows relatively small bed forms whose average size increases slightly downstream in the limited field of view.

Section 4-11

Run 10

The mean flow velocity during the initial data set of Run 10 was very similar to that of Run 3. In Run 10 the mean flow velocity was gradually increased from approximately 31 cm/s to 32 cm/s during the first 15 minutes of the run, whereas in Run 3 the mean flow velocity was gradually increased from approximately 30 cm/s to 32 cm/s during the first 15 minutes of the run. The mean flow conditions during both of these runs were in the ripple stability field as delineated by Costello (1974) and Costello and Southard (1981).

In Run 10 the first bed forms to develop propagated from the false bottom in basically the same way as bed forms propagated from the false bottom in Run 3. In

general, the shape of the propagating bed-form front and the bed forms appeared similar to those in Run 3. Both the longitudinal variation in the appearance and average size of the bed forms upstream from the bed-form front at a given time and the variation in the appearance and average size of the bed forms at a given longitudinal position as a function of time were similar to those for Run 3. Figure 4-25 is a plan view (centered at 650 cm) of the sediment bed when the bed-form front had propagated downstream from the false bottom to about 850 cm (about six hours and 25 minutes after start-up). This figure illustrates how three-dimensional the bed forms became upstream from the bed-form front (away from the false bottom); the average size of the bed forms at this location was still increasing. As in the preceding runs, the time-lapse movie photography of newly developed bed forms shows that slipfaces were migrating at different rates and began overtaking or being overtaken immediately after they developed.

The sediment bed downstream from the propagating bed-form front initially remained a planar bed. Sediment movement on the planar bed was basically the same as that in Run 3 and was similar to that in all of the preceding runs. At a given location on the planar bed, the sediment movement occurred in intermittent bursts of grain motion that rapidly propagated a short distance downstream in

narrow, fan-shaped streaks, roughly parallel to the mean flow direction, and then subsided. The bursts appeared to propagate downstream much faster than the individual grains appeared to be moving. When individual grains were moved in bursts, the grains rolled or moved in short trajectories like ballistic trajectories; commonly, an individual grain moved several times in series before coming to rest. This continued motion of individual grains in a burst sustained the burst for a brief moment after the initial surge of motion had passed downstream and subsided. As in Run 3, the subparallel, fan-shaped bursts of sediment movement resulted in a charactersitic streaky or hummocky planar-bed micro-topography.

The hummocky micro-topography became particularly pronounced on about the first half meter of the planar bed immediately downstream from the downstream end of the water-surface plate (i.e., the plexiglass plate suspended on the water surface for the plan-view, time-lapse movie photography). By the time the bed-form front had propagated about 4.5 meters downstream from the false bottom, two bed forms had developed directly from features of the planar-bed micro-topography at the downstream end of the particularly hummocky section of planar bed: 1) a small bed form with a zigzag crest and 2) a small elongated mound with a small slipface and a narrow, V-shaped crest (open end facing downstream). Figure 4-26

is a plan view (centered at 850 cm) of the sediment bed 4 hours and 33 minutes after start-up; this figure shows these features after several small bed forms had propagated from the bed form with the zigzag crest and a second mound had begun to develop downstream from the mound with the V-shaped crest. This figure also shows the markedly hummocky section of planar bed immediately upstream from these features. Bed forms continued to propagate downstream from the bed form with the zigzag crest but did not continue to propagate downstream from the mound with the V-shaped crest; the two mounds decayed.

The decay of the two mounds proceeded sequentially from upstream; the upstream mound with the V-shaped crest was eroded before the downstream mound. After Figure 4-26 was taken, the mound downstream from the V-shaped crest initially continued to increase in size. As the upstream mound was eroded, the trough downstream began to be filled with sediment, and the height and slope of the small slipface gradually decreased. At some time after the upstream mound began to decrease in size, the downstream mound stopped increasing in size. Figure 4-27 is a plan view (centered at 850 cm) of these features 28 minutes after Figure 4-26 was taken. By that time the upstream mound had been reduced almost to the size of the features of the planar-bed micro-topography, the slipface with the V-shaped crest no longer existed, the trough downstream had

become a shallow depression, and the downstream mound was beginning to be eroded.

Figure 4-27 also shows a newly developing slipface with an irregular crest immediately upstream from the decaying mound which is farthest upstream. This bed form also developed directly from the planar-bed micro-topography at the downstream end of the particularly hummocky section of planar bed immediately downstream from the water-surface plate. Initially, relatively two-dimensional bed forms propagated downstream from this bed form in a narrow patch near the centerline of the flume. Later, however, three-dimensional bed forms developed from both sides of this patch of bed forms and propagated rapidly in narrow spurs diagonally downstream toward both sidewalls, in basically the same manner as three-dimensional bed forms propagated across the planar bed in Run 3. Earlier, a spur of three-dimensional bed forms also developed from the patch of bed forms that propagated from the bed form with the zigzag crest in Figure 4-26; these three-dimensional bed forms developed from the righthand (facing downstream) side of the slipface which is farthest downstream in Figure 4-26 and propagated rapidly diagonally downstream toward the righthand sidewall.

In Run 3, unlike in Run 10, no bed forms developed directly from the hummocky planar-bed micro-topography before bed forms had propagated throughout the full length

of the flume from the false bottom and sidewalls. However, in Run 10, the only bed forms that developed directly from the planar-bed micro-topography were the bed forms that developed at the downstream end of the markedly hummocky section of planar bed immediately downstream from the water-surface plate. The bed forms propagating from the false bottom and the bed forms that developed directly from the hummocky planar-bed micro-topography eventually covered the entire sediment bed.

At a given longitudinal position in the test section of the flume, the average size of the bed forms increased until the equilibrium value for that position was reached. By the time the false bottom was covered with sediment and the average size of the bed forms at a given longitudinal position had reached the equilibrium value for that position, the average spacing of the bed forms in the section of the flume immediately downstream from the false bottom no longer was larger than the average spacing of the equilibrium bed forms in the test section; the average spacing of the bed forms immediately downstream from the false bottom appeared to be slightly smaller than the average spacing of the equilibrium bed forms downstream.

Section 4-12

Run 11

The mean flow velocity during the initial development of bed forms in Run 11 was most similar to that in Run 8. In Run 11 the mean flow velocity was increased to approximately 39 cm/s during the first minute of the run; in Run 8 the mean flow velocity was between approximately 39 cm/s and 41 cm/s during the first 100 minutes of the run. The mean flow conditions during both of these runs were in the two-dimensional dune stability field as delineated by Costello (1974) and Costello and Southard (1981). In general, the initial development of bed forms in Run 11 was similar to that in Run 8. However, in Run 11, the water-surface plate affected the rate of development of bed forms and consequently altered the longitudinal variation in the average size and appearance of bed forms while the average size of the bed forms was increasing.

In Run 11 the first bed forms to develop propagated from the false bottom in basically the same way as in Run 8. However, as in Run 8, the sediment movement on the planar bed downstream rapidly resulted in the development of small bed forms directly from the planar bed. As soon as the velocity was increased at the beginning of Run 11, the sediment movement on the planar bed produced narrow, longitudinal furrows and ridges, a few grain diameters in

relief, which initially gave a streaky appearance to the planar bed. The planar-bed micro-topography rapidly became increasingly hummocky; within two or three minutes subparallel, crisscross, diagonal lineations formed by the sides of hummocks gave the appearance of faint, diamond-shaped patterns over most of the planar bed.

Small bed forms first developed directly from the hummocky planar-bed micro-topography in the section of the planar bed underneath the water-surface plate. Within less than two minutes of setting the velocity, a series of small slipfaces with somewhat irregular crests developed almost simultaneously, directly from diamond-shaped hummocks about a quarter of the way downstream from the upstream end of the water-surface plate; the hummocks appeared to increase in size fairly continuously until recognizable slipfaces developed. The small bed forms that developed underneath the water-surface plate continued to increase in size and propagated downstream. Figure 4-28 is a plan view (centered at 700 cm) of the sediment bed underneath the water-surface plate about two minutes after the velocity was set. The crests of the bed forms farthest upstream in Figure 4-28 are somewhat irregular and zigzag, while the crests of the bed forms downstream are straighter and more continuous. Immediately upstream from the bed forms with the irregular zigzag crests, there are diagonal and zigzag lineations on the planar bed. In general, the bed forms

appear similar to newly developed bed forms in Run 8. As in preceding runs, the time-lapse movie photography of newly developed bed forms shows that slipfaces were migrating at different rates and began overtaking or being overtaken almost immediately after they developed.

Bed forms initially developed and increased in size most rapidly immediately downstream from the false bottom and underneath the water-surface plate. The almost simultaneous development of bed forms in these two areas and the subsequent propagation of bed forms downstream from these areas initially resulted in two consecutive longitudinal sequences of developing bed forms, each similar to the initial longitudinal sequence for the full length of the flume in Run 8. In Run 11 the initial longitudinal variation in the bed configuration downstream from the false bottom was as follows: 1) bed forms propagating from the false bottom, 2) hummocky planar bed with small bed forms developing directly from the planar-bed micro-topography, 3) bed forms that developed underneath the water-surface plate propagating downstream, and 4) hummocky planar bed again with small bed forms developing directly from the planar bed. The bed forms propagating from the false bottom and from underneath the water-surface plate and the bed forms that developed directly from the planar bed downstream from each of these areas merged with one another as in Run 8. By 15 minutes

after the velocity was set, there was a single, continuous train of bed forms from the false bottom to the tailbox with planar bed of varying widths on either side. No spurs of highly three-dimensional bed forms developed on the planar bed.

As in the preceding runs, at a given longitudinal position the average size of the bed forms initially increased with time; at a given longitudinal position in the test section of the flume, the average size of the bed forms increased until the equilibrium value for that position was reached. In general, the sequence of changes in the average size and appearance of the bed forms at a given longitudinal position as a function of time was similar to tha described for Runs 7 through 9. However, while the average size of the bed forms was increasing, the longitudinal variation in the average size and appearance of the bed forms as a function of time was more complicated in Run 11 than that in the preceding runs because of the effects of the water-surface plate. Nevertheless, the longitudinal variation in the average size of the bed forms as a function of time reflected the dependence of both the growth rate and the size of the bed forms on the bed configuration upstream.

The longitudinal variation in the average size of the bed forms as a function of time underneath the water-surface plate and immediately upstream and downstream from

the plate is particularly illustrative. Initially the bed forms underneath the water-surface plate increased in size more rapidly than those immediately upstream or downstream from the plate; the bed forms upstream and downstream from the plate were smaller than those underneath the plate. However, once the average spacing of the bed forms about a quarter of the way downstream from the upstream end of the water-surface plate became about 15 cm, the average size of the bed forms at that location remained approximately the same as long as the bed forms immediately upstream from the plate were relatively small. The bed forms immediately downstream from the water-surface plate initially continued to increase in size and became larger than those underneath the plate. With time, progressively larger bed forms and growth rates propagated downstream both from underneath the water-surface plate and from the false bottom as described for Run 9. Once the bed forms immediately upstream from the water-surface plate became almost as large as those about a quarter of the way downstream from the upstream end of the plate, the average size of the bed forms underneath the plate began to increase again.

Figures 4-29 and 4-30 are overlapping plan views (centered at 650 cm and 750 cm, respectively) about 11 minutes after the velocity was set. These figures show the sediment bed underneath the water-surface plate and the sediment bed immediately upstream and downstream from the

plate. At that time, the bed forms underneath the plate were larger than those either upstream or downstream from the plate. The bed forms immediately upstream from the plate developed directly from the planar-bed micro-topography: at that time, there was not a continuous train of bed forms from the false bottom to the water-surface plate. Figures 4-31 and 4-32 are overlapping plan views (centered at 650 cm and 750 cm, respectively) of the same section of the sediment bed about 30 minutes after Figures 4-29 and 4-30 were taken. In Figure 4-31 the bed forms about a quarter of the way downstream from the upstream end of the water-surface plate are not much larger than those in Figure 4-29; however, in Figure 4-32 the bed forms immediately downstream from the plate are markedly larger than those in Figure 4-30.

By the time the second data set of Run 11 was started, about 19 hours after start-up, the false bottom was covered with sediment and the average size of the bed forms increased downstream from the flume inlet. The water-surface plate no longer appeared to be significantly affecting the longitudinal variation in the average size and appearance of the bed forms.

Section 4-13

Run 12

The mean flow velocity during the initial data set of Run 12 was approximately the same as that of Run 9; in both runs the mean flow velocity was increased to 47.6 cm/s during the first few minutes of the run. The mean flow conditions during both of these runs were in the three-dimensional dune stability field as delineated by Costello (1974) and Costello and Southard (1981). In general, the development of bed forms in Run 12 from the time the gate valves were completely opened was basically the same as that in Run 9. As in Run 9, by the time the gate valves were completely opened, the entire sediment bed was covered with relatively small, straight-crested, two-dimensional bed forms. However, as in Run 11, the water-surface plate affected the rate of development of bed forms and likewise altered the longitudinal variation in the average size and appearance of bed forms while the average size of the bed forms was increasing.

The initial development of the bed forms was observed and documented most carefully underneath the water-surface plate. As the gate valves were being opened at the beginning of Run 12, the sediment movement on the planar bed almost immediately produced a streaky micro-topography on the planar bed, as described for Run 11. The planar-bed micro-topography very rapidly became increasingly hummocky.

Within approximately half a minute of starting to increase the flow velocity, a short series of faint, small slipfaces with somewhat irregular crests developed almost simultaneously, directly from hummocks on the planar bed underneath the water-surface plate as in Run 11; the hummocks appeared to increase in size fairly continuously until recognizable slipfaces developed. The newly developed bed forms continued to increase in size and propagated downstream. Small bed forms developed in the same manner at many points throughout the flume and rapidly merged with one another, completely covering the sediment bed within a few minutes of start-up.

Figures 4-33 through 4-35 are a series of close-up plan views (centered at 700 cm) of the sediment bed underneath the water-surface plate, taken at 28 second intervals beginning a few seconds after start-up (the field of view is approximately 80 cm long). This series illustrates the initial development of bed forms directly from the planar bed. Figure 4-33 shows the slightly streaky appearance of the planar bed a few seconds after start-up. Figure 4-34 shows a series of incipient slipfaces developing directly from the hummocky micro-topography on the planar bed and the appearance of the micro-topography immediately prior to the development of recognizable slipfaces. Figure 4-35 shows small bed forms which appear to cover the entire field of view; however, in

a few places hummocks do not have distinct slipfaces.

As in all of the preceding runs, newly developed slipfaces migrated at different rates and began overtaking adjacent slipfaces downstream or being overtaken almost immediately after they developed. The overtaking phenomenon was particularly apparent at the beginning of Run 12 because of the relatively rapid migration rates of the small, newly developed slipfaces. Just before a slipface was overtaken from upstream, the local sediment transport rate on the upper part of the stoss side of the bed form being overtaken appeared to decrease markedly and the migration rate of the bed form appeared to decrease. In some cases, the slipface being overtaken was almost obliterated before the slipface was actually overtaken. As the slipface being overtaken decayed, the spacing appeared to increase suddenly; the spacing between the slipface immediately upstream from the decaying slipface and the slipface immediately downstream was greater than the average spacing at that location had previously been. The overtaking phenomenon appeared to be an integral part of the initial growth process of the developing bed forms.

Figures 4-36 through 4-38 are a series of close-up plan views (centered at 700 cm) of the sediment bed underneath the water-surface plate, taken at 14-second intervals beginning about four minutes after start-up (the field of view is approximately 80 cm long). This series

illustrates the overtaking phenomenon. The third slipface from the lefthand side of Figure 4-36 is being overtaken by the slipface immediately upstream. In Figure 4-37 the slipface being overtaken is decaying; part of the slipface is almost indiscernible. In Figure 4-38 the original slipface that was being overtaken no longer exists; parts of the slipface were completely obliterated before being overtaken and the remainder was overtaken by the slipface immediately upstream. Examination of Figure 4-36 through 4-38 indicates that the slipface that overtook the original slipface is likewise being overtaken from upstream.

As in Run 11, bed forms initially developed and increased in size most rapidly immediately downstream from the false bottom and underneath the water-surface plate. Consequently, similar to Run 11, there were initially two consecutive longitudinal sequences of developing bed forms, each similar to the initial longitudinal sequence for the full length of the flume in Run 9. As in the preceding runs, at a given longitudinal position the average size of the bed forms initially increased with time; at a given longitudinal position in the test section of the flume, the average size of the bed forms increased until the equilibrium value for that position was reached. As the average size of the bed forms increased, the local sediment transport rates on the stoss sides of the bed forms also appeared to increase. Even the increase in the average

size of the bed forms underneath the water-surface plate during the first five minutes of Run 12 was sufficient to result in an apparent increase in the local sediment transport rates.

In general, the sequence of changes in the average size and appearance of the bed forms at a given longitudinal position as a function of time was similar to that described for Runs 7 through 9. As in Run 11, while the average size of the bed forms was increasing, the longitudinal variation in the average size and appearance of the bed forms as a function of time was relatively complicated because of the effects of the water-surface plate but likewise reflected the dependence of both the growth rate and the size of the bed forms on the bed configuration upstream.

The sequence of development of the bed forms underneath the water-surface plate and immediately upstream and downstream from the plate was generally similar to that for Run 11. Initially the bed forms underneath the water-surface plate increased in size much more rapidly than those immediately upstream or downstream from the plate. These bed forms were relatively straight-crested, and two-dimensional. However, the average size of the bed forms underneath the water-surface plate remained relatively small as long as the bed forms immediately upstream from the plate were relatively small. The bed forms immediately

downstream from the water-surface plate initially continued to increase in size and became larger and more three-dimensional than those underneath the plate. Once the bed forms immediately upstream from the water-surface plate became almost as large as those about a quarter of the way downstream from the upstream end of the plate, the average size of the bed forms underneath the plate began to increase again and the bed forms gradually became more three-dimensional. Once the bed forms underneath the water-surface plate reached a certain critical size, relatively small slipfaces began to develop on the stoss sides of the larger bed forms just upstream from the slipfaces of the larger bed forms. As the average spacing of the larger bed forms continued to increase, progressively longer trains of small bed forms developed on the stoss sides of the larger bed forms.

By the time the second data set of Run 12 was started, about 23 hours after start-up, the longitudinal variation in the average size and appearance of the bed forms downstream was similar to that for the second data set of Run 9; the false bottom was covered with sediment and the average size of the bed forms increased downstream from the flume inlet. As in Run 11, once the average size of the bed forms at a given longitudinal position had reached the equilibrium value, the water-surface plate no longer

appeared to affect significantly the longitudinal variation in the average size and appearance of the bed forms.

CHAPTER 5

OBSERVATIONS OF FULLY DEVELOPED BED FORMS

Section 5-1

Introduction

This chapter consists of observations of the sediment bed after the initial data set for each flume experiment. These observations include: 1) descriptions of the bed forms from direct observations, plan-view photography, and longitudinal sediment-bed profiles; 2) observations of the kinematics of the bed forms from both direct observations and time-lapse movie photography; and 3) observations of the sediment movement.

For Runs 1 through 9, the observations of the fully developed or equilibrium bed forms are presented as a function of flow velocity in the same way as the observations of the initial development of bed forms in Chapter 4. However, for Runs 10, 11, and 12 the observations are presented by topic; for each topic the similarities and differences as a function of flow velocity for these three runs are directly compared. These runs were carried out to observe and compare directly within a relatively short time period bed forms in the three different stability fields observed in Runs 1 through 9: ripples, two-dimensional dunes, and three-dimensional dunes. Therefore, the comparisons of these three runs

provide a summary of the main observations of fully developed bed forms for the range of flow velocities of these experiments.

Contrary to expectations, the kinematics and dynamics of the fully developed bed forms appeared to be basically the same over the entire range of flow conditions of these experiments. The differences in the bed forms as a function of flow velocity seemed to result from differences in the relative rates at which processes occurred, such as the rates of development and growth of new slipfaces, in addition to differences in the maximum size the bed forms could attain. The differences in relative rates of different processes as a function of flow velocity are discussed in the observations for Runs 10, 11, and 12.

The overtaking phenomenon was the dominant characteristic of the kinematics of the bed forms for the entire range of flow conditions. In addition, both the size and shape of individual bed forms continually changed, and new slipfaces continually developed.

The modes of sediment movement and the longitudinal variation in the sediment movement patterns over the bed forms were basically the same for all the experiments despite the large differences in the mean sediment transport rates. Three-dimensional scour pits were common for the entire range of flow conditions.

A particularly important observation is that the

sediment movement on the stoss sides of bed forms was dominated by coherent bursts of sediment movement that originated from the apparent reattachment area downstream from slipfaces. Even sediment movement on the upper stoss sides of bed forms just upstream from slipfaces resulted from bursts of sediment movement emanating from the reattachment area. The nature of these bursts of sediment movement appeared to determine the micro-topography on the stoss sides of the bed forms, the development of new slipfaces, and ultimately the bed geometry. This observation resulted in the examination of some new quantitative measures of the bed-form geometry.

The interactions between these bursts of sediment movement and the development and progression of new slipfaces were most evident for the higher velocity runs because of the much greater sediment transport rates and therefore the much more rapid and immediate changes in the bed topography. The most detailed descriptions of the development and progression of new slipfaces are presented in Runs 7 and 9. The differences in the development of new slipfaces as a function of flow velocity are discussed in Runs 10, 11, and 12.

As in Chapter 4, parallel organization is used for all the runs to facilitate locating data. As the flow velocity was increased, the changes in the relative rates of processes, etc., occurred smoothly and gradationally.

Therefore, it is possible to get an overview of the fully developed bed forms by reading the descriptions selectively.

Section 5-2

Run 1

The average of the mean flow velocities for all of the data sets of Run 1, excluding the initial data set, is 28.6 cm/s. The mean flow conditions during this run were in the ripple stability field as delineated by Costello (1974) and Costello and Southard (1981).

The equilibrium bed forms were relatively small; the mean length or spacing of the major bed forms is 19.9 cm and the mean height is 1.61 cm. The definitions of bed-form length and height as used in these experiments are presented in Chapter 6, Section 6-2.0.0. At a given time, the size of the bed forms in the test section of the flume varied greatly up to the maximum size for the mean flow conditions of this run. Data on the size of the bed forms are presented in more detail in Chapter 6. In general, the bed forms were relatively three-dimensional; most crestlines were sinuous, and three-dimensional scour pits occurred locally at various locations downstream from slipfaces. The crestlines of many of the bed forms were long compared to the spacing of the bed forms. Some crestlines extended across the full width of the flume, but

most were discontinuous across the flume. Bed-form height generally varied along slipfaces.

At a given time, the detailed geometry of the bed forms varied substantially throughout the test section of the flume. At times, relatively straight-crested, evenly spaced bed forms were adjacent to highly three-dimensional bed forms, and series of relatively small bed forms were intermixed with larger bed forms. Similar variations in the detailed geometry of the bed forms were observed at a given longitudinal position as a function of time. Figures 5-1 and 5-2 are close-up plan views (centered at 725 cm and 825 cm, respectively) of the sediment bed during Run 1-13. The field of view of each figure is approximately 80 cm long. These figures show the large variation in the size of the bed forms at a given time in adjacent areas of the test section of the flume.

Bed forms were superimposed on one another: slipfaces with relatively small heights occurred on the stoss sides of larger bed forms. In order to differentiate apparently minor slipfaces from the major bed forms, slipfaces whose heights were markedly smaller than the apparent mean height for a given run were arbitrarily designated as ripplets. Figure 5-3 is a close-up plan view (centered at 750 cm) of the sediment bed during Run 1-3. Several slipfaces with small heights are superimposed on the stoss side of a bed form in the upper righthand part of this figure. This

figure also illustrates the spatial variability of the detailed geometry of the bed forms.

The longitudinal centerline profiles of the sediment bed show that the slipfaces of major bed forms were not migrating in a single plane; the low points at the base of adjacent slipfaces are not in a single plane. Some of the slipfaces appear to be migrating up the stoss side of the adjacent bed form downstream and overtaking the slipface downstream. The side-view, time-lapse movie photography clearly illustrates that bed forms were not migrating in a single plane; slipfaces were migrating at different rates and overtaking the adjacent slipface downstream or being overtaken. Plots of the centerline profiles of the sediment bed with a vertical exaggeration of five show that there were alternating highs and lows in the local mean bed elevation with wavelengths or spacings at least several times the mean spacing of the bed forms.

The centerline profiles of the sediment bed also show that the shape of the stoss sides of the bed forms varies considerably; however, the slipfaces appear to be roughly near the angle of repose of the sediment in water. The profiles of the bed forms are not uniform and not roughly triangular, and sometimes the identity of individual bed forms is ambiguous. The slopes of the stoss sides of the bed forms range from being positive with respect to the flume bottom for all or most of the distance downstream to

the slipface (i.e., the elevation of the stoss side increases downstream) to being slightly negative for the entire distance downstream to the slipface when the slipface is being overtaken.

The kinematics of the bed forms were examined using the side-view, time-lapse movie photography of the sediment bed. At a given time the migration rates of different slipfaces varied greatly. In addition, the migration rates of individual slipfaces increased in spurts and then decreased. Spurts of relatively rapid migration commonly appear to propagate to successive slipfaces downstream.

A dominant characteristic of the kinematics of the bed forms is the continual overtaking of the slipfaces. The overtaking phenomenon is unambiguously shown by the time-lapse movie photography. Slipfaces migrated up the stoss side of the adjacent bed form downstream and overtook the slipface downstream. Shortly before a slipface was overtaken by the slipface immediately upstream, the migration rate of the slipface being overtaken tended to decrease markedly. At times, several slipfaces in series were simultaneously migrating up the stoss side of the adjacent bed form downstream; each successive slipface upstream was migrating more rapidly than the adjacent slipface downstream.

As the bed forms migrated downstream, the size and shape of the longitudinal profiles changed or deformed.

The height and length of individual bed forms both increased and decreased with time. A common deformation sequence of the longitudinal profiles gives the appearance of a mound of sediment migrating downstream through a bed form.

The following changes typically occurred in the longitudinal profile of a bed form as a mound of sediment appeared to migrate downstream through the bed form:

1) the bed elevation of the farthest upstream section of the profile decreased and the profile of that section became more convex upstream, while immediately downstream the bed elevation of the profile increased, resulting in a hump-backed profile with a slight mound developing on the stoss side of the bed form a short distance downstream from the upstream trough;

2) as the mound migrated downstream, the profile became rounded and relatively symmetric with the slope of the stoss side first increasing downstream to the top of the mound then decreasing downstream to the slipface;

3) finally, as the top of the mound approached the slipface, the slope of the stoss side became relatively steeply positive downstream (i.e., the elevation of the stoss side increased downstream to the slipface).

Sometimes the downstream slope of a mound became unstable before the mound had migrated all the way through a bed form and developed into a new slipface on the stoss

side of the original bed form. However, more often, mounds of sediment migrated through bed forms without developing slipfaces.

The modes and relative rates of sediment movement varied with both the longitudinal position on a given bed form and with the geometry of the bed. The general patterns of sediment movement on the stoss sides of bed forms appeared to depend primarily on whether the upstream slipface was relatively two-dimensional or whether an active, three-dimensional scour pit had developed in the trough downstream from the slipface.

The longitudinal variation in the general sediment movement patterns downstream from relatively two-dimensional slipfaces are described below. In the trough area immediately downstream from a slipface, there tended to be very little sediment movement on the bed. Downstream from this protected area part way up the stoss side of the bed form where the flow appeared to reattach to the sediment bed, the sediment movement occurred in intermittent, radial bursts of grain motion with multiple grains moving simultaneously a short distance in all directions from a common center. The radial bursts of grain motion resulted in a pitted or cratered micro-topography. Most of the occasional grain motion which did occur in the protected trough area upstream appeared to originate from the radial bursts in the pitted or cratered

area. The grain motion in the trough area was predominantly upstream or lateral in direction.

At the downstream end of the apparent reattachment area, the sediment movement occurred in intermittent bursts that propagated predominantly downstream. The strength of the bursts of sediment movement varied: many of the bursts propagated all or most of the way to the slipface downstream, but some propagated only part way over the stoss side before subsiding. As the bursts propagated downstream, they tended to spread laterally, forming fans of grain motion parallel and subparallel to the mean flow direction on the stoss sides of the bed forms. Most of the sediment movement on the stoss sides of the bed forms downstream from the reattachment area appeared to result from the bursts of sediment movement originating at the downstream end of the reattachment area. Once a burst of downstream sediment movement occurred, grain motion tended to be sustained in a given swath for a few moments after the initial wave of sediment movement passed downstream. The parallel and subparallel fan-shaped bursts of sediment movement resulted in a relatively smooth micro-topography with faint lineations parallel to the direction of grain motion.

Individual grains moved both by rolling over the surface and by hopping or saltating in short, low trajectories. Once a grain was set in motion on the stoss

side of a bed form downstream from the apparent reattachment area, it seemed more likely than average to continue to be moved; commonly a given grain moved in a series of hops before coming to rest. At the slipface downstream, grains tended to overshoot the top of the slipface and land just downstream from the brink of the slipface on the upper part of the slipface. Grains on the slipface appeared to be protected from further motion by direct fluid forces. Periodically the upper part of the slipface oversteepened to the point that it became unstable and slumped or avalanched to the base of the slipface. By this process, slipfaces migrated downstream.

The longitudinal variation in the general sediment movement patterns associated with active, three-dimensional scour pits was somewhat different from that downstream from relatively two-dimensional slipfaces. The apparent flow patterns and consequent sediment movement patterns associated with active, three-dimensional scour pits appeared to be essentially the same as those described in Chapter 4, Run 2 for the propagation of highly three-dimensional bed forms from the side of a patch of relatively two-dimensional bed forms on a planar bed. Scour pits seemed to occur preferentially downstream from where there was a marked contrast in the height of adjacent sections of a slipface or where a slipface pinched out laterally. The flow appeared to be channeled through the

low section, curl around the adjacent high section, and then spiral diagonally downstream forming a relatively strong separation vortex at about a 45° angle to the mean flow direction in the trough downstream from the high section of the slipface. Commonly the adjacent high section of the slipface was oriented diagonally downstream, roughly parallel to the vortex. As during the propagation of three-dimensional bed forms, sediment in the trough along the slipface was transported fairly continuously back up the slipface by the vortex and deposited on the slipface, forming a ridge part way up the slipface which extended downstream on the stoss side of the bed form. Immediately downstream from the separation vortex, sediment movement occurred in fairly continuous, broad, sweeping bursts of sediment movement which propagated diagonally downstream at about a 65° angle to the axis of the vortex and at about a 20° angle to the mean flow direction. Figure 4-4 is a schematic of these approximate geometric relationships. Figure 5-4 is a close-up plan view (centered at 725 cm) of the sediment bed during Run 1-6 (the field of view is approximately 80 cm long). The bed geometry characteristically associated with active scour pits is illustrated by the three-dimensional bed form just to the left of the center of this figure.

One of the most striking differences in the sediment movement associated with active, three-dimensional scour

pits and two-dimensional slipfaces was that the local sediment transport rates associated with active, three-dimensional scour pits were markedly greater than those associated with relatively two-dimensional slipfaces. As noted in Chapter 4, Run 2, this difference was also strikingly evident during the propagation of highly three-dimensional bed forms and relatively two-dimensional bed forms onto a planar bed.

Section 5-3

Run 2

The average of the mean flow velocities for all of the data sets of Run 2, excluding the initial data set, is 30.0 cm/s. The mean flow conditions during this run were in the ripple stability field as delineated by Costello (1974) and Costello and Southard (1981).

The mean length or spacing of the major bed forms is 21.5 cm and the mean height is 1.68 cm. As in Run 1, at a given time the size of the bed forms in the test section of the flume varied greatly up to the maximum size for the mean flow conditions of this run. In general, the bed forms were relatively three-dimensional; most crestlines were sinuous, and three-dimensional scour pits with longitudinal ridges extending downstream occurred locally at various locations downstream from slipfaces. The occurrence of three-dimensional scour pits does not

necessarily imply that the crests were discontinuous; scour pits occurred locally downstream from slipfaces that extended across the entire width of the flume. As in Run 1, the crestlines of many of the bed forms were relatively long compared to the spacing of the bed forms. Bed-form height generally varied along slipfaces. As in Run 1, there were substantial variations in the detailed geometry of the bed forms both at a given time as a function of longitudinal position in the test section of the flume and at a given longitudinal position as a function of time. In addition, bed forms were superimposed on one another; slipfaces with relatively small heights occurred on the stoss sides of larger bed forms.

As in Run 1, the longitudinal centerline profiles of the sediment bed show that the slipfaces of major bed forms were not migrating in a single plane. Some slipfaces appear to be migrating up the stoss side of the adjacent bed form downstream and overtaking the slipface downstream. The overtaking phenomenon is illustrated by the side-view, time-lapse movie photography. Plots of the centerline profiles show that there were alternating highs and lows in the local mean bed elevation with wavelengths at least several times the mean spacing of the bed forms.

The shape of the longitudinal profiles of the stoss sides of the bed forms varies considerably. The variation in shape is similar to that in Run 1. The slopes of the

stoss sides range from being positive with respect to the flume bottom for all or most of the distance downstream to the slipface to being slightly negative for the entire distance downstream to the slipface.

The kinematics of the bed forms observed using the side-view, time-lapse movie photography of the sediment bed appear to be similar to those of Run 1. The continual overtaking of the slipfaces is a dominant feature of the kinematics. The large variation in the migration rates of different slipfaces at a given time resulted in slipfaces overtaking or being overtaken. In addition, the sporadic, spurt-like nature of the migration rates of individual slipfaces is evident. For example, a given slipface might remain almost stationary for a noticeable period of time, and then suddenly begin to migrate downstream as rapidly or more rapidly than the average migration rate for this run. As in Run 1, spurts of relatively rapid migration appear to propagate to successive slipfaces downstream.

As the bed forms migrated downstream, the size and shape of the longitudinal profiles changed or deformed. The height and length of individual bed forms both increased and decreased as functions of time; for example, the height of a given slipface might first increase as the bed form migrated downstream, then decrease, and then increase again.

As in Run 1, a common deformation sequence of the

longitudinal profiles gives the appearance of a mound of sediment migrating downstream through the bed form. At times, the downstream slope of a mound became unstable and developed into a new slipface on the stoss side of the original bed form. Commonly the new slipface continued to migrate over the stoss side of the original bed form and overtook the original slipface. However, occasionally, if the new slipface developed far enough upstream from the original slipface and the original slipface migrated as rapidly as the new slipface, the formation of the new slipface effectively resulted in the breakup of the original bed form into two bed forms.

The sediment movement over the bed forms was similar to that in Run 1. However, the average sediment transport rate appeared to be greater; bursts of sediment movement appeared to be more frequent and more grains appeared to move in individual bursts. The sediment movement patterns downstream from relatively two-dimensional slipfaces were essentially the same as those described in Run 1. Most of the sediment movement on the stoss sides of bed forms seemed to be controlled by the bursts of sediment movement that originated where the flow appeared to reattach to the sediment bed downstream from slipfaces; even sediment movement high on the stoss sides of bed forms just upstream from slipfaces seemed to result from bursts of sediment movement emanating from the apparent reattachment area. As

in Run 1, the micro-topography of the reattachment area was pitted and cratered; downstream from this area, the sediment bed appeared smoother, with faint lineations in the direction of grain motion.

The sediment movement patterns associated with active, three-dimensional scour pits were also essentially the same as those described in Run 1. Slipfaces with active, three-dimensional scour pits downstream and the bed form downstream were observed to become relatively two-dimensional with time. The relatively strong, diagonal vortices subsided, crests became oriented more nearly perpendicular to the flow, and longitudinal ridges gradually blended into the stoss sides of bed forms. As described in Chapter 4, Run 2, this phenomenon was also observed for three-dimensional bed forms that propagated diagonally downstream across the planar bed. As in Run 1, the local sediment transport rates associated with active, three-dimensional scour pits were markedly greater than those associated with relatively two-dimensional slipfaces.

Section 5-4

Run 3

The average of the mean flow velocities for all of the data sets of Run 3, excluding the initial data set, is 32.1 cm/s. The mean flow conditions during this run were in the ripple stability field as delineated by

Costello (1974) and Costello and Southard (1981).

The mean length of the major bed forms is 24.8 cm and the mean height is 1.78 cm. As in Runs 1 and 2, at a given time the size of the bed forms in the test section of the flume varied greatly up to the maximum size for the mean flow conditions of this run. In general, the bed forms were relatively three-dimensional; most crestlines were sinuous, and three-dimensional scour pits with longitudinal ridges extending downstream occurred locally downstream from slipfaces. As in Runs 1 and 2, the crestlines of many of the bed forms were relatively long compared to the spacing of the bed forms. Bed-form height generally varied along slipfaces. As in Runs 1 and 2, there were substantial variations in the detailed geometry of the bed forms both at a given time as a function of longitudinal position and at a given longitudinal position as a function of time.

Small slipfaces were superimposed on larger bed forms; occasional ripplets seemed more common than in Runs 1 and 2. Figure 5-5 is a plan view (centered at 560 cm) of the sediment bed after the flume was drained at the end of Run 3-12 (the field of view of this figure is approximately 155 cm long). Two slipfaces with very small heights are superimposed on the stoss side of the relatively long bed form located close to the near sidewall in the center of this figure; these slipfaces appear to have propagated from

the slightly higher slipface immediately upstream with a similarly shaped crestline. This figure also illustrates the spatial variability of both the size and the detailed geometry of the bed forms.

As in Runs 1 and 2, the longitudinal centerline profiles of the sediment bed show that the slipfaces of the major bed forms were not migrating in a single plane; many slipfaces appear to be overtaking or being overtaken. The centerline profiles show that there were alternating highs and lows in the local mean bed elevation with wavelengths at least several times the mean spacing of the bed forms. In addition, the variation in the shape of the longitudinal profiles of individual bed forms is similar to that of Run 1 and Run 2.

The kinematics of the bed forms observed using the side-view, time-lapse movie photography of the sediment bed appear to be similar to those of Runs 1 and 2. A dominant characteristic of the kinematics is the continual overtaking of slipfaces migrating at different rates. In addition, the migration rates of individual slipfaces vary in a sporadic, spurt-like manner as described in Run 2. Spurts of relatively rapid migration appear to propagate to successive slipfaces downstream, giving the impression of waves of relatively rapid migration passing downstream through the field of view.

As the bed forms migrated downstream, the size and

shape of the longitudinal profiles changed. As in Runs 1 and 2, the height and length of individual bed forms both increased and decreased as functions of time and the longitudinal profiles commonly deformed in such a way that a mound of sediment appears to migrate downstream through the bed form. Observing the changes in the profiles of bed forms by means of the time-lapse movie photography shows that the identity of a given bed form was transitory. Bed forms lost their identity by being overtaken from upstream, by being broken up into more than one bed form as a result of a new slipface developing on the stoss side of the original bed form, or by the slipface decreasing in height and blending gradually into the stoss side of the bed form downstream.

The sediment movement over the bed forms was similar to that in Runs 1 and 2, but the average sediment transport rate appeared to be greater. Both the sediment movement patterns associated with relatively two-dimensional slipfaces and those associated with active, three-dimensional scour pits were essentially the same as those described for Runs 1 and 2. The features of the micro-topography on the upper stoss sides of some of the bed forms downstream from relatively two-dimensional slipfaces appeared more pronounced than those in Runs 1 and 2; the micro-topography appeared similar to the streaky or hummocky micro-topography that developed on the planar bed.

The most striking difference between the sediment movement associated with relatively two-dimensional slipfaces and that associated with active, three-dimensional scour pits was the markedly greater local sediment transport rates that appeared to result from the strong diagonal vortices associated with three-dimensional scour pits. Strong diagonal vortices appeared to be particularly transient: with time, diagonal vortices tended to subside and three-dimensional bed forms tended to become relatively two-dimensional.

Section 5.5

Run 4

The average of the mean flow velocities for all of the data sets of Run 4, excluding the initial data set, is 34.1 cm/s. The mean flow conditions during this run were at the low-velocity end of the two-dimensional dune stability field as delineated by Costello (1974) and by Costello and Southard (1981).

The mean length of the major bed forms is 30.3 cm and the mean height is 1.75 cm. As in Runs 1 through 3, at a given time the size of the bed forms in the test section of the flume varied greatly up to the maximum size for the mean flow conditions of this run. In general, the bed forms were relatively three-dimensional; most crestlines were sinuous, and three-dimensional scour pits with

longitudinal ridges extending downstream occurred locally downstream from slipfaces. The crestlines of the bed forms did not appear as long relative to the spacing of the bed forms as during the lower velocity runs; a smaller percentage of the crestlines seemed to extend across the full width of the flume. Bed-form height generally varied along slipfaces. At a given longitudinal position, the size of the bed forms tended to vary across the width of the flume. At times, bed forms with greater lengths occurred near the centerline of the flume; however, occasionally, unusually long, narrow bed forms developed along the sidewalls. As in Runs 1 through 3, there were substantial variations in the detailed geometry of the bed forms both at a given time as a function of longitudinal position and at a given longitudinal position as a function of time.

Small slipfaces were superimposed on larger bed forms; ripplets seemed more common than in the lower velocity runs. Ripplets appeared to occur most frequently on the upper stoss sides of the longer bed forms.

As in Runs 1 through 3, the longitudinal centerline proflies of the bed forms show that the bed forms were not migrating in a single plane; many slipfaces appear to be overtaking or being overtaken. The centerline profiles show that there were alternating highs and lows in the local mean bed elevation with wavelengths at least several

times the mean spacing of the bed forms. The variation in shape of the longitudinal profiles of individual bed forms is similar to that in the lower velocity runs, but on average the profiles of individual bed forms appear more elongated than in the lower velocity runs. (Data on the length/upstream-height ratios of the bed forms are presented in Chapter 6.)

The kinematics of the bed forms observed using the side-view, time-lapse movie photography of the sediment bed appear to be similar to those of the lower velocity runs. The dominant characteristics of the kinematics are the continual overtaking of slipfaces migrating at different rates and the sporadic, spurt-like nature of the migration rates of individual slipfaces.

As in the lower velocity runs, the size and shape of the longitudinal profiles of the bed forms changed as the bed forms migrated downstream, and the identity of individual bed forms was transitory. New slipfaces developed on the stoss sides of existing bed forms in the same way as described for the lower velocity runs. At times, when a new slipface developed far enough upstream on the stoss side of a longer bed form, a second new slipface developed downstream from the first new slipface on the stoss side of the same bed form: the second new slipface appeared to propagate from the first new slipface. Sometimes, both new slipfaces migrated downstream and

sequentially overtook the original slipface, and at other times the original bed form was broken up into two or three separate bed forms.

The sediment movement over the bed forms was similar to that in the lower velocity runs, but the average sediment transport rate appeared to be greater. The sediment movement patterns associated with relatively two-dimensional slipfaces were essentially the same as those observed in Runs 1 through 3. Most of the sediment movement on the stoss sides of bed forms downstream from relatively two-dimensional slipfaces seemed to be controlled by the bursts of sediment movement that emanated from the apparent reattachment area downstream from slipfaces. The overlapping, parallel and subparallel, fan-shaped bursts of sediment movement resulted in a markedly hummocky micro-topography on the upper stoss sides of some of the longer bed forms. The more markedly hummocky micro-topography on the bed forms with greater lengths seemed to be due to a smaller percentage of the bursts of sediment movement propagating all the way to the slipface downstream before subsiding than on bed forms with shorter lengths. As on the planar bed, in places this hummocky micro-topography coalesced to form diagonal and zigzag lineations and diamond-shaped patterns. Figure 5-6 is a plan view (center at 935 cm) of the sediment bed during Run 4-12 (the field of view of this figure is approximately 155 cm long).

The hummocky micro-topography with diagonal and zigzag lineations is evident on the upper stoss sides of the two longest bed forms in this figure, located near the center of the figure; the diagonal lineations on the stoss side of the farther upstream of these two bed forms are particularly pronounced. This figure also shows the spatial variability of both the size and detailed geometry of the bed forms. In places, the features of the hummocky micro-topography developed into well defined slipfaces that migrated downstream. Initially these slipfaces were identified as ripplets.

The sediment movement patterns associated with active, three-dimensional scour pits were also essentially the same as those observed in Runs 1 through 3. As in the lower velocity runs, the local sediment transport rates associated with active, three-dimensional scour pits were markedly greater than those associated with relatively two-dimensional slipfaces.

Section 5-6

Run 5

The average of the mean flow velocities for all of the data sets of Run 5, excluding the initial data set, is 36.1 cm/s. The mean flow conditions during this run were in the two-dimensional dune stability field as delineated by Costello (1974) and Costello and Southard (1981).

The mean length of the major bed forms is 37.6 cm and the mean height is 1.75 cm. As in Runs 1 through 4, at a given time the size of the bed forms in the test section of the flume varied greatly up to the maximum size for the mean flow conditions of this run. In general, the bed forms were relatively three-dimensional; three-dimensional scour pits with longitudinal ridges extending downstream occurred locally downstream from slipfaces. The crestlines did not tend to extend across the full width of the flume. Bed-form height generally varied along slipfaces.

At a given longitudinal position, the size of the bed forms tended to vary across the width of the flume. The variation in size was more noticeable than for the lower velocity runs because of the greater maximum length or spacing of the bed forms. Occasionally, unusually long, narrow bed forms developed along the sidewalls. These bed forms seemed to be generated preferentially downstream from active, three-dimensional scour pits that developed downstream from slipfaces oriented at an acute angle (opening downstream) with the sidewall. With time, these unusually long, narrow bed forms were observed to break up into several bed forms with shorter lengths. Figure 5-7 is a plan view (centered at 810 cm) of the sediment bed during Run 5-3 (the field of view of this figure is approximately 155 cm long). The long, narrow stretch of sediment bed along the near sidewall in this figure is the farthest

upstream 90 cm of the stoss side of a bed form that was 130 cm long; this bed form had a relatively high slipface 40 cm downstream from the downstream end of the field of view. The upstream scour pit is no longer evident, but the remnants of the upstream slipface are still oriented at an acute angle with the sidewall. By approximately three hours after this bed form was first observed, the bed form had broken up into a series of fairly evenly spaced bed forms, each approximately 15 cm long. This figure also shows the spatial variability of both the size and detailed geometry of the bed forms at a given time. As in Runs 1 through 4, there were substantial variations in the detailed geometry of the bed forms both at a given time as a function of longitudinal position and at a given longitudinal position as a function of time.

Small slipfaces were superimposed on larger bed forms. Individual ripplets and/or faint diagonal or V-shaped lineations were common on the upper stoss sides of most of the longer bed forms. Occasionally, ripplets occurred in series. Some ripplet slipfaces were observed to increase in height sufficiently as they migrated downstream to result in the breakup of the bed form on which they developed.

As in Runs 1 through 4, the longitudinal centerline profiles of the sediment bed show that the slipfaces of the major bed forms were not migrating in a single plane; many

slipfaces appear to be overtaking or being overtaken. The centerline profiles show that there were alternating highs and lows in the local mean bed elevation with wavelengths at least several times the mean spacing of the bed forms. The variation in shape of the longitudinal profiles of individual bed forms was similar to that in the lower velocity runs, but on average the profiles appear noticeably more elongated and stretched out than in the lower velocity runs (i.e., the length/upstream-height ratios of many of the bed forms appear noticeably larger).

The kinematics of the bed forms observed using the side-view, time-lapse movie photography of the sediment bed appear to be similar to those of the lower velocity runs. The continual overtaking of slipfaces migrating at different rates and the variable, spurt-like nature of the migration rates of individual slipfaces are the dominant characteristics of the kinematics.

As in the lower velocity runs, the size and shape of the longitudinal profiles of the bed forms changed as the bed forms migrated downstream, and the identity of individual bed forms was transitory. As the maximum length of the bed forms increased with velocity, on average there were fewer bed forms in the field of view of the movie camera at a given time. As a result, the changes in the longitudinal profiles of the longer bed forms can not be observed for as great a distance relative to their lengths

as in the lower velocity runs. On a couple of occasions during Run 5, the stoss side of a single bed form extended across the entire field of view, which was 75 cm long. As in the lower velocity runs, a common deformation sequence gives the impression of a mound of sediment migrating downstream through the bed form; at times, the downstream slope of a mound became unstable and developed into a new slipface. Sometimes a new slipface that developed far enough upstream on the stoss side of a relatively long bed form appeared to propagate sequentially a series of new slipfaces downstream on the stoss side of the original bed form. At times, the development of a series of new slipfaces resulted in the breakup of the original bed form.

The sediment movement over the bed forms was similar to that in the lower velocity runs, but the average sediment transport rate appeared to be greater. The general sediment movement patterns associated with relatively two-dimensional slipfaces were essentially the same as those observed in Runs 1 through 4. Sediment movement on the stoss sides of bed forms downstream from relatively two-dimensional slipfaces seemed to be dominated by the intermittent bursts of sediment movement that emanated from the reattachment area downstream from the slipfaces. The bursts appeared to originate from almost point sources in the reattachment area and then propagate downstream. As the bursts propagated downstream they

tended to spread laterally somewhat, forming fan-shaped streaks of grain motion parallel and subparallel to the mean flow direction. Once a burst of sediment movement occurred, grain motion tended to be sustained in a given longitudinal swath for a few moments after the initial wave of sediment movement passed downstream. As a result, at a given time the most intense grain motion on the stoss side of a bed form tended to be laterally spaced in longitudinal fans; sediment movement did not occur in a continuous sheet of grain motion across the entire width of the bed form. On the upper stoss sides of most of the longer bed forms, the overlapping, fan-shaped bursts of sediment movement resulted in a markedly hummocky micro-topography with diagonal and zigzag lineations and diamond-shaped patterns. In places, features of the hummocky micro-topography developed into ripplets.

On the stoss sides of bed forms, individual grains moved both by rolling over the surface and by hopping or saltating in low trajectories. When viewed from above, the trajectories of the saltating grains along with the greater sediment transport rates gave a somewhat softened appearance to the sediment bed. Upon a cursory glance, the saltating grains gave the impression that more grains were moving at a given time than actually appeared to be the case upon closer examination. At the slipface downstream, grains tended to overshoot the brink of the slipface

somewhat farther, on average, than at lower velocities, but still tended to be deposited mostly on the upper part of the slipface. The slumping or avalanching process on slipfaces appeared to be essentially the same as during the lower velocity runs, but slumping was more frequent. The overtaking process modified the pattern of deposition and avalanching on slipfaces. As the trough area of an overtaking slipface approached the brink of the slipface downstream, the slipface that was being overtaken was usually sheltered, so very little sediment was deposited on its slipface. Then, as the slipface was overtaken, extensive avalanching occurred.

The general sediment movement patterns associated with active, three-dimensional scour pits were also essentially the same as those observed in Runs 1 through 4. As in the lower velocity runs, the local sediment transport rates associated with active, three-dimensional scour pits were markedly greater than those associated with relatively two-dimensional slipfaces. In contrast to the relatively two-dimensional bed forms, the sediment movement immediately downstream from the diagonal separation vortices occurred in fairly continual, broad, sweeping bursts that tended to span the entire width of the bed form downstream from the vortex. Individual bursts of sediment movement tended to be as wide as the lateral extent of the vortex.

If the bed form downstream was long enough, not all of

the bursts of sediment movement propagated to the slipface downstream before subsiding. The repeated subsidence of fairly strong, broad, sweeping bursts of sediment movement on the stoss side of the bed form downstream tended to result in the formation of low but well defined slipfaces which were designated as ripplets. The ripplets that developed downstream from active, three-dimensional scour pits tended to have fairly continuous, curved crestlines convex downstream. Frequently, as a newly developed ripplet slipface propagated downstream, subsiding bursts from the scour pit resulted in the formation of another new ripplet slipface upstream from the first ripplet slipface. In this way series of ripplets were formed.

As new slipfaces developed, migrated downstream, and increased in height, the sediment transport patterns between existing ripplet slipfaces were continually altered. Sometimes an existing ripplet slipface was effectively starved of sediment by the development of a new slipface upstream, while at other times an existing ripplet slipface continued to increase in height after the development of a new slipface upstream.

Section 5-7

Run 6

The average of the mean flow velocities for all of the data sets of Run 6, excluding the initial data set, is

38.0 cm/s. The mean flow conditions during this run were in the two-dimensional dune stability field as delineated by Costello (1974) and Costello and Southard (1981).

The mean length of the major bed forms is 57.8 cm and the mean height is 1.96 cm. As in Runs 1 through 5, at a given time the size of the bed forms in the test section of the flume varied greatly up to the maximum size for the mean flow conditions of this run. In general, the bed forms were relatively three-dimensional; three-dimensional scour pits with longitudinal ridges extending downstream occurred locally downstream from slipfaces. The crestlines of some of the larger bed forms extended across the full width of the flume, but the crestlines of most of the bed forms were discontinuous across the flume. Bed-form height generally varied along slipfaces. At a given longitudinal position, the size of the bed forms tended to vary across the width of the flume; at times, unusually long, narrow bed forms developed along the side walls as described in Run 5. As in Runs 1 through 5, there were substantial variations in the detailed geometry of the bed forms both at a given time as a function of longitudinal position and at a given longitudinal position as a function of time.

Small slipfaces were superimposed on larger bed forms; ripplets were noticeably more common than in the lower velocity runs. Individual ripplets, ripplets in series, and/or diagonal or V-shaped lineations occurred on the

upper stoss sides of most of the bed forms with greater lengths. Ripplets in series occurred most frequently downstream from large, three-dimensional scour pits on the stoss sides of longer bed forms; Run 6 was the lowest velocity run in which ripplets in series were fairly common downstream from large scour pits. Figure 5-8 is a plan view (centered at 950 cm) of the sediment bed during Run 6-6 (the field of view of this figure is approximately 155 cm long). In the center of this figure, there is a series of ripplets downstream from an active, three-dimensional scour pit on the stoss side of a particularly large bed form; these ripplets exhibit the characteristic geometry described in Run 5. In the upper left corner of this figure there are ripplets with more zigzag crestlines which developed downstream from a relatively two-dimensional slipface (not in the field of view); these ripplets are fairly characteristc of incipient ripplets that developed downstream from relatively two-dimensional slipfaces. The geometry of these ripplets is similar to that of the bed forms that initially developed directly from the hummocky micro-topography on the planar bed.

As in Runs 1 through 5, the longitudinal centerline profiles of the sediment bed show that the bed forms were not migrating in a single plane; many slipfaces appear to be overtaking or being overtaken. The centerline profiles show that there were alternating highs and lows in the

local mean bed elevation with wavelengths longer than the mean spacing of the bed forms. However, underlying patterns are not as obvious as for the lower velocity runs because the mean spacing of the bed forms is relatively large compared to the length of the profiles. The variation in the shape of the longitudinal profiles of individual bed forms is similar to that in the lower velocity runs, but on average the profiles appear even more elongated and stretched out than in Run 5 (i.e., the length/upstream-height ratios of many of the bed forms appear larger).

The kinematics of the bed forms observed using the side-view, time-lapse movie photography of the sediment bed appear to be similar to those of the lower velocity runs. As noted in Run 5, as the maximum length of the bed forms increased, the longer bed forms can not be observed in the films for as great a distance relative to their lengths as in the lower velocity runs. At times, the stoss side of a single bed form extended across the entire field of view. Obviously, when this occurs in the films, it is not possible to observe the interaction of adjacent bed forms or a series of bed forms. Nonetheless, the overtaking phenomenon and the variable, spurt-like nature of the migration rates of individual slipfaces are clearly evident and appear to be the dominant characteristics of the kinematics.

As in the lower velocity runs, the size and shape of the longitudinal profiles of the bed forms changed as the bed forms migrated downstream, and the identity of individual bed forms was transitory. Because of the limited length of the field of view of the movie camera, the changes in the longitudinal profiles are most readily observed for the bed forms with shorter lengths; the deformation patterns appear to be similar to those in the lower velocity runs. As described in Run 5, new slipfaces that developed far enough upstream on the stoss side of a relatively long bed form sometimes appeared to propagate sequentially a series of new slipfaces downstream on the stoss side of the original bed form. New slipfaces were also observed to develop and then blend gradually back into the stoss side of the bed form on which they developed.

The sediment movement over the bed forms was similar to that in the lower velocity runs, but the average sediment transport rate appeared to be greater. The general sediment movement patterns downstream from relatively two-dimensional slipfaces were essentially the same as those observed in Runs 1 through 5. As described for Run 5, the overlapping, fan-shaped bursts of sediment movement emanating from the reattachment area resulted in a markedly hummocky micro-topography on the upper stoss sides of most of the longer bed forms. In Run 6, features of the micro-topography developed into ripplets more commonly than

in the lower velocity runs. The greater amount of sediment moved in individual bursts seemed to result in more rapid development of larger bed roughness elements, which in turn seemed to develop more readily into ripplets. As illustrated in Figure 5-9, ripplets that developed downstream from relatively two-dimensional slipfaces initially tended to have diagonal, V-shaped, or zigzag crestlines, similar to those of bed forms that initially developed directly from the hummocky micro-topography on the planar bed. As new slipfaces developed upstream from preexisting ripplet slipfaces and migrated downstream, the sediment transport patterns and the bed geometry of the upper stoss side of the bed form on which the ripplets developed continually changed. Newly developed slipfaces tended to overtake preexisting ripplet slipfaces or be overtaken by newer slipfaces as they migrated downstream. Some newly developed slipfaces increased in height sufficiently as they migrated downstream to result in the breakup of the bed form on which they developed, while others decreased in height until they blended into the stoss side of the bed form. At times, overtaking ripplets resulted in the original major slipface downstream becoming very irregular and/or poorly defined.

The general sediment movement patterns associated with active, three-dimensional scour pits were also essentially the same as those observed in Runs 1 through 5. As in the

lower velocity runs, the local sediment transport rates associated with active, three-dimensional scour pits were markedly greater than those associated with relatively two-dimensional slipfaces. As described in Run 5 and illustrated in Figure 6-9, ripplets that developed downstream from active, three-dimensional scour pits tended to have fairly continuous, curved crestlines which were convex downstream. In general, ripplets that developed in series downstream from three-dimensional scour pits appeared more regular than those that developed downstream from relatively two-dimensional slipfaces. The more regular appearance seemed to result in part from single bursts of sediment movement being as wide as the lateral extent of the vortex. Despite their more regular appearance, these ripplets also tended to overtake the adjacent ripplet slipface downstream or be overtaken and increase or decrease in height as described above for ripplets that developed downstream from relatively two-dimensional slipfaces.

Section 5-8

Run 7

The average of the mean flow velocities for all of the data sets of Run 7, excluding the initial data set, is 40.9 cm/s. The mean flow conditions during this run were in the two-dimensional dune stability field as delineated

by Costello (1974) and Costello and Southard (1981).

The mean length of the major bed forms is 68.5 cm and the mean height is 2.45 cm. As in Runs 1 through 6, at a given time the size of the bed forms in the test section of the flume varied greatly up to the maximum size for the mean flow conditions of this run. In general, the bed forms were relatively three-dimensional; three-dimensional scour pits with longitudinal ridges extending downstream occurred locally downstream from slipfaces.

The crestlines of many of the larger bed forms extended across the full width of the flume. The orientation of the crestlines varied: some were roughly perpendicular to the mean flow, some extended diagonally across the flume, while others pointed downstream with plan profiles shaped like truncated arrowheads (the crestline was roughly penpendicular to the mean flow in the center section of the flume but formed acute downstream angles with each of the sidewalls near the sidewall). This variation in the orientation of the crestlines was also observed for the longer bed forms that extended across the full width of the flume in lower velocity runs. Bed-form height generally varied along slipfaces. Slipfaces that did not extend across the full width of the flume tended to decrease in height gradually as they blended laterally into the stoss side of an adjacent bed form. As in Runs 1 through 6, there were substantial variations in the

detailed geometry of the bed forms both at a given time as a function of longitudinal position and at a given longitudinal position as a function of time.

Small slipfaces were superimposed on larger bed forms; ripplets appeared to be much more common than in any of the lower velocity runs. Ripplets occurred in series on the upper stoss sides of almost all of the longer bed forms and commonly extended across the full width of the bed form. Run 7 was the lowest velocity run in which ripplets occurred in series on the stoss sides of most of the longer bed forms independent of whether or not an active, three-dimensional scour pit occurred upstream. In general, the only bed forms with relatively high slipfaces but no ripplets superimposed on their stoss sides had relatively short lengths. Figure 5-10 is a plan view (centered at 850 cm) of the sediment bed during Run 7-2 (the field of view of this figure is approximately 155 cm long). In the center of this figure there are two bed forms in series which have fairly high slipfaces but do not have ripplets superimposed on their stoss sides; both have relatively short lengths. The bed form immediately upstream from these bed forms with ripplets in series superimposed on its upper stoss side is more than twice as long as these bed forms. Figure 5-10 also shows the spatial variability of both the size and detailed geometry of the bed forms at a given time.

On average, the bed forms in the most upstream section of the flume, upstream of the test section, appeared to be smaller in both height and length than those in the test section. Run 7 was the first run for which the difference in size of the bed forms in the two sections of the flume was particularly evident; on average, the size of the bed forms increased downstream toward the test section. Smaller bed forms occurred interspersed with larger bed forms in the test section of the flume throughout the run, but after the false bottom was covered with sediment, larger bed forms with more extensive series of ripplets superimposed on their stoss sides were not observed to occur in the most upstream section of the flume.

As in Runs 1 through 6, the longitudinal centerline profiles of the sediment bed show that the slipfaces of major bed forms were not migrating in a single plane; many slipfaces appear to be overtaking or being overtaken. The centerline profiles show that there were alternating highs and lows in the local mean bed elevation with wavelengths longer than the mean spacing of the bed forms. However, as noted in Run 6, underlying patterns are difficult to discern because the mean length of the bed forms is relatively large compared to the length of the profiles. In general, the variation in the shape of the longitudinal profiles of individual bed forms is similar to that in the lower velocity runs. On average, the height of the bed

forms appears to have increased proportionately more than the length with the increase in velocity from Run 6 to Run 7; on average, the length/upstream-height ratios of the bed forms appear somewhat smaller than those in Run 6.

The kinematics of the bed forms observed using the side-view, time-lapse movie photography of the sediment bed appear to be similar to those of the lower velocity runs. As noted in Runs 5 and 6, the longer bed forms can only be observed in the films for a relatively short distance compared to their lengths. As a result, it is not possible to observe the interaction of a series of longer bed forms. However, the dominant characteristics of the kinematics appear to be the overtaking of slipfaces migrating at different rates and the variable, spurt-like nature of the migration rates of individual slipfaces.

As in the lower velocity runs, the size and shape of the longitudinal profiles of the bed forms changed as the bed forms migrated downstream, and the identity of individual bed forms was transitory. The deformation patterns appear to be similar to those in the lower velocity runs. New slipfaces commonly formed on the stoss sides of existing bed forms in the same way as described for lower velocity runs. At times, a new slipface appeared to propagate sequentially more new slipfaces downstream on the stoss side of the original bed form. Once new slipfaces developed on the stoss sides of existing bed

forms their subsequent progression varied greatly: sometimes the development of new slipfaces resulted in the breakup of the original bed form, sometimes new slipfaces overtook the original slipface, while at other times they blended back into the stoss side of the original bed form before overtaking its slipface. Occasionally, a whole series of new slipfaces was observed to develop and then blend back into the stoss side of the original bed form. Shortly before a slipface was overtaken, its migration rate tended to decrease markedly and, frequently, its height also decreased.

On the upper stoss sides of some of the bed forms, very low slipfaces, which are barely preceptible in profile in the films, appear to develop and migrate relatively extremely rapidly downstream. The development and migration of these very low slipfaces occur so rapidly in the time-lapse films and the heights of these slipfaces are so low that the details of their development and motion are not discernible.

The sediment movement over the bed forms was similar to that in the lower velocity runs, but the average sediment transport rate appeared to be greater. The general sediment movement patterns associated with relatively two-dimensional slipfaces were essentially the same as those observed in Runs 1 through 6. Sediment movement on the stoss sides of bed forms downstream from

relatively two-dimensional slipfaces seemed to be dominated by the intermittent bursts of sediment movement that emanated from the reattachment area downstream from the slipface. Despite the relatively large average sediment transport rate, at a given time there tended to be no sediment movement on the bed at some locations in the trough area upstream from the reattachment area. As in the lower velocity runs, most of the grain motion in the trough area appeared to originate from radial bursts in the reattachment area. In contrast to three-dimensional scour pits, a strong reverse flow pattern was not evident downstream from relatively two-dimensional slipfaces. In the reattachment area, the sediment moved in intermittent, radial bursts which, on average, appeared stronger than in the lower velocity runs; more sediment moved in individual bursts and individual grains tended to move farther, both vertically and radially.

As in the lower velocity runs, at the downstream end of the reattachment area, bursts of sediment movement propagated predominantly downstream in fan-shaped swaths. The nature of the micro-topography on the upper stoss side of the bed form seemed to be determined by the bursts of sediment movement emanating from the reattachment area. Positive micro-relief seemed to occur where bursts of sediment movement subsided and at the lateral extent of bursts. Some single bursts appeared to be sufficiently

strong to produce immediately noticeable micro-topography: incipient ripplet slipfaces or longitudinal ridges and furrows. When most bursts of sediment movement emanating from the reattachment area propagated all the way to the next slipface downstream before subsiding, the stoss side of the bed form tended to be relatively smooth (i.e., the features of the micro-topography tended to be less pronounced) and ripplet slipfaces did not tend to form. As a bed form increased in length, a smaller percentage of the bursts of sediment movement seemed to propagate all the way to the next slipface before subsiding. In the region where bursts subsided, the bed tended to become markedly hummocky and incipient ripplet slipfaces tended to develop.

The resulting longitudinal variation in the micro-topography on the stoss side of a sufficiently long bed form was generally as follows: 1) in the trough and reattachment areas, the bed tended to be pitted or cratered; 2) downstream on the stoss side of the bed form, the bed was usually relatively smooth or slightly streaky; 3) in the area where bursts of sediment movement first appeared to be subsiding, the bed became increasingly hummocky downstream with incipient ripplet slipfaces developing; and 4) downstream on the upper stoss side of the bed form, ripplets became more fully developed with the heights of slipfaces tending to increase downstream. As noted in Run 6, ripplets that developed downstream from

relatively two-dimensional slipfaces initially tended to have diagonal, V-shaped, or zigzag crestlines; as the ripplets became more fully developed, the crests tended to become longer, straighter, and oriented more nearly perpendicular to the mean flow direction.

Upon a cursory glance, ripplets in series appeared more regular and systematic than actually was the case upon closer examination. Once a ripplet slipface developed downstream from a slipface, its subsequent progression tended to be variable: some increased in height, while others were subsequently eroded or overtaken by a newer slipface from upstream. When bursts of sediment movement did not continue to propagate beyond an existing ripplet slipface or continued with an apparently reduced strength, the slipface seemed to increase in height. On the other hand, when subsequent bursts repeatedly propagated over an existing ripplet slipface, the slipface tended to be eroded. As ripplet slipfaces increased in height, the bursts of sediment movement on the bed downstream from the ripplet slipface seemed to become more independent of the bursts emanating from the reattachment area downstream from the original major slipface upstream.

At times, ripplet slipfaces increased in height sufficiently to break up the downstream end of the bed form on which they developed. As noted in Run 6, ripplets in series tended to overtake the adjacent ripplet downstream

or be overtaken as they migrated downstream; at a given time, the migration rates of adjacent ripplet slipfaces were not the same and, in addition, the migration rates of individual slipfaces seemed to vary as a function of time.

The general sediment movement patterns associated with active, three-dimensional scour pits were essentially the same as those observed in Runs 1 through 6. As in the lower velocity runs, the local sediment transport rates associated with active, three-dimensional scour pits were markedly greater than those associated with relatively two-dimensional slipfaces. The apparent relationships between bursts of sediment movement downstream from reattachment and the development and progression of ripplets described above for ripplets that developed downstream from relatively two-dimensional slipfaces are also generally applicable to ripplets that developed downstream from three-dimensional scour pits. However, the greater sediment transport rates and much wider bursts of sediment movement repeatedly occurring in the same area seemed to result in the more rapid development of ripplets downstream from three-dimensional scour pits; on average, the subsidence of fewer bursts seemed sufficient to generate incipient ripplet slipfaces. The wide, sweeping bursts also seemed to result in the ripplets being more regular in appearance. As described in Runs 5 and 6, ripplets that developed downstream from active, three-dimensional scour

pits tended to have fairly continuous, curved crestlines which were convex downstream; incipient slipfaces that developed from the subsidence of a single burst of sediment movement also had this configuration. As described for ripplets that developed downstream from relatively two-dimensional slipfaces, ripplets in series migrated at different rates and tended to overtake the adjacent ripplet downstream or be overtaken.

Section 5-9

Run 8

The average of the mean flow velocities for all of the data sets of Run 8, excluding the initial data set, is 43.8 cm/s. The mean flow conditions during this run were in the two-dimensional dune stability field as delineated by Costello (1974) and Costello and Southard (1981).

The mean length of the major bed forms is 60.8 cm and the mean height is 2.60 cm. As in Runs 1 through 7, at a given time, the size of the bed forms in the test section of the flume varied greatly up to the maximum size for the mean flow conditions of this run. In general, the bed forms were relatively three-dimensional; three-dimensional scour pits with longitudinal ridges extending downstream occurred locally downstream from slipfaces. As in Run 7, the crestlines of many of the larger bed forms extended across the full width of the flume; the orientation of the

crestlines varied in the same ways as described for Run 7. Bed-form height generally varied along slipfaces. As in Runs 1 through 7, there were substantial variations in the detailed geometry of the bed forms both at a given time as a fuction of longitudinal position and at a given longitudinal position as a function of time.

Small slipfaces were superimposed on larger bed forms; as in Run 7, ripplets were very common. Ripplets occurred singly on the upper stoss sides of some of the bed forms with shorter lengths and occurred in extensive series on the upper stoss sides of most of the bed forms with greater lengths; ripplets commonly extended across the full width of the bed form. As in Run 7, ripplets occurred in series on the stoss sides of most of the longer bed forms independent of whether or not an active, three-dimensional scour pit occurred upstream. The bed forms that did not have ripplets superimposed on their stoss sides tended to have relatively short lengths.

As for Run 7, on average, the size of the bed forms increased progressively downstream from the flume inlet toward the test section. The bed forms farthest upstream were similar in size to bed forms that developed directly from the planar bed or to ripplets that developed on the stoss sides of larger bed forms. Within several meters, the average size of the bed forms increased downstream from ripplet-sized to somewhat larger bed forms without

superimposed ripplets, to still larger bed forms with one or two incipient ripplets just upstream from their slipfaces, to even larger bed forms with series of ripplets superimposed on their upper stoss sides. The longitudinal sequence of bed forms downstream from the flume inlet was similar to the sequence that occurred at a given longitudinal position as a function of time at the beginning of the run when the average size of the bed forms was initially increasing to the equilibrium size. As described for Run 7, smaller bed forms occurred interspersed with larger bed forms in the test section of the flume throughout the run. After the false bottom was covered with sediment, however, larger bed forms with extensive series of ripplets were not observed to occur in the most upstream section of the flume. The average size of the bed forms in the meter of the test section farthest upstream appeared to be slightly smaller than that of the bed forms in the rest of the test section. The largest bed forms in this section tended to have only one or two ripplets superimposed on their stoss sides.

As in Runs 1 through 7, the longitudinal centerline profiles of the sediment bed show that the slipfaces of major bed forms were not migrating in a single plane; many slipfaces appear to be overtaking or being overtaken. The centerline profiles show that there were alternating highs and lows in the local mean bed elevation with wavelengths

longer than the mean spacing of the bed forms. However, as noted in Runs 6 and 7, underlying patterns are difficult to discern because the mean length of the bed forms is relatively large compared to the length of the profiles. In general, the variation in the shape of the longitudinal profiles of individual bed forms is similar to that in the lower velocity runs.

The kinematics of the bed forms observed using the side-view, time-lapse movie photography of the sediment bed appear to be similar to those of the lower velocity runs. As noted in Runs 5 through 7, the longer bed forms can only be observed in the films for a relatively short distance compared to their lengths; frequently, only portions of two adjacent bed forms were in the field of view of the movie camera at a given time. However, the overtaking of slipfaces migrating at different rates and the variable, spurt-like nature of the migration rates of individual slipfaces appear to be the dominant characteristics of the kinematics.

As in the lower velocity runs, the size and shape of the longitudinal profiles of the bed forms changed as the bed forms migrated downstream, and the identity of individual bed forms was transitory. The deformation patterns appear to be similar to those in the lower velocity runs. The details of the changes in the profiles are somewhat more difficult to observe than for the lower

velocity runs because the average migration rate of the bed forms increased more rapidly than the rate at which the individual movie frames were taken. As described for Run 7, very low slipfaces developed on the upper stoss sides of many of the bed forms and appeared to migrate relatively extremely rapidly downstream. As these initially low slipfaces migrated downstream, they appeared to increase in height noticeably more than similar slipfaces in Run 7. The development, growth, rapid migration, and overtaking of initially low slipfaces on the upper stoss sides of bed forms continually changed the downstream portion of the longitudinal profiles of these bed forms. The changes occur so rapidly in the time-lapse films that the details of the development and motion of the initially low slipfaces are not really distinguishable. At times in the films, the increase in height of initially low slipfaces appeared to result in the decrease of the migration rate and/or height of the original major slipface downstream.

In general, the sediment movement over the bed forms was similar to that in the lower velocity runs, but the average sediment transport rate appeared to be substantially greater. The general sediment movement patterns on the bed forms downstream from relatively two-dimensional slipfaces were essentially the same as those observed in Runs 1 through 7. However, the sediment movement patterns appeared noticeably more exaggerated than

for the lower velocity runs because of the greater sediment transport rates. The sediment movement on the stoss sides of the bed forms seemed to be dominated by the bursts of sediment movement that emanated from the reattachment area downstream from the slipface. On average, the bursts of sediment movement appeared stronger than for lower velocity runs: more grains moved in individual bursts and the individual grains appeared to move farther. In addition, the rate at which bursts of sediment movement occurred appeared greater.

As described for Run 7, the nature of the micro-topography on the stoss sides of the bed forms seemed to be determined by the bursts of sediment movement emanating from the reattachment area; positive micro-relief seemed to occur where bursts subsided and at the lateral extent of bursts. On average, the greater strength and more rapid rate of the bursts of sediment movement resulted in the micro-topography changing more rapidly than in the lower velocity runs. Longitudinal ridges and furrows constantly shifted position and, on average, fewer bursts seemed necessary for the development of incipient ripplets. As described for Run 7, when most bursts of sediment movement emanating from the reattachment area propagated all the way to the next slipface downstream before subsiding, ripplet slipfaces did not tend to form. As a bed form increased in length, a smaller percentage of the bursts seemed to

propagate all the way to the next slipface before subsiding, and incipient ripplet slipfaces tended to develop. In general, the longitudinal variation in the micro-topography on the stoss side of a bed form was the same as described for Run 7.

Once a ripplet developed on the stoss side of a bed form, its subsequent progression appeared to be largely determined by the nature of the subsequent bursts of sediment movement emanating from the reattachment area, as described for Run 7. Some ripplets increased in height, while others were eroded or overtaken by a newer ripplet from upstream. The strength of individual bursts of sediment movement in a succession of bursts tended to vary; consequently the progression of ripplets varied. For example, several bursts in succession might result in a ripplet slipface initially increasing in height, and then the next few bursts might be stronger, propagate over the ripplet slipface, and consequently result in the slipface being eroded. As ripplet slipfaces increased in height, the bursts of sediment movement on the bed downstream from the ripplet slipface seemed to become more independent of the bursts emanating from the reattachment area downstream from the original major slipface upstream. Sometimes, when a new ripplet slipface developed upstream from an existing ripplet slipface and a large percentage of the subsequent bursts of sediment movement did not continue to propagate

beyond the new slipface, the preexisting slipface would be eroded and effectively replaced by the newer slipface from upstream. Frequently, when a ripplet slipface immediately upstream from a major slipface had increased sufficiently in height, the major slipface appeared to be starved of sediment in a similar manner. Commonly both the migration rate and the height of the major slipface would decrease. Sometimes a ripplet slipface increased sufficiently in height far enough upstream from the next major slipface downstream to break up the bed form. At times the downstream end of the original bed form became a separate bed form with a high slipface but a relatively short length and with no superimposed ripplets.

On the stoss sides of bed forms, individual grains appeared to move predominantly by saltating in ballistic trajectories. On average, the trajectories appeared longer than for lower velocity runs. As the average sediment transport rate increased with velocity, the trajectories of the saltating grains, when viewed from above, gave an increasingly softened appearance to the sediment bed on the stoss sides of bed forms, but when viewed from the side, the trajectories of the individual grains were clearly distinguishable.

At the slipface downstream, grains tended to overshoot the brink of the slipface and be deposited mostly on the upper part of the slipface, but some grains overshot the

brink by the entire length of the slipface in the flow direction. The slumping or avalanching process of the slipfaces appeared to be essentially the same as during the lower velocity runs: the upper part of the slipface oversteepened until it became unstable and slumped or avalanched to the base of the slipface. On average slumping seemed to occur more frequently than for the lower velocity runs. As described for Run 5, the overtaking process modified the pattern of deposition and avalanching on slipfaces. Just prior to being overtaken, a slipface appeared to be sheltered; less sediment tended to be deposited on the slipface, so avalanching occurred less frequently. As the slipface was overtaken, extensive avalanching occurred.

The general sediment movement patterns associated with three-dimensional scour pits were essentially the same as those observed in Runs 1 through 7. The three-dimensional scour pits seemed to occur preferentially downstream from where there was a marked contrast in the height of adjacent sections of a slipface or where a slipface pinched out laterally. The flow appeared to be channeled through the relatively low section, curl around the adjacent high section, and then spiral diagonally downstream in the trough downstream from the high section of the slipface. Commonly, the high section of the slipface was oriented diagonally downstream roughly parallel to the vortex, but

at times the slipface was oriented more nearly perpendicular to the mean flow, and the axis of the vortex formed an acute angle with the baseline of the slipface. As in the lower velocity runs, the local sediment transport rates associated with active, three-dimensional scour pits were markedly greater than those associated with relatively two-dimensional slipfaces.

As noted for Run 7, the apparent relationships between bursts of sediment movement downstream from reattachment and the development and progression of ripplets that developed downstream from relatively two-dimensional slipfaces are generally applicable to ripplets that developed downstream from three-dimensional scour pits. The secondary differences in the development and progression of ripplets downstream from two-dimensional slipfaces and three-dimensional scour pits were essentially the same as those described for Run 7.

Section 5-10

Run 9

The average of the mean flow velocities for all of the data sets of Run 9, excluding the initial data set, is 47.4 cm/s. The mean flow conditions during this run were in the three-dimensional dune stability field as delineated by Costello (1974) and Costello and Southard (1981).

The mean length of the major bed forms is 54.2 cm and

the mean height is 2.74 cm. As in Runs 1 through 8, at a given time the size of the bed forms in the test section of the flume varied greatly up to the maximum size for the mean flow conditions of this run. In general, the bed forms were relatively three-dimensional; three-dimensional scour pits with longitudinal ridges extending downstream occurred locally downstream from slipfaces. As in Runs 7 and 8, the crestlines of many of the larger bed forms extended across the full width of the flume; the orientation of the crestlines varied in the same ways as described for Run 7. Bed-form height generally varied along slipfaces. As in Runs 1 through 8, there were substantial variations in the detailed geometry of the bed forms both at a given time as a function of longitudinal position and at a given longitudinal position as a function of time.

Small slipfaces were superimposed on larger bed forms; as in Runs 7 and 8, ripplets were very common. Ripplets occurred in extensive series on the upper stoss sides of most of the bed forms with greater lengths independent of whether or not a three-dimensional scour pit occurred upstream. Ripplets also occurred singly on the upper stoss sides of some of the bed forms with shorter lengths. The bed forms that did not have any ripplets superimposed on their stoss sides tended to have relatively short lengths. Figures 5-11 and 6-12 are plan views (centered at 850 cm)

of the sediment bed taken during Runs 9-5 and 9-7, respectively (the field of view of each figure is approximately 155 cm long). These figures show both the variation in the occurrence of ripplets and the large variation in the geometry of the bed forms at a given longitudinal position as a function of time. The bed forms in the center of Figure 5-10 have relatively short lengths and either have no ripplets superimposed on their stoss sides or very few ripplets. The bed form downstream from the three-dimensional scour pit at the top of Figure 5-10 has ripplets in series superimposed on its stoss side; these ripplets are fairly evenly spaced and have curved crestlines convex downstream characteristic of ripplets that developed downstream from active, three-dimensional scour pits. The large bed form in the center of Figure 5-11 has extensive series of ripplets on its stoss side; the upstream slipface (not in the field of view) was relatively two-dimensional. The ripplets are somewhat less regular in appearance than those in Figure 5-10 downstream from the three-dimensional scour pit and are fairly typical of ripplets that developed downstream from relatively two-dimensional slipfaces. The relatively high ripplet slipfaces immediately upstream from the major slipface in the center of Figure 5-11 appear to have increased in height at the expense of the major slipface, as described in Run 8. Frequently, when the ripplet slipfaces

immediately upstream from a major slipface became relatively high, both the height and migration rate of the major slipface tended to decrease. In this way, the length or spacing of the bed forms appeared to be limited.

As for Run 7 and 8, on average, the size of the bed forms increased progressively downstream from the flume inlet toward the test section. In general, the longitudinal sequence of bed forms downstream from the flume inlet was the same as that described for Run 8. In the test section of the flume, smaller bed forms occurred interspersed with larger bed forms throughout the run, but after the false bottom was covered with sediment, larger bed forms with extensive series of ripplets were not observed to occur in the most upstream section of the flume. As in Run 8, the average size of the bed forms in the farthest upstream meter of the test section appeared to be slightly smaller than that of the bed forms in the rest of the test section.

As in Runs 1 through 8, the longitudinal centerline profiles of the sediment bed show that the slipfaces of major bed forms were not migrating in a single plane; many slipfaces appear to be overtaking or being overtaken. The centerline profiles show that there were alternating highs and lows in the local mean bed elevation with wavelengths longer than the mean spacing of the bed forms. However, as noted in Runs 6 through 8, underlying patterns are

difficult to discern because the mean spacing of the bed forms is relatively large compared to the length of the profiles. In general, the variation in the shape of the longitudinal profiles of individual bed forms is similar to that in the lower velocity runs.

The kinematics of the bed forms observed using the side-view, time-lapse movie photography of the sediment bed appear to be similar to those of the lower velocity runs. As noted in Runs 5 through 8, the longer bed forms can be observed in the films only for a relatively short distance compared to their lengths. Nevertheless, the overtaking of slipfaces migrating at different rates and the variable, unsteady nature of the migration rates of individual slipfaces appear to be the dominant characteristics of the kinematics.

As in the lower velocity runs, the size and shape of the longitudinal profiles of the bed forms changed as the bed forms migrated downstream, and the identity of individual bed forms was transitory. In the films, the changes in the profiles occur more rapidly than in any of the lower velocity runs; the average migration rate of the bed forms relative to the rate at which individual movie frames were taken is larger than for any of the other runs. As a result, some changes, particularly those in the smaller and intermediate-sized bed forms, occur too rapidly to distinguish unambiguously the apparent sequence of

events. However, in general, the deformation patterns appear to be similar to those in the lower velocity runs.

As described for Runs 7 and 8, low slipfaces developed on the upper stoss sides of many of the bed forms and appeared to migrate relatively extremely rapidly downstream. On average, these initially low slipfaces appeared to increase in height more as they migrated downstream than similar slipfaces in Run 8. The development, growth, migration, and interaction of newly developed, initially low slipfaces occurred so rapidly relative to the rate at which individual movie frames were taken that the details of the changes in the profiles are not distinguishable in the films. At times, the profile of what seemed to be the downstream end of a relatively large bed form gives the impression of a series of small to intermediate-sized slipfaces rapidly migrating downstream and overtaking one another.

In general, the sediment movement over the bed forms was similar to that in the lower velocity runs; however, the average sediment transport rate appeared to be dramatically greater. As a result of the greater sediment transport rates, the sediment movement patterns appeared much more exaggerated than in the lower velocity runs. At times in Run 9, some sediment appeared to act briefly almost as flow markers: once set in motion, the sediment appeared to move briefly with the flow. The general

sediment movement patterns on the bed forms downstream from relatively two-dimensional slipfaces were essentially the same as those observed in Runs 1 through 8. The sediment movement on the stoss sides of the bed forms seemed to be dominated by the bursts of sediment movement that emanated from the reattachment area downstream from the slipface. On average, the bursts appeared stronger and more exaggerated than those in Run 8 and seemed to occur more frequently. At times, sediment moved in bursts in the reattachment area appeared to be gustily whipped around in all directions by the flow. Despite the large average sediment transport rate and violent bursts of sediment movement, at a given time there tended to be no sediment movement on the bed at some locations in the trough area upstream from the reattachment area. As in the lower velocity runs, most of the grain motion in the trough area appeared to originate from radial bursts of sediment movement in the reattachment area. In contrast to three-dimensional scour pits, a strong reverse flow pattern was <u>not</u> evident downstream from relatively two-dimensional slipfaces. In general, there did not appear to be strong reverse flow patterns downstream from relatively two-dimensional slipfaces for any of the average flow conditions of these experiments.

As in the lower velocity runs, at the downstream end of the reattachment area, bursts of sediment movement

propagated predominantly downstream in fan-shaped swaths. Sometimes grains moved in these bursts appeared to change direction laterally as they moved downstream in the flow. Also, at times, grains moved at the downstream extent of a burst of sediment movement appeared to be flipped up by the flow. As described for lower velocity runs, the nature of the micro-topography on the stoss sides of the bed forms seemed to be determined by the bursts of sedimennt movement emanating from the reattachment area. On average, the greater strength of the bursts of sediment movement and the more rapid rate of the bursts resulted in the micro-topography changing relatively very rapidly; commonly, enough sediment was moved in individual bursts to result in immediately noticeable changes in the micro-topography. As described for Runs 7 and 8, when most bursts of sediment movement emanating from the reattachment area propagated all the way to the next slipface downstream before subsiding, ripplet slipfaces did not tend to form. As a bed form increased in length, a smaller percentage of the bursts seemed to propagate all the way to the next slipface before subsiding and incipient ripplet slipfaces tended to develop. In general, the longitudinal variation in the micro-topography on the stoss side of a bed form was the same as described for Run 7.

Once a ripplet developed on the stoss side of a bed form, its subsequent progression appeared to be largely

determined by the nature of the subsequent bursts of sediment movement emanating from the reattachment area in the ways described for Runs 7 and 8. The apparent relationship between the bursts of sediment movement and the development and progression of ripplets was more evident than in lower velocity runs because of the greater strength of the bursts and, consequently, the more immediately noticeable changes in the ripplets. The strength of individual bursts in a succession of bursts tended to vary; consequently the progression of ripplets varied. Once ripplet slipfaces developed, some continued to increase in height while others were eroded or overtaken by a newer ripplet slipface from upstream. As noted for Run 7, ripplet slipfaces seemed to increase in height when bursts of sediment movement did not continue to propagate beyond the slipface or continued with an apparently reduced strength. Existing ripplet slipfaces seemed to be eroded either when subsequent bursts repeatedly propagated over the existing slipface or when a new ripplet slipface developed upstream from the existing slipface and a large percentage of the subsequent bursts did not continue to propagate beyond the new slipface, apparently effectively starving the preexisting slipface of sediment.

For this average flow velocity, noticeable changes occurred in ripplets very rapidly. Some incipient ripplet slipfaces were observed to be completely eroded in roughly

half a minute. The trajectories of saltating grains on the stoss sides of ripplets seemed to result in the ripplet slipfaces appearing higher than they actually were; at times, when there was a brief pause in the bursts, some ripplet slipfaces with low heights became barely noticeable. As noted for lower velocity runs, ripplets in series migrated at different rates and tended to overtake the adjacent ripplet downstream or be overtaken as they migrated downstream.

Despite the noticeably greater average sediment transport rate, the basic sediment transport modes of individual grains on the stoss sides of bed forms appeared to be predominantly the same as in the lower velocity runs; individual grains appeared to move mostly by saltating in ballistic trajectories. On average the trajectories appeared noticeably longer than for lower velocity runs. At times some grains appeared to be briefly carried with the flow. When viewed from above, the trajectories gave an even more softened appearance to the sediment bed on the stoss sides of bed forms than for Run 8, but the trajectories of individual grains were still distinguishable. The slumping or avalanching process of slipfaces appeared to be essentially the same as during the lower velocity runs; however, because of the greater average sediment transport rate, slumping seemed to occur much more frequently.

The general sediment movement patterns associated with active, three-dimensional scour pits were essentially the same as those observed in Runs 1 through 8. As in the lower velocity runs, the local sediment transport rates associated with active, three-dimensional scour pits were markedly greater than those associated with relatively two-dimensional slipfaces. The similarities and differences in the development and progression of ripplets downstream from relatively two-dimensional slipfaces and downstream from three-dimensional scour pits were essentially the same as those described for lower velocity runs. The nature of the bursts of sediment movement downstream from reattachment appeared to be the dominant influence in the development and progression of ripplets. As observed in the lower velocity runs, the relatively strong, diagonal vortices associated with active three-dimensional scour pits appeared to be particularly transient. With time, three-dimensional scour pits tended to become more two-dimensional. After the subsidence of a strong, diagonal vortex, the sediment movement downstream from the scour pit tended to be basically the same as that downstream from relatively two-dimensional slipfaces even while the bed geometry was still roughly similar to that when the scour pit was active. The local sediment transport rates tended to be greatly reduced and sediment movement occurred in less frequent, apparently more random, relatively narrow,

fan-shaped bursts of movement, as opposed to fairly continual, broad, sweeping bursts of sediment movement spanning the entire width of the bed form downstream from the vortex. Longitudinal ridges gradually blended into the stoss sides of bed forms. The length of the bed forms downstream from three-dimensional scour pits varied; both bed forms with short lengths and no superimposed ripplets and bed forms with relatively very long lengths and ripplets in series were observed downstream from three-dimensional scour pits. Some bed forms downstream from active three-dimensional scour pits that had short lengths and high slipfaces with no superimposed ripplets when they were first observed, later, after the vortex subsided, were observed to have much longer lengths with ripplets in series superimposed on their stoss sides.

Section 5-11

Runs 10, 11, and 12

Runs 10, 11, and 12 are supplementary runs, carried out to observe and compare directly within a relatively short time period bed forms in the three different stability fields observed in Runs 1 through 9. The mean flow velocities for Runs 10, 11,and 12 were 32.3 cm/s, 38.4 cm/s, and 47.4 cm/s, respectively, and the mean flow conditions during these runs were in the ripple, two-dimensional dune, and three-dimensional dune stability

fields, respectively.

The sizes of the equilibrium bed forms for each of these runs were within the range of sizes observed for the primary runs with similar mean flow conditions. As for all the primary runs, the size of the bed forms in the test section of the flume at a given time varied greatly up to the maximum size for the mean flow conditions of the run.

The general appearance of the bed forms and the variation in the appearance of the bed forms for each of these runs were likewise similar to those observed for the primary runs with similar mean flow conditions. In general, the bed forms were relatively three-dimensional; the occurrence of active, three-dimensional scour pits locally downstream from slipfaces was common for all three runs.

As for all the primary runs, the detailed geometry and size of the bed forms varied substantially at a given location as a function of time. This variation seemed to reflect at least in part the continual generation and growth of new slipfaces on the stoss sides of existing bed forms (thereby limiting the length of the existing bed forms) and the erosion and being overtaken of existing slipfaces.

Figures 5-12 and 5-13 are plan views (centered at 750 and 770 cm, respectively) of the sediment bed taken during Run 11-2 (the field of view of each figure is

approximately 155 cm long); these figures illustrate relatively long bed forms being broken up by the development of smaller bed forms on their stoss sides. In Figure 5-12, there are two unusually long bed forms with very few small slipfaces superimposed on their stoss sides. Figure 5-13 shows these same major bed forms one hour and 35 minutes later after smaller bed forms had developed on their stoss sides and were starting to break up the original bed forms. By this time the major slipface downstream from the large bed form near the far wall in Figure 5-12 was no longer clearly defined. Approximately three hours later, the bed forms in this same section of the flume were intermediate in size between the smaller bed forms in Figure 5-13 and the unusually long bed forms in Figure 5-12.

Figures 5-14 and 5-15 are plan views (centered at 880 cm) of the sediment bed taken during Run 10-3; these figures illustrate relatively small bed forms increasing in size with time. There is a series of relatively small bed forms in the upper righthand section of Figure 5-14. Figure 5-15 shows this same series of bed forms approximately 30 minutes later; the average length of the bed forms in the series has increased and the relatively high slipface downstream appears to be about to be overtaken. Figure 5-14 and Figure 5-15 also illustrate the spatial variability of both the size and the detailed

geometry of the bed forms.

Small slipfaces were superimposed on larger bed forms in all three runs; the occurrence of ripplets for each of these runs was similar to that observed for the primary runs with similar mean flow conditions. In Run 10 very low slipfaces most frequently occurred singly; however, short series of very low slipfaces were occasionally observed. Diagonal and/or V-shaped lineations occurred on the upper stoss sides of longer bed forms. In Run 11 ripplets were noticeably more common than in Run 10. Individual ripplets, ripplets in series, and/or diagonal or V-shaped lineations occurred on the upper stoss sides of most of the longer bed forms; however, as illustrated in Figure 5-12, for limited time periods some unusually long bed forms were observed to have very few superimposed ripplets. In Run 12 ripplets were very common; ripplets occurred singly on the upper stoss sides of some of the bed forms with shorter lengths and occurred in series on the stoss sides of bed forms with greater lengths. Longer bed forms with no superimposed ripplets were not observed, even for short time periods.

The longitudinal centerline profiles of the sediment bed show that the slipfaces of major bed forms were not migrating in a single plane for any of these runs. As for all the primary runs, some slipfaces appear to be migrating up stoss side of the adjacent bed form downstream and

overtaking the slipface downstream, while other slipfaces appear to be being overtaken. The overtaking phenomenon is illustrated by the time-lapse movie photography. For all three runs, the centerline profiles show that there tended to be alternating highs and lows in the local mean bed elevation with wavelengths longer than the mean spacing of the bed forms. The variation in the shape of the longitudinal profiles of the bed forms for each of these runs is similar to that for the primary runs with similar mean flow conditions.

The kinematics of the bed forms were examined using plan-view, time-lapse movie photography. As for all the primary runs, the continual overtaking of slipfaces migrating at different rates and the variable, unsteady nature of the migration rates of individual slipfaces appear to be the dominant characteristics of the kinematics for all three runs.

In addition, the bed configuration continually changed for all three runs; the variable nature of the bed configuration is particularly noticeable in the plan-view films. As for all the primary runs, the size of individual bed forms continually changed; the changes in the lengths of the bed forms are most evident because of the overhead perspective of the photography. The different and variable migration rates of adjacent slipfaces resulted in the lengths of the bed forms increasing and/or decreasing with

time in variable patterns. In addition, the development of new slipfaces on the stoss sides of existing bed forms and the erosion of existing slipfaces changed the length between adjacent slipfaces. As for all the primary runs, the identity of individual bed forms was transitory and, at times, ambiguous; the most readily identifiable feature of a bed form is the slipface.

The generation of new slipfaces is more evident in the plan-view films than in the side-view films; smaller differences in elevation are distinguishable. In Run 10 new slipfaces most frequently developed singly on the stoss side of a bed form; new slipfaces tended to grow into a major slipface, overtake the next slipface downstream, or be eroded before another new slipface developed upstream from the original new slipface. Faint lineations or low slipfaces developed repeatedly on the upper stoss sides of some of the bed forms and then overtook the major slipface downstream, but they usually did not develop rapidly enough to form a series of very low slipfaces. At times a new slipface appeared to propagate one or more new slipfaces downstream on the stoss side of an existing bed form. In Runs 11 and 12 new slipfaces developed so rapidly compared to the rate at which the individual movie frames were taken that the details of the development and progression of most individual slipfaces, while they were relatively low, are not distinguishable; however, general patterns are

evident. In Run 12, new slipfaces appeared to develop most commonly in relatively rapid succession immediately upstream from the most recently developed slipface on the stoss side of a bed form, thereby forming series of relatively low slipfaces. When a new slipface developed downstream from a major slipface, more new slipfaces appeared to develop upstream from the original new slipface before it had increased in size substantially, had overtaken the next major slipface downstream, or had been eroded. In Run 11 new slipfaces did not appear to develop as rapidly as in Run 12; however, they commonly developed rapidly enough to form series of ripplets as described for Run 12. At times, a series of new slipfaces appeared to develop by a new slipface propagating more new slipfaces downstream on the stoss side of a bed form as opposed to the repeated development of new slipfaces immediately upstream from the most recently developed slipface.

The erosion of existing slipfaces is also more evident in the plan-view films than in the side-view films. For all three runs, slipfaces at various stages of development were observed to be eroded. Sometimes new slipfaces were eroded shortly after they developed while, at other times, relatively high, major slipfaces that were being overtaken were completely eroded before being overtaken.

In general, as for the primary runs, the modes of sediment movement and longitudinal variation in the

sediment movement patterns on bed forms were observed to be basically the same for all three runs. However, some aspects of the sediment movement became more evident as the mean flow velocity increased because 1) the processes occurred more rapidly and 2) more sediment was involved in the processes. As for the primary runs, for a given mean flow velocity, the general patterns of sediment movement on the stoss sides of bed forms varied somewhat depending on whether the upstream slipface was relatively two-dimensional or whether an active, three-dimensional scour pit had developed in the trough downstream from the slipface. The development of three-dimensional scour pits was common for all three runs. In both cases, the sediment movement on the stoss sides of bed forms appeared to be dominated by the nature of the bursts of sediment movement emanating from the apparent reattachment area; consequently the nature of the micro-topography on the stoss sides of the bed forms and ultimately the bed geometry appeared to be determined by these bursts, as described for the primary runs. For a given mean flow velocity, differences in the bed geometry downstream from relatively two-dimensional slipfaces and downstream from three-dimensional scour pits appeared to result from secondary differences in the nature of the bursts of sediment movement emanating from the reattachment area. Likewise, differences in the bed geometry as the mean flow

velocity increased appeared to result from changes in the nature of these bursts of sediment movement as the flow velocity increased.

The general sediment movement patterns on the bed forms downstream from relatively two-dimensional slipfaces were the same as those described for the primary runs. As the mean flow velocity increased, the nature of the bursts of sediment movement downstream from reattachment changed in the same ways as observed for the primary runs; both the rate at which bursts occurred and the amount of sediment moved in individual bursts increased. In Run 10 there tended to be pauses in the sediment movement between successive bursts emanating from a given section of the reattachment area, and the amount of sediment moved in a individual burst tended to result in barely noticeable changes in the micro-topography. However, if a given area on the upper stoss side of a bed form was closely observed for a period of time, changes could be seen in the micro-topography which were due to the cumulative effect of multiple bursts of sediment movement having subsided in approximately the same area.

In contrast, in Run 12 successive bursts of sediment movement emanating from a given section of the reattachment area commonly began before the preceding burst from that section had subsided, and frequently enough sediment was moved in individual bursts to result in immediately

noticeable changes in the bed topography. If a bed form was long enough so that most bursts of sediment movement subsided before reaching the next major slipface downstream, ripplet slipfaces tended to develop on the stoss side of the bed form. New ripplet slipfaces tended to develop rapidly enough compared to the rate of growth, migration, or erosion of existing ripplet slipfaces to form series of ripplets on the stoss side of the bed form. The general relationships between bursts of sediment movement downstream from reattachment and the development and progression of ripplets were the same as described for the primary runs. The basic processes appeared to be the same both downstream from two-dimensional slipfaces and downstream from three-dimensional scour pits.

In Run 11, the frequency and strength of bursts of sediment movement varied and appeared to be intermediate between that in Run 10 and that in Run 12. Series of ripplets were fairly common on the stoss sides of the longer bed forms, but, as noted earlier, for limited periods of time some unusually long bed forms were observed to have very few superimposed smaller bed forms. Ripplet slipfaces did not always tend to develop rapidly enough to form series of ripplets by the repeated development of new ripplet slipfaces upstream from existing ripplet slipfaces.

The laterally spaced, overlapping, fan-shaped bursts of sediment movement downstream from relatively two-

dimensional slipfaces resulted in ripplets that initially tended to have diagonal, V-shaped, or zigzag crestlines. The ripplet crestlines tended to become longer, straighter, and oriented more nearly perpendicular to the mean flow as the ripplet slipfaces increased in height.

As for the primary runs, strong reverse flow patterns were not observed downstream from relatively two-dimensional slipfaces in any of these runs. Even for Run 12, as for Run 9, there tended to be relatively little grain motion in the trough area downstream from the slipface and upstream from the reattachment area; most of the grain motion in this area appeared to originate from radial bursts of sediment movement in the reattachment area.

The basic sediment transport modes of individual grains on the stoss sides of bed forms appeared to be predominantly the same for all three runs despite the greatly different average sediment transport rates: individual grains appeared to move mostly by saltating in ballistic trajectories. As for the primary runs, as the mean flow velocity increased, the trajectories appeared to become longer. Also, as the average sediment transport rate increased with the mean flow velocity, the trajectories gave a more softened appearance to the sediment bed when viewed from above.

For Run 10, at a given location on the stoss side of a

bed form, there tended to be pauses in the sediment movement: a burst of sediment movement would propagate downstream, grain motion would be sustained for a few moments in the given swath made by the burst, and then the sediment movement would subside until the next burst. Once a sediment grain was set in motion, it seemed more likely than average to continue to be moved. Grains that were moved in a series of hops sometimes zigzagged downstream as observed in Run 9: sometimes, successive hops had oppositely directed lateral components of motion.

For Run 12, successive bursts of sediment movement occurred rapidly enough that there tended to be some sediment movement in a given area on the upper stoss side of a bed form all of the time; however, as successive bursts of sediment movement propagated downstream and subsided, the intensity of the grain movement varied with time.

For Run 11, at different times and at different locations, the frequency and strength of bursts of sediment movement varied substantially: at times, the sediment movement on a given area of the sediment bed appeared more like that described for Run 10 while, at other times, it appeared more similar to that for Run 12, though not as great.

The slumping or avalanching process of slipfaces appeared to be essentially the same for all three runs, but

as for the primary runs, as the average sediment transport rate increased with mean flow velocity, the slumping occurred more frequently.

As for the primary runs, the development of three-dimensional scour pits was common for all three runs. The apparent flow patterns and consequent sediment movement patterns associated with three-dimensional scour pits were basically the same for the entire range of conditions of these experiments. These patterns were also essentially the same as those described for the propagation of highly three-dimensional bed forms on the planar bed. The three-dimensional scour pits seemed to occur preferentially downstream from where there was a marked contrast in the height of adjacent sections of a slipface or where a slipface pinched out laterally. The flow appeared to be channeled through the low section, curl around the adjacent high section, and then spiral diagonally downstream forming a relatively strong separation vortex in the trough downstream from the high section of the slipface; the diagonal vortices were commonly oriented at about a 45^{o} angle to the mean flow or the sidewalls.

As noted for the primary runs, for a given mean flow velocity the most striking difference between the sediment movement associated with relatively two-dimensional slipfaces and that associated with active, three-dimensional scour pits was the markedly greater, local

sediment transport rates that appeared to result from the relatively strong, diagonal vortices associated with three-dimensional scour pits. For all three runs, the reverse flow in the scour pits was very pronounced: sediment was transported almost continuously back up the slipface forming a ridge on the slipface which extended downstream as described for the primary runs. Downstream from the reattachment area, the sediment movement occurred in broad, sweeping bursts that tended to span the entire width of the bed form downstream from the vortex. Both the rate at which these bursts of sediment movement occurred and the amount of sediment moved in individual bursts were greater than those downstream from relatively two-dimensional slipfaces.

As noted above, the axes of the unusually strong, vortices were oriented at an acute angle to the mean flow or sidewalls, commonly at roughly a 45^{o} angle. The unusual strength of the vortices might be due to the chance orientation of the axes of the vortices with the mean strain rate as the flow curls around the side or edge of a slipface (i.e., at an acute angle with a boundary). As noted by Tennekes and Lumley (1972), "the most powerful eddies thus are those that can absorb energy from the shear flow more effectively than others. Evidence suggests that the eddies that are more effective than most ... in extracting energy from the mean flow are vortices whose

principal axis is roughly aligned with that of the mean strain rate."

For a given mean flow velocity, the differences in the bed geometry downstream from relatively two-dimensional slipfaces and downstream from three-dimensional scour pits appeared to result from the differences in the nature of the bursts of sediment movement downstream from reattachment as described for the primary runs. Both the greater local sediment transport rates and the much wider, more directed bursts of sediment movement downstream from three-dimensional scour pits seemed to result in the more rapid development of ripplets and, consequently, the greater probability of series of ripplets. The much wider, more directed bursts also seemed to result in the development of somewhat more regular ripplets with fairly continuous, characteristically curved crestlines. In addition, unusually long, narrow bed forms seemed to occur preferentially downstream from three-dimensional scour pits; the width of the bed form tended to be approximately the same as the length of the vortex.

For the primary runs, series of ripplets and unusually long bed forms tended to occur downstream from three-dimensional scour pits at lower mean flow velocities than they tended to occur downstream from relatively two-dimensional slipfaces, apparently primarily as a result of the greater, local sediment transport rates associated with

three-dimensional scour pits. In Run 11 a similar effect was illustrated by changes observed in the development of ripplets downstream from a three-dimensional scour pit as the diagonal vortex subsided.

The following changes were observed for an unusually long bed form that had developed downstream from a three-dimensional scour pit along the sidewall. While the scour pit was active, ripplet slipfaces repeatedly developed on the stoss side of the bed form, forming series of ripplets. However, after the vortex subsided, new ripplet slipfaces did not tend to form, and existing ripplet slipfaces were eroded or overtook the major slipface downstream. After the vortex subsided, the sediment movement downstream from the scour pit was basically the same as that downstream from relatively two-dimensional slipfaces. Both the rate at which bursts of sediment movement occurred and the amount of sediment moved in individual bursts were markedly reduced from when the scour pit was active. Eventually, the bed form was broken up into a series of smaller bed forms by a new slipface developing on the stoss side of the unusually long bed form and then propagating more new slipfaces downstream, as opposed to a series of ripplets forming by the repeated development of new ripplet slipfaces upstream from existing ripplet slipfaces. However, at the same time, at other locations on the sediment bed, ripplets were developing rapidly enough

downstream from some relatively two-dimensional slipfaces to form series of ripplets. The low rate of development of ripplets was probably due to the lower flow velocity near the sidewall and therefore lower local sediment transport rates.

As the mean flow velocity increased, the frequency and strength of bursts of sediment movement downstream from three-dimensional scour pits increased as they did downstream from relatively two-dimensional slipfaces. However, because of the relatively greater local sediment transport rates associated with three-dimensional scour pits, changes in the bed geometry occurred even more rapidly and seemed even more noticeable.

As for the primary runs, the relatively strong, diagonal vortices associated with active, three-dimensional scour pits appeared to be particularly transient for all three runs. After the subsidence of the diagonal vortex, the sediment movement downstream from the scour pit tended to be basically the same as that downstream from relatively two-dimensional slipfaces, even while the bed geometry was still roughly similar to that when the scour pit was active. With time, the bed geometry tended to become more two-dimensional.

CHAPTER 6

EXPERIMENTAL RESULTS:

THE GEOMETRIC PROPERTIES OF THE BED FORMS

Section 6-1.0.0

Introduction

The experimental results on the geometric properties of the bed forms are presented in this chapter. The definitions of the bed form height, length, and length/upstream-height are presented in Sections 6-2.0.0 to 6-2.3.0. The criterion for excluding data due to the overtaking phenomenon are presented in Sections 6-3.0.0 to 6-3.1.0. The procedure for correcting the bed-form length which includes data on the average migration rates of the slipfaces is presented in Sections 6-4.0.0 to 6-4.3.0. The experimental results on the geometric properties are presented in Sections 6-5.1.0 to 6-5.3.2. The results include histograms of the geometric properties for each mean flow velocity, means of the geometric properties as functions of mean flow velocity, and statistical analyses and discussion of the data. The main results are summarized in Section 6-6.0.0.

Section 6-2.0.0

Definition of Bed-Form Height, Length, and Length/Upstream-Height

As noted in the qualitative descriptions of the bed forms, the identity of individual bed forms is both ambiguous and transitory. As a result of the continual overtaking of the slipfaces and the large variation in the magnitude of both the heights of slipfaces and the distances between adjacent slipfaces, the division of a longitudinal profile of the sediment bed into individual bed forms is subjective. Slipfaces are well defined, but the longitudinal profiles between adjacent slipfaces vary greatly in shape and commonly do not delineate easily distinguishable, individual elements with roughly triangular profiles.

For these experiments, the height of a slipface was defined as the distance perpendicular to the mean plane of the sediment bed (i.e., perpendicular to the flume rails) from the break in slope at the top of the slipface (the brink) to the low point in the trough downstream. The length or spacing between two slipfaces was defined as the longitudinal distance parallel to the mean plane of the sediment bed (i.e., parallel to the flume rails) from the brink of one slipface to the brink of the next slipface downstream. The length/upstream-height ratio was defined as the length between two slipfaces divided by the height

of the slipface upstream. All measurements of the geometric properties were made along the longitudinal centerline of the flume. From the observations, the examination of certain categories of height, length, and length/upstream-height seemed to be potentially particularly useful in understanding more about the dynamics of the bed forms.

Section 6-2.1.0

Bed-Form Height

Commonly, in the bed-form literature, slipfaces with relatively small heights have been viewed as small bed forms superimposed on larger bed forms and have been treated as secondary features: usually only the heights and lengths of the larger bed forms have been used to describe the bed geometry. From the observations, slipfaces with the smallest heights frequently were formed relatively recently and also tended to have small lateral extent or crestlines that were discontinuous laterally. A slipface appeared secondary if its height was unusually small along the entire lateral extent of the slipface and/or the crestline was unusually short.

For these experiments, slipfaces whose heights at the intersection with the centerline appeared markedly smaller than the apparent mean height for a given run and that also appeared to be secondary slipfaces as described above were

arbitrarily designated as ripplets. Occasionally, slipfaces that did not appear to be secondary pinched out laterally near the centerline and, consequently, also had unusually small heights at the intersection with the centerline. Both ripplets and major slipfaces that pinched out laterally near the centerline were noted at the time the centerline profile of the sediment bed was taken. All slipfaces that were not designated as ripplets were considered to be major slipfaces.

Slipfaces designated as ripplets tended to be similar in height for all of the runs. Most ripplets were less than 1.0 cm high and, on average, tended to be approximately 0.5 cm high. For a given run, ripplets appeared to make up the low end of the frequency distribution of the heights. There appeared to be a continuum of heights from ripplets to the highest slipfaces: there were no breaks in the height distributions.

The heights of major slipfaces, denoted H_m, were subdivided into two categories based on the type of slipface immediately downstream: 1) the height of a major slipface immediately upstream from a ripplet slipface, H_{m-r}, or 2) the height of a major slipface immediately upstream from another major slipface, H_{m-m}. Category 1, major slipfaces immediately upstream from ripplet slipfaces, seemed to be composed mostly of slipfaces that

were immediately upstream from the most recently formed slipfaces. The heights of all slipfaces, denoted H, is the combination of the heights of major slipfaces, H_m, plus the heights of ripplets, denoted H_r.

Section 6-2.2.0

Bed-Form Length

The lengths downstream from major slipfaces were divided into three categories also based on the type of slipface immediately downstream: 1) the length from a major slipface to an immediately adjacent major slipface downstream, L_m; 2) the length from a major slipface to an immediately adjacent ripplet slipface downstream, L_r; and 3) the length from a major slipface immediately upstream from a ripplet to the next major slipface downstream (i.e., a composite with ripplets: the length between two major slipfaces with one or more ripplet slipfaces in between), L_c.

Figure 7-1 illustrates the different types of bed-form length. The slipfaces are numbered sequentially from upstream: slipfaces 3 and 4 are ripplets and slipfaces 1, 2, and 5 are major slipfaces. The length between slipfaces 1 and 2 is an example of category 1, L_m; the length between slipfaces 2 and 3 is an example of category 2, L_r; and the length between slipfaces 2 and 5 is an example of category 3, L_c.

The combination of categories 1 and 3, the lengths between immediately adjacent major slipfaces, L_m, and the lengths of composites with ripplets, L_c, comprises all lengths between major slipfaces - the set of lengths most commonly used to represent the lengths of the bed forms. The combination of these two categories, L_m and L_c, is denoted by L_{m-m}.

The combination of categories 1 and 2, the lengths between immediately adjacent major slipfaces, L_m, and the lengths downstream from major slipfaces to immediately adjacent ripplet slipfaces, L_r, comprises all lengths downstream from major slipfaces to the next slipface regardless of the height of the slipface downstream. The combination of these two categories, L_m and L_r, is denoted by L_{m-a}. From the observations of the sediment transport, this set of lengths appeared to be potentially important in terms of the dynamics of the bed forms, as will be discussed later in Section 6-5.2.2.

Section 6-2.3.0

Bed-Form Length/Upstream-Height

The length/upstream-height ratios for lengths downstream from major slipfaces were divided into three categories based on the category of length in the ratio: 1) the length from a major slipface to an immediately adjacent major slipface downstream divided by the height of

the slipface upstream, L_m/H_u; 2) the length from a major slipface to an immediately adjacent ripplet slipface downstream divided by the height of the slipface upstream, L_r/H_u; and 3) the length between two major slipfaces with one or more ripplet slipfaces in between divided by the height of the slipface upstream, L_c/H_u.

The combination of categories 1, L_m/H_u, and 3, L_c/H_u, comprises all length/upstream-height ratios for lengths between major slipfaces. The combination of these two categories is denoted L_{m-m}/H_u. The combination of categories 1, L_m/H_u, and 2, L_r/H_u, comprises all length/upstream-height ratios for lengths downstream from major slipfaces to the next slipface regardless of the height of the slipface downstream. The combination of these two categories is denoted L_{m-a}/H_u.

Section 6-3.0.0

Dynamic Considerations

From the qualitative descriptions of the sediment transport downstream from slipfaces, the bursts of sediment movement emanating from the apparent reattachment area appeared to be important in determining the bed geometry downstream: the area where bursts repeatedly subsided appeared to be where a new slipface developed. However, where a slipface was migrating up the stoss side of the bed form immediately downstream and overtaking the adjacent

slipface, the bursts from the reattachment area downstream from the overtaking slipface no longer appeared to be dominant in determining the distance to the next slipface: as the overtaking slipface approached the next slipface, the bursts tended to continue over the next slipface and no longer tended to subside before reaching the slipface. Consequently, when a slipface was overtaking another slipface, the bursts of sediment movement (i.e., the flow patterns downstream from the slipface: the flow separation and reattachment, etc.) did not appear to be the limiting factor in determining the length downstream from the overtaking slipface. In this instance, the differential migration rates of the slipfaces appeared to be the dominant factor limiting bed-form length. The lengths determined by the bursts of sediment movement appeared to be the maximum lengths possible downstream from slipfaces for a given set of flow conditions.

Section 6-3.1.0

Exclusion Criterion

In order to examine the set of lengths that appeared to be predominantly limited by the bursts of sediment movement on the stoss sides of bed forms (i.e., the flow patterns downstream from slipfaces), the lengths downstream from major slipfaces that were overtaking the next major slipface downstream were excluded when constructing

histograms and calculating means of the different categories of length. Ratios of length/upstream-height using lengths downstream from major slipfaces that were overtaking the next major slipface downstream were also excluded. The following criterion was used to distinguish whether a slipface was overtaking the next slipface downstream: if the low point downstream from the upstream slipface was higher than one-third of the height of the downstream slipface (relative to the flume rails), the upstream slipface was considered to be overtaking the downstream slipface.

This criterion is illustrated in Figure 6-2. In Figure 6-2a, slipface 1 is considered to be overtaking slipface 2, because the low point downstream from slipface 1 is higher than one-third of the height of slipface 2 relative to the flume rails. (The length between slipfaces 1 and 2 would be excluded from the data for histograms and means and the length/upstream-height using the length between slipfaces 1 and 2 would also be excluded.) In Figure 6-2b, slipface 3 is not considered to be overtaking slipface 4, because the low point downstream from slipface 3 is higher than the low point downstream from slipface 4 relative to the flume rails but is lower than one-third of the height of slipface 4. This criterion excludes the set of lengths that appeared to be predominantly limited by the overtaking phenomenon (i.e.,

the differential migration rates of adjacent slipfaces) as opposed to being limited by the bursts of sediment movement on the stoss sides of bed forms (i.e., the flow patterns downstream from slipfaces).

Section 6-4.0.0

Correction of Bed-Form Length

Centerline profiles of the sediment bed were taken while the flume was running. The profiles were taken from the downstream end of the test section of the flume to the upstream end. As a result, the measured length between two slipfaces is shorter than the real length (at the time the position of the slipface downstream was measured) by the distance the slipface upstream migrated while the profile of the sediment bed was being taken between the two slipfaces.

Figure 6-3 illustrates the relationship between the measured and real lengths between slipfaces A and B. The solid line shows the sediment bed profile at time T_1 when the position of slipface B was measured, and the dashed line shows the upstream section of the profile at time T_2 when the position of slipface A was measured. Let X equal the average migration rate of the slipface upstream, slipface A, and let Y equal the average rate at which the bed profile was taken. Let T represent the time interval from T_1 to T_2. Therefore, the average migration rate of

the slipface upstream is equal to the difference between the real and measured lengths divided by the time interval, T:

$$X = (\text{real length} - \text{measured length}) / T.$$

Likewise, the average rate at which the profile was taken is equal to the measured length divided by the time interval, T:

$$Y = (\text{measured length}) / T.$$

Eliminating T by combining the above two expressions yields the following relationship between the measured and real lengths:

$$(\text{real length}) = (\text{measured length}) (1 + X/Y).$$

Therefore, in order to determine the real length, a correction equal to the measured length times the ratio of the average migration rate of the slipface upstream and the average rate at which the profile was taken must be added to the measured length. When the average migration rate of the slipfaces is very slow compared to the rate at which the profile is taken, the correction to the measured length is negligible.

In order to estimate the magnitude of the correction to the lengths measured while the flume was running, both the average migration rate of the major slipfaces and the average rate of taking the bed profile were determined for each mean flow velocity. The ratio of these two quantities was used to approximate the ratio of the average migration rate of the slipface upstream and the average rate at which the profile was taken in the above relationship between the measured and real lengths.

Section 6-4.1.0

Determination of Average Migration Rates of Major Slipfaces

Two methods were used to determine the average migration rate of the major slipfaces for each mean flow velocity: 1) from comparison of the location of slipfaces in the last bed profile with the flume running and in the bed profile with the flume off at the end of the run and 2) from the side-view, time-lapse movie photography. The results from these two different methods were then combined to estimate the average migration rate of the major slipfaces for each mean flow velocity.

1) Comparison of the last flume-on bed profile and the flume-off profile at the end of the run.

The distance each major slipface migrated from the time its position was measured during the last flume-on

profile until the flume was turned off at the end of the run was determined by noting the difference in position of each major slipface in the flume-off and the last flume-on profiles. The corresponding time interval was determined by interpolating the time when the position of the slipface was measured from times recorded at one-meter intervals while taking the profile and then subtracting this time from the time when the flume was shut off at the end of the run. The average migration rate of each major slipface was calculated by dividing the distance the slipface migrated by the corresponding time interval. The mean and standard deviation of the average migration rates of the major slipfaces were then calculated for each mean flow velocity. This method was not used for Runs 8 and 9. For these runs, the sediment bed profiles changed sufficiently between the last flume-on profile and the flume-off profile that most of the major slipfaces in the last flume-on profile could not be unambiguously identified in the flume-off profile.

2) Side-view, time-lapse movie photography.

The side-view, time-lapse movies were analyzed using a microfilm reader. This made it possible to follow the migration of an individual slipface frame by frame through the field of view of the movie camera. In general, each major slipface was followed from near a vertical scale at the upstream end of the field of view: 1) until just

before the slipface became indistinguishable, 2) for a preset distance (approximately 50 cm or 75 cm), or 3) for 100 frames, whichever occurred first. Slipfaces were followed for 50 cm for Runs 1 through 7 and for 75 cm for Runs 8 and 9. The starting and ending positions for tracking a given slipface and the corresponding times were recorded. In addition, the number of movie frames from the starting to ending positions was also counted to provide an independent measure of the time period while the slipface was being tracked. The time period was determined by multiplying the number of movie frames by the time interval at which the frames were taken. The average migration rates of individual slipfaces were calculated using the difference in ending and starting positions and the corresponding time period determined from the number of movie frames. The mean and standard deviation of the average migration rates of the major slipfaces were then calculated for each mean flow velocity.

The estimates of the average migration rates of the major slipfaces using the two different methods are in good agreement. In order to determine a more accurate estimate of the average migration rate for each mean flow velocity, the data from the above two methods were combined. The estimates obtained by combining both sets of data are presented in Figure 6-4, which shows the average migration

rate of the major slipfaces with 90% confidence intervals on the mean as a function of mean flow velocity.

Section 6-4.2.0

Determination of Average Rates of Taking the Bed Profile

The average rate of taking a bed profile was determined for each mean flow velocity using times that were recorded at one-meter intervals while the bed profiles were being taken. The mean and standard deviation of the average rates of taking the bed profile for one-meter intervals for all flume-on profiles were calculated for each mean flow velocity.

Section 6-4.3.0

Ratio of Average Migration Rate of Major Slipfaces to Average Rate of Taking the Bed Profile

Using the above values, determined as described in Sections 6-4.1.0 and 6-4.2.0, the ratio of the average migration rate of the major slipfaces to the average rate of taking the bed profile was calculated for each mean flow velocity. The results are presented in Table 6-1. These ratios were used to estimate the magnitude of the corrections to the measured lengths. The ratio times the measured length approximates the correction that must be added to the measured length to determine the real length. For Runs 1 through 5, the major slipfaces migrated

relatively very slowly compared to the rate at which the bed profiles were taken: the major slipfaces migrated approximately 2% or less as fast as the profiles were taken and the corrections to the measured lengths were considered to be negligible. For Runs 6 through 9, however, the major slipfaces migrated relatively more rapidly compared to the rate at which the bed profiles were taken: for these runs, the ratios were used to correct the measured lengths.

Section 6-5.0.0

Experimental Results

For each run, 1 through 9, histograms were constructed for the bed-form height and length. In addition, for each run the mean, standard deviation, and 90% confidence interval for the mean were calculated for each of the categories of the height, length, and length/upstream-height, as defined in Sections 6-2.0.0 to 6-2.3.0. Hypothesis testing regarding the means was performed both to examine trends in the data as functions of mean flow velocity and to examine similarities and differences in the different categories of the geometric properties for a given mean flow velocity. Data from all of the flume-on bed profiles (except that of the propagating ripple front) for each run were used in constructing the histograms and calculating the means.

Section 6-5.1.0

Bed-Form Height

Section 6-5.1.1

Histograms of Bed-Form Height

For each mean flow velocity the three different categories of height (H_r, H_{m-r}, H_{m-m}) are shown on the same histogram. No heights are excluded from the histograms. Figures 6-5a through 6-5i present the histograms of bed-form height for Runs 1 through 9; the histograms are arranged in order of increasing mean flow velocity. The sample size for each histogram, n, is given on the histogram. The median value of all the heights for each histogram is marked with an arrow.

On average, the range of the heights increases as the mean flow velocity increases: the minimum values are approximately the same for all the flow velocities, while the maximum values increase as a function of mean flow velocity. Because of the increasing percentage of relatively small slipfaces through Run 7, however, the median actually decreases from Run 3 to a minimum at Run 7 (even though the maximum value of the height is increasing) and then increases again. On average, the shape of the histograms becomes increasingly skewed to small values as the mean flow velocity increases through Run 7: the percentage of small values increases as the maximum value increases. The shape of the histograms becomes less skewed

from Run 7 to Run 9 because of the decreasing percentage of small slipfaces.

From the qualitative descriptions, ripplet slipfaces seemed to develop more readily as the mean flow velocity increased: fewer bursts of sediment movement seemed necessary for them to develop. The decreasing percentage of ripplets from Run 7 to 9 might be due, in part, to newly developed slipfaces being more easily eroded. Also, for Runs 8 and 9 some ripplets migrated so rapidly as they passed under the point gauge that it was not possible to measure their height; these ripplets were recorded as "ripplet passed", but no height was recorded. Consequently, these ripplets are not represented in the histograms. In addition, the mean length of the bed forms is a maximum for Run 7 and then decreases to Run 9, as will be presented later. This decrease in length is probably a consequence of the restricted length of the flume: as noted in the observations for Runs 8 and 9, the mean size of the bed forms was still increasing downstream within the test section of the flume (additional evidence that the decrease in mean length from Run 7 to Run 9 is probably an artifact of the restricted length of the flume is presented later). The decrease in the percentage of ripplets from Run 7 to Run 9 may reflect, in part, that the mean length of the bed forms had not reached the equilibrium value.

The histograms in Figure 6-5 show that bed-form height

for a given mean flow velocity is not readily characterized by a single value. For each mean flow velocity the height ranges from barely perceptible slipfaces to the maximum height for that mean flow velocity with no major breaks in size: there is a continuum of sizes from ripplets to the slipfaces with the maximum heights.

The data on bed-form height for all of the mean flow velocities of these experiments were combined in a single histogram for comparison with histograms prepared by other authors for a range of flow conditions, as opposed to a single set of flow conditions. Such histograms have been used to determine whether there are any natural breaks in bed- form size over the range of conditions examined. Figure 6-6 shows the histogram combining the data on bed-form height for all of the mean flow velocities of these experiments. In combining the data, the data from each run were weighted equally. This histogram includes the heights of 1952 slipfaces. The histogram is very smooth with a single mode: there are no marked breaks in height within the range of heights. The histogram is skewed toward small values with a long tail to higher values.

Section 6-5.1.2

Means of Bed-Form Height

Although the histograms of bed form height for given mean flow velocities are not sharply and symmetrically

peaked about single values, trends in the mean show the similarities and differences in the different populations of bed-form height. Relatively long running times were used for Runs 1 through 9, in part to obtain large sample sizes for the data on the geometric properties of the bed forms for a given set of mean flow conditions. As a result, in these experiments the value of the mean is usually well defined, even though the standard deviations are large. Sample sizes range up to almost 300.

For each run, 1 through 9, the mean, standard deviation, and 90% confidence interval for the mean were calculated for each of the three categories of bed-form height: H_r, H_{m-r}, and H_{m-m}. In addition, these quantities were determined for the height of all major slipfaces, H_m (i.e., the combination of H_{m-r} plus H_{m-m}), and for the height of all slipfaces, H (i.e., the combination of H_m plus H_r).

Hypothesis testing was performed to examine the trends in the means of the different categories of height as functions of mean flow velocity. The significance of the difference between the means of a given category of height for different mean flow velocities was calculated.

Figure 6-7 shows the mean height of major slipfaces, H_m, with 90% confidence intervals as a function of mean flow velocity. The mean height of the major slipfaces increases as a function of mean flow velocity.

At the 10% level of significance,

. the mean height of the major slipfaces in Run 1 is less than that in Run 3, 4, or 5;

. the mean height of the major slipfaces in Run 3, 4, and 5 are each less than that in Run 6;

. the mean height of major slipfaces in Run 6 is less than that in Run 7 or 8; and

. the mean height of major slipfaces in Run 7 is less than that in Run 9.

Figure 6-8 shows the mean height of ripplets, H_r, with 90% confidence intervals as a function of mean flow velocity. The mean values range from 0.44 cm to 0.65 cm. The mean heights of the slipfaces with the smallest heights that developed for each mean flow velocity are similar in magnitude for all the mean flow velocities of these experiments. As previously noted, the slipfaces with the smallest heights are commonly the most recently formed slipfaces. Therefore, despite the increase in the mean height of major slipfaces as a function of mean flow velocity, the height of incipient slipfaces remains similar with increasing mean flow velocity.

Figure 6-9 shows the mean height of all slipfaces, H, with 90% confidence intervals as a function of mean flow velocity. As with the median height of all slipfaces, the mean height of all slipfaces decreases from Run 4 to Run 6 or 7 then increases to Run 9. At the 10% level of

significance, the mean heights in Runs 1, 2, 3, and 4 are not significantly different from one another. The mean height in each of these runs is greater than that in Run 6 or 7, and the mean height in Run 6 or 7 is less than that in Run 8, which in turn is less than that in Run 9. For each run the median of the height of all slipfaces is less than the mean.

Hypothesis testing was performed to examine the similarities and differences between the different categories of height for a given mean flow velocity. The significance of the difference between the means for different categories of height for a given mean flow velocity was calculated. Only means with sample sizes greater than 15 are presented: the statistical tests that were used are not appropriate for smaller samples. For direct comparison, the means of H_r, H_{m-r}, H_{m-m}, and H as functions of mean flow velocity are shown together in Figure 6-10.

The mean height of ripplets, H_r, is significantly less than that of major slipfaces, H_m, for each mean flow velocity for Runs 2 through 9 at less than a 1% level of significance. On average, the slipfaces whose heights appeared to be markedly smaller than the apparent mean height for a given mean flow velocity and which also appeared to be secondary have smaller heights than the slipfaces that appeared to be major slipfaces.

The mean height of major slipfaces immediately upstream from a ripplet slipface, H_{m-r}, is significantly greater than that of major slipfaces immediately upstream from another major slipface, H_{m-m}, for each mean flow velocity for Runs 5 through 9 at a 2% level of significance. On average, the major slipfaces that are immediately upstream from slipfaces with the smallest heights are higher than those immediately upstream from other major slipfaces. As noted earlier, the slipfaces with the smallest heights frequently were the most recently formed; therefore, new slipfaces tend to develop preferentially downstream from the higher slipfaces.

This result is consistent with the observation that new slipfaces formed more readily when the bursts of sediment movement were stronger and, therefore, more sediment grains were moved in a given burst. The higher the upstream slipface is, the greater the acceleration of the flow over the top of the slipface, and so the stronger the bursts of sediment movement emanating from the reattachment area downstream. This conclusion is important in relation to the conditions favoring the generation of new slipfaces.

Section 6-5.2.0

Bed-Form Length

Section 6-5.2.1

Histograms of Bed-Form Length

Two separate histograms of bed-form length were constructed for each mean flow velocity; two of the three categories of length are shown on each histogram (Figures 6-11a through 6-11i and Figures 6-12a through 6-12i). One histogram comprises the lengths between major slipfaces, L_{m-m}, which is the set of lengths most commonly used to represent bed form length. This histogram consists of the lengths from major slipfaces to an immediately adjacent major slipface downstream, L_m, and the lengths from major slipfaces immediately upstream from a ripplet to the next major slipface downstream (i.e., the lengths of composites with one or more ripplets), L_c.

The other histogram comprises lengths downstream from major slipfaces to the next slipface regardless of the height of the slipface downstream, L_{m-a}. This histogram consists of the lengths from major slipfaces to an immediately adjacent major slipface downstream, L_m, and the lengths from major slipfaces to an immediately adjacent ripplet slipface downstream, L_r. As described in Section 6-3.1.0, lengths downstream from major slipfaces that were overtaking the next major slipface downstream are excluded from the histograms. All other lengths downstream from

major slipfaces are included in the histograms.

The histograms of length were first constructed with 5-cm intervals using the uncorrected lengths measured while the flume was running. Then for Runs 6 through 9 the end points of the length intervals were corrected as described in Section 6-4.0.0. Histograms of the corrected length with 5-cm intervals were constructed by assuming that the values of the length were uniformly distributed within the corrected intervals. For Runs 1 through 5 the histograms were not corrected: the correction to the lengths is negligible, as presented in Section 6-4.3.0.

Figures 6-11a through 6-11i show the histograms of the lengths between major slipfaces, L_{m-m}, for Runs 1 through 9, and Figures 6-12a through 6-12i show the histograms of lengths downstream from major slipfaces to the next slipface regardless of the height of the slipface downstream, L_{m-a}, for Runs 1 through 9. The histograms are arranged in order of increasing mean flow velocity. The sample size for each histogram, n, is indicated on the histogram.

On average, the range of the lengths between major slipfaces, L_{m-m}, increases as a function of mean flow velocity through Run 6: the minimum values are approximately the same, while the maximum values increase as a function of mean flow velocity. For Runs 6 through 9, the value of the maximum length does not follow a simple

trend: the greatest length measured was in Run 8 and the second largest was in Run 9. However, the percentage of lengths greater than an arbitrarily choosen value tends to increase with mean flow velocity. For example, for Runs 6 through 9 the percentage of lengths greater than 105 cm increases with mean flow velocity from 5% for Run 6, to 7% for Run 7, to 8% for both Runs 8 and 9. The minimum values for Runs 6 through 9 are slightly greater than those for Runs 1 through 5, but not substantially: for Runs 1 through 5 the minimum length is approximately 5 cm, while for Runs 6, 8, and 9 the minimum length is approximately 10 cm.

As the range of the lengths between major slipfaces, L_{m-m}, increases with mean flow velocity, the histograms become more skewed with an increasing tail to larger values.

Comparison of Figures 6-11a through 6-11i with Figures 6-12a through 6-12i shows that the lengths from major slipfaces to an immediately adjacent major slipface downstream, L_m, are more similar to the lengths from major slipfaces to an immediately adjacent ripplet slipface downstream, L_r, than to the lengths of composites with one or more ripplets, L_c. On average, the ranges for the histograms of the lengths downstream from major slipfaces to the next slipface, regardless of the height of the slipface downstream, L_{m-a}, are less than the ranges for the

histograms of the lengths between major slipfaces, L_{m-m}.

The histograms in Figures 6-11a through 6-11i and Figures 6-12a through 6-12i show that the bed-form length for a given mean flow velocity is not readily characterized by a single value. For each mean flow velocity the length ranges from approximately 5 or 10 cm to the maximum length for that mean flow velocity with no major breaks in size. For all the mean flow velocities of these experiments, smaller lengths were intermixed with the larger lengths: larger lengths were not observed to occur exclusively without the presence of smaller lengths for any of the mean flow velocities of these experiments. The ranges of the length for the individual sediment bed profiles taken during a given run tended to be approximately the same as those shown in the histograms in Figures 6-11a through 6-11i and Figures 6-12a through 6-12i, which include the data from all of the profiles of the run. If the lengths downstream from major slipfaces that were overtaking the next major slipface downstream had been included, the range of the lengths for each mean flow velocity would be even greater. On average, the excluded lengths are less than the lengths that were not excluded.

The data on the bed-form length for all of the mean flow velocities of these experiments (as opposed to a single set of flow conditions) were combined in two single histograms: 1) a histogram of the lengths between major

slipfaces, L_{m-m}, and 2) a histogram of the lengths downstream from major slipfaces to the next slipface regardless of the height of the slipface downstream, L_{m-a} (Figure 6-13a and 6-13b). As for the height, these histograms were constructed to compare with similar histograms for a range of flow conditions prepared by other authors and to determine whether there are any natural breaks in the bed-form length over the range of conditions examined.

The histograms of L_{m-m} and L_{m-a} combining the data on the bed form length for all the mean flow velocities of these experiments are presented in Figures 6-13a and 6-13b, respectively. In combining the data, the data for each run was weighted equally. Both histograms are smooth with single modes: there are no marked breaks in length within the range of lengths. Both histograms are skewed toward small values with tails to larger values. The range of L_{m-m} extends to larger values than that of L_{m-a}, and so the tail to larger values is longer. The shapes of the histograms in Figures 6-11a through 6-11i and Figures 6-12a through 6-12i are such that as the mean flow velocity is increased, the minimum values remain approximately the same while the maximum values increase; therefore, even if longer bed forms would have developed in a longer flume for the higher flow velocities, the shapes of the above two histograms would probably still be fairly similar to those

in Figures 6-13a and 6-13b, but with longer tails to larger values.

Section 6-5.2.2

Means of Bed-Form Length

As with the bed-form height, trends in the mean of the bed-form length show the similarities and differences in the different populations of bed form length. For each run, 1 through 9, the mean, standard deviation and 90% confidence interval for the mean were calculated for each of the three categories of bed-form length: L_m, L_r, and L_c. In addition, these quantities were determined for the lengths between major slipfaces, L_{m-m}, and for the lengths downstream from major slipfaces to the next slipface regardless of the height of the slipface downstream, L_{m-a}.

Hypothesis testing was performed to examine the trends in the means of different categories of length as functions of mean flow velocity. The significance of the difference between the means of a given category of length for different mean flow velocities was calculated.

Figure 6-14 shows the mean length between major slipfaces, Lm-m, with 90% confidence intervals as a function of mean flow velocity. The mean length between major slipfaces increases as a function of mean flow velocity through Run 7 and then decreases from Run 7 through Run 9. At the 10% level of significance the mean

length for each run is significantly different from that of the adjacent runs. For Runs 1 through 7 the mean length of each run is significantly greater than that of the preceding run, and for Runs 8 and 9 the mean length of each run is significantly less than that of the preceding run. As shown in Figure 7-14 the mean length between major slipfaces, which is the length most commonly used to represent bed-form length, changes very smoothly as a function of mean flow velocity.

As noted earlier, the decrease in the mean length between major slipfaces, L_{m-m}, from Run 7 through 9 is probably due to the restricted length of the flume. As noted in Section 6-5.1.1, for Runs 8 and 9 the mean size of the bed forms was still increasing downstream within the test section of the flume. Also, even though the mean length was greatest for Run 7, the longest individual length measured was in Run 8 and the second longest was in Run 9. Most importantly, the mean lengths of bed forms generated under mean flow conditions fairly similar to Runs 8 and 9, but in a much longer flume, were significantly longer (Simons, Richardson, and Albertson, 1961). The above evidence suggests that if the flume had been longer, longer bed forms would have developed for these runs.

Apart from the issue of what the length between major slipfaces, L_{m-m}, would be, given an ideal flume, the data show that as the mean flow velocity is systematically

increased, the mean length of the bed forms changes smoothly and systematically in response to even small changes in mean flow velocity. The mean length of the bed forms depends on the mean flow velocity for the entire range of flow conditions of these experiments. Even an increase of 2 cm/s in mean flow velocity within the ripple stability field results in a measurable increase in the mean length. Large sample sizes make it possible to determine even the small differences in the value of the mean length for the lower mean flow velocities of these experiments: the larger the the sample size is, the better defined the mean is.

The observations suggest that the mean length downstream from major slipfaces to the next slipface regardless of the height of the slipface downstream, L_{m-a}, is possibly a more fundamental length than the mean length between major slipfaces, L_{m-m}. This length, L_{m-a}, is a measure of the longitudinal distance downstream from major slipfaces to the first discontinuity in height. From the observations, this length appears to be the sum of the distance downstream to the reattachment area plus the distance from the reattachment area to where the bursts of sediment movement have been repeatedly subsiding. Once a new slipface develops downstream from a major slipface on the stoss side of an existing bed form, the bursts of sediment movement emanating from the reattachment area

downstream from the major slipface no longer seem to influence as strongly the sediment movement on the upper stoss side of the preexisting bed form downstream from the new slipface. The distance downstream from a major slipface to where a new slipface develops seems to be an indication of the distance over which the flow patterns associated with the major slipface (i.e., the flow separation and subsequent reattachment) strongly infuence the sediment movement. Downstream from the new slipface the sediment movement appears more independent of the flow patterns associated with the major slipface upstream. Once a new slipface develops, the distance downstream to the next major slipface seems to become somewhat decoupled from the major slipface upstream.

Figure 6-15 shows the mean length downstream from major slipfaces to the next slipface regardless of the height of the downstream slipface, L_{m-a}, with 90% confidence intervals as a function of mean flow velocity. The mean length downstream from major slipfaces to the next slipface increases as a function of mean flow velocity through Run 7 and then decreases from Run 7 through Run 9. At the 10% level of significance the mean length for each run is significantly different from that of the adjacent runs. For Runs 1 through 7 the mean length of each run is significantly greater than that of the preceding run, and for Runs 8 and 9 the mean length of each run is

significantly less than that of the preceding run. As for the mean length between major slipfaces, the mean length downstream from major slipfaces to the next slipface changes very smoothly and systematically as a function of mean flow velocity. The mean value of L_{m-a} depends on the mean flow velocity for the entire range of mean flow conditions of these experiments. Small changes in the mean flow velocity result in measurable changes in the mean length.

Hypothesis testing was performed to examine the similarities and differences between the different categories of length for a given mean flow velocity. The significance of the difference between the means of different categories of length for a given mean flow velocity was calculated. For direct comparison, the means of L_m, L_r, L_c, and L_{m-a} as functions of mean flow velocity are shown together in Figure 6-16.

The mean length of composites with one or more ripplets, L_c, is significantly greater than the mean length from major slipfaces to an immediately adjacent major slipface downstream, L_m, for each mean flow velocity for Runs 5 through 9 at the 5% level of significance. For a given flow velocity the mean length between major slipfaces is significantly greater if there are one or more ripplet slipfaces between the major slipfaces than if there are no intervening ripplet slipfaces. The mean length of

composites with one or more ripplets is significantly greater than the mean length between major slipfaces with no intervening ripplets.

The mean length of composites with one or more ripplets, L_c, is significantly greater than the mean length from major slipfaces to an immediately adjacent ripplet slipface downstream, L_r, for each mean flow velocity for Runs 5 through 9 at the 5% level of significance. This result is a natural consequence of the definitions of L_c and L_r. For any given major slipface that is immediately upstream from a ripplet slipface, the longitudinal distance to the next major slipface downstream is greater than the distance to the immediately adjacent ripplet.

The mean length from major slipfaces to an immediately adjacent ripplet slipface downstream, L_r, is significantly greater than the mean length from major slipfaces to an immediately adjacent major slipface downstream, L_m, for each mean flow velocity for Runs 5, and 7 through 9 at the 5% level of significance. For a given mean flow velocity the distance from a major slipface to the next slipface downstream tends to be greater if the next slipface downstream is a ripplet than if it is another major slipface. (Note: by definition, L_m is the length between major slipfaces with no intervening ripplets.) This result is consistent with the result that the mean height of major slipfaces immediately upstream from a ripplet slipface,

H_{m-r}, is significantly greater than the mean height of major slipfaces immediately upstream from another major slipface, H_{m-m}, for each mean flow velocity. The possible significance of this result will be discussed later.

Section 6-5.3.0

Bed Form Length/Upstream-Height

The bed-form length/upstream-height ratio may be viewed as a dimensionless measure of the bed-form length or a dimensionless measure of bed-form shape. This ratio is potentially a particularly useful measure of the geometry in terms of understanding more about the dynamics of the bed forms. The ratio of the distance downstream from a negative step to the height of the step is commonly used in examining phenomena associated with flow over a negative step. As noted in the observations, the sediment transport on the stoss sides of bed forms appears to be dominated by the bursts of sediment movement emanating from the reattachment area downstream from slipfaces. This observation suggests that the flow separation over slipfaces and subsequent reattachment of the flow downstream are important in the dynamics of the bed forms. For a given set of mean flow conditions, a constant value of length/upstream-height suggests that the flow and sediment dynamics are similar.

Section 6-5.3.1

Means of Bed-Form Length/Upstream-Height

Trends in the mean of the bed form length/upstream-height provide an indication of the similarities and differences in the different populations of bed form length/upstream-height. For each Run, 1 through 9, the mean, standard deviation, and 90% confidence interval for the mean were calulated for each of the three categories of this ratio: L_m/H_u, L_r/H_u, and L_c/H_u. In addition, these quantities were determined for the lengths between major slipfaces divided by the upstream height, $(L_{m-m})/H_u$, and for the lengths downstream from major slipfaces to the next slipface regardless of the height of the slipface downstream divided by the upstream height, $(L_{m-a})/H_u$.

Hypothesis testing was performed to examine the trends in the means of different categories of length/upstream-height as functions of mean flow velocity. The significance of the difference between the means of a given category of length/upstream-height for different mean flow velocities was calculated.

Figure 6-17 shows the mean length between major slipfaces divided by the upstream height, $(L_{m-m})/H_u$, with 90% confidence intervals as a function of mean flow velocity. This ratio increases through Run 6 then decreases from Run 6 through Run 9. For Runs 3 through 6 this ratio for each run is significantly greater than that

of the preceding run, and for Runs 8 and 9 this ratio for each run is significantly less than that of the preceding run at the 10% level of significance. The mean length between major slipfaces divided by the upstream height varies smoothly as a function of mean flow velocity.

Figure 6-18 shows the mean length downstream from major slipfaces to the next slipface regardless of the height of the slipface downstream divided by the upstream height, $(L_{m-a})/H_u$, with 90% confidence intervals as a function of mean flow velocity. This ratio increases through Run 6 and then decreases from Run 7 through Run 9. For Runs 3 through 6 this ratio for each run is significantly more than that of the preceding run, and for Runs 7 through 9 this ratio for each run is significantly less than that of the preceding run at the 10% level of significance. The mean length downstream from major slipfaces to the next slipface, regardless of the height of the slipface downstream, divided by the upstream height varies smoothly as a function of mean flow velocity.

Hypothesis testing was performed to examine the similarities and differences between the different categories of length/upstream-height for a given mean flow velocity. The significance of the difference between the means for different categories of length/upstream-height for a given mean flow velocity was calculated.

For direct comparison the different categories of

length/upstream-height are presented together in Figure 6-19. The mean length of composites with one or more ripplets divided by the upstream height, L_c/H_u, is significantly greater than the mean length from major slipfaces to an immediately adjacent major slipface downstream divided by the upstream height, L_m/H_u, for each mean flow velocity for Runs 5 through 9 at the 10% level of significance. For a given mean flow velocity the dimensionless length between major slipfaces is significantly greater if there are one or more ripplet slipfaces between the major slipfaces than if there are no intervening ripplet slipfaces. The dimensionless length of composites with ripplets is significantly different from the dimensionless length from major slipfaces to an immediately adjacent major slipface. This result suggests that the fluid and sediment dynamics determining the length downstream from a major slipface to the next major slipface when there are one or more ripplet slipfaces between the major slipfaces are different than when there are no intervening ripplet slipfaces. The dimensionless length between major slipfaces is not represented by a single value.

The mean length of composites with one or more ripplets divided by the upstream height, L_c/H_u, is significantly greater than the mean length from major slipfaces to an immediately adjacent ripplet slipface

downstream divided by the upstream height, L_r/H_u, for each mean flow velocity for Runs 5 through 9 at the 5% level of significance. As for the lengths on which these ratios are based, this result is a natural consequence of the definitions of the variables.

The mean length from major slipfaces to an immediately adjacent ripplet slipface downstream divided by the upstream height, L_r/H_u, is not significantly different from the mean length from major slipfaces to an immediately adjacent major slipface downstream divided by the upstream height, L_m/H_u, for each mean flow velocity for Runs 5 through 9 at the 5% level of significance. For a given mean flow velocity the mean length from major slipfaces to the next slipface downstream divided by the upstream height is not significantly different regardless of whether the next slipface is a ripplet or another major slipface. The dimensionless length from a major slipface to the next slipface downstream does not depend on the height of the slipface downstream. This result suggests that the fluid and sediment dynamics determining the length from a major slipface to the next slipface downstream are similar regardless of the height of the slipface downstream.

The above results comparing the different categories of length/upstream-height support the hypothesis that the mean length downstream from major slipfaces to the next slipface regardless of the height of the slipface

downstream, L_{m-a}, is a more fundamental length in terms of the fluid and sediment dynamics than the mean length between major slipfaces, L_{m-m}. These results suggest that the fluid and sediment dynamics determining the length downstream from a major slipface to the next slipface, L_{m-a}, are similar regardless of whether the slipface downstream is a ripplet or a major slipface, but that the dynamics determining the length between major slipfaces, L_{m-m}, are different depending on whether or not there are intervening ripplet slipfaces. Therefore, L_{m-a} is a length associated with all major slipfaces that appears to be determined by similar dynamics.

These results on the length/upstream-height are consistent with the observations that lead to the hypothesis that L_{m-a} is a more fundamental length than L_{m-m}. Once a new slipface develops downstream from a major slipface on the stoss side of an existing bed form, the bursts of sediment movement emanating from the reattachment area downstream from the major slipface no longer appear to influence as strongly the sediment movement on the upper stoss side of the preexisting bed form downstream from the new slipface. The distance to the next major slipface downstream no longer appears to be as strongly affected by the bursts of sediment movement emanating from the reattachment area downstream from the major slipface upstream. The development of the new slipface between the

existing major slipfaces seems to decouple, at least partially, the dynamics between the major slipfaces.

Section 6-6.0.0

Summary of the Experimental Results

Below are presented the main results from the examination and analysis of the geometric properties of the bed forms.

For both the bed-form height and the bed-form length, the range of sizes increases as a function of mean flow velocity. The minimum values remain approximately the same as the mean flow velocity is increased, while the maximum values increase as the mean flow velocity is increased. For a given mean flow velocity neither the height nor the length is readily characterized by a single value. For all of the mean flow velocities of these experiments, the full range of sizes for the given mean flow conditions occur intermixed: larger heights and lengths were not observed to occur without the presence of smaller heights and lengths. The histograms of both the height and the length are fairly continuous, with no marked breaks. The histograms tend to be skewed to small values with tails to larger values.

The histograms of the height and the length that were constructed using data for all of the mean flow velocities of these experiments, as opposed to a single set of flow

conditions, are smooth with single modes. There are no marked breaks in either the height or the length over the range of mean flow conditons examined. For both the height and the length, the histograms are skewed toward small values with long tails to higher values.

The main results for the mean height are summarized below:

1) The mean height of the major slipfaces, H_m, increases with mean flow velocity.

2) The mean height of ripplets, H_r, remains fairly similar as the mean flow velocity is increased: the mean values range only from 0.44 cm to 0.65 cm. Despite the increase in the mean height of major slipfaces with mean flow velocity, the height of incipient slipfaces remains similar as the mean flow velocity increases.

3) The mean height of ripplets, H_r, is significantly less than that of major slipfaces, H_m, for each mean flow velocity.

4) The mean height of major slipfaces immediately upstream from a ripplet slipface, H_{m-r}, is significantly greater than that of major slipfaces immediately upstream from another major slipface for each mean flow velocity for Runs 5 through 9. The slipfaces with the smallest heights occur preferentially downstream from the higher slipfaces; new slipfaces tend to develop preferentially downstream from the higher slipfaces.

The main results for the mean length are summarized below:

1) The mean length between major slipfaces, L_{m-m}, and the mean length downstream from major slipfaces to the next slipface regardless of the height of the slipface downstream, L_{m-a}, both increase with mean flow velocity through Run 7 and then decrease from Run 7 through Run 9. As discussed in Section 6-5.2.2, the decrease in the mean length from Run 7 through 9 is probably due to the restricted length of the flume.

2) The mean length of the bed forms depends on the mean flow velocity for the entire range of mean flow conditions of these experiments. As the mean flow velocity is systematically increased, both L_{m-m} and L_{m-a} change smoothly and systematically in response to even small changes in mean flow velocity. Even an increase of 2 cm/s in mean flow velocity within the ripple stability field results in a measureable increase in the mean length.

3) The mean length of composites with one or more ripplets, L_c, is significantly greater than the mean length from major slipfaces to an immediately adjacent major slipface downstream, L_m, for each mean flow velocity for Runs 5 through 9. The mean length of composites with one or more ripplets is significantly greater than the mean length between major slipfaces with no intervening ripplets.

4) The mean length from major slipfaces to an immediately adjacent ripplet slipface downstream, L_r, is significantly greater than the mean length from major slipfaces to an immediately adjacent major slipface downstream, L_m, for each mean flow velocity for Runs 5 and Runs 7 through 9. The distance from a major slipface to the next slipface downstream tends to be greater if the next slipface downstream is a ripplet than if it is another major slipface.

The main results for the mean length/upstream-height are summarized below:

1) The mean length of composites with one or more ripplets divided by the upstream height, L_c/H_u, is significantly greater than the mean length from major slipfaces to an immediately adjacent major slipface downstream divided by the upstream height, L_m/H_u, for each mean flow velocity for Runs 5 through 9. The dimensionless length between major slipfaces is significantly greater if there is one or more ripplet slipfaces between the major slipfaces than if there are no intervening ripplet slipfaces. This result suggests that the fluid and sediment dynamics determining the length downstream from a major slipface to the next major slipface are different depending on whether or not there are intervening ripplet slipfaces.

2) The mean length from major slipfaces to an immediately adjacent ripplet slipface downstream divided by the upstream height, L_r/H_u, is not signficantly different from the mean length from major slipfaces to an immediately adjacent major slipface divided by the upstream height, L_m/H_u, for each mean flow velocity for Runs 5 through 9. The dimensionless length from a major slipface to the next slipface downstream does not depend on the height of the slipface downstream. This result suggests that the fluid and sediment dynamics determining the length from a major slipface to the next slipface downstream are similar regardless of the height of the slipface downstream (i.e., regardless of whether the slipface downstream is a ripplet or another major slipface).

3) The above two results on the dimensionless length suggest that the mean length downstream from major slipfaces to the next slipface regardless of the height of the slipface downstream, L_{m-a}, may be a more fundamental length in terms of the fluid and sediment dynamics than the mean length between major slipfaces, L_{m-m}.

CHAPTER 7

DISCUSSION AND CONCLUSION:

A QUALITATIVE MODEL FOR LOWER-FLOW-REGIME BED FORMS

Section 7-1

Introduction

The observations on the bed forms described in Chapters 4 and 5 and the experimental results on the geometric properties of the bed forms presented in Chapter 6 can be explained by a single model for the generation and continued existence (lack of attenuation) of bed forms. The bed forms over the entire range of these experiments appeared to be governed by basically the same kinematics and dynamics, and the geometric properties of the bed forms changed smoothly and systematically as functions of mean flow velocity. No abrupt changes in bed-form kinematics, bed-form dynamics, or bed-form size were observed with changes in mean flow velocity.

The single model proposed in this chapter is based on the hypothesis that the nonconstant sediment transport rate caused by the phenomenon of fluid bursting at the base of the turbulent boundary layer results in both the development and continued existence (lack of attenuation) of the bed forms. (The sediment conservation equation requires that in order for bed forms to develop from a planar bed, the sediment discharge in the direction of flow

must not be constant.) Once slipfaces develop, the bursting phenomenon is altered in such a way as to augment the development of more new slipfaces and therefore keep the bed forms from being attenuated. In addition, the overtaking and coalescence of slipfaces inhibits the attenuation of the bed forms. This model is an extension of the work of Raudkivi (1963) and Williams and Kemp (1971) on the development of ripples from a planar bed.

Section 7-2

Fluid Bursting

The phenomenon of fluid bursting is described in the discussion of the work of Williams and Kemp (1971) in Chapter 1. The topic is reviewed by Cantwell (1981). High velocity eddies or vortices called "sweeps" spiral toward the boundary and result in alternate high and low velocity streaks of fluid laterally spaced at the boundary. The high velocity fluid interacts with low velocity fluid at the boundary which is then ejected away from the boundary as a turbulent "burst". The turbulent bursts include the liftup, sudden oscillation and then breakup of streaks of fluid. The high velocity sweeps and subsequent turbulent bursts are referred to as bursting or the burst-sweep cycle. Most of the turbulent shear stress near the boundary results from the bursting phenomenon. Bursting does not depend on the existence of a viscuous sublayer:

it also occurs for rough boundaries where no viscuous sublayer exists.

In these experiments the bursting phenomenon was indirectly inferred from observing the sediment movement on the bed. What are referred to as "bursts" of sediment movement on a planar bed are assumed to result from the high velocity "sweeps" of fluid of the burst-sweep cycle.

The nature of the bursts of sediment movement on the stoss sides of bed forms appeared to be basically the same as the bursts of sediment movement on a planar bed except that they were stronger and originated preferentially from the reattachment area downstream from slipfaces as opposed to from random locations on the stoss sides of bed forms. Bursts of sediment movement were not observed to originate on the upper stoss sides of bed forms (unless the slipface was being overtaken and thus a reattachment area occurred on the upper stoss side). The sediment-movement patterns on the stoss sides of bed forms suggest that subparallel, high-velocity streaks or sweeps of fluid originate at the reattachment area, spread downstream, and end where the bursts of sediment movement subside. The focusing of the origin of high velocity sweeps in the reattachment area by the flow separation and subsequent reattachment appeared to be important in the development of new slipfaces downstream.

Both on the planar bed and on the stoss sides of bed

forms, the bursts of sediment movement appeared to emanate from almost point sources and propagate downstream in subparallel, fan-shaped swaths until they subsided.

Section 7-3

Qualitative Model

For the entire range of mean flow conditions of these experiments, the first slipfaces that developed from a planar bed were very similar in height. All seemed to develop as a result of the nonconstant sediment transport rate due to the fluid bursting at the base of the boundary layer. At the higher flow velocities, new, low slipfaces were observed to develop directly from the hummocky micro-topography on the planar bed; this micro-topography was formed by subparallel bursts of sediment movement caused by the high-velocity fluid sweeps of the burst-sweep cycle. At the lower flow velocities, new slipfaces propagated downstream from the negative step formed by the false bottom over the full length of the sediment bed before slipfaces developed directly from the hummocky micro-topography on the planar bed. Except at the lowest flow velocity, however, slipfaces would have eventually developed directly from the hummocky planar bed, as at the higher velocities, if the slipfaces that propagated from the false bottom had been artificially levelled as they developed (c.f. Costello and Southard, 1981).

The initial development of a slipface downstream from the false bottom on the planar bed appeared to result from the bursts of sediment movement emanating from the reattachment area downstream from the negative step formed by the false bottom. The bursts of sediment movement subsided within a given distance downstream; an initial slipface developed where bursts of sediment movement were repeatedly subsiding. This process was repeated downstream from the initial slipface. The negative step formed by the exposed false bottom and subsequently by the farthest downstream slipface appeared to alter the fluid bursting in such a way as to increase the rate at which new slipfaces developed on the planar bed (as will be discussed later). As the bed forms propagated downstream onto the planar bed, the new slipfaces that developed at the bed-form front were very similar in size to those that developed directly on the planar bed at the higher flow velocities, and also similar in size to ripplets (i.e., the smallest slipfaces that developed once the average size of the bed forms had reached some sort of quasi-equilibrium).

Once they developed, the slipfaces tended to migrate at different velocities and overtake one another. When slipfaces overtook one another, they coalesced to form a new slipface. The height of the resulting new slipface was commonly greater than that of either of the original slipfaces. In this way the height of the slipfaces

sometimes increased fairly quickly in a discontinuous manner. The overtaking and coalescence of slipfaces appeared to be important in the continued existence or lack of attenuation of the bed forms.

Also, once slipfaces developed, the fluid flow over the sediment bed was altered and, consequently, the pattern of fluid bursting was altered. Flow separation developed downstream from the slipfaces, and high-velocity streaks or sweeps of fluid originated in the reattachment area and spread downstream resulting in bursts of sediment movement. As noted above, these bursts appeared to be basically the same as those on the planar bed. However, they were stronger or more exaggerated and originated preferentially from the reattachment area as opposed to from random locations on the bed forms. The bursts of sediment movement subsided within a given distance downstream; new slipfaces tended to develop where bursts of sediment movement were repeatedly subsiding.

The flow separation and subsequent reattachment appeared to cause high-velocity streaks or sweeps of fluid to start preferentially in the reattachment area. The focusing of the origin of high velocity sweeps of fluid in the reattachment area appeared to be very important to the development of new slipfaces downstream. As noted in the observations on the bed forms, the bursts of sediment movement caused by these high velocity sweeps appeared to

dominate the sediment transport on the stoss sides of the bed forms. The continuity of these bursts of sediment movement longitudinally from the reattachment area to where they subsided appeared important in determining the distance to the next slipface. New slipfaces tended to develop where these bursts of sediment movement were repeatedly subsiding.

The high velocity sweeps of fluid emanating from the reattachment area may not be strictly the same phenomenon as the high velocity sweeps on a planar bed. However, the effects of the two phenomena on sediment transport are very similar. In any case, the bursts of sediment movement emanating from the reattachment area appeared to be extremely important in determining the bed geometry.

For a given mean flow velocity, the higher the upstream slipface, the stronger the bursts of sediment movement in the reattachment area appeared to be. The experimental results indicate that new slipfaces developed preferentially downstream from the higher slipfaces. New slipfaces tended to develop where bursts of sediment movement were repeatedly subsiding. If the distance to the next slipface was greater than this distance, a new slipface developed on the stoss side of the existing bed form. In this way, new slipfaces were continually generated downstream from existing slipfaces.

It is hypothesized that the continual generation of

new slipfaces due to the fluid bursting phenomenon keeps the bed forms from being attenuated with time. Theoretically, if a mound of sediment is placed on a planar sediment bed with a constant mean flow velocity sufficient to transport sediment, the sediment on the top of the mound will be eroded and deposited on the downstream slope, resulting in the development of a slipface at the downstream end of the mound (Exner, 1920). With time, the slipface will migrate downstream and the mound will become longer and lower until it is eventually levelled off. If an existing slipface migrates farther downstream than the distance most bursts of sediment movement travel before subsiding, a new slipface develops on the stoss side of the existing bed form. The development of new slipfaces upstream from existing slipfaces offsets the tendency of an existing slipface or mound on the sediment bed to be levelled off with time. (The tendency of an existing mound or slipface to be levelled off with time if it is not supported from upstream was frequently observed.) Therefore, in this model, the generation of new slipfaces is critical to the continued existence of the bed forms, as opposed to the new slipfaces being secondary features that develop locally as a consequence of local flow conditions on the stoss side of an existing bed form.

The basic process resulting in the development of new slipfaces upstream from existing slipfaces appeared to be

the same for the entire range of mean flow conditions of these experiments. However, the rate of generation of new slipfaces was much slower at the lower mean flow velocities than at the higher. At the lower mean flow velocities, so little sediment was moved in a single burst of sediment movement that the subsidence of a much larger number of bursts in a given area was required for a new slipface to develop and, consequently, the area over which bursts subsided was more diffuse. From the time-lapse movie photography, mounds of sediment were observed to develop on the stoss side of bed forms and migrate downstream. At times, the downstream side of a mound became unstable and developed into a new slipface.

At the higher mean flow velocities, so much more sediment was moved in a single burst of sediment movement that the generation of new slipfaces by the repeated subsidence of bursts of sediment movement in a given area could be observed directly. The new slipfaces generated were similar to those that developed directly from a planar bed. Despite the necessity of the subsidence of many more bursts of sediment movement at lower flow velocities to result in the development of a new slipface and consequently the more diffuse nature of the deposition of the sediment, the basic process of the generation of the new slipfaces appeared to be the same for the entire range of mean flow conditions of these experiments.

The continual generation of new slipfaces downstream from existing slipfaces results in the large range of heights for a given mean flow velocity. All slipfaces initially have relatively small heights. With time, the heights of at least some of the slipfaces increase; heights increase both directly by the deposition of sediment upstream from the slipface and by the overtaking and coalescing of slipfaces. The skewed nature of the histograms of the height toward small values with tails to larger values is consistent with the continual generation of new slipfaces with small heights, with the height of only a small percentage of the slipfaces increasing to the maximum height.

The large range of heights consequently results in the large range of lengths for a given mean flow velocity. The height of a slipface determines the size of the flow separation and also appears to affect the strength of the bursts of sediment movement emanating from the reattachment area downstream. As noted in Section 6-5.2.2, the sum of these two distances appears to be the length downstream from major slipfaces to the next slipface regardless of the height of the slipface downstream, Lm-a, when the major slipface upstream is not overtaking the slipface downstream. The lengths between slipfaces that are less than the sum of the above two distances appear to be determined by the kinematics or relative migration rates of

the slipfaces rather than by the hydrodynamics downstream from a slipface.

Hypothetically, the maximum possible height of slipfaces for a given set of flow conditions is, in turn, ultimately limited by the length downstream from major slipfaces to the next slipface regardless of the height of the slipface downstream, Lm-a. Consider the case where the flow is sufficiently deep that the height of slipfaces is not limited by the mean flow depth. For a given value of Lm-a, as the height of the slipface downstream from Lm-a increases, the acute angle between the stoss side and the mean slope of the sediment bed increases. The maximum possible height is limited by how great this angle can become. A good first approximation of the maximum value of this angle might be the angle of repose of the sediment. For these experiments, especially at the lower flow velocities, there were some examples of bed forms with almost symmetrical longitudinal profiles where the acute angles that the stoss and lee slopes each formed with the mean bed slope were approximately the same.

In nature or experimental flumes, other factors such as the flow depth, the longitudinal extent of the sediment bed, the duration of the flow generating the bed forms, etc., probably limit or restrict the maximum possible height to a greater extent than Lm-a.

The dependence of the mean length on the mean flow

velocity and the increase in the average size of the bed forms as a function of mean flow velocity are both consistent with the above model. The length downstream from major slipfaces to the next slipface regardless of the height of the slipface downstream, Lm-a, depends strongly on the distance travelled by bursts of sediment movement before they subside. This distance might be expected to increase as the mean flow velocity increases, because the sediment-transporting ability of the flow increases with mean flow velocity.

As a result of the continual generation of new slipfaces and evolution from small scales to larger scales, there is no characteristic size for the bed forms for a given set of flow conditions. Bed-form height and length appear to be determined by the dynamics of the production and growth of slipfaces. If the distance from a given slipface to the next slipface downstream becomes greater than the distance to where bursts of sediment movement are repeatedly subsiding, a new slipface develops on the stoss side of the existing bed form. Once a new slipface develops, the sediment movement downstream from the new slipface on the upper stoss side of the preexisting bed form no longer appears to be as strongly influenced by the bursts of sediment movement originating upstream from the new slipface. The distance downstream from a given slipface to where a new slipface develops appears to

indicate the distance over which the flow patterns associated with the slipface upstream strongly influence the sediment movement and thus the bed geometry downstream.

Downstream from the new slipface the sediment movement seems more independent of the flow patterns associated with the slipface upstream from the new slipface. The length downstream from the new slipface to the next slipface appears to be determined by the relative migration rates of the slipfaces, although in some cases, if the preexisting bed geometry permits, the flow patterns associated with the new slipface result in the development of another new slipface downstream.

By the above hypothesis, the maximum length that can be sustained downstream from a given slipface to the next slipface is determined by the hydrodynamics downstream from the given slipface (i.e., the size of the flow separation and the distance over which most of the bursts of sediment movement from the reattachment area travel before subsiding). The best measure of this length is probably the length downstream from a slipface to where a new slipface is developing; the development of a new slipface occurs when most of the bursts of sediment movement subside before reaching the existing slipface downstream. The development of a new slipface indicates that the length downstream to the preexisting slipface is greater than the length the flow patterns associated with the slipface

upstream can maintain: the preexisting slipface downstream has migrated farther downstream than where most bursts of sediment movement are subsiding or, in some instances, the slipface upstream from the new slipface has changed configuration.

The experimental results on the geometric properties of the bed forms are consistent with the idea that if an existing slipface migrates farther downstream than the distance most bursts of sediment movement travel before subsiding, a new slipface develops on the stoss side of the existing bed form. As presented in Section 6-5.1.2, new slipfaces develop preferentially downstream from slipfaces with the larger heights. On average, for a given mean flow velocity the slipfaces with the larger heights migrate more slowly. Therefore, there is a greater than average probability that the slipfaces immediately downstream from the higher slipfaces will migrate more rapidly than the higher slipfaces and thus will eventually migrate farther downstream than where most bursts of sediment movement subside.

In addition, as noted in Section 6-5.1.2, the preferential development of new slipfaces downstream from slipfaces with the larger heights is consistent with the observation that new slipfaces form more readily when the bursts of sediment movement are stronger and therefore more grains are moved in a single burst; slipfaces with larger

heights appeared to result in stronger, more exaggerated bursts of sediment movement downstream. The higher the upstream slipface is, the greater the acceleration of the flow over the top of the slipface, and consequently the stronger the bursts of sediment movement emanating from the reattachment area downstream. Both the probable relative migration rates of slipfaces and the hydrodynamics downstream from slipfaces with the larger heights favor the preferential development of new slipfaces downstream from the slipfaces with the larger heights.

According to the proposed model the length downstream from a major slipface to the next slipface, L_{m-a}, is dominantly determined by the hydrodynamics downstream from the slipface when the slipface is not overtaking the slipface downstream. Also, the fluid and sediment dynamics determining the length downstream from a major slipface to the next slipface are similar regardless of the height of the slipface downstream. The data on the length/upstream-height ratios presented in Section 6-5.3.1 support this hypothesis. The lack of a difference in the mean values of L_r/H_u and L_m/H_u suggests that the fluid and sediment dynamics determining the length downstream from a major slipface to the next slipface are similar regardless of whether the next slipface is a ripplet or another major slipface. (L_r/H_u is the length from a major slipface to an adjacent ripplet downstream divided by the height of the

slipface upstream, and L_m/H_u is the length from a major slipface to an immediately adjacent major slipface downstream divided by the height of the slipface upstream.) This result also suggests that the length downstream from major slipfaces to the next slipface, L_{m-a}, may be a more fundamental length in terms of the fluid and sediment dynamics than the length between major slipfaces, L_{m-m}, as had been previously assumed.

As noted above, new slipfaces develop preferentially downstream from slipfaces with larger heights (i.e., on average H_{m-r} is greater than H_{m-m}). (H_{m-r} is the height of a major slipface upstream from a ripplet, and H_{m-r} is the height of a major slipface immediately upstream from another major slipface.) This result and the lack of a difference in the mean values of L_r/H_u and L_m/H_u naturally lead to the result that on average the length downstream from a major slipface to the next slipface is greater if the slipface downstream is a ripplet than if it is another major slipface (i.e., on average L_r is greater than L_m).

The result that on average L_r is greater than L_m is consistent with the above model but is not consistent with the common assumption that ripplets are secondary features that develop locally as a consequence of local flow conditions on the stoss side of an existing bed form. In the above model, the maximum length that can be sustained downstream from a slipface is the length downstream to

where a new slipface (i.e., a ripplet) is developing. This length is Lr. The development of a new slipface indicates that the length downstream to the preexisting slipface has become greater than the length the flow patterns associated with the slipface upstream can maintain.

Lengths shorter than the length determined by the hydrodynamics downstream from a slipface appear to result from the preexisting bed geometry and the kinematics or relative migration rates of the slipfaces. Interestingly, both processes which limit the length inhibit the attenuation of the bed forms. In the first case, if the distance downstream to the next slipface becomes greater than the distance most of the bursts of sediment movement travel before subsiding, a new slipface is generated, and in the second case, when slipfaces overtake one another and coalescence, the height of the resulting slipface is commonly greater than that of either of the individual slipfaces.

The histograms of the height and length are consistent with the continual generation of new slipfaces and evolution from small scales to larger scales with the maximum size increasing as a function of mean flow velocity. For both the height and the length, the range of sizes increases as a function of mean flow velocity; the minimum values remain approximately the same as the mean flow velocity is increased, while the maximum values

increase as the mean flow velocity is increased. For all the mean flow velocities of these experiments, the full range of sizes for the given mean flow velocity occur interspersed. The histograms are skewed to small values with tails to higher values, and there are no marked breaks in the histograms. In large part, differences in the details of the histograms for the different flow velocities reflect the differences in the rate of generation and growth of slipfaces and the differences in the maximum size that the bed forms can attain for different flow velocities.

Even if larger bed forms would have developed in a longer flume for the higher flow velocities, as is discussed in Section 6-5.2.2, the basic dynamics of the production and growth of the slipfaces from small scales to larger scales would still result in the continuum of bed form sizes from small to large and no single characteristic size for a given set of flow conditions. The continual evolution of slipfaces from small scales to larger scales was observed for all the mean flow velocities of these experiments; larger heights and lengths were not observed to occur without the presence of smaller heights and lengths interspersed. A natural consequence of this continual evolution of slipfaces from small scales to larger scales is the absence of a major break in bed-form size or an intermediate range of sizes over which no bed

forms exist within the range of flow conditions of these experiments.

This conclusion appears to contradict data presented by other authors suggesting that there is a natural break in bed form size within the range of mean flow conditions examined in these experiments. The apparent contradiction is a consequence of the method used by previous authors to present data. The data on bed-form length of Guy et al. (1966) presented by Allen (1982) is frequently cited as evidence for a natural break in bed-form size within this range. This data is presented in a histogram using a logarithmic scale for the size intervals and mean values of the length. The distribution appears strongly bimodal. However, a unimodal distribution which is skewed to small values with a long tail to higher values on a linear scale can appear bimodal when presented using a logarithmic scale. The data on bed-form length used by Allen (1982) when presented in a histogram using a linear scale and the number of class intervals indicated by Sturges' equation (Daniel, 1978) is a unimodal distribution skewed to small values with a long tail to higher values. Logarithmic scales are frequently used in presenting data on the size of bed forms.

The continual generation of new slipfaces and the differential migration rates of the slipfaces naturally result in the superposition of smaller slipfaces on the

stoss sides of larger bed forms. A difference in dynamics in bed forms of different size is not necessary in order to explain the superposition of bed forms. The superposition of bed forms is consistent with the single model for the generation and continued existence of bed forms proposed above.

Section 7-4

Conclusion

These experiments were carried out to examine both quantitatively and observationally the similarities and differences between the different kinds of flow-transverse bed forms previously delineated by other authors in flume studies: ripples, two-dimensional dunes, and three-dimensional dunes. More detailed quantitative data on the bed geometry was obtained than has generally been available. Long running times were used for the flume experiments in order to obtain large sample sizes for the data on the geometric properties of the bed forms for each set of mean flow conditions. The large sample sizes made it possible to construct well defined histograms of the different geometric properties for each mean flow velocity. The large sample sizes also made it possible to analyze trends in the data statistically as functions of mean flow velocity and to examine the similarities and differences in the various categories of the geometric properties for a

given set of mean flow conditions. The geometric properties of the bed forms changed smoothly and systematically as functions of mean flow velocity; there are no marked breaks in the size distributions. A summary of the main results on the geometric properties of the bed forms is given in Section 6-6.0.0.

In order to document and examine the transitions between the three different kinds of bed forms the experiments were conducted at closely spaced velocity intervals over the range of mean flow velocities where these transitions were expected to occur. Careful observations of the sediment bed were made many times during each flume run. Included were observations of the sediment movement, the initial development of bed forms from a planar bed, the evolution of the bed forms with time, and the kinematics of the bed forms. The closely spaced velocity intervals were purposely used to make it possible to observe the supposedly abrupt change in the bed forms from ripples to dunes. For the 15-cm flow depth of these experiments, no abrupt changes in bed-form size, kinematics, or apparent dynamics were observed with changes in mean flow velocity. The experimenter was anticipating a change and observed even more carefully when it did not become evident.

Both the kinematics and the dynamics of the bed forms appeared to be basically the same over the entire range of

flow conditions of these experiments. For all the mean flow velocities of these experiments the initial bed forms that developed from a planar bed were very similar in size and appeared to result from similar processes. With time the average size of the bed forms increased until some bed forms of the maximum size for the given set of flow conditions developed. The evolution from the initial bed forms to larger bed forms was similar for the entire range of flow conditions. As the average size of the bed forms increased, new small slipfaces continued to be generated. As a result the size distributions of the bed forms are skewed to small values with tails to larger values. The bed forms did not evolve to a single characteristic size. The continual generation of new slipfaces and the evolution from small scales to larger scales are dominant features of the bed-form dynamics for the entire range of flow conditions of these experiments. The above data do not support any theory of bed forms that results in a single characteristic bed-form size for a given set of flow conditions.

The experimental results on the geometric properties of the bed forms and the observations on the bed forms suggest that ripples and dunes may not be two dynamically different kinds of bed forms. The main reasons for this possible conclusion are summerized below:

(1) The geometric properties of the bed forms changed smoothly and systematically as functions of mean flow velocity over the entire range of mean flow conditions of these experiments. There are no marked breaks in the size distributions: there is a continuum of bed-form sizes.

(2) In addition, both the kinematics and the dynamics of the bed forms appear to be basically the same over the range of mean flow conditions where the transitions between the three different kinds of bed forms were expected to occur. The modes of sediment movement and the sediment movement patterns were observed to be basically the same for the entire range of flow conditions. However, as the mean flow velocity increased, certain aspects of sediment movement such as the development of three-dimensional scour pits became more noticeable both because the processes occurred more rapidly and more sediment was involved in the processes; the development of three-dimensional scour pits was common in all of the flume runs. As a result, a cursory examination of the sediment bed might give the impression of greater differences than can be substantiated upon closer examination.

(3) Also, a difference in dynamics in ripples and dunes (ie., bed forms of different size) is not necessary in order to explain the superposition of bed forms. The continual generation of new slipfaces and the differential migration rates of slipfaces naturally result in the

superposition of smaller slipfaces on the stoss sides of larger bed forms. The superposition of bed forms is an inherent characteristic of the process of bed form development.

This conclusion is similar to that of a symposium on "Classification of Large-Scale Flow-Transverse Bedforms" that concluded that all large flow-transverse bed forms are similar phenomena (Ashley et al., 1990). Different scales of large-scale bed forms have been considered to be possibly dynamically different primarily because of apparent discontinuities in size and differences in shape for different flow conditions, and the superposition of different scales of large-scale bed forms on one another. In this report, Flemming's (1988) log-log plot of spacing vs. height of bed forms with spacings ranging from 0.01 m (1.0 cm) to over 1000 m (1.0 X 10^6 cm) is used to show that "large bedforms occur as a continuum of sizes not as discrete groups."

The superposition of different scales of large-scale bed forms has been used to infer a difference in dynamics. The symposium concluded that "superposition should not form the basis of classification, but could be a useful second order descriptor (ie., simple or compound)." However, this conclusion is reached for reasons different from those presented in the above model. Ashley notes that the consensus of the panel "is based on the assumption that

superposition reflects processes other than fundamental processes of bedform genesis." In the report, it is suggested that "larger bed forms generate a boundary layer in which the smaller bed forms are locally stable (Smith and Mclean, 1977; Rubin and McCulloch, 1980)." The implicit assumption is that the smaller bed forms are secondary: the stability of the larger bed forms does not depend on the smaller bed forms. The boundary layer generated by the larger bed forms creates local conditions in which the smaller bed forms are locally stable.

In the model presented in this thesis, the superposition of bed forms is considered to be an integral part of bed-form development resulting from the continual generation of new slipfaces and the differential migration rates of slipfaces. These processes appeared to be essential to the continued existence of the bed forms and thus are fundamental processes of bed-form development or genesis.

The single model of lower-flow-regime bed forms proposed in this thesis is consistent with the observations on the bed forms and the experimental data on the geometric properties of the bed forms obtained in these experiments. This model represents a fundamentally different interpretation of bed forms. In this model, the size of the bed forms is determined by the dynamics of the continual generation of new slipfaces and the evolution

from small scales to larger scales. The size of individual bed forms is continually changing. No single size of bed form is stable, even locally.

For the range of flow conditions of these experiments, the geometric properties of the bed forms change smoothly and systematically and both the kinematics and dynamics of the bed forms appear to be basically the same. These results suggest that ripples and dunes may not be two dynamically different kinds of bed forms. However, the range of flow conditions of these experiments are limited compared to natural environments. Detailed quantitative data on the geometric properties of the bed forms and data on the kinematics and dynamics of the bed forms for greater flow depths and a wider range of flow velocities would be important in resolving whether ripples and dunes are geometrically and dynamically distinct bed phases. Experiments for greater flow depths and a wider range of flow velocities might show that bed forms in the ripple and dune stability fields are dominated by different processes with a continuous transition between the two kinds of bed forms.

The flow depth of 15 cm in these experiments is very shallow compared with the range of flow depths in which ripples and dunes are observed. For greater flow depths, the sizes of the bed forms in the ripple stability field would probably be similar to those in these experiments

whereas the maximum size of the bed forms in the dune stability field would probably be larger. The greater difference in the mean size would enhance the difference in appearance between bed forms in the ripple and dune stability fields.

Inferences about the distinction between ripples and dunes which are based on the shapes of curves of mean geometric properties of the bed forms as functions of flow velocity would be strengthened by data for a wider range of flow velocities on either side of the possible transitional region. If curves of mean geometric properties for a wider range of flow velocities showed the presence of two branches with relatively gentle curvature at the low-velocity and high-velocity extremes and a strongly curved intermediate segment, then such data could be viewed as evidence for the existence of two distinct bed phases whose dynamics are different. If, on the other hand, curves of mean geometric properties for a wider range of flow velocities showed no substantial differences in degree of curvature over the entire range of flow velocities, then such data would be evidence for a single bed phase whose properties and dynamics vary gradually over a wide range of flow conditions.

If data were obtained for a wider range of flow conditions, it would be important to determine whether or not the distributions of the geometric properties of the

bed forms for individual sets of flow conditions exhibit the same basic characteristics as those for these experiments. It would also be important to obtain data on the kinematics of the bed forms and observations on the sediment movement patterns on the bed forms.

Hopefully, both the observational and quantitative data and the ideas presented in this thesis will provide some new insights into the problem of bed-form development and will indicate possible areas for future research.

REFERENCES

Allen, J.R.L., 1963, Asymmetrical ripple marks and the origin of water-laid cosets of cross-strata: Liverpool Manchester Geol. J., 3, 187-236.

Allen, J.R.L., 1968, Current Ripples; Their Relation to Patterns of Water and Sediment Motion: Amsterdam, North Holland, 433 p.

Allen, J.R.L., 1982, Sedimentary Structures; Their Character and Physical Basis: Amsterdam, Elsevier, 2 vols.

ASME (American Society of Mechanical Engineers), 1959, Flow Measurement, 4, PTC 19.5, 92 p.

Ashley et al., 1990, Classification of large-scale subaqueous bed forms: a new look at an old problem. SEPM Bedforms and Bedding Structures Research Symposium: Jour. Sed. Petrology, 60, in press.

Bevington,P.R., 1969, Data Reduction and Error Analysis for the Physical Sciences: New York, NY, McGraw-Hill, 336 p.

Cantwell, B.J., 1981, Organized motion in turbulent flow: Ann. Rev. Fluid Mech., 13, 457-515.

Costello, W.R., and Southard, J.B., 1981, Flume experiments on lower-flow-regime bed forms in coarse sand: Jour. Sed. Petrology, 51, 849-864.

Daniel, Wayne, 1987, Biostatistics: a Foundation for Analysis in Health Sciences, 4th ed.: New York, John Wiley and Sons, Inc., 737 p.

Engelund, F., 1970, Instability of erodible beds: J. Fluid Mech., 42, 225-244.

Engelund, F., and Fredsoe, J., 1974, Transition from dunes to plane bed in alluvial channels: Tech. Univ. Denmark, Inst. Hydraul. Eng., Series Paper 4.

Exner, F.M., 1920, Zur Physik der dunen: Akad. Wiss. Wien, Sitzungsver, Math.-Nat. Kl., Abt. IIa, 129, 929-952.

Flemming, B.W., 1988, Zur Klassifikation subaquatischer, stromungstransversaler Transportkorper: Boch. geol. u. geotechn. Arb., 29, 44-47.

Gilbert, G.K., 1914, The transportation of debris by running water: U.S. Geol. Surv. Prof. Paper 86, 263 p.

Guy, H.P., Simons, D.B., and Richardson, E.V., 1966, Summary of alluvial channel data from flume experiments, 1956-61: U.S. Geol. Surv. Prof. Paper 462-I, 96 p.

Johnson, Palmer O., 1949, Statistical Methods in Research: New York, Prentice Hall, Inc., 377 p.

Kennedy, J.F., 1963, The mechanics of dunes and antidunes in erodible bed channels: J. Fluid Mech., 16, 521-544.

Kennedy, J.F., 1969, The formation of sediment ripples, dunes and antidunes: Annual Review of Fluid Mechanics, W.R. Sears (ed.) 1, 147-168.

Middleton, G.V., and Southard, J.B., 1984, Mechanics of Sediment Movement: 2nd ed. SEPM Short Course No. 3, Soc. of Econ. Paleo, Mineral. Tulsa, OK, 401 p.

Pratt, C.J., and Smith, K.V.H., 1972, Ripple and dune phases in a narrowly graded sand: Am. Soc. Civil Engrs. Proc., Jour. Hydraul. Div., 98, 859-874.

Raudkivi, A.J., 1963, Study of sediment ripple formation: Proc. Amer. Soc. Civ. Eng., J. Hydraul, Div., 89, (HY 6), 15-33.

Reynolds, A.J., 1965, Waves on the erodible bed of an open channel: J. Fluid Mech., 22, 113-133.

Richards, 1980, The formation of ripples and dunes on an erodible bed: J. Fluid Mech., 99, 597-618.

Rubin, D.M., and McCulloch, D.S., 1980, Single and superimposed bedforms: a synthesis of San Francisco Bay and flume observations: Sed. Geology, 26, 207-231.

Simons, D.B., Richardson, E.V., and M.L. Albertson, 1961, Flume studies using medium sand (0.45), Geological Survey Water-Supply Paper 1498-A.

Smith, J.D., 1970, Stability of a sand bed subjected to a shear flow of low Froude Number: J. Geophys. Res., 75, 5928-5939.

Smith, J.D., and McLean, S.R., 1977, Spatially averaged flow over a wavy surface: J. Geophys. Res., 82, 1735-1746.

Southard, J.B., 1971, Representation of bed configurations in depth-velocity-size diagrams: J. Sed. Petrol., 41, 903-915.

Southard, J.B., and Dingler, J.R., 1971, Flume study of ripple propagation behind mounds of flat sand beds: Sedimentology, 16, 251-263.

Southard, J.B., and Boguchwal, L.A., 1990, Bed Configurations in Steady Unidirectional Water Flows, Part 2, Synthesis of Flume Data: J. Sed. Petrol., 60, 658-679.

Weast, Robert C., 1988, CRC Handbook of Chemistry and Physics, 69th ed., 2488p.

Williams, G.E., 1971, Flood Deposits of the Sand-Bed Ephemeral Streams of Central Australia: Sedimentology, 17, 1-40.

Williams, P.B., and Kemp, P.H., 1971, Initiation of ripples on flat sediment beds: Proc. Am. Soc. Civ. Eng., J. Hydraul. Div., 97(4), 505-522.

TABLES

APPENDICES

FIGURES

TABLES

TABLE 3-1

FLOW DEPTH

Run Number	Mean Flow Depth (cm)	Sample Standard Deviation (cm)
1	14.70	0.45
2	15.04	0.48
3	14.97	0.12
4	14.95	0.20
5	14.97	0.20
6	15.03	0.20
7	15.06	0.31
8	15.07	0.28
9	15.07	0.27
10	15.16	--
11	15.22	--
12	15.02	--

TABLE 3-2

FLOW VELOCITY

Run Number	Mean Flow Velocity (cm/s)	Sample Standard Deviation (cm/s)
1	28.59	0.88
2	30.02	1.11
3	32.05	0.26
4	34.13	0.44
5	36.10	0.46
6	37.96	0.47
7	40.86	0.82
8	43.81	0.82
9	47.41	0.80
10	32.30	--
11	38.37	--
12	47.38	--

TABLE 3-3

WATER-SURFACE SLOPE

Run Number	Mean Water-Surface Slope	Sample Standard Deviation
1	-5.97×10^{-4}	0.78×10^{-4}
2	-6.91×10^{-4}	0.83×10^{-4}
3	-6.58×10^{-4}	0.86×10^{-4}
4	-4.88×10^{-4}	1.34×10^{-4}
5	-4.64×10^{-4}	1.30×10^{-4}
6	-4.72×10^{-4}	0.91×10^{-4}
7	-6.72×10^{-4}	1.43×10^{-4}
8	-6.65×10^{-4}	1.26×10^{-4}
9	-9.72×10^{-4}	3.02×10^{-4}
10	-6.28×10^{-4}	--
11	-0.89×10^{-4}	--
12	-16.43×10^{-4}	--

TABLE 3-4

BED-SURFACE SLOPE

Run Number	Mean Bed-Surface Slope	Sample Standard Deviation
1	-4.0×10^{-4}	19.0×10^{-4}
2	12.8×10^{-4}	8.3×10^{-4}
3	4.4×10^{-4}	9.5×10^{-4}
4	-24.7×10^{-4}	15.5×10^{-4}
5	-20.1×10^{-4}	13.7×10^{-4}
6	-37.1×10^{-4}	22.4×10^{-4}
7	-30.4×10^{-4}	22.2×10^{-4}
8	-51.5×10^{-4}	14.6×10^{-4}
9	-59.5×10^{-4}	15.8×10^{-4}
10	-3.9×10^{-4}	--
11	-67.5×10^{-4}	--
12	-69.9×10^{-4}	--

TABLE 3-5

BOUNDARY SHEAR STRESS

Run Number	Mean Boundary Shear Stress ($dyne/cm^2$)
1	8.58
2	10.1
3	9.65
4	7.16
5	6.80
6	6.92
7	9.91
8	9.81
9	14.4
10	9.33
11	1.32
12	24.1

TABLE 3-6

WATER TEMPERATURE

Run Number	Mean Water Temperature (°C)	Sample Standard Deviation (°C)
1	26.43	0.84
2	26.56	0.39
3	26.87	0.29
4	27.30	0.52
5	28.22	0.41
6	28.70	0.64
7	28.68	0.25
8	28.22	0.40
9	26.08	0.30
10	26.40	--
11	26.55	--
12	26.05	--

TABLE 3-7

WATER DENSITY, VISCOSITY, AND KINEMATIC VISCOSITY

Run Number	Mean Water Density (g/cm^3)	Mean Viscosity (g/s cm)	Mean Kinematic Viscosity (cm/s)
1	0.9967	0.008622	0.008651
2	0.9966	0.008597	0.008626
3	0.9965	0.008538	0.008568
4	0.9964	0.008457	0.008487
5	0.9962	0.008288	0.008320
6	0.9960	0.008202	0.008235
7	0.9960	0.008205	0.008238
8	0.9962	0.008288	0.008320
9	0.9968	0.008690	0.008718
10	0.9967	0.008628	0.008657
11	0.9966	0.008599	0.008628
12	0.9968	0.008696	0.008724
average for Runs 1-9	0.9964	0.008432	0.008462

TABLE 3-8

REYNOLDS NUMBER AND FROUDE NUMBER

Run Number	Reynolds Number	Froude Number
1	4.86×10^4	0.238
2	5.23×10^4	0.247
3	5.60×10^4	0.265
4	6.01×10^4	0.282
5	6.50×10^4	0.298
6	6.93×10^4	0.313
7	7.47×10^4	0.336
8	7.94×10^4	0.360
9	8.20×10^4	0.390
10	5.65×10^4	0.265
11	6.77×10^4	0.314
12	8.16×10^4	0.390

TABLE 3-9

SEDIMENT DISCHARGE

Run Number	Mean Sediment Discharge[1] (g/cm s)
1	0.21×10^{-3}
2	1.29×10^{-3}
3	1.70×10^{-3}
4	1.55×10^{-3}
5	3.52×10^{-3}
6	1.83×10^{-3}
7	2.14×10^{-3}
8	11.3×10^{-3}
9	16.7 x 10-3

[1]per unit width of the flume

TABLE 6-1

$$\frac{X}{Y} = \frac{\text{AVERAGE MIGRATION RATE OF MAJOR SLIPFACES}}{\text{AVERAGE RATE OF TAKING THE BED PROFILE}}$$

Run Number	X/Y
1	0.013
2	0.013
3	0.019
4	0.021
5	0.023
6	0.044
7	0.078
8	0.150
9	0.325

APPENDICES

Appendix A: Summary of Data

run	mean flow depth (cm)	mean flow velocity (cm/s)	mean flow discharge (cm^3/s)	mean water surface slope	mean bed surface slope	mean water temperature (deg C)	mean water density (g/cm^3)
1	14.7	28.6	38,700	-0.000597	-0.00040	26.4	0.9967
2	15.0	30.0	41,400	-0.000691	0.00128	26.6	0.9966
3	15.0	32.1	44,300	-0.000658	0.00044	26.9	0.9965
4	15.0	34.1	47,100	-0.000488	-0.00247	27.3	0.9964
5	15.0	36.1	49,800	-0.000464	-0.00201	28.2	0.9962
6	15.0	38.0	52,400	-0.000472	-0.00371	28.7	0.9960
7	15.1	40.9	56,800	-0.000672	-0.00304	28.7	0.9960
8	15.1	43.8	60,800	-0.000665	0.00515	28.2	0.9962
9	15.1	47.4	65,800	-0.000972	-0.00595	26.1	0.9968
10	15.2	32.3	45,200	-0.000628	-0.00039	26.4	0.9967
11	15.2	38.4	53,700	-0.000089	-0.00675	26.6	0.9966
12	15.0	47.4	65,400	-0.001643	-0.00699	26.1	0.9968

run	mean viscosity (g/cm-s)	mean kinematic viscosity (cm/s)	Reynolds number	Froude number	mean sediment discharge (g/cm-s)	boundary shear stress ($dyne/cm^2$)
1	0.008622	0.008651	48,600	0.238	0.00021	8.58
2	0.008597	0.008626	52,300	0.247	0.00129	10.13
3	0.008538	0.008568	56,000	0.265	0.00170	9.65
4	0.008457	0.008487	60,100	0.282	0.00155	7.16
5	0.008288	0.008320	65,000	0.298	0.00352	6.80
6	0.008202	0.008235	69,300	0.313	0.00183	6.92
7	0.008205	0.008238	74,700	0.336	0.00214	9.91
8	0.008288	0.008320	79,400	0.360	0.01133	9.81
9	0.008690	0.008718	82,000	0.390	0.01672	14.35
10	0.008628	0.008657	56,500	0.265		9.33
11	0.008599	0.008628	67,700	0.314		1.32
12	0.008696	0.008724	81,600	0.390		24.10

Appendix B: Summary of Geometric Properties

Run	Mean Height					Mean Length					Mean Length / Upstream Height				
	H_m (cm)	H_r (cm)	H (cm)	H_{m-m} (cm)	H_{m-r} (cm)	L_{m-m} (cm)	L_{m-a} (cm)	L_m (cm)	L_r (cm)	L_c (cm)	$\frac{L_{m-m}}{H_u}$	$\frac{L_{m-a}}{H_u}$	$\frac{L_m}{H_u}$	$\frac{L_r}{H_u}$	$\frac{L_c}{H_u}$
1	1.6		1.6	1.6		19.9	19.5	19.7			14.5	14.2	14.5		
2	1.7	0.5	1.6	1.7		21.5	20.5	20.9			13.9	13.2	13.3		
3	1.8	0.6	1.6	1.8		24.8	23.6	24.2			15.5	14.8	15.2		
4	1.8	0.5	1.6	1.8		30.3	29.0	29.5			18.4	17.6	17.8		
5	1.8	0.4	1.5	1.7	2.5	37.6	35.0	32.9	44.8	61.4	22.2	20.7	21.0	19.0	28.0
6	2.0	0.5	1.3	1.7	2.5	57.8	47.7	45.8	50.0	73.8	32.7	27.0	29.7	24.1	36.7
7	2.4	0.5	1.4	2.2	2.7	68.5	53.3	48.0	55.6	78.8	28.4	23.8	21.4	24.7	32.0
8	2.6	0.6	1.7	2.3	3.0	60.8	49.0	40.7	55.4	77.9	24.4	20.4	19.5	21.0	28.6
9	2.7	0.6	2.0	2.5	3.4	54.2	44.4	38.0	52.4	76.7	20.8	17.4	17.3	17.5	25.7

FIGURES

Figure 3–1

Mean Flow Depth vs. Mean Flow Velocity

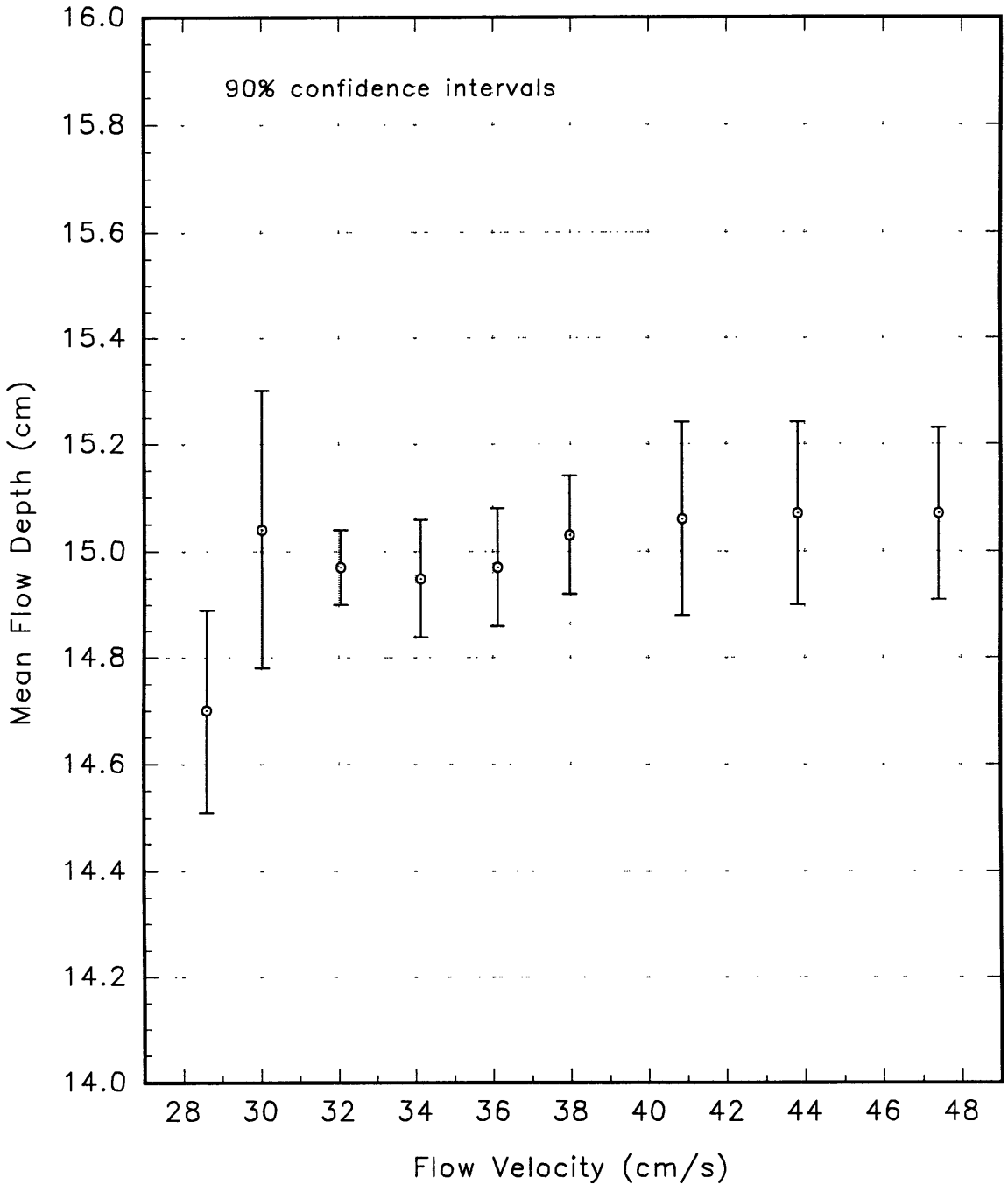

Figure 3–2

Mean Flow Velocity vs. Run Number

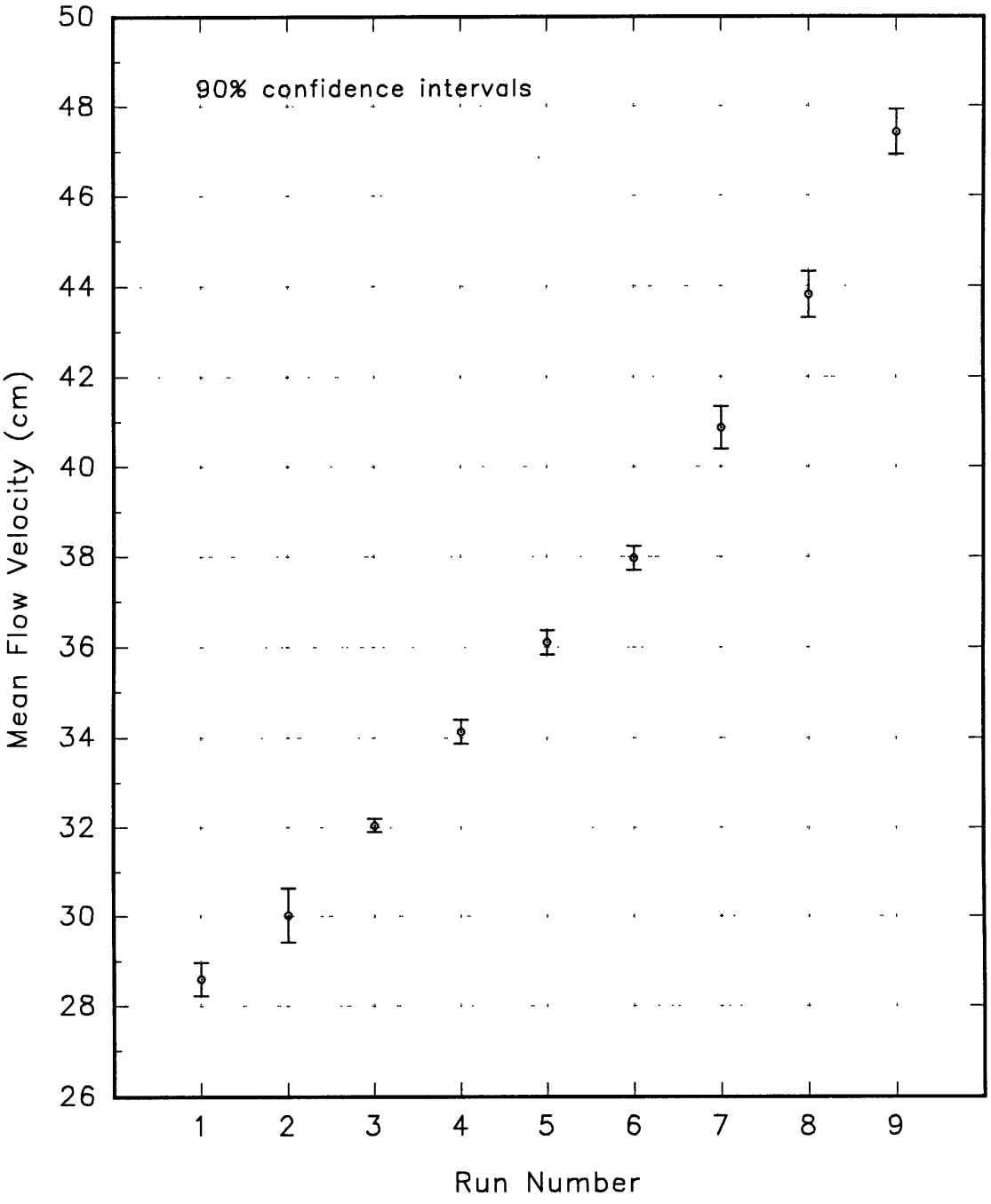

Figure 3-3

Mean Water-Surface Slope vs. Mean Flow Velocity

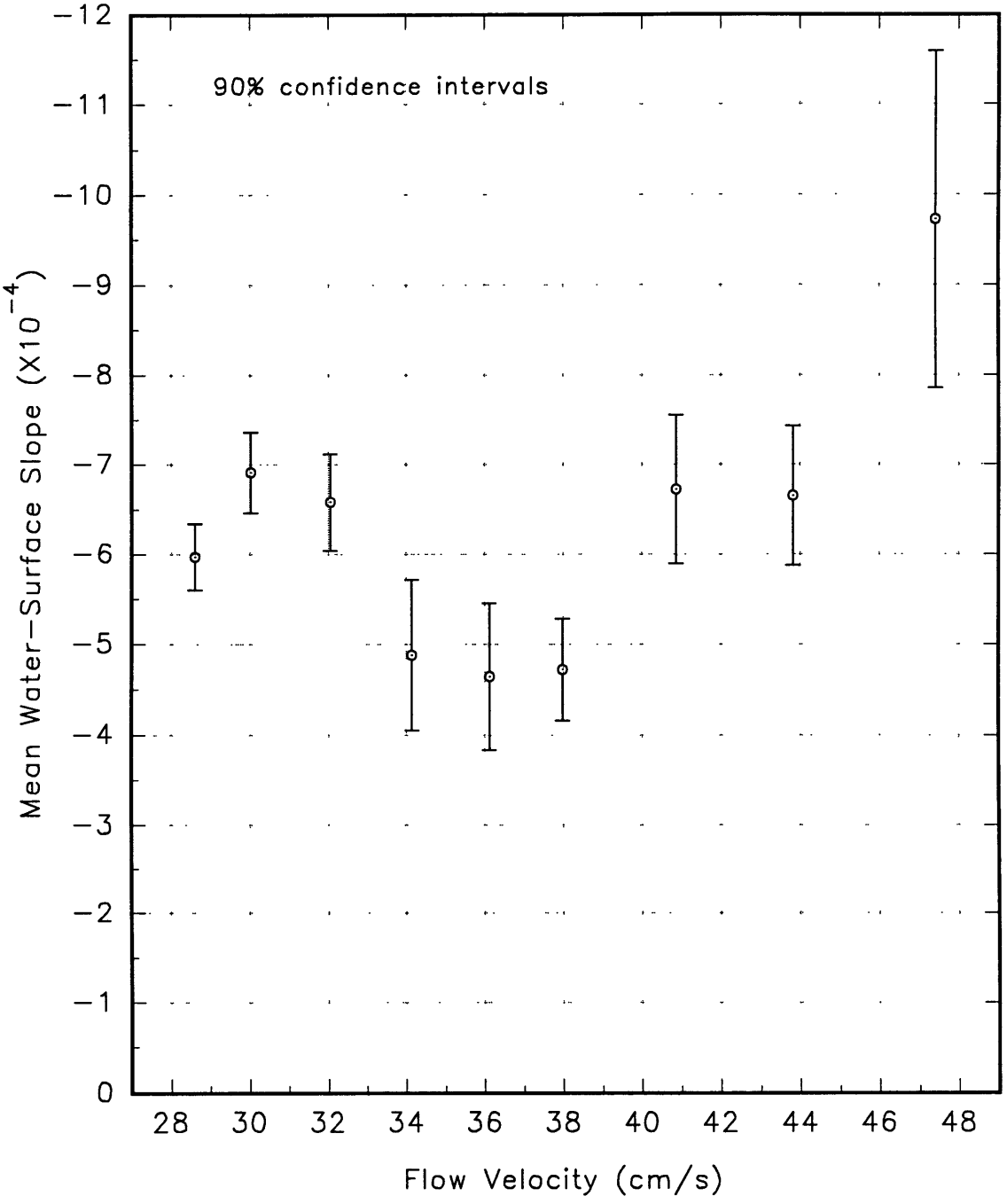

Figure 3–4

Mean Bed–Surface Slope vs. Mean Flow Velocity

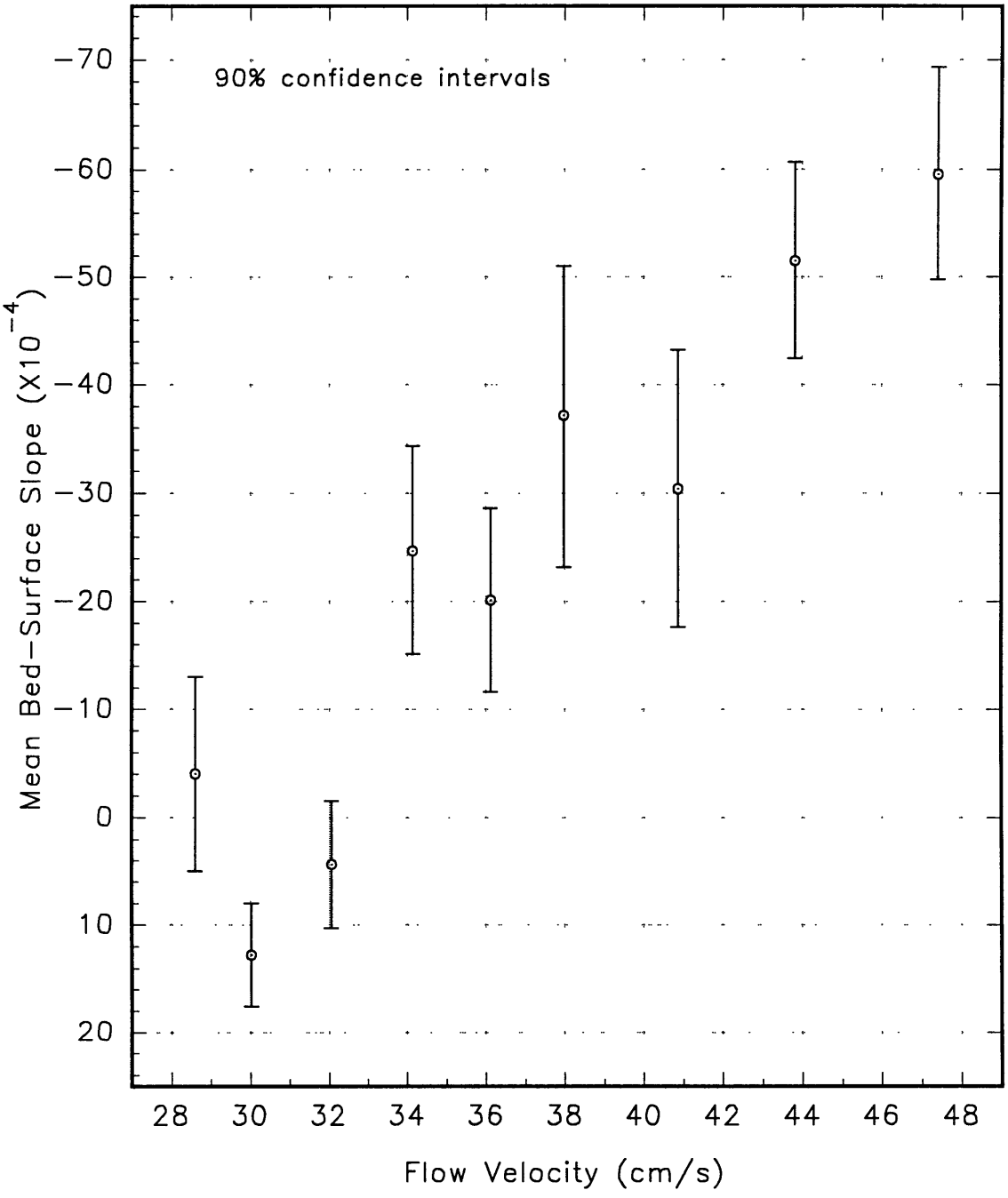

Figure 3–5

Mean Water–Surface and Mean Bed–Surface Slopes

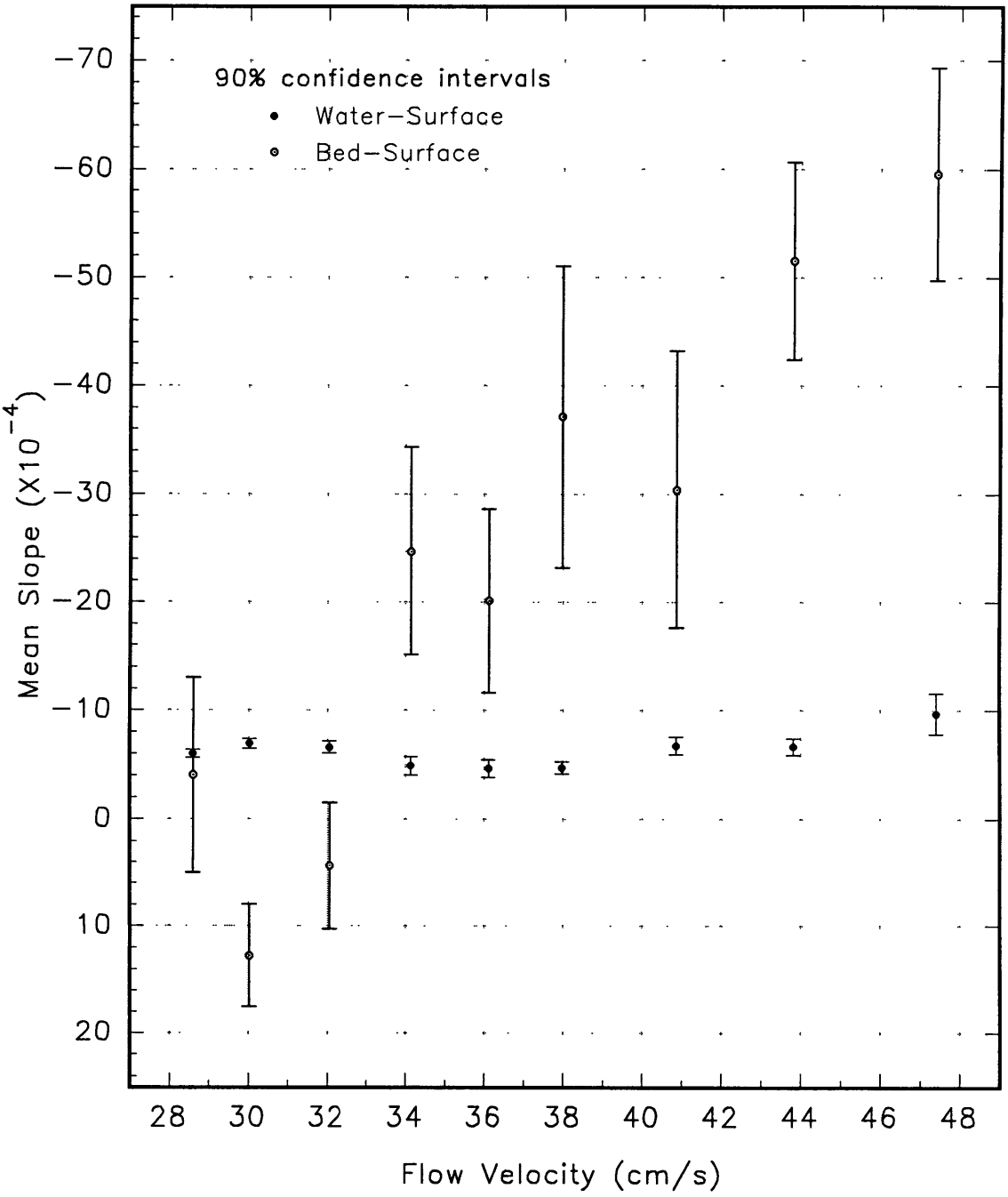

Figure 3–6

Mean Sediment Discharge vs. Mean Flow Velocity

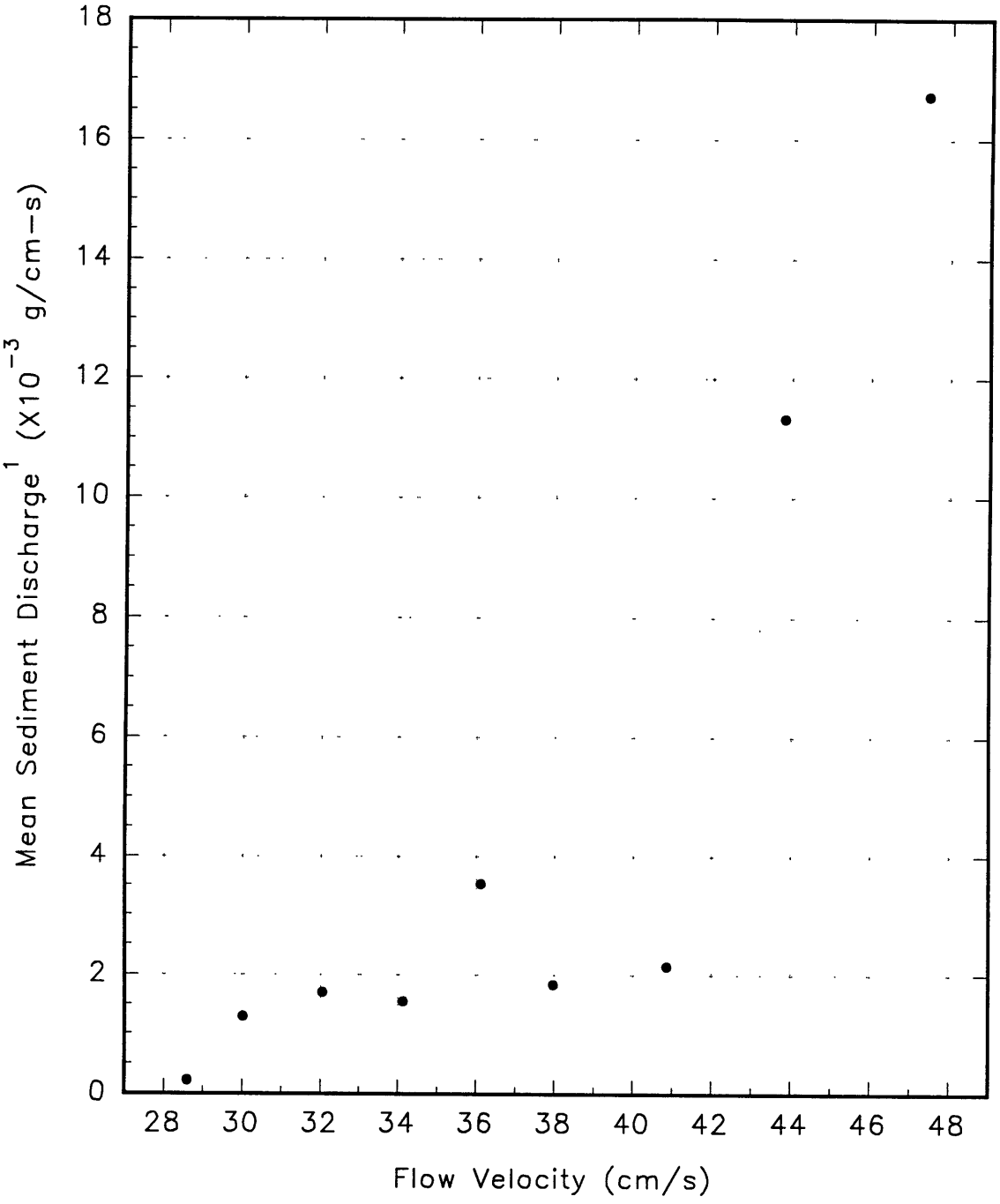

[1] per unit width of the flume

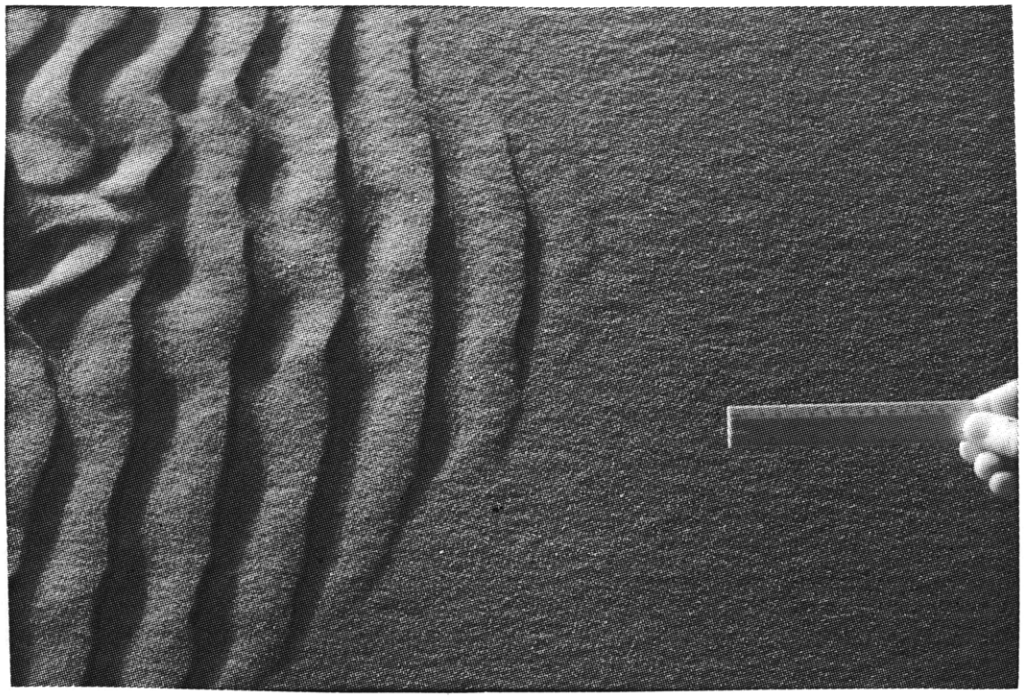

Figure 4-1. Close-up plan view of propagating bed-form front about 13 hours after start-up. This figure shows a new bed form developing downstream from the front and also the beginnings of an even newer disturbance on the planar bed immediately downstream from this newly developing bed form. (Run 1-1, V = 28.6 cm/s, centered at 470 cm, ruler = 15 cm, flow from left to right)

Figure 4-2. Upstream view of propagating bed-form front about 13 hours after start-up. This figure shows the shape of the bed-form front and the more three-dimensional bed forms upstream from the front. (Run 1-1, V = 28.6 cm/s, channel width = 91 cm)

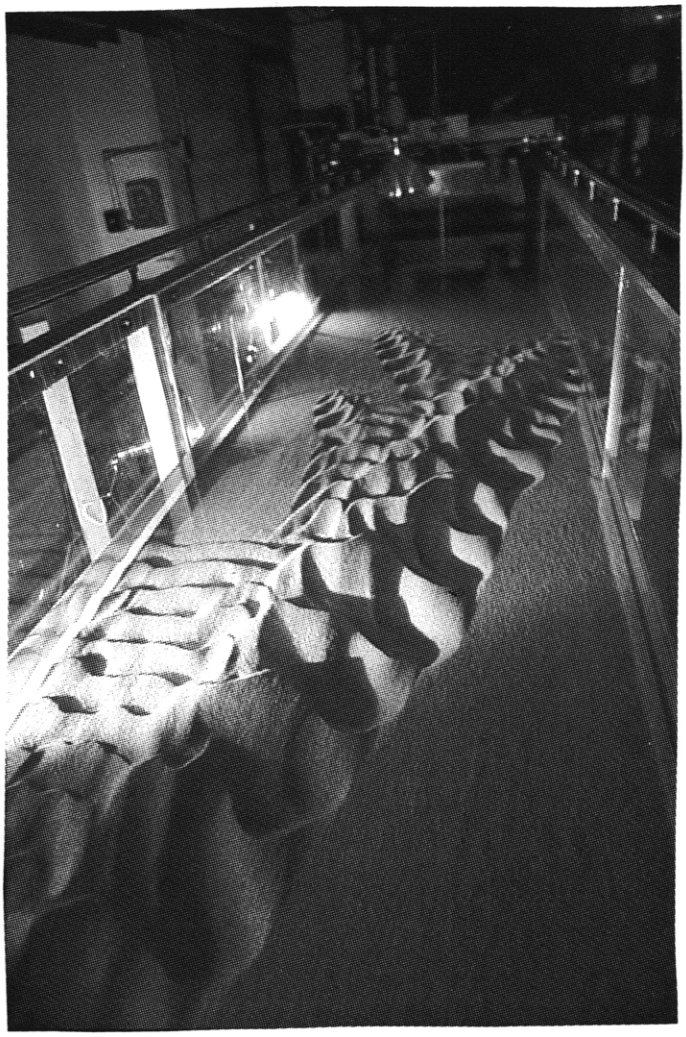

Figure 4-3. Downstream view of diagonal spurs of three-dimensional bed forms about nine hours and 15 minutes after start-up. See text. (Run 1-1, V = 28.6 cm/s)

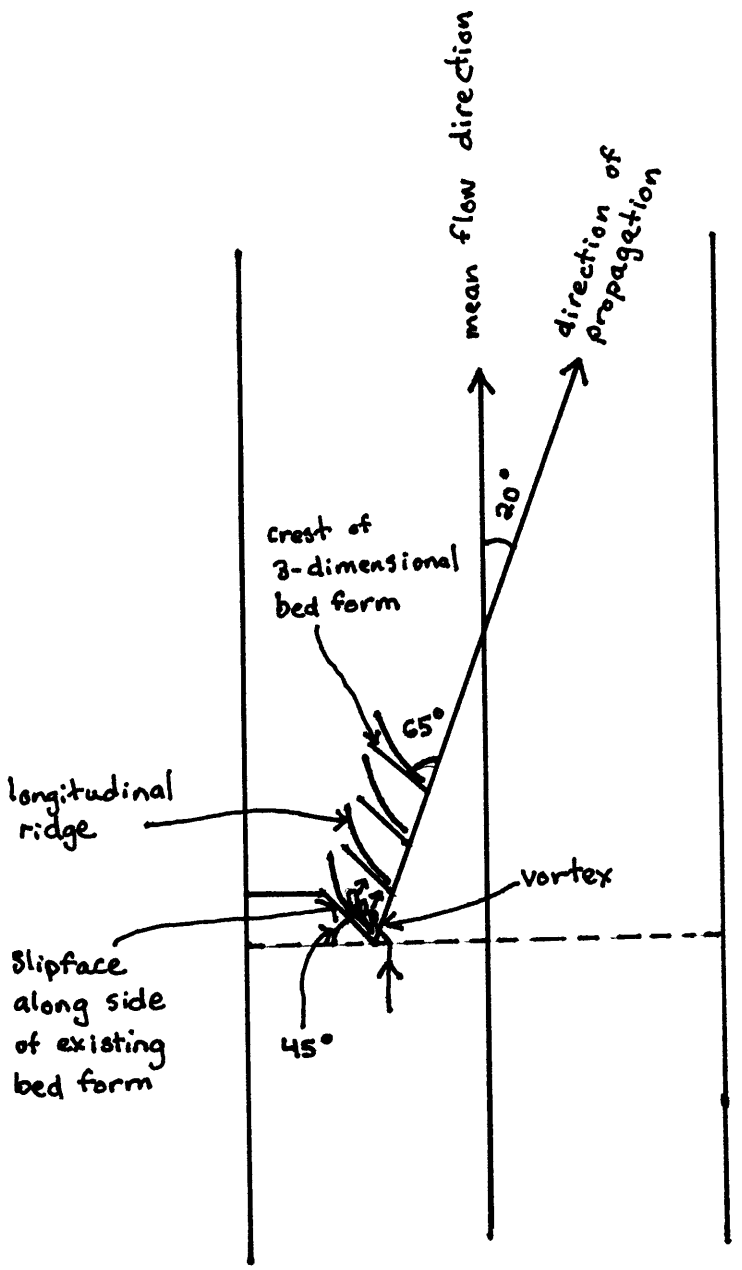

Figure 4-4. Schematic of the approximate geometric relationships that characterize the propagation of 3-dimensional bed forms.

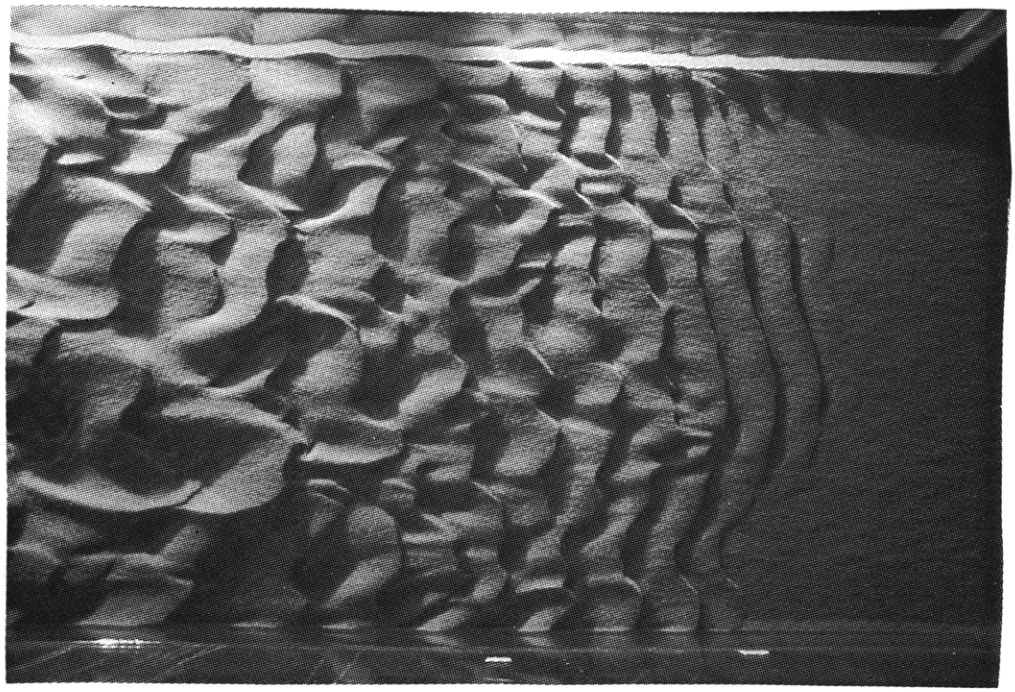

Figure 4-5. Plan view of propagating bed-form front about five hours and ten minutes after start-up. This figure shows the relatively small, straight-crested, two-dimensional bed forms near the bed form front and the larger, more three-dimensional bed forms upstream. (Run 3-1, V = 32.1 cm/s, centered at 460 cm, length of field of view = 155 cm, flow from left to right)

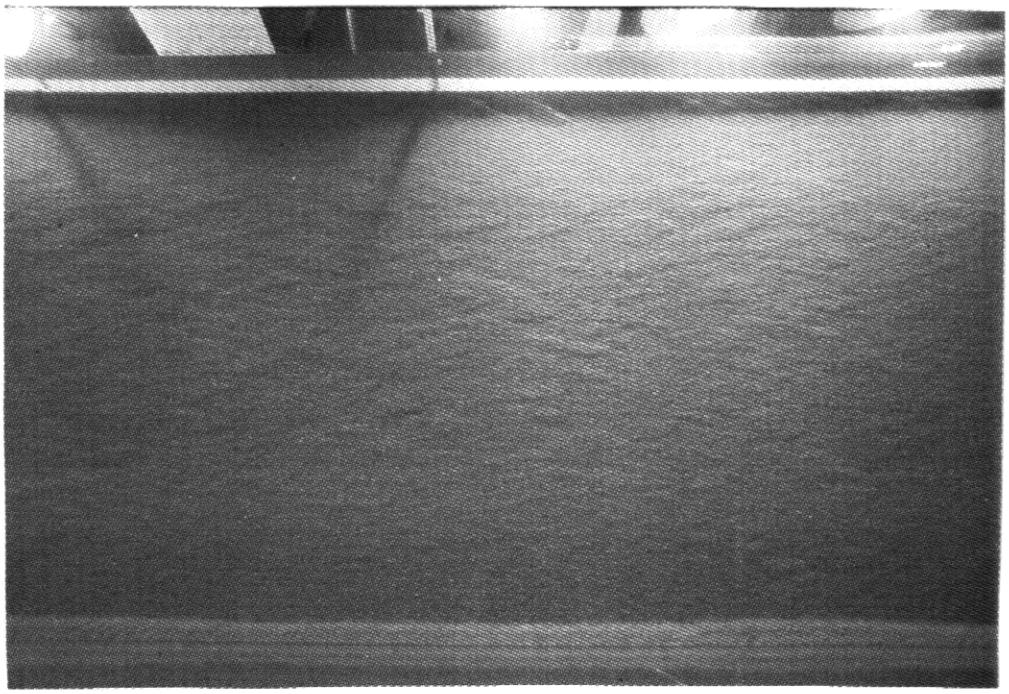

Figure 4-6. Plan view of hummocky planar-bed micro-topography about 5 hours and 20 minutes after start-up. (Run 3-1, V = 32.1 cm/s, centered at 920 cm, length of the field of view = 155 cm, flow from left to right)

Figure 4-7. Close-up plan view of newly developed three-dimensional bed forms propagating diagonally downstream about 5 hours and 30 minutes after start-up. This figure shows the characteristic geometry of three-dimensional bed forms and also shows a newly developing scour pit and the beginnings of the associated longitudinal ridge, extending downstream onto the planar bed. (Run 3-1, V = 32.1 cm/s, length of field of view = 64 cm, flow from left to right)

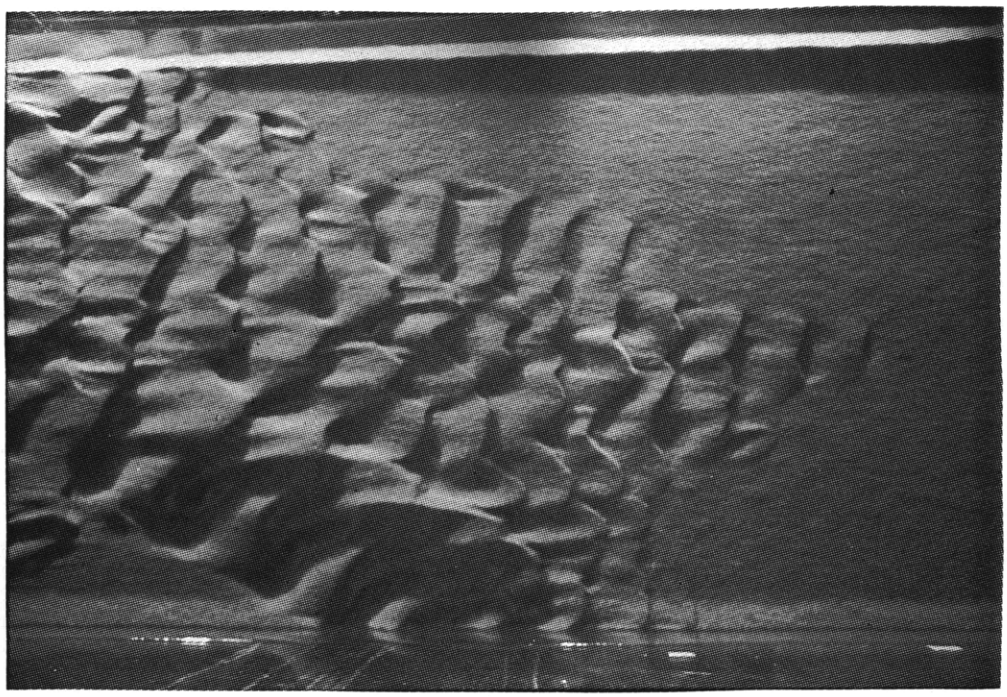

Figure 4-8. Plan view of propagating bed-form front one hour and 48 minutes after start-up. This figure shows a spur of three-dimensional bed forms and also shows the pointed shape of the front of relatively two-dimensional bed forms. See text. (Run 5-1, V = 36.1 cm/s, centered at 460 cm, length of field of view = 155 cm, flow from left to right)

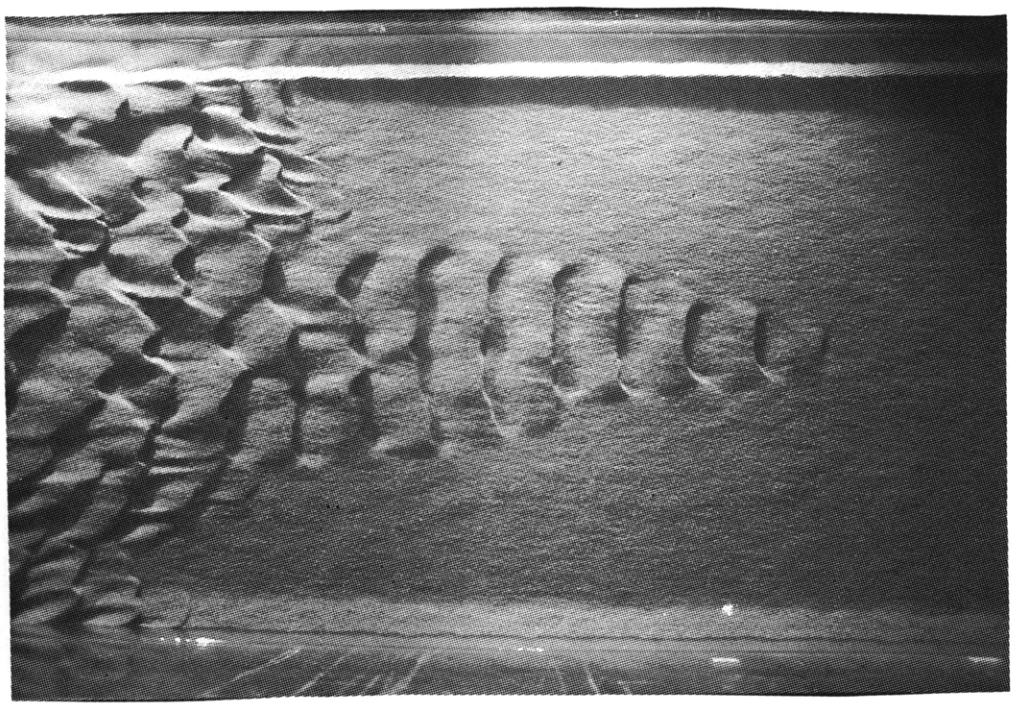

Figure 4-9. Plan view of propagating bed-form front one hour and 10 minutes after start-up. See text. (Run 6-1, V = 38.0 cm/s, centered at 450 cm, length of field of view = 155 cm, flow from left to right)

Figure 4-10. Plan view of a slipface that developed directly from the hummocky planar-bed micro-topography and then propagated another slipface downstream. This figure also shows some distinct, diagonal and zigzag lineations on the surrounding planar-bed micro-topography. See text. (Run 6-1, V = 38.0 cm/s, centered at 780 cm, length of field of view = 155 cm, flow from left to right)

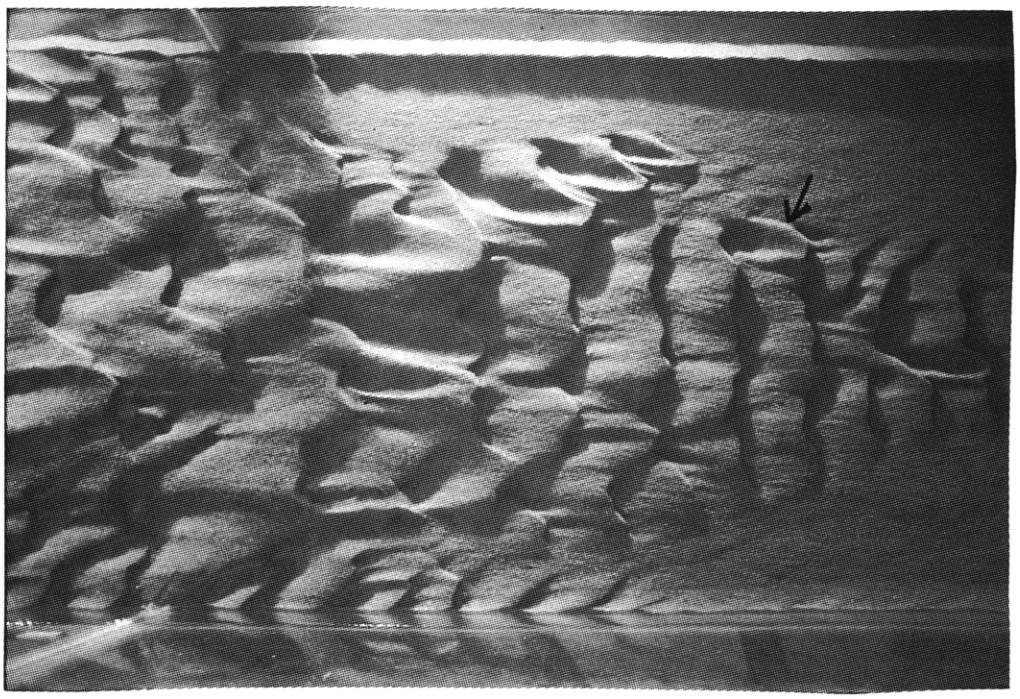

Figure 4-11. Plan view of propagating bed-form front and a diagonal spur of three-dimensional bed forms. This figure also shows the side of the bed form from which a second spur of three-dimensional bed forms developed (indicated by an arrow). See text. (Run 6-1, V = 38.0 cm/s, centered at 600 cm, length of field of view = 155 cm, flow from left to right)

Figure 4-12. Downstream view of propagating bed-form front and two parallel diagonal spurs of three-dimensional bed forms taken 20 minutes after Figure 4-11. See text. (Run 6-1, V = 38.0 cm/s)

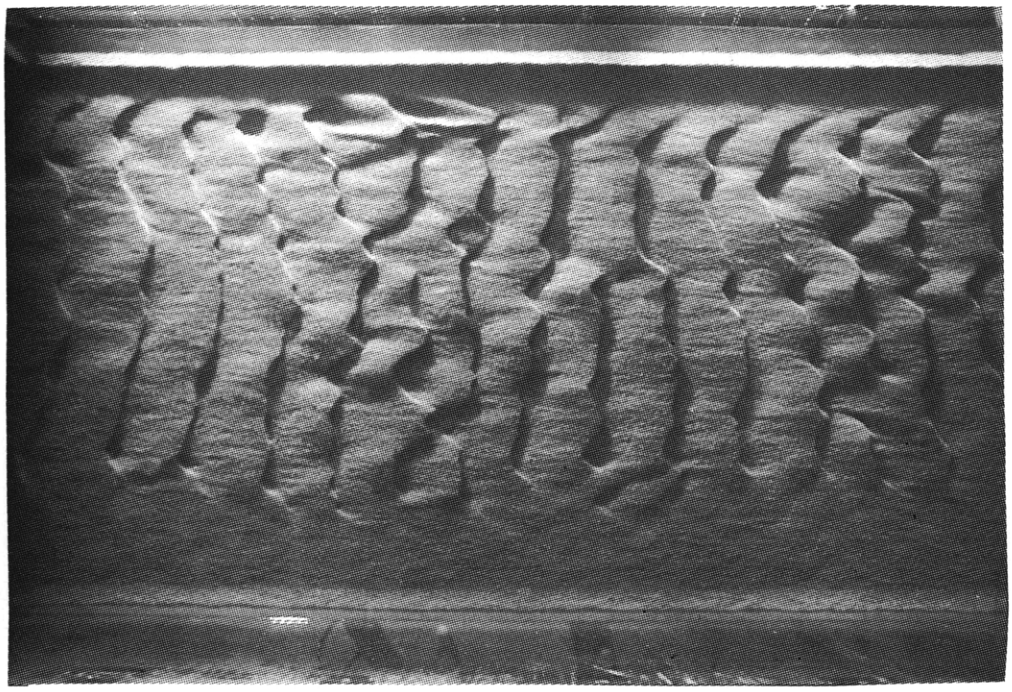

Figure 4-13. Plan view of relatively small two-dimensional bed forms 48 minutes after start-up. See text. (Run 7-1, V = 40.9 cm/s, centered at 650 cm, length of field of view = 155 cm, flow from left to right)

Figure 4-14. Plan view of sediment bed 15 minutes after start-up. This figure shows two discontinuous strips of bed forms that developed directly from the planar-bed micro-topography. See text. (Run 8-1, V = 43.8 cm/s, centered at 700 cm, length of field of view = 155 cm, flow from left to right)

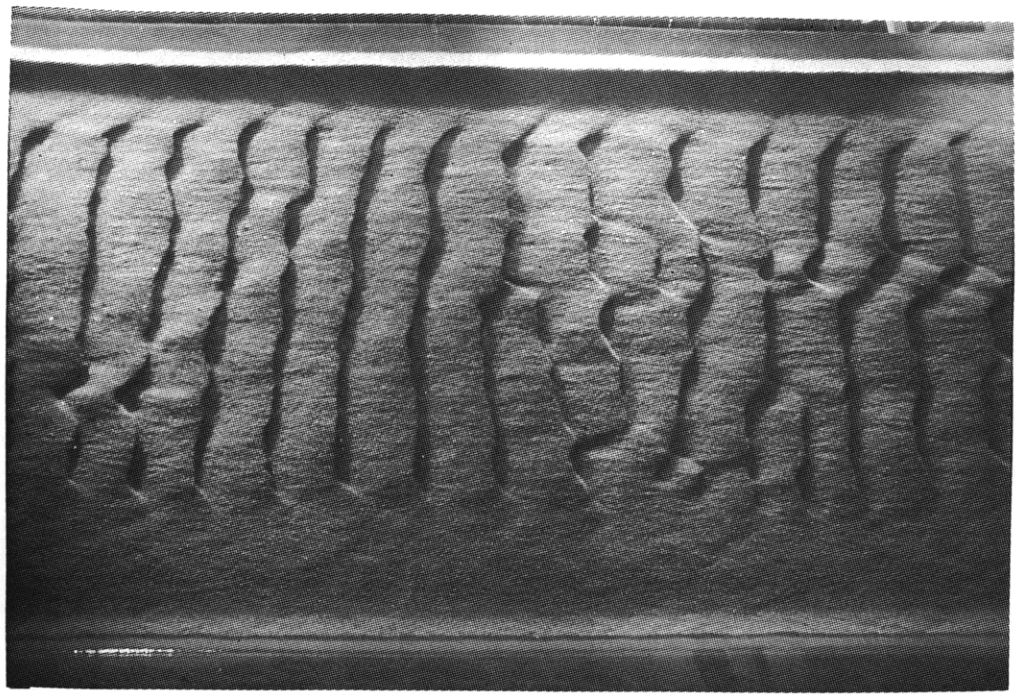

Figure 4-15. Plan view of relatively small two-dimensional bed forms 17 minutes after Figure 4-14 was taken. See text. (Run 8-1, V = 43.8 cm/s, centered at 650 cm, length of field of view = 155 cm, flow from left to right)

Figure 4-16. Upstream view of entire sediment bed seven minutes after start-up. In Run 9 within two minutes of start-up, the entire sediment bed was covered with relatively small, two-dimensional bed forms which were similar in size and appearance to newly developed bed forms near the propagating bed-form fronts in the lower velocity runs. See text. (Run 9-1, V = 47.4 cm/s)

Figures 4-17 through 4-21 are plan views of the sediment bed (centered at 850 cm) taken at 18-minute to 38-minute intervals during the first two hours of Run 9 (V = 47.4 cm/s). These figures illustrate the characteristic sequence of development of bed forms at the beginning of a run: the sequence of changes in the average size and appearance of bed forms at a given longitudinal position as a function of time.

Figure 4-17. Plan view of bed forms 5 minutes after start-up. The bed forms are relatively small and two-dimensional. (Run 9-1, V = 47.4 cm/s, centered at 850 cm, length of field of view = 155 cm, flow from left to right)

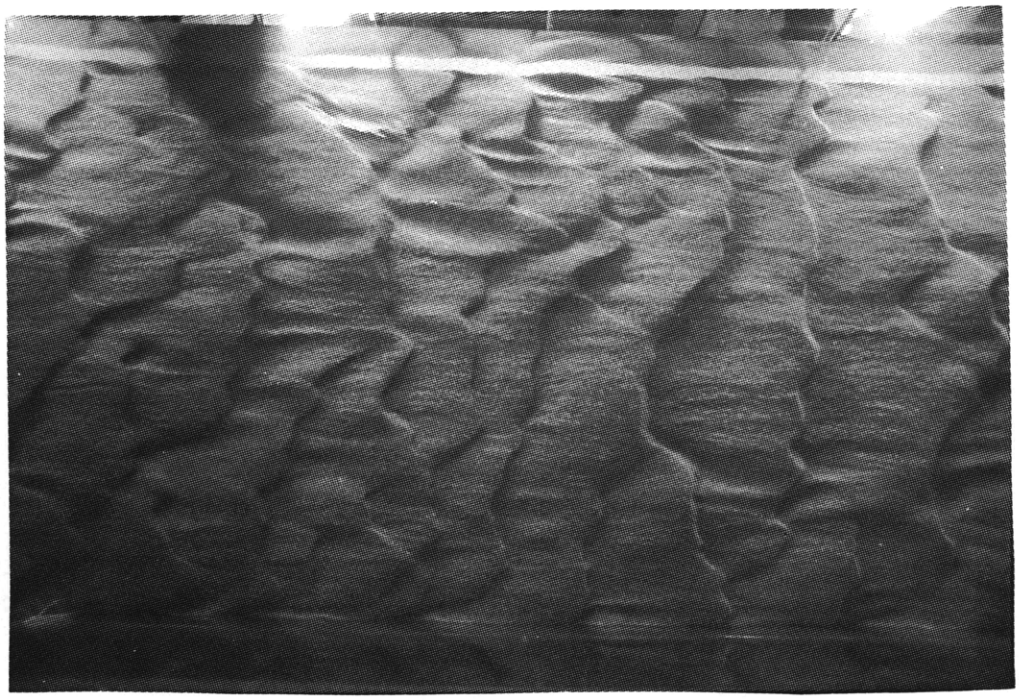

Figures 4-18. Plan view of bed forms 23 minutes after start-up. The mean size of the bed forms is greater and the bed forms are more three-dimensional than in Figure 4-17. Crests are less continuous and more sinuous than in Figure 4-17, and some three-dimensional scour pits are present downstream from slipfaces. (Run 9-1, V = 47.4 cm/s, centered at 850 cm, length of field of view = 155 cm, flow from left to right)

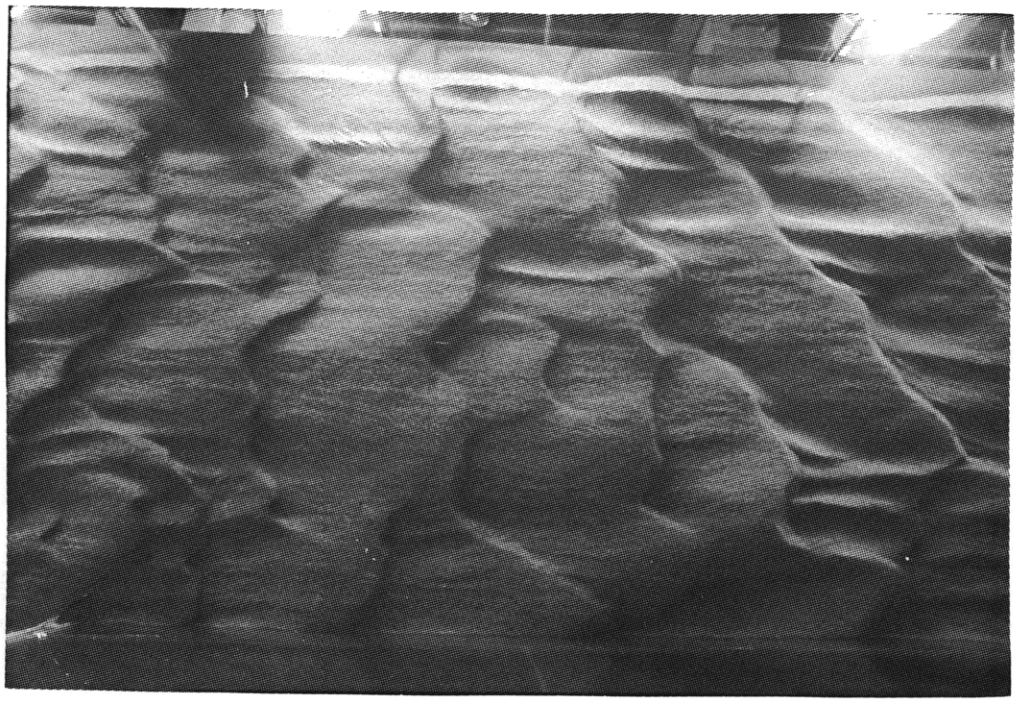

Figures 4-19. Plan view of bed forms 41 minutes after start-up. The mean size of the bed forms is greater than in Figure 4-18. (Run 9-1, V = 47.4 cm/s, centered at 850 cm, length of field of view = 155 cm, flow from left to right)

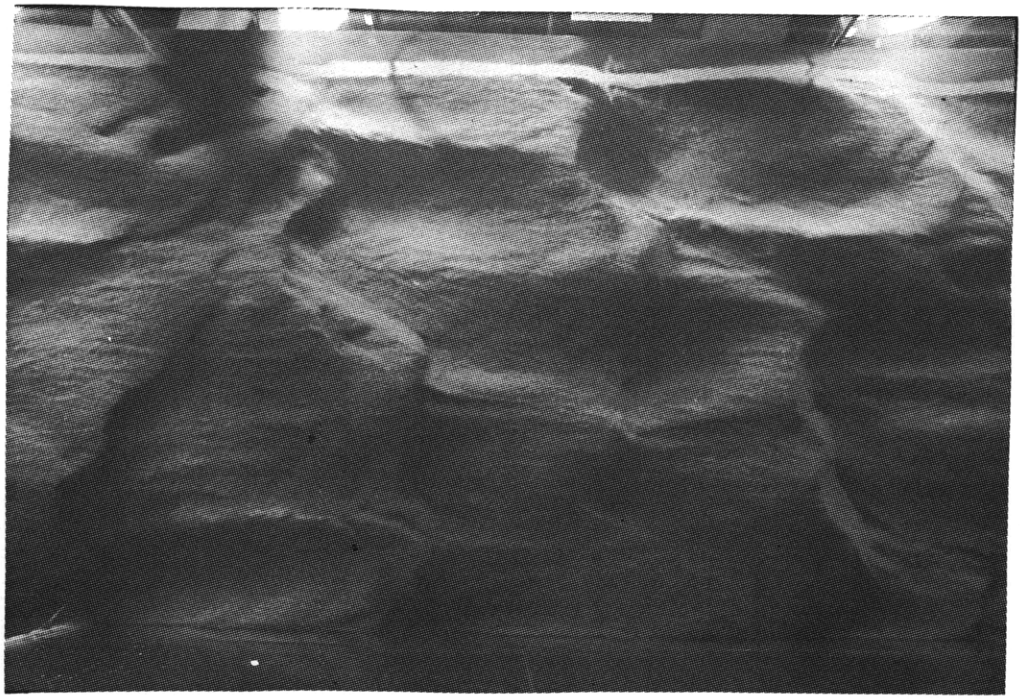

Figure 4-20. Plan view of bed forms 77 minutes after start-up. The mean size of the bed forms is greater than the preceding figures, and small slipfaces are present on the stoss sides of some of the longer bed forms just upstream from the slipfaces of the longer bed forms. (Run 9-1, V = 47.4 cm/s, centered at 850 cm, length of field of view = 155 cm, flow from left to right)

Figure 4-21. Plan view of bed forms 111 minutes after start-up. The mean size of the bed forms is greater than in Figure 4-20 and longer trains of small bed forms are present on the stoss sides of the longer bed forms. The small slipfaces that are farthest downstream in the trains appear to have the largest heights. (Run 9-1, V = 47.4 cm/s, centered at 850 cm, length of field of view = 155 cm, flow from left to right)

Figure 4-22. Plan view of bed forms 16 hours and 20 minutes after start-up. The difference in appearance of the bed forms in Figures 4-21 and 4-22 is similar to differences observed at a given longitudinal position for different data sets once the average size of the bed forms had reached the equilibrium value. See text. (Run 9-2, V = 47.4 cm/s, centered at 850 cm, length of field of view = 155 cm, flow from left to right)

Figure 4-23. Plan view of sediment bed just downstream from the false bottom 36 minutes after start-up before the false bottom was covered with sediment. The negative step formed by the exposed edge of the false bottom effects the sediment bed geometry like an artificial upstream slipface. This figure shows the first bed form immediately downstream from the false bottom with small slipfaces on its stoss side. The small slipfaces that are farthest downstream have become so large that they appear to be breaking up the downstream end of this bed form into separate bed forms. (Run 9-1, V = 47.4 cm/s, centered at 250 cm, length of field of view = 155 cm, flow from left to right)

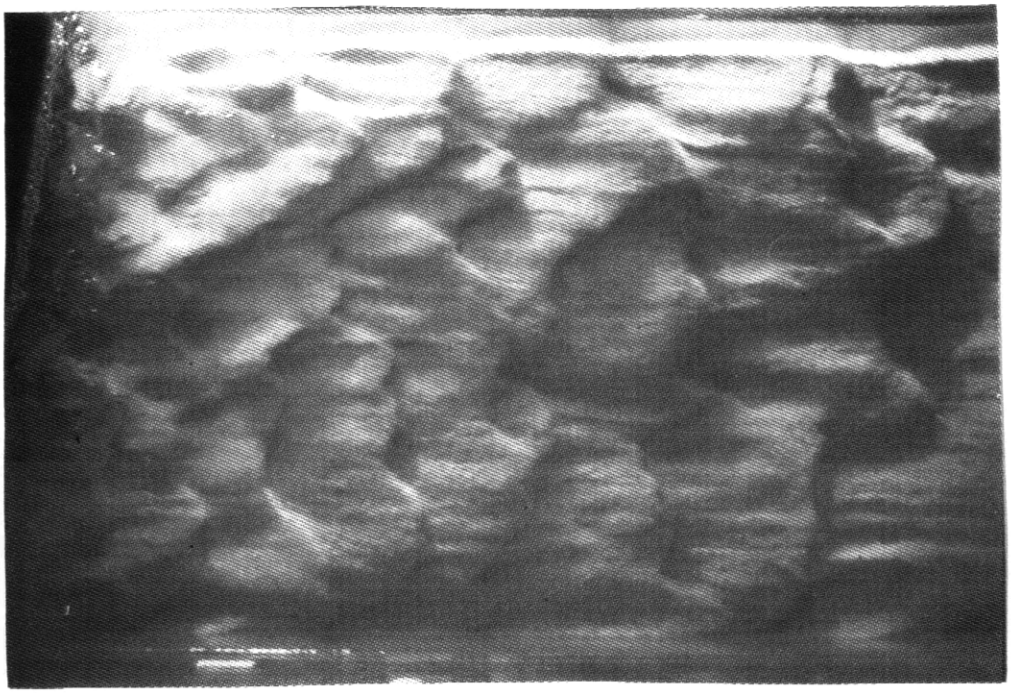

Figure 4-24. Plan view of sediment bed just downstream from the false bottom 39 hours and 15 minutes after start-up after the false bottom was covered with sediment. In contrast to Figure 4-23, this figure shows relatively small bed forms whose average size increases slightly downstream in the limited field of view. See text. (Run 9-4, V = 47.4 cm/s, centered at 250 cm, length of field of view = 155 cm, flow from left to right)

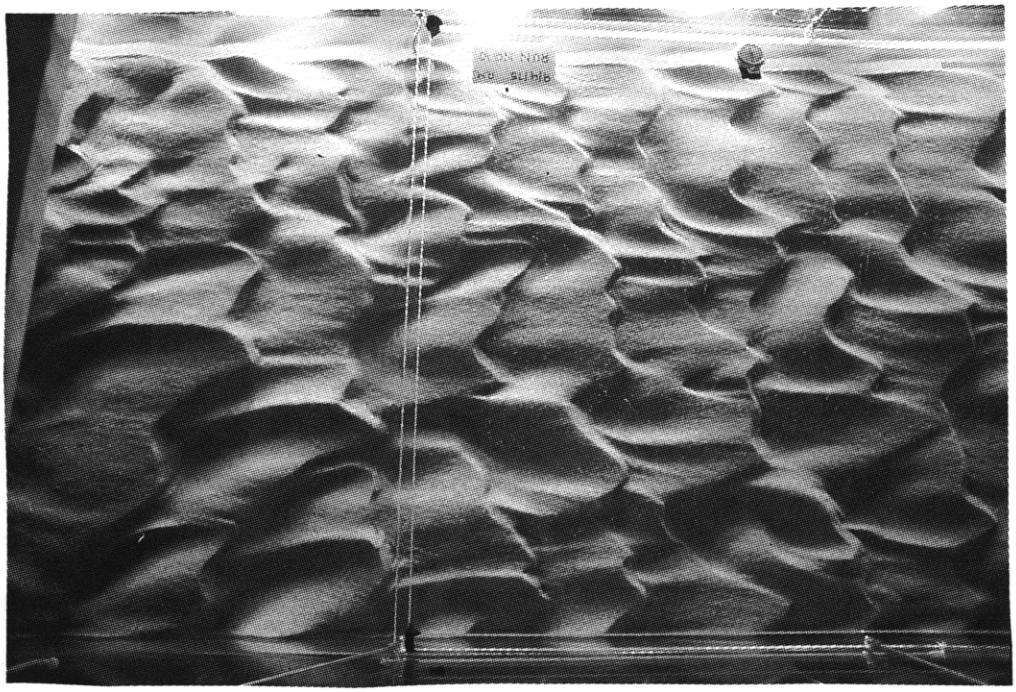

Figure 4-25. Plan view of bed forms about two meters upstream from the propagating bed-form front about six hours and 25 minutes after start-up. This figure illustrates how three-dimensional the bed forms became upstream from the bed form front (away from the false bottom); the average size of the bed forms at this location was still increasing. See text. (Run 10-1, V = 32.3 cm/s, centered at 650 cm, length of field of view = 155 cm, flow from left to right)

Figure 4-26. Plan view of bed forms that developed directly from the hummocky planar-bed micro-topography and are propagating downstream about 4 hours and 33 minutes after start-up. See text. (Run 10-1, V = 32.3 cm/s, centered at 850 cm, length of field of view = 155 cm, flow from left to right)

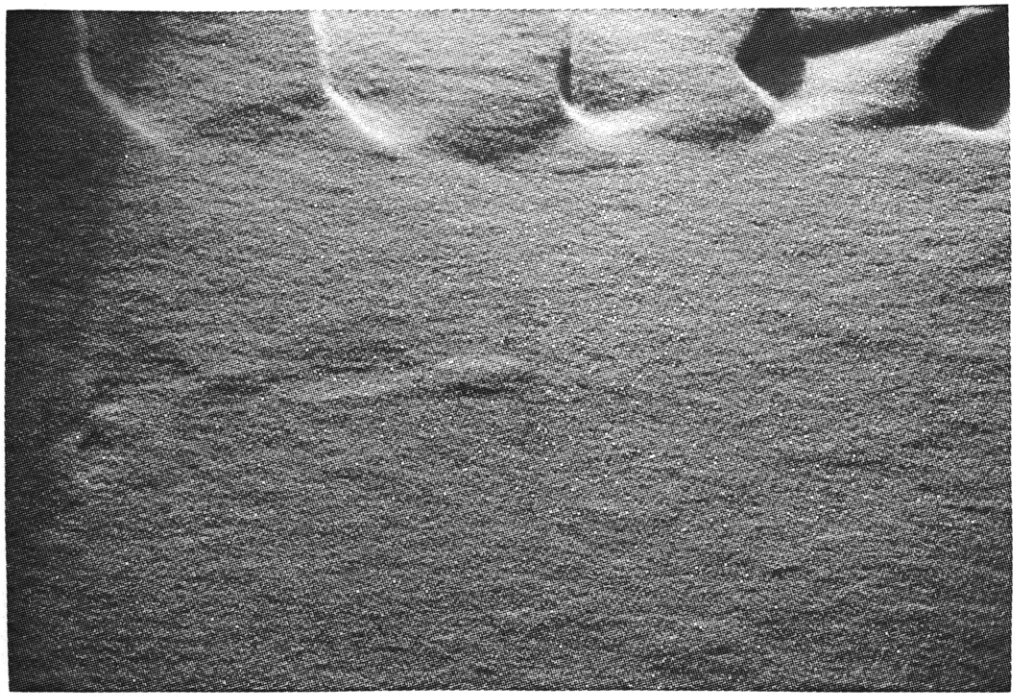

Figure 4-27. Close-up plan view of the remnants of the sequential decay from upstream of the incipient bed forms in the center of Figure 4-26, 28 minutes after Figure 4-26 was taken. The upstream mound with the V-shaped crest in Figure 4-26 was eroded before the downstream mound. See text. (Run 10-1, V = 32.3 cm/s, centered at 850 cm, length of field of view = 155 cm, flow from left to right)

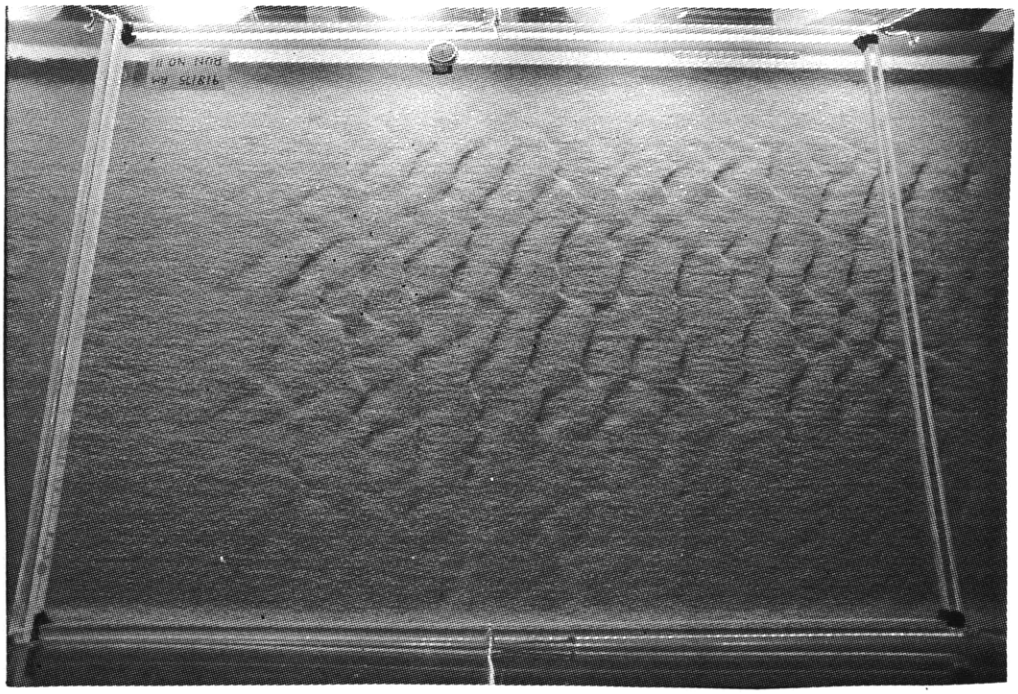

Figure 4-28. Plan view of the sediment bed underneath the water-surface plate about three minutes after start-up. See text. (Run 11-1, V = 38.4 cm/s, centered at 700 cm, length of field of view = 155 cm, flow from left to right)

Figures 4-29 through 4-32 on the following two pages illustrate the dependence of both the growth rate and size of the bed forms on the bed configuration upstream. See text.

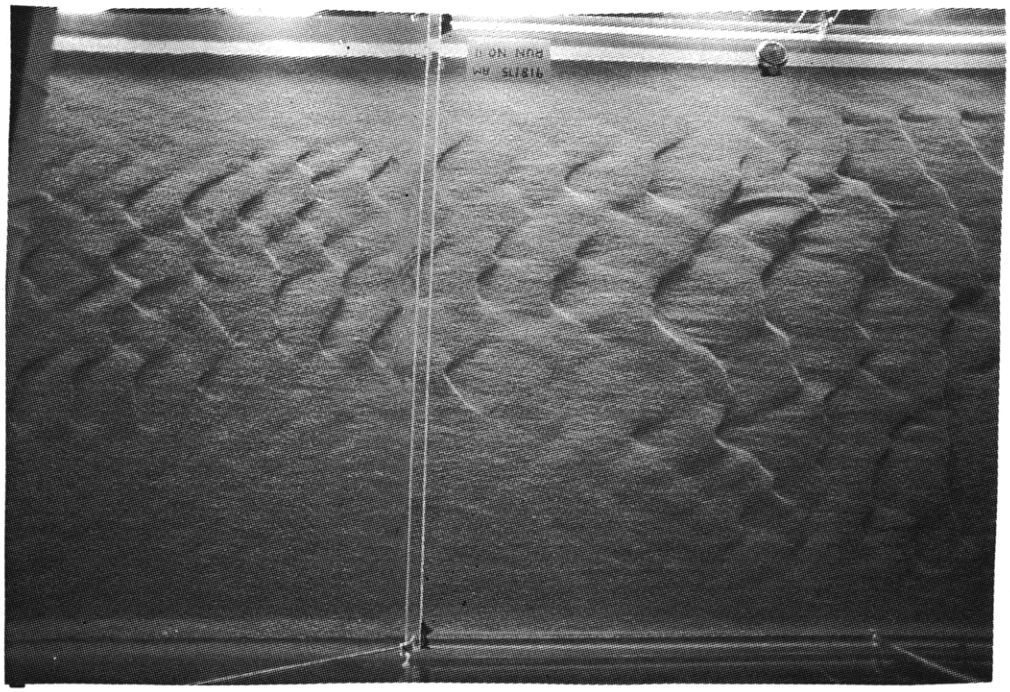

Figure 4-29. Plan view of sediment bed underneath the water-surface plate and immediately upstream from the plate 12 minutes after start-up (overlaps with Figure 4-30). (Run 11-1, V = 38.4 cm/s, centered at 650 cm, length of field of view = 155 cm, flow from left to right)

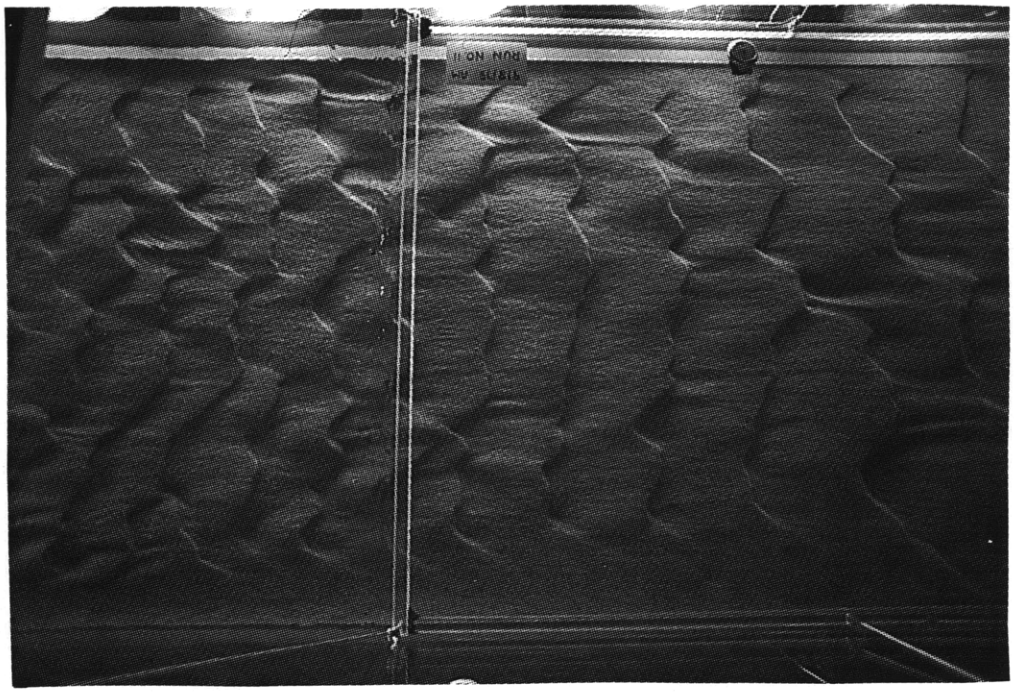

Figure 4-31. Plan view of the same section of the sediment bed as Figure 4-29, 30 minutes after Figure 4-29 was taken (overlaps with Figure 4-32). (Run 11-1, V = 38.4 cm/s, centered at 650 cm, length of field of view = 155 cm, flow from left to right)

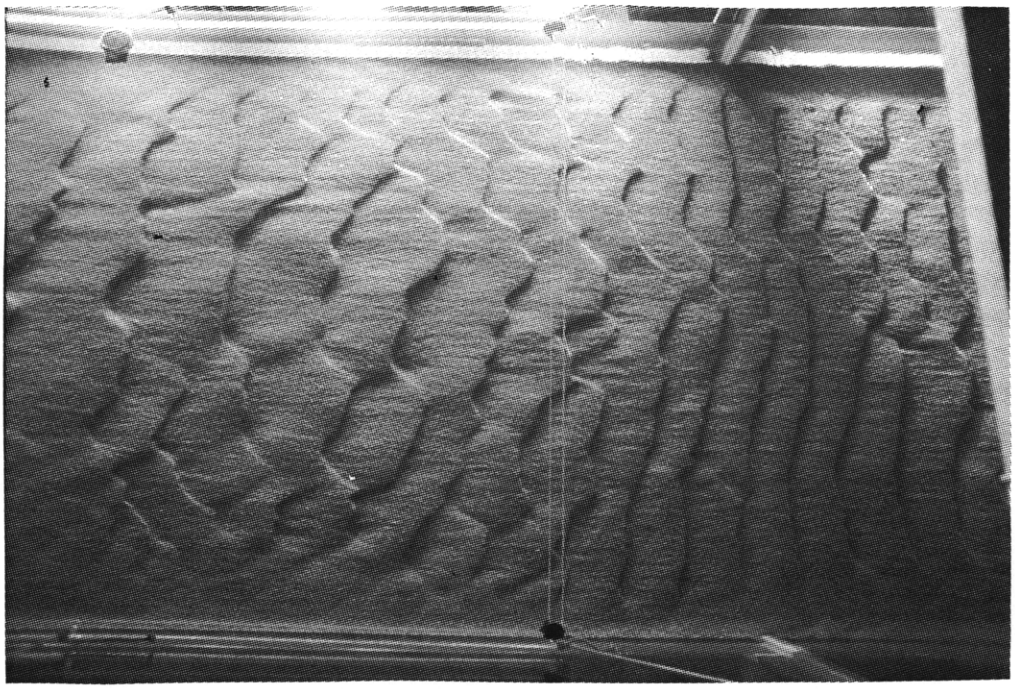

Figure 4-30. Plan view of sediment bed underneath the water-surface plate and immediately downstream from the plate, 12 minutes after start-up (overlaps with Figure 4-29). (Run 11-1, V = 38.4 cm/s, centered at 750 cm, length of field of view = 155 cm, flow from left to right)

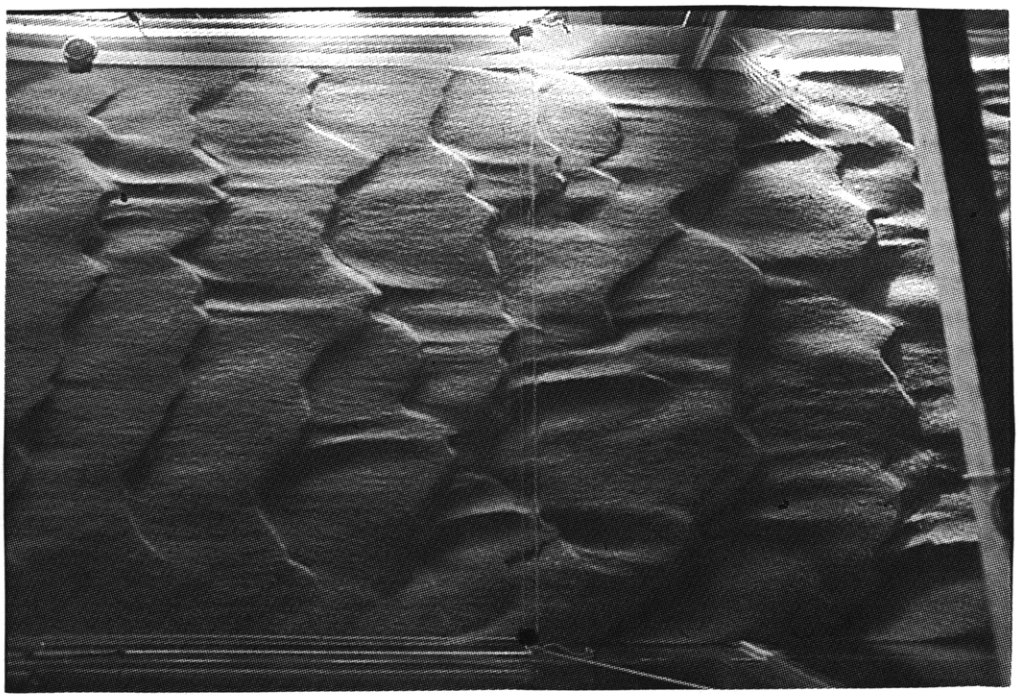

Figure 4-32. Plan view of the same section of the sediment bed as Figure 4-30, 30 minutes after Figure 4-30 was taken (overlaps with Figure 4-31). (Run 11-1, V = 38.4 cm/s, centered at 750 cm, length of field of view = 155 cm, flow from left to right)

Figures 4-33 through 4-35 illustrate the initial development of bed forms directly from the planar bed.

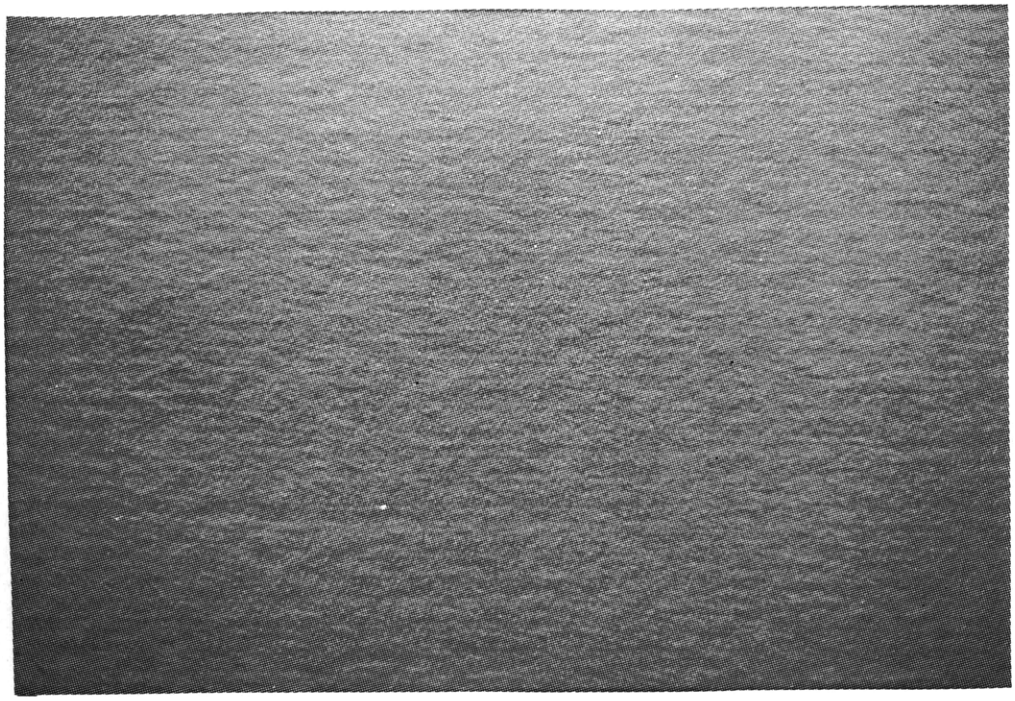

Figure 4-33. Close-up plan view of the sediment bed underneath the water-surface plate a few seconds after start-up. This figure shows the slightly streaky appearance of the planar bed. (Run 12-1, V = 47.4 cm/s, centered at 700 cm, length of field of view = 80 cm, flow from left to right)

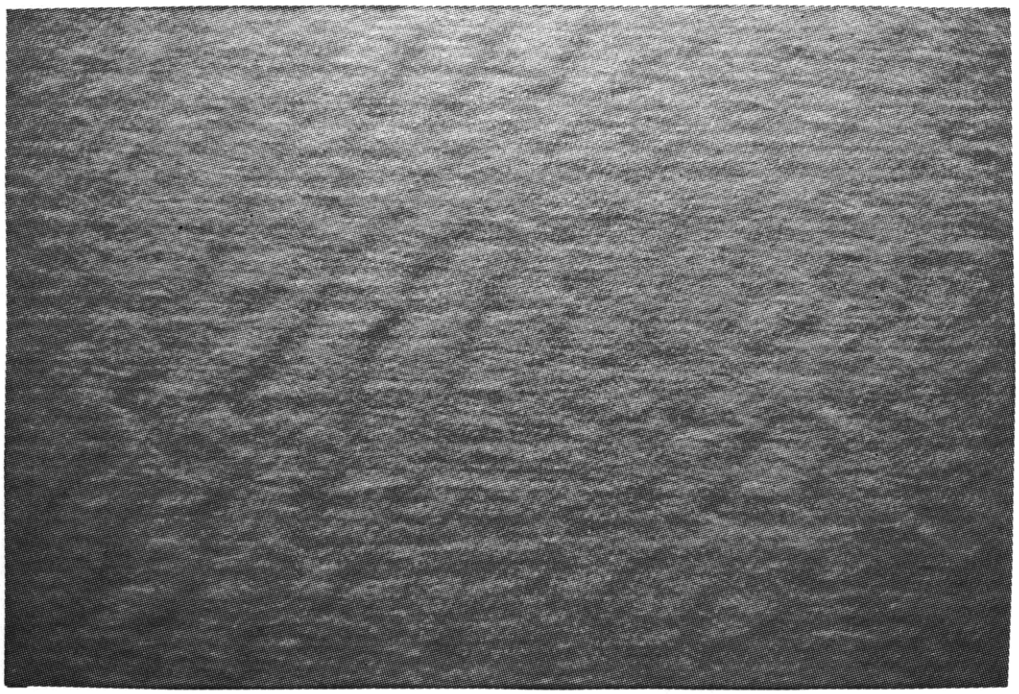

Figure 4-34. Close-up plan view of the same area of the sediment bed as in Figure 4-33, 28 seconds after Figure 4-33 was taken. This figure shows incipient slipfaces developing directly from the hummocky micro-topography immediately prior to the development of recognizable slipfaces. (Run 12-1, V = 47.4 cm/s, centered at 700 cm, length of field of view = 80 cm, flow from left to right)

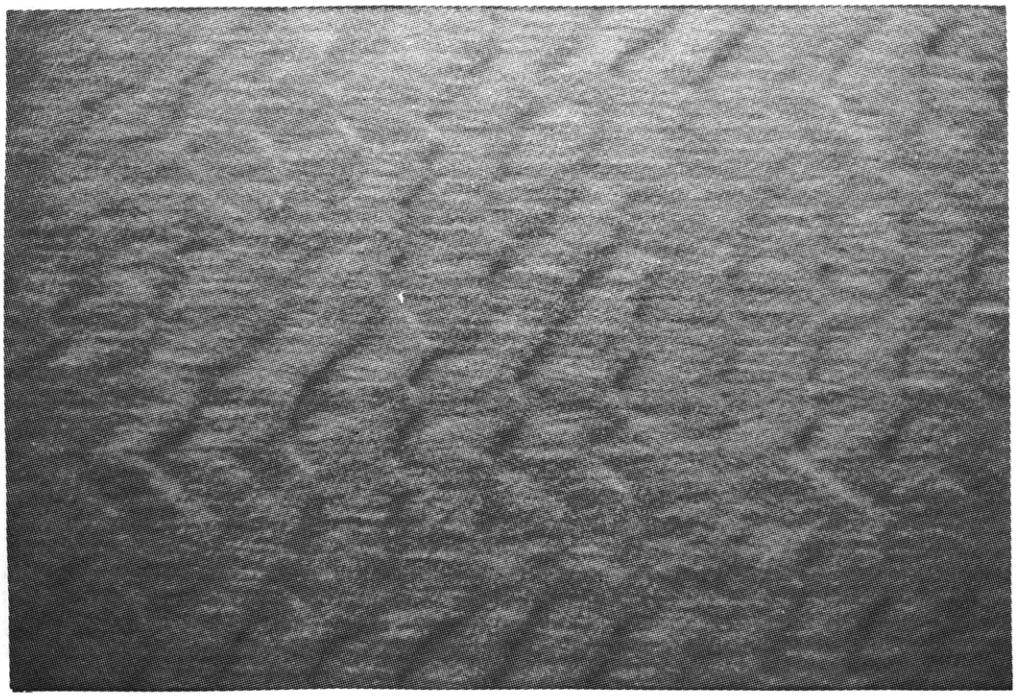

Figure 4-35. Close-up plan view of the same area of the sediment bed as Figures 4-33 and 4-34, 28 seconds after Figure 4-34 was taken. Small bed forms appear to cover the entire field of view; however, in a few places hummocks do not have distinct slipfaces. (Run 12-1, V = 47.4 cm/s, centered at 700 cm, length of field of view = 80 cm, flow from left to right)

Figures 4-36 through 4-38 illustrate the overtaking phenomenon. (Run 12-1, V = 47.4 cm/s, centered at 700 cm, length of field of view - 80 cm, flow from left to right)

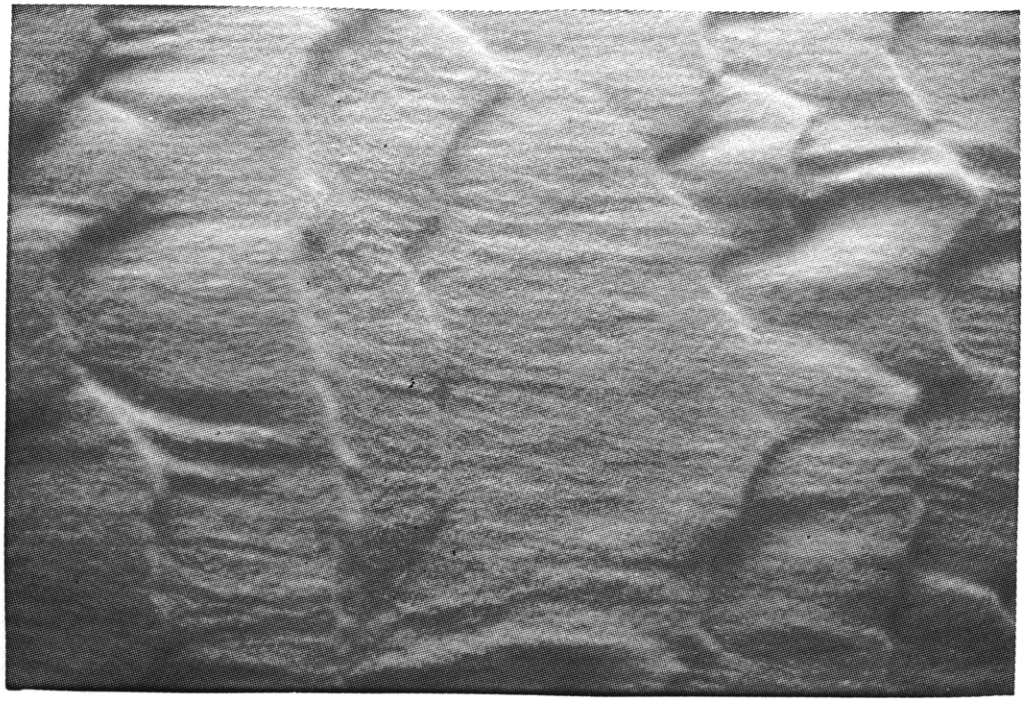

Figure 4-36. Close-up plan view of sediment bed underneath the water-surface plate about four minutes after start-up. The third slipface from the lefthand side is being overtaken by the slipface immediately upstream.

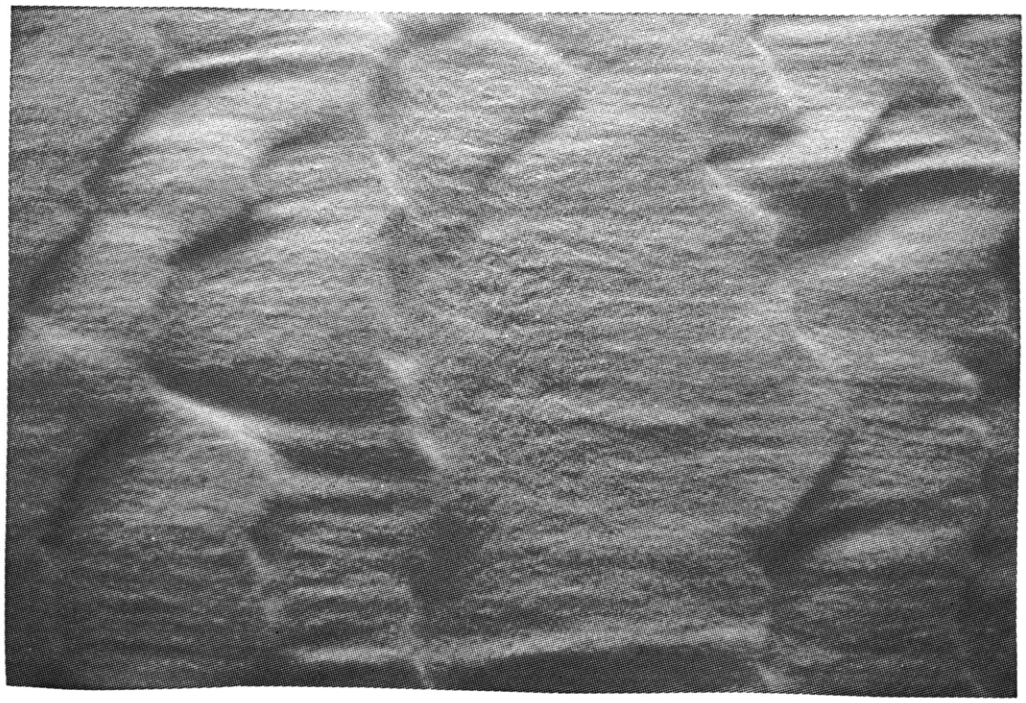

Figure 4-37. Same view 14 seconds after Figure 4-36 was taken. The slipface being overtaken in Figure 4-36 is decaying; part of the slipface is almost indiscernible.

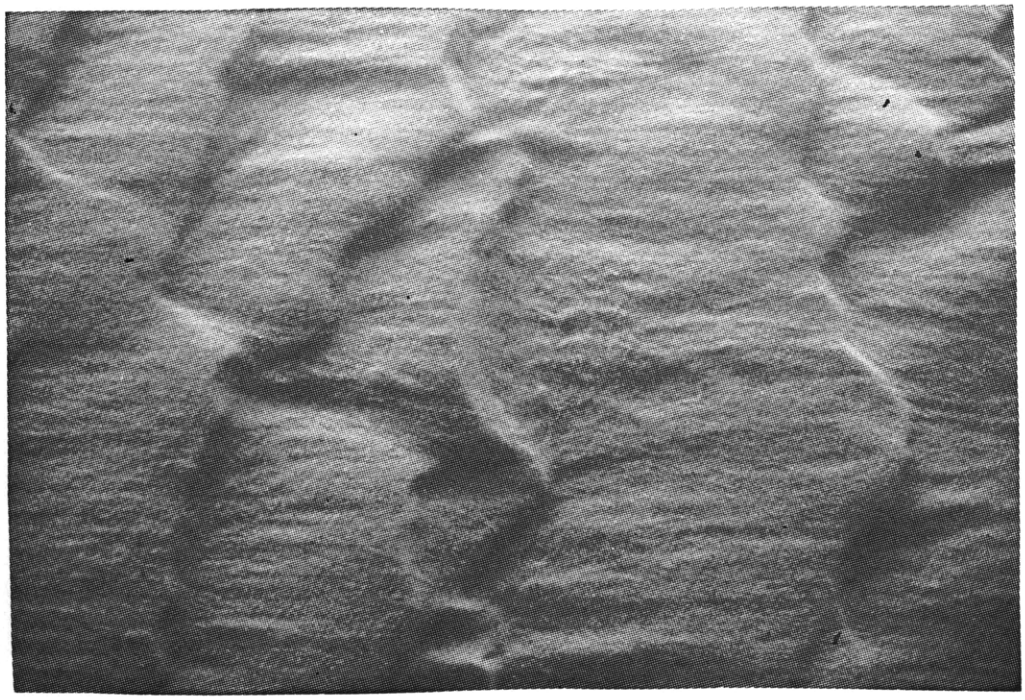

Figure 4-38. Close-up plan view of the same area of the sediment bed as in Figures 4-36 and 4-37, 14 seconds after Figure 4-37 was taken. The original slipface that was being overtaken in Figure 4-36 no longer exists; parts of the slipface were obliterated before being overtaken and the remainder was overtaken by the slipface immediately upstream. Also, the slipface that overtook the original slipface is likewise being overtaken. (Run 12-1, V = 47.4 cm/s, centered at 700 cm, length of field of view = 80 cm, flow from left to right)

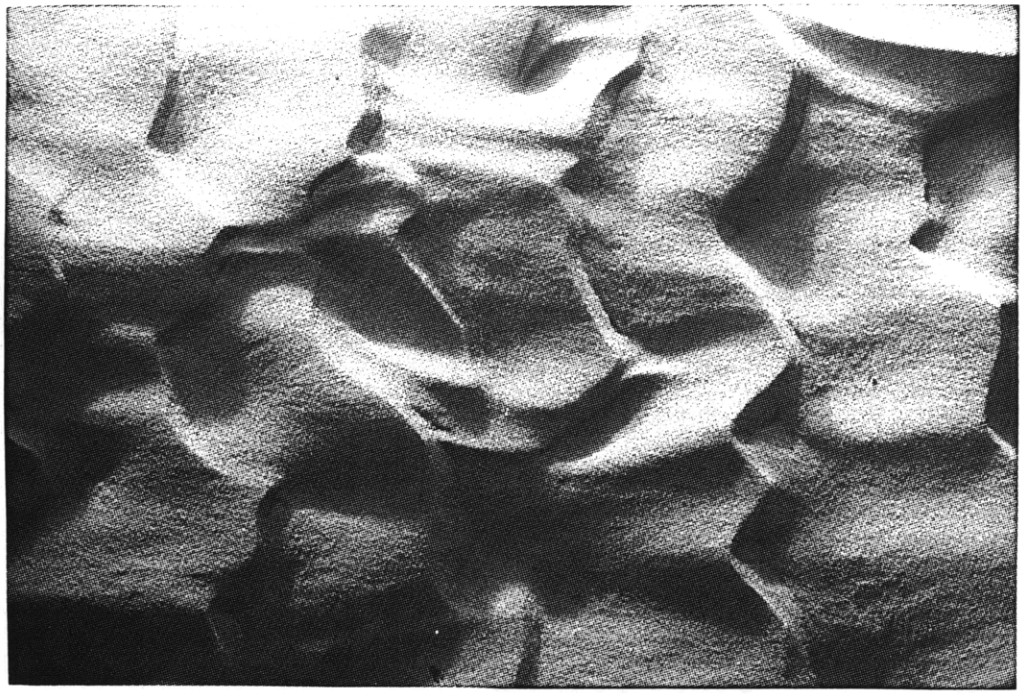

Figure 5-1. Close-up plan view of sediment bed. (Run 1-13, V = 28.6 cm/s, centered at 725 cm, length of field of view = 80 cm, flow from left to right)

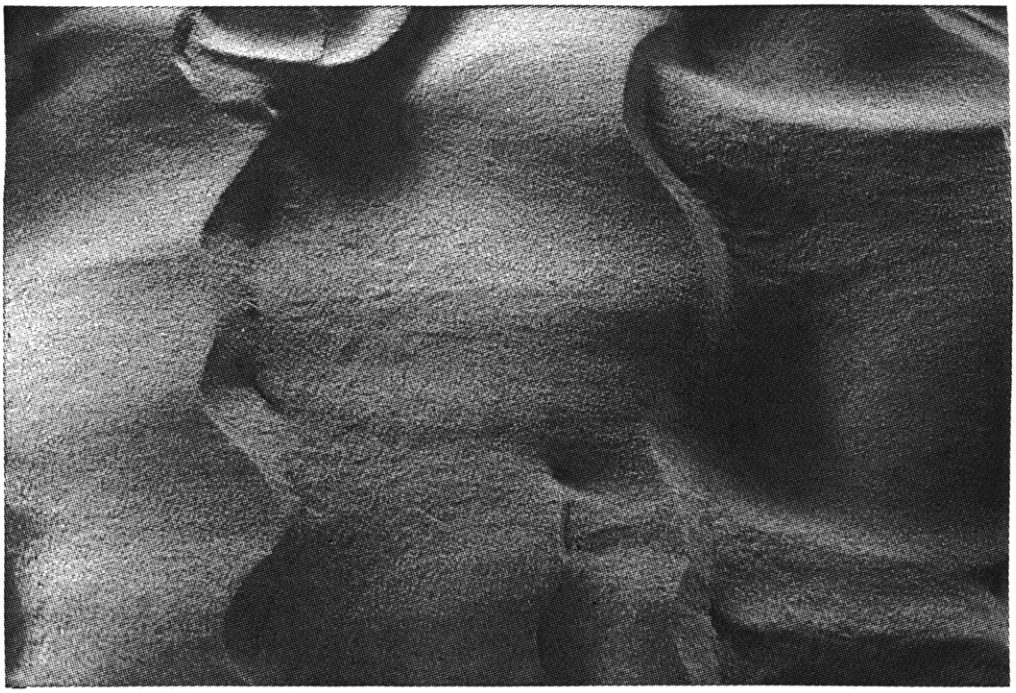

Figure 5-2. Close-up plan view of sediment bed adjacent to that in Figure 5-1. Figures 5-1 and 5-2 illustrate the large variation in the size of the bed forms at a given time in adjacent areas of the test section of the flume. (Run 1-13, V = 28.6 cm/s, centered at 825 cm, length of field of view = 80 cm, flow from left to right)

Figure 5-3. Close-up plan view of sediment bed. Slipfaces with heights markedly smaller than the apparent mean height (i.e., ripplets) are superimposed on the stoss side of a bed form in the upper righthand section. (Run 1-3, V = 28.6 cm/s, centered at 750 cm, flow from left to right)

Figure 5-4. Close-up plan view of sediment bed. The bed geometry characteristically associated with active three-dimensional scour pits is illustrated by the bed form to the left of center. (Run 1-6, v = 28.6 cm/s, centered at 725 cm, length of field of view = 80 cm, flow from left to right)

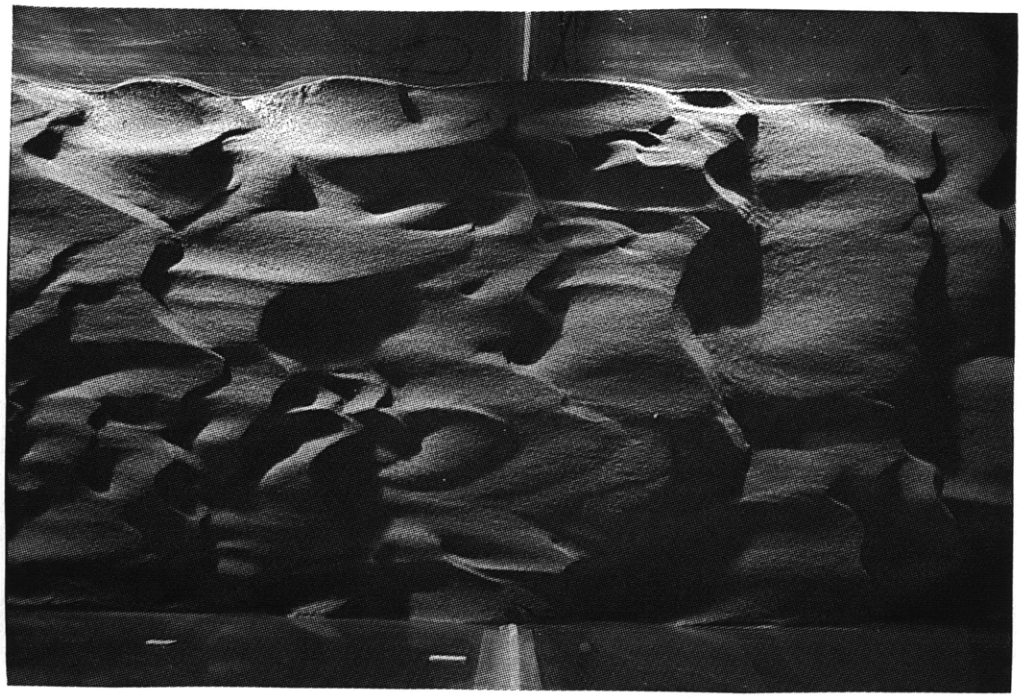

Figure 5-5. Plan view of sediment bed. Two slipfaces with small heights (i.e., ripplets) are superimposed on the stoss side of the relatively long bed form close to near sidewall in the center of the figure. (Run 3-12, V = 32.1 cm/s, centered at 560 cm, length of field of view = 155 cm, flow from left to right)

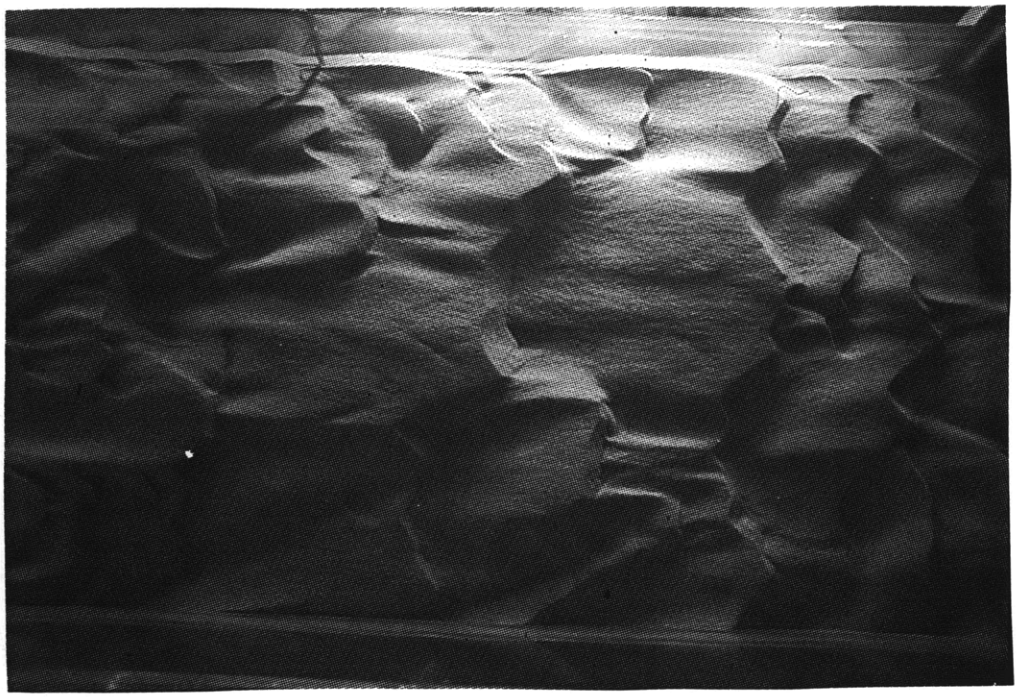

Figure 5-6. Plan view of sediment bed. Hummocky, micro-topography with diagonal and zigzag lineations is evident on the upper stoss sides of the two longest bed forms near the center. (Run 4-12, v = 34.1 cm/s, centered at 935 cm, length of field of view = 155 cm, flow from left to right)

Figure 5-7. Plan view of sediment bed. This figure shows an example of unusally long narrow bed forms that developed along the sidewalls downstream from active three-dimensional scour pits. The long narrow stretch along the near sidewall is the farthest upstream 90 cm of the stoss side of a bed form 130 cm long. The upstream scour pit is no longer active, but the remnants of the upstream slipface are still oriented at an acute angle with the sidewall. See text. (Run 5-3, V = 36.1 cm/s, centered at 810 cm, length of field of view = 155 cm, flow from left to right)

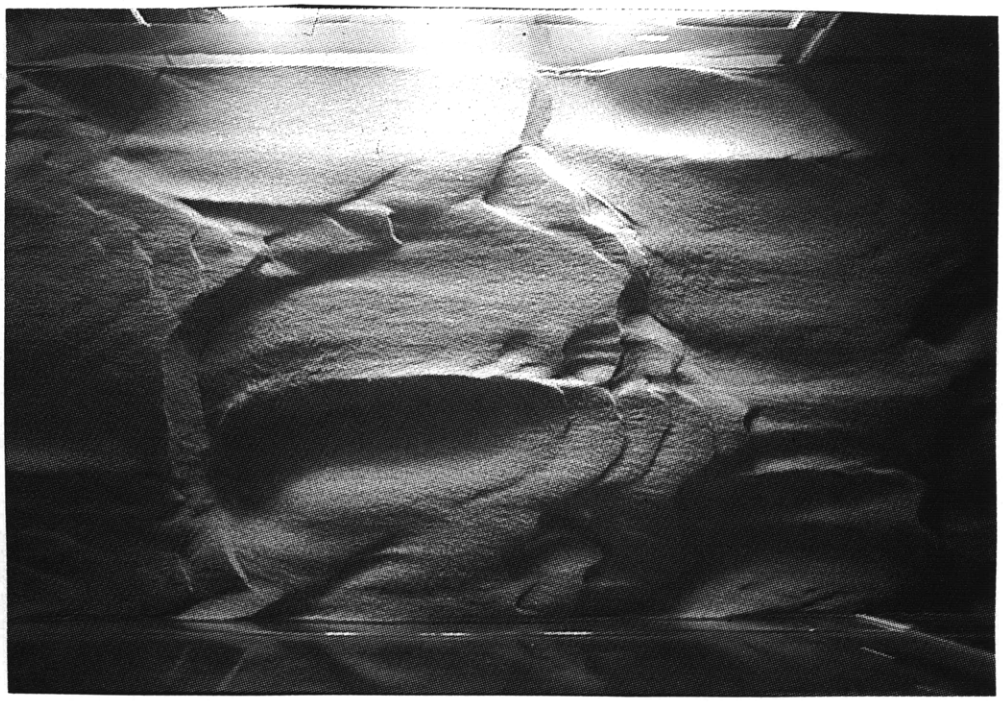

Figure 5-8. Plan view of sediment bed. In the center of this figure is a series of ripplets downstream from an active three-dimensional scour pit on the stoss side of a relatively long bed form. These ripplets exhibit the characteristic geometry of ripplets that developed downstream from three-dimensional scour pits. See text. Ripplets in upper left corner with more zigzag crestlines are characteristic of ripplets that developed downstream from relatively two-dimensional slipfaces. See text. (Run 6-6, V = 38.0 cm/s, centered at 950 cm, length of field of view = 155 cm, flow from left to right)

Figure 5-9. Plan view of sediment bed. In the center of this figure are two examples of bed forms with relatively high slipfaces and no superimposed ripplets; the lengths are relatively short. The bed form immediately upstream with ripplets in series is more than twice as long as the bed forms in the center. See text. (Run 7-2, V = 40.9 cm/s, centered at 850 cm, length of field of view = 155 cm, flow from left to right)

Figure 5-10. Plan view of sediment bed. (Run 9-5, V = 47.4, centered at 850 cm, length of field of view = 155 cm, flow from left to right)

Figure 5-11. Same view as Figure 5-10 but during a different data set of Run 9. Figures 5-10 and 5-11 show both the variation in the occurrence of ripplets and the large variation in the geometry of the bed forms at a given longitudinal position as a function of time for a given flow velocity. (Run 9-7, V = 47.4, centered at 850 cm, length of field of view = 155 cm, flow from left to right)

Figure 5-12. Plan view of sediment bed. (Run 11-2, V = 38.4 cm/s, centered at 750 cm, length of field of view = 155 cm, flow from left to right)

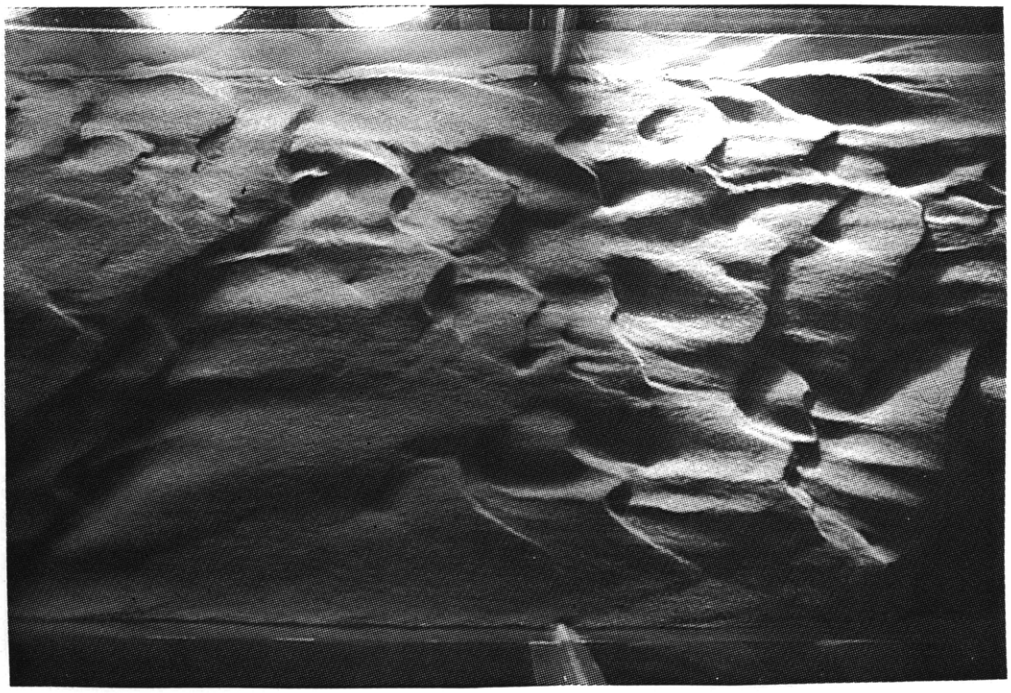

Figure 5-13. Plan view of the same section of the sediment bed as in Figure 5-12, one hour and 35 minutes after Figure 5-12 was taken. Figures 5-12 and 5-13 illustrate relatively long bed forms being broken up by the development of smaller bed forms on their stoss side. See text. (Run 11-2, V = 38.4 cm/s, centered at 770 cm, length of field of view = 155 cm, flow from left to right)

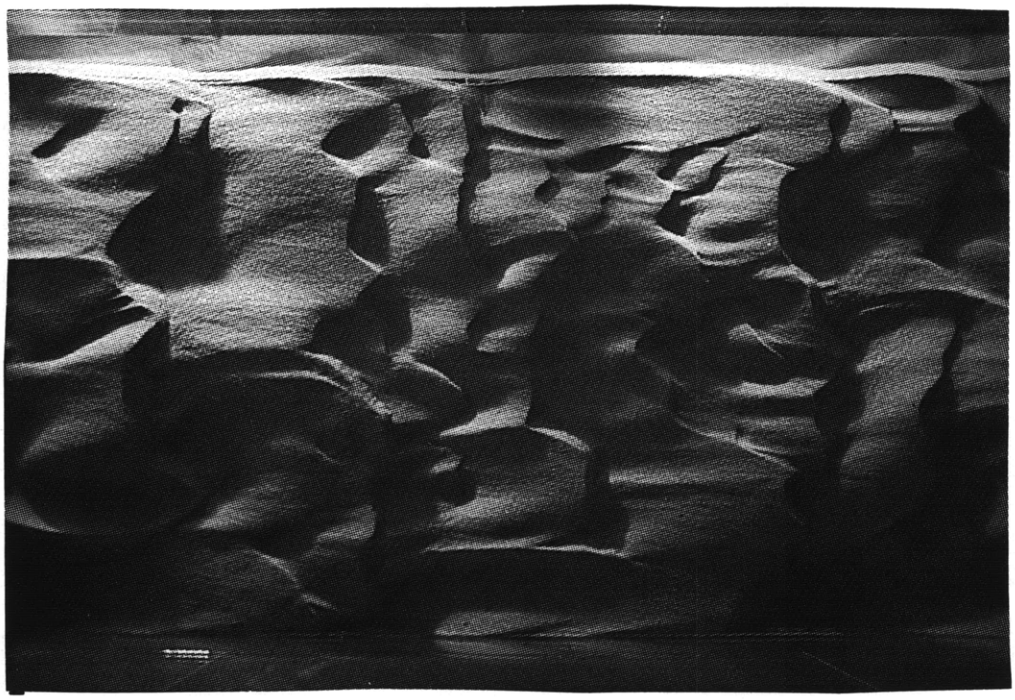

Figure 5-14. Plan view of sediment bed. (Run 10-3, V = 32.3 cm/s, centered at 880 cm, length of field of view = 155 cm, flow from left to right)

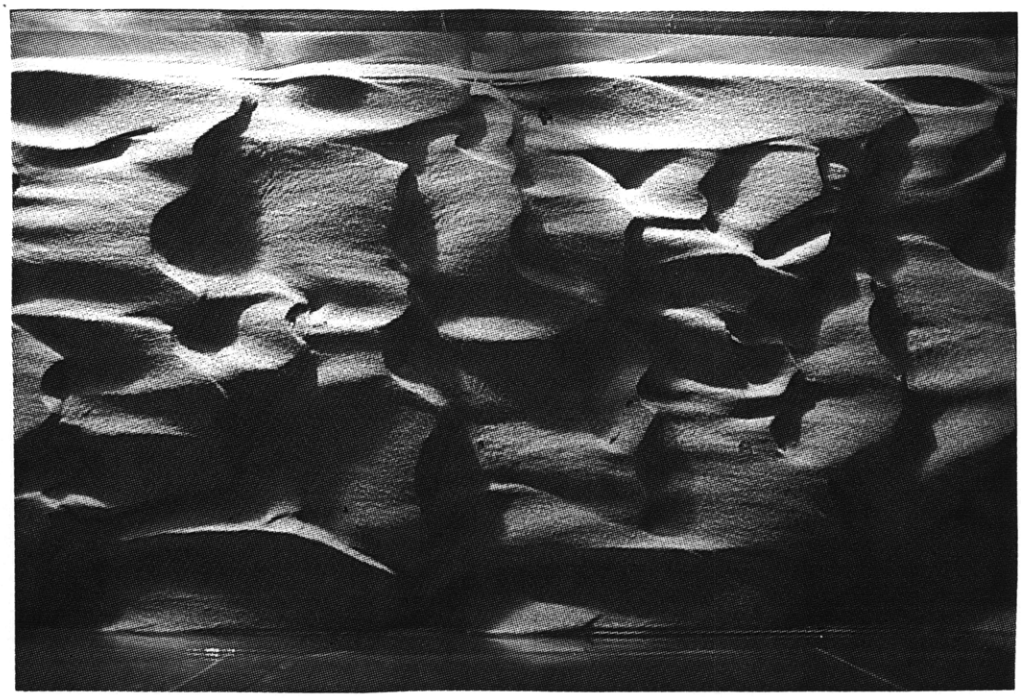

Figure 5-15. Plan view of the same section of the sediment bed as in Figure 5-14, 30 minutes after Figure 5-14 was taken. The series of bed forms on the upper righthand sections of Figures 5-14 and 5-15 illustrate relatively small bed forms increasing in size with time. See text. (Run 10-3, V = 32.3 cm/s, centered at 880 cm, length of field of view = 155 cm, flow from left to right)

Figure 6-1: Definition Drawing of Bed Forms
1, 2, and 5: major slipfaces
3 and 4: ripplets

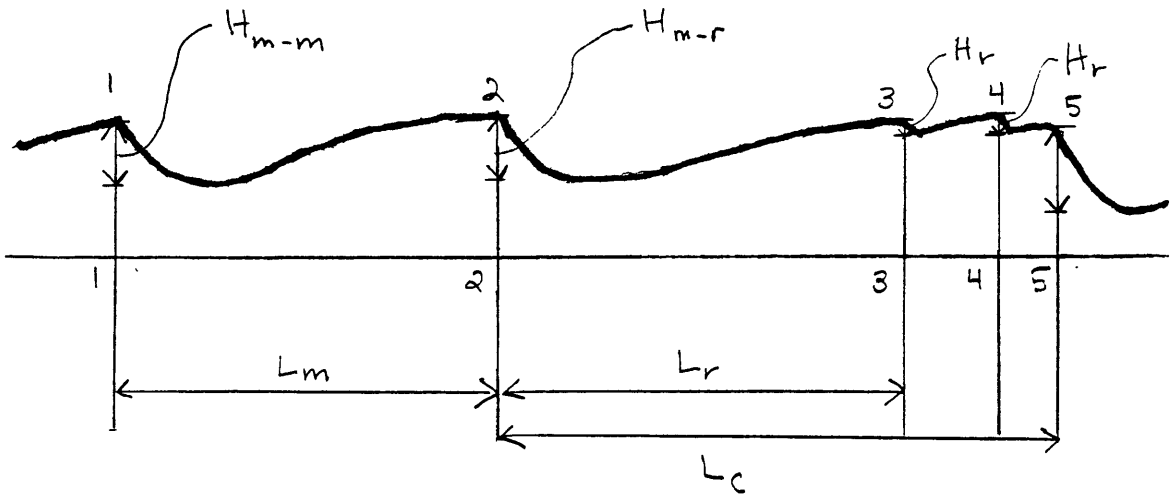

HEIGHT

H_r: height of a ripplet

H_{m-m}: height of a major slipface immediately upstream from another major slipface

H_{m-r}: height of a major slipface immediately upstream from a ripplet slipface

H_m: height of a major slipface (subcategories: H_{m-m} and H_{m-r})

H: height of a slipface (subcategories: H_m and H_r)

LENGTH

L_m: length from a major slipface to an immediately adjacent major slipface downstream

L_r: length from a major slipface to an immediately adjacent ripplet slipface downstream

L_c: length from a major slipface immediately upstream from a ripplet to the next major slipface downstream (composite with ripplets: the length between two major slipfaces with one or more ripplet slipfaces in between)

L_{m-m}: length between major slipfaces - set of lengths most commonly used (subcategories: L_m and L_c)

L_{m-a}: length downstream from a major slipface to the next slipface regardless of the height of the slipface downstream (subcategories: L_m and L_r)

Figure 6-2: Overtaking Criteria

A slipface is considered to be overtaking the next slipface downstream if the low point downstream from the upstream slipface is higher than one-third of the height of the downstream slipface.

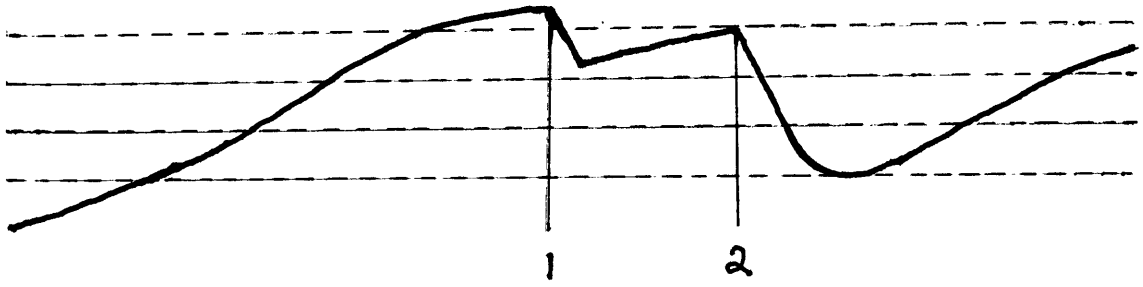

Figure 6-2A: Slipface 1 is overtaking Slipface 2. The low point downstream from slipace 1 is higher than one-third of the height of slipface 2.

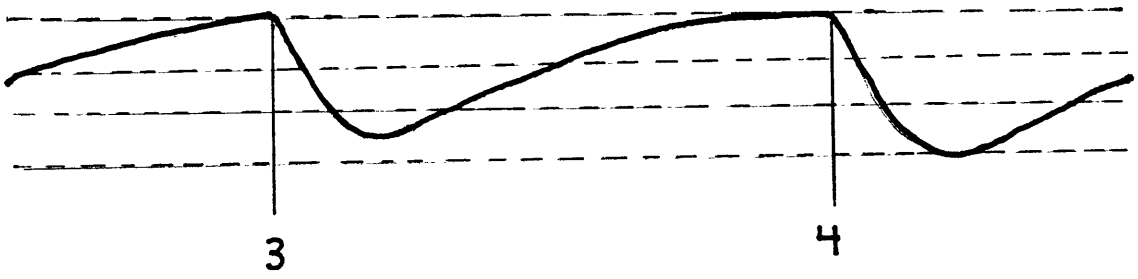

Figure 6-2b: Slipface 3 is not overtaking slipface 4. The low point downstream from slipface 3 is higher than the low point downstream from slipface 4 but is lower than one-third of the height of slipface 4.

Figure 6-3: Length Correction

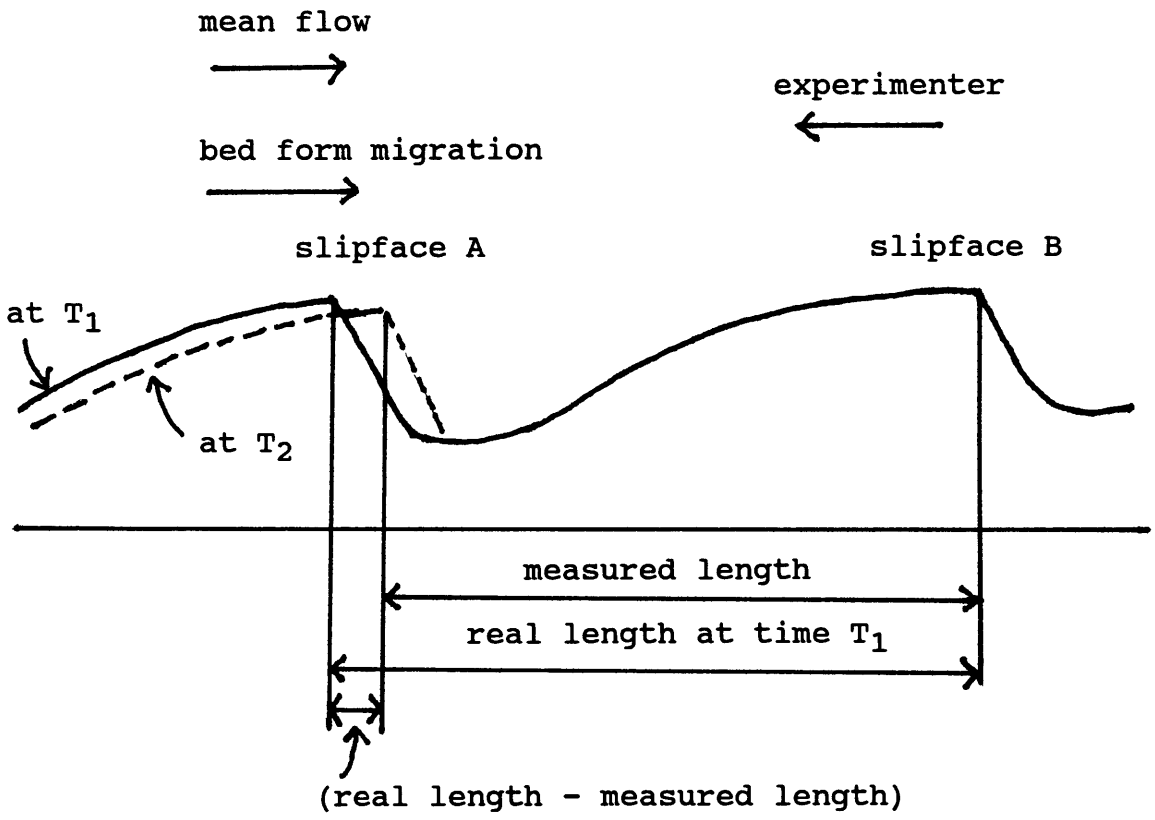

$$T = T_2 - T_1$$

X = average migration rate of slipface A during T

$$X = (\text{real length} - \text{measured length}) / T$$

Y = average rate of taking the bed profile during T

$$Y = (\text{measured length}) / T$$

$$(\text{real length}) = (\text{measured length})(1 + X/Y)$$

Figure 6–4

Mean Migration Rate of Major Slipfaces

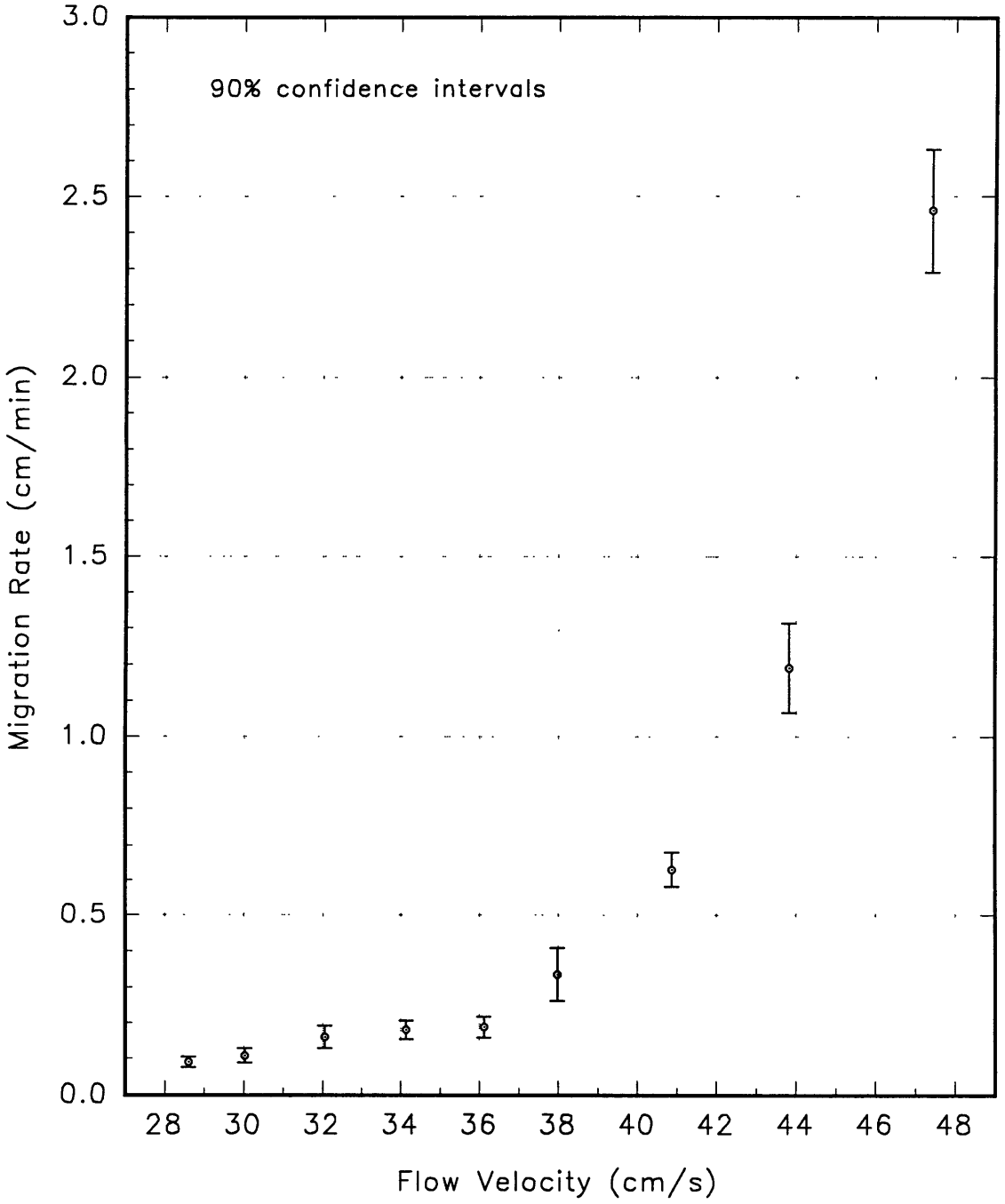

Histograms of Bed–Form Heights

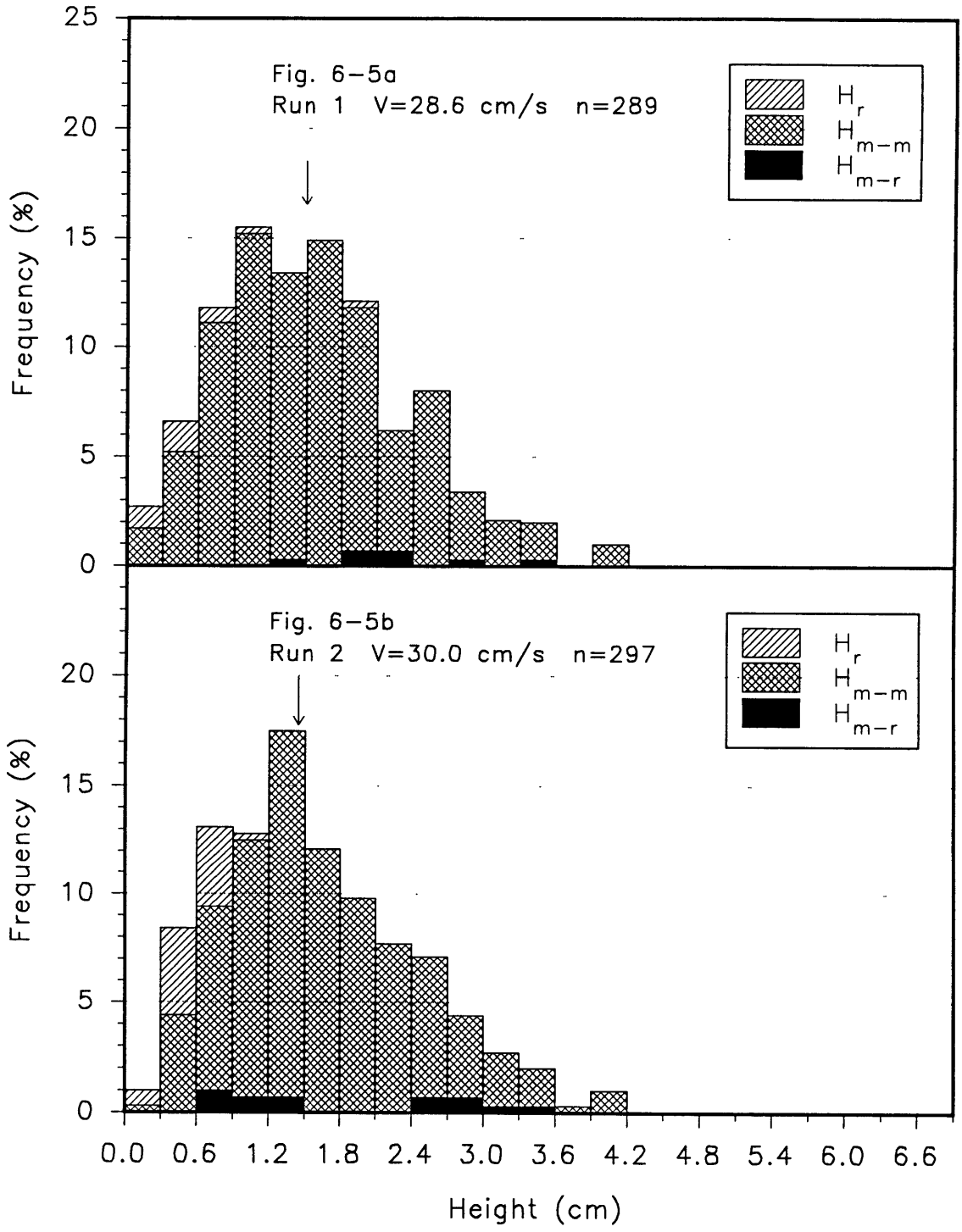

Histograms of Bed–Form Heights

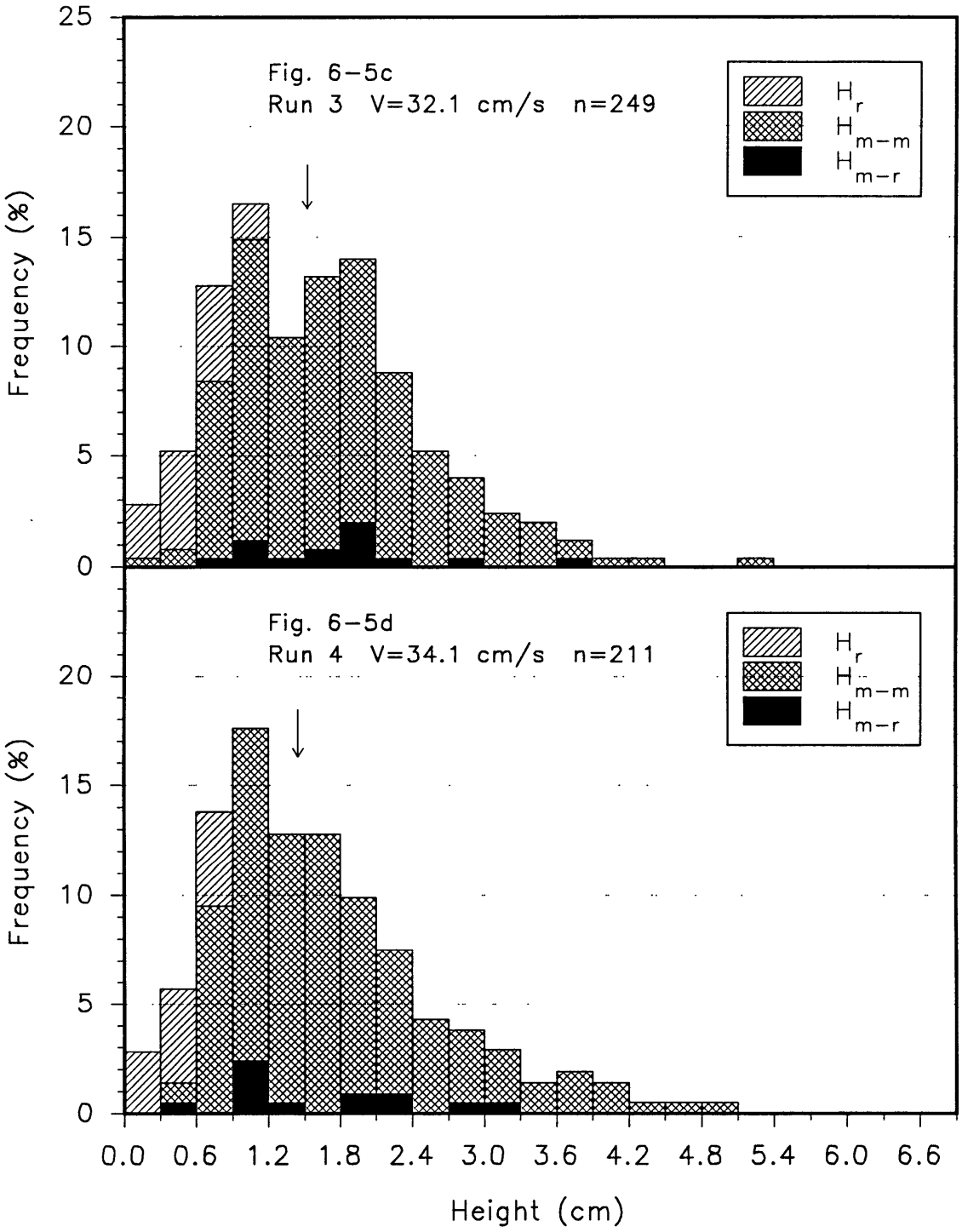

Histograms of Bed–Form Heights

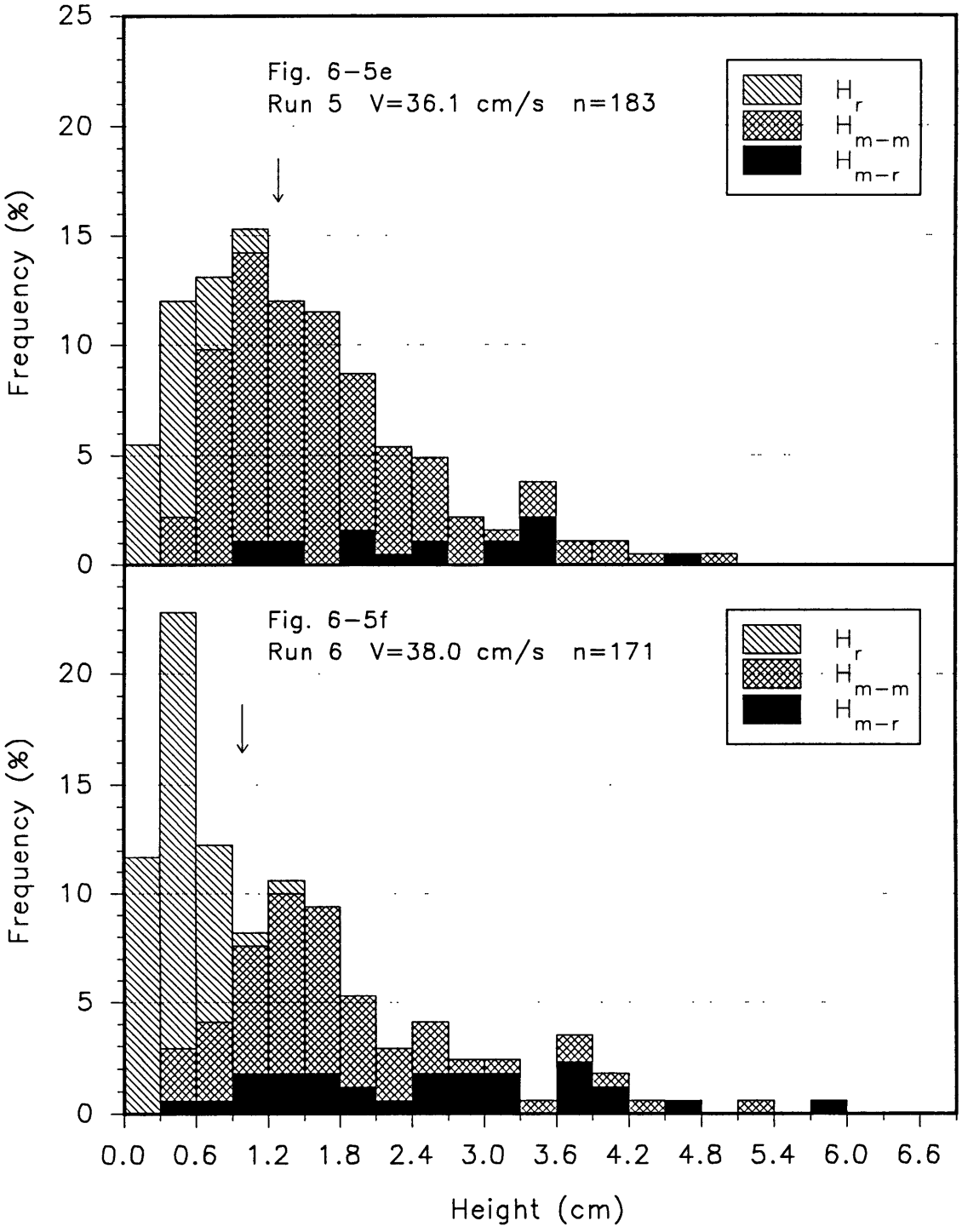

Histograms of Bed-Form Heights

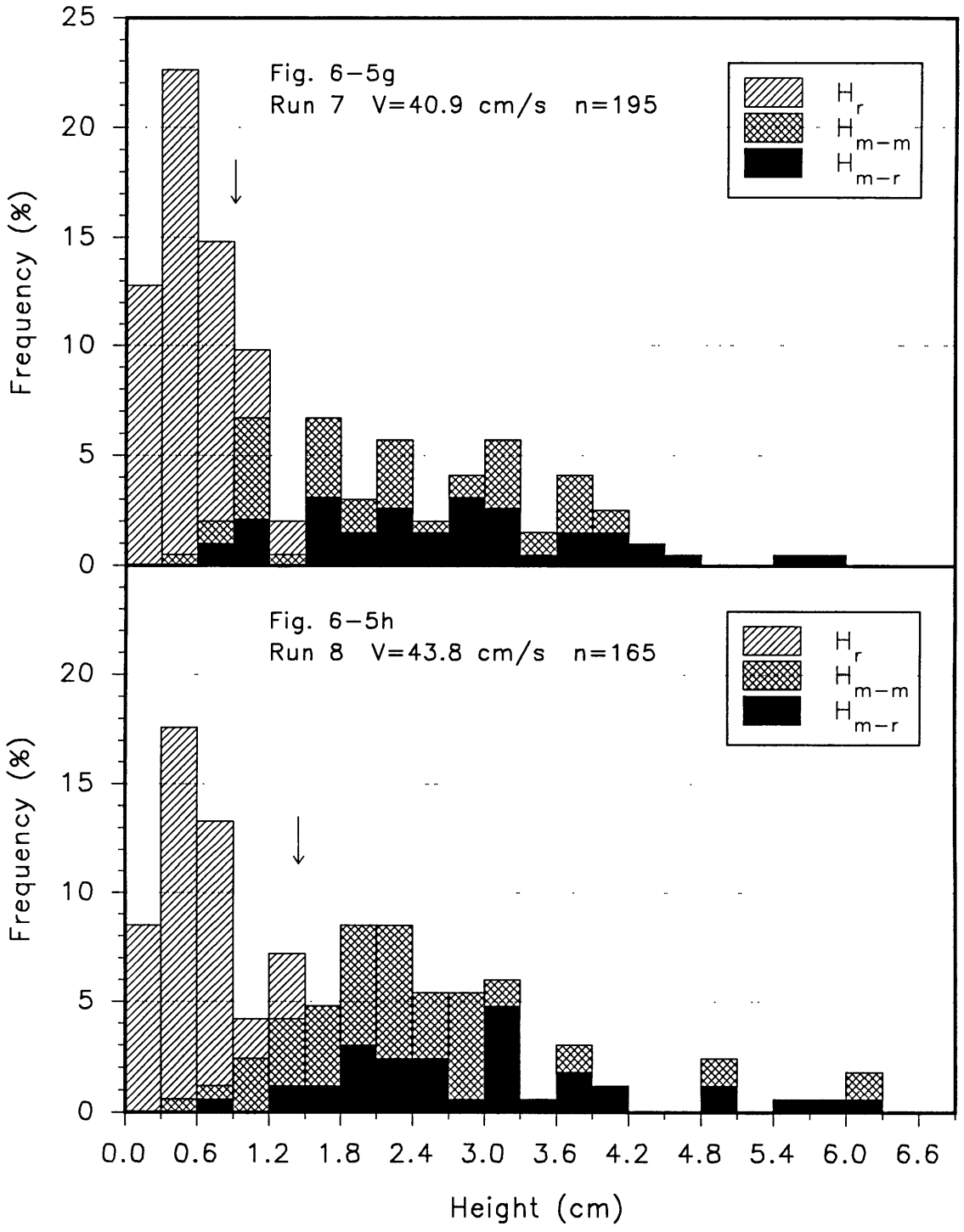

Histograms of Bed–Form Heights

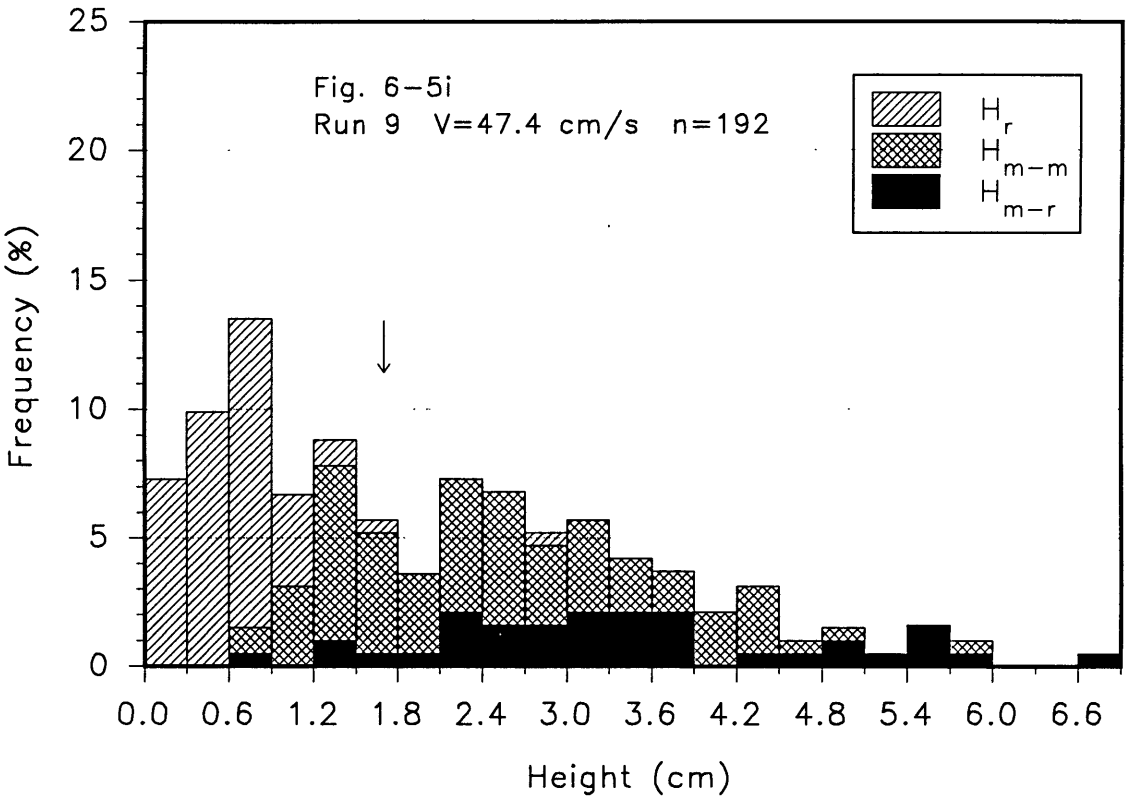

Histogram of Bed-Form Heights

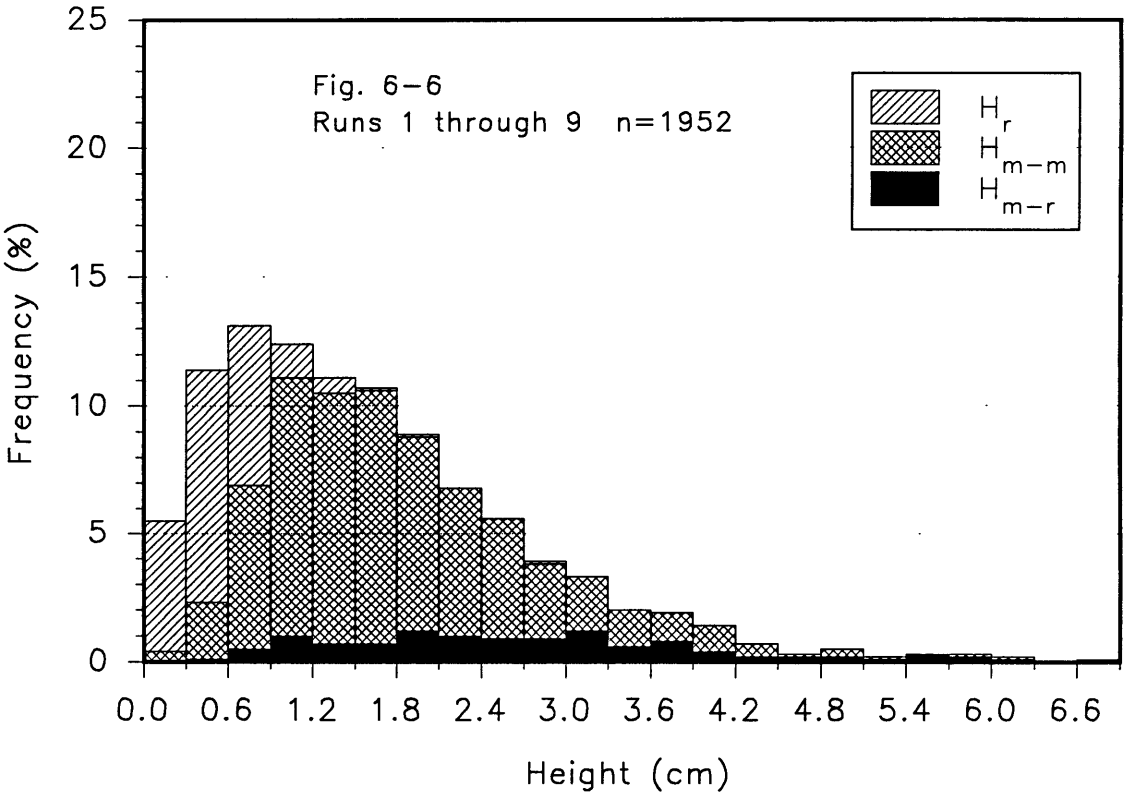

Figure 6–7

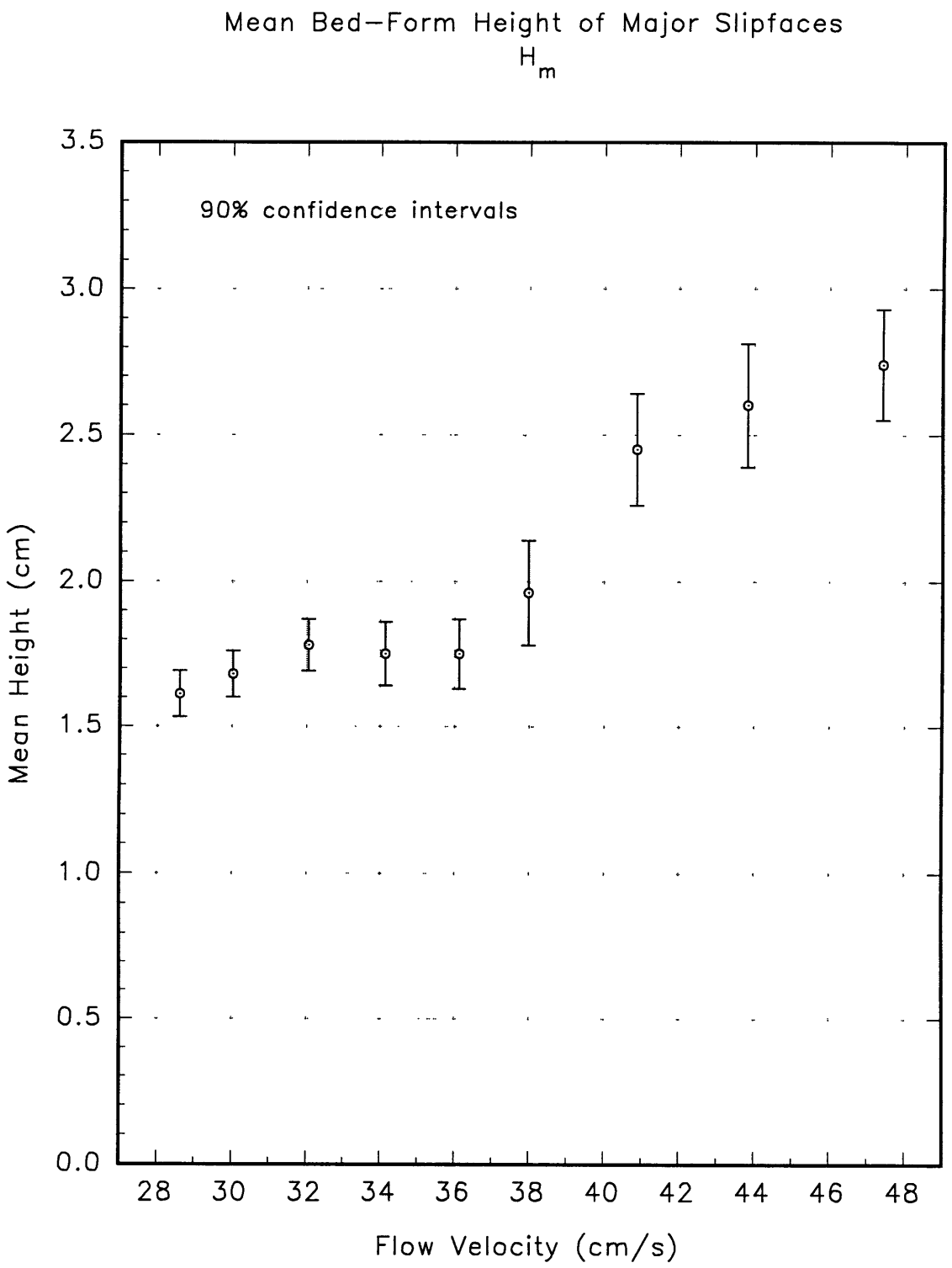
Mean Bed–Form Height of Major Slipfaces
H_m
90% confidence intervals
Mean Height (cm)
3.5
3.0
2.5
2.0
1.5
1.0
0.5
0.0
28
30
32
34
36
38
40
42
44
46
48
Flow Velocity (cm/s)

Figure 6–8

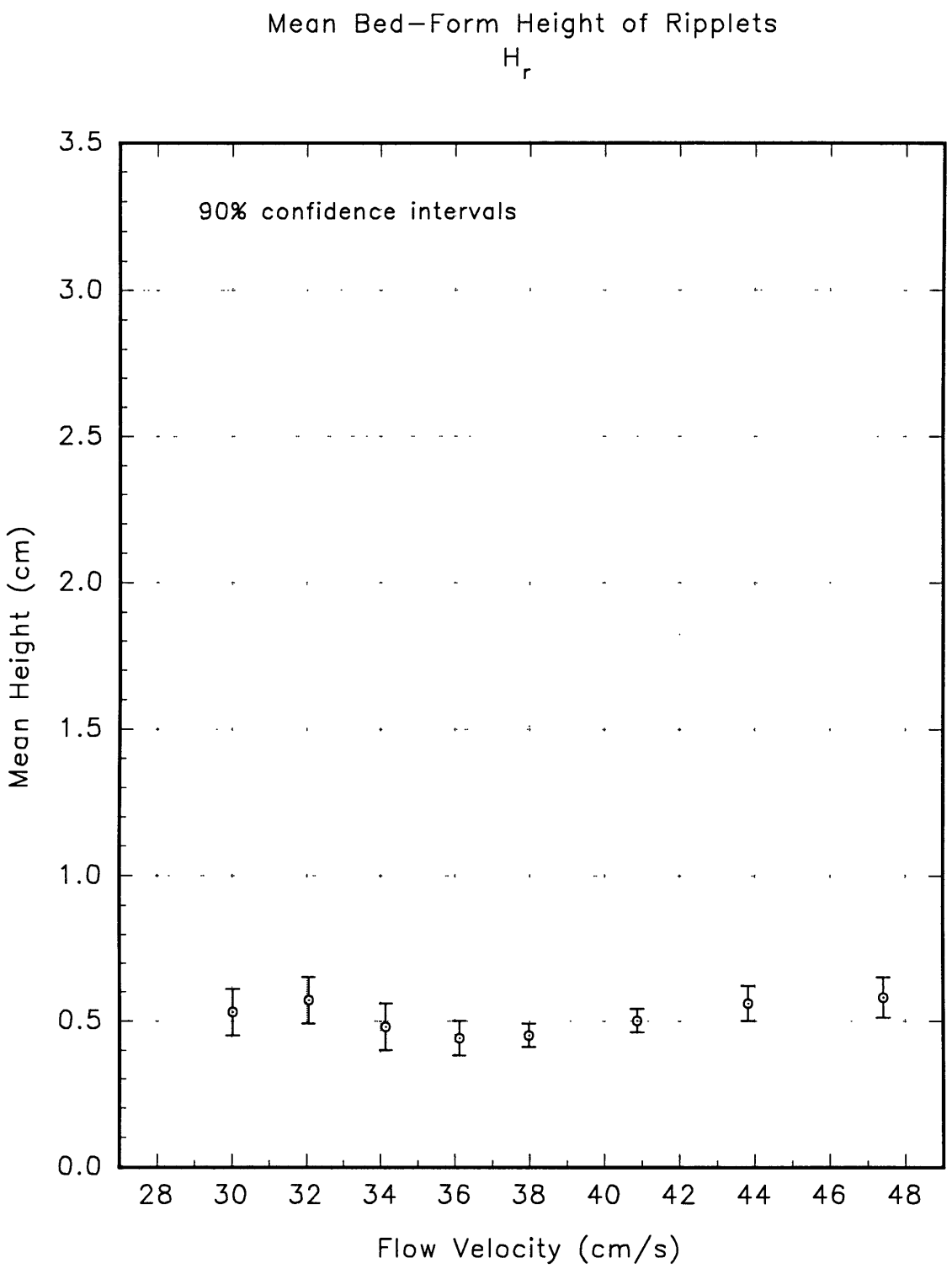
Mean Bed–Form Height of Ripplets
H_r
90% confidence intervals
Mean Height (cm)
3.5
3.0
2.5
2.0
1.5
1.0
0.5
0.0
28
30
32
34
36
38
40
42
44
46
48
Flow Velocity (cm/s)

Figure 6–9

Mean Bed–Form Height of All Slipfaces
H

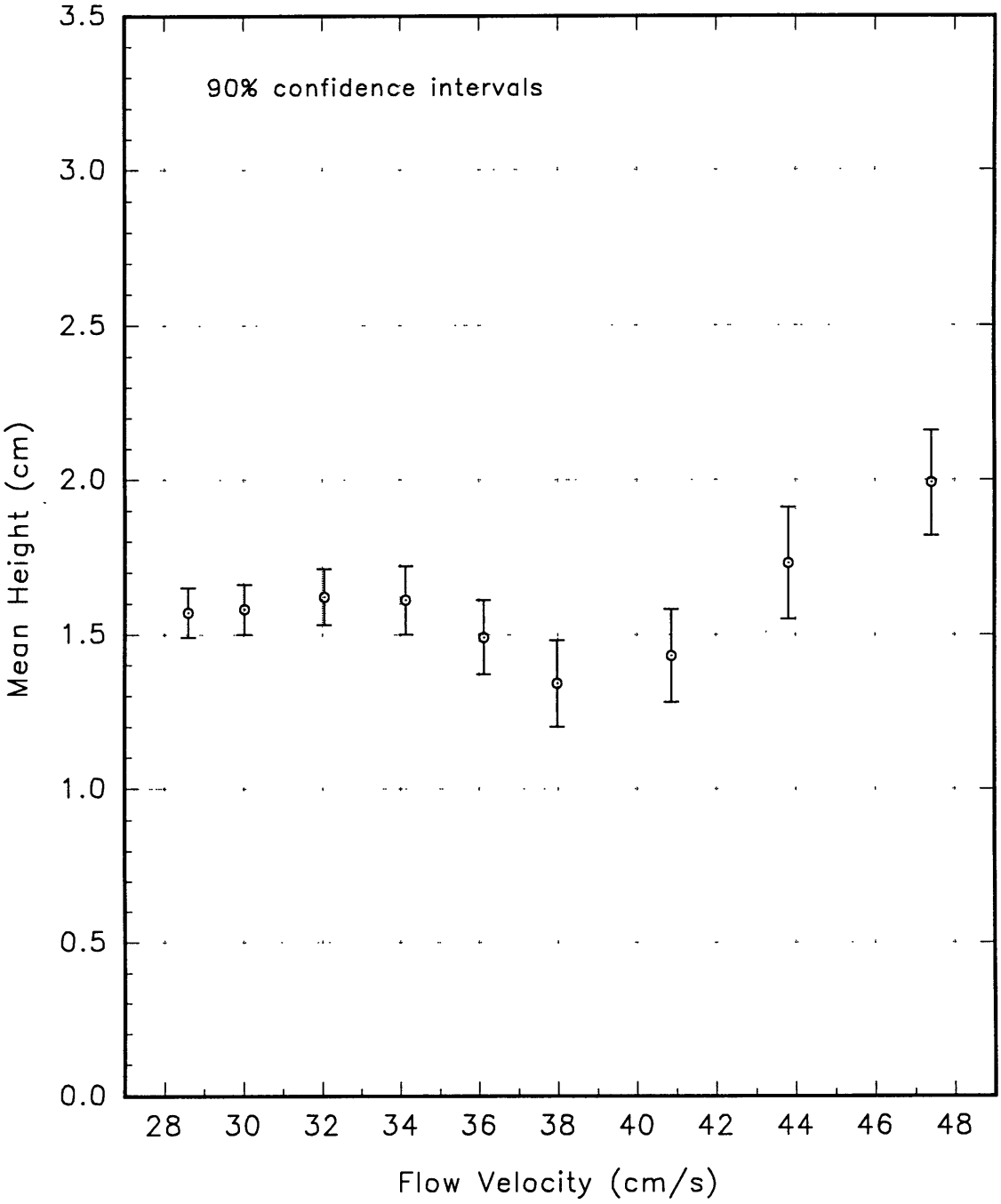

Figure 6–10

Comparison of Bed–Form Heights

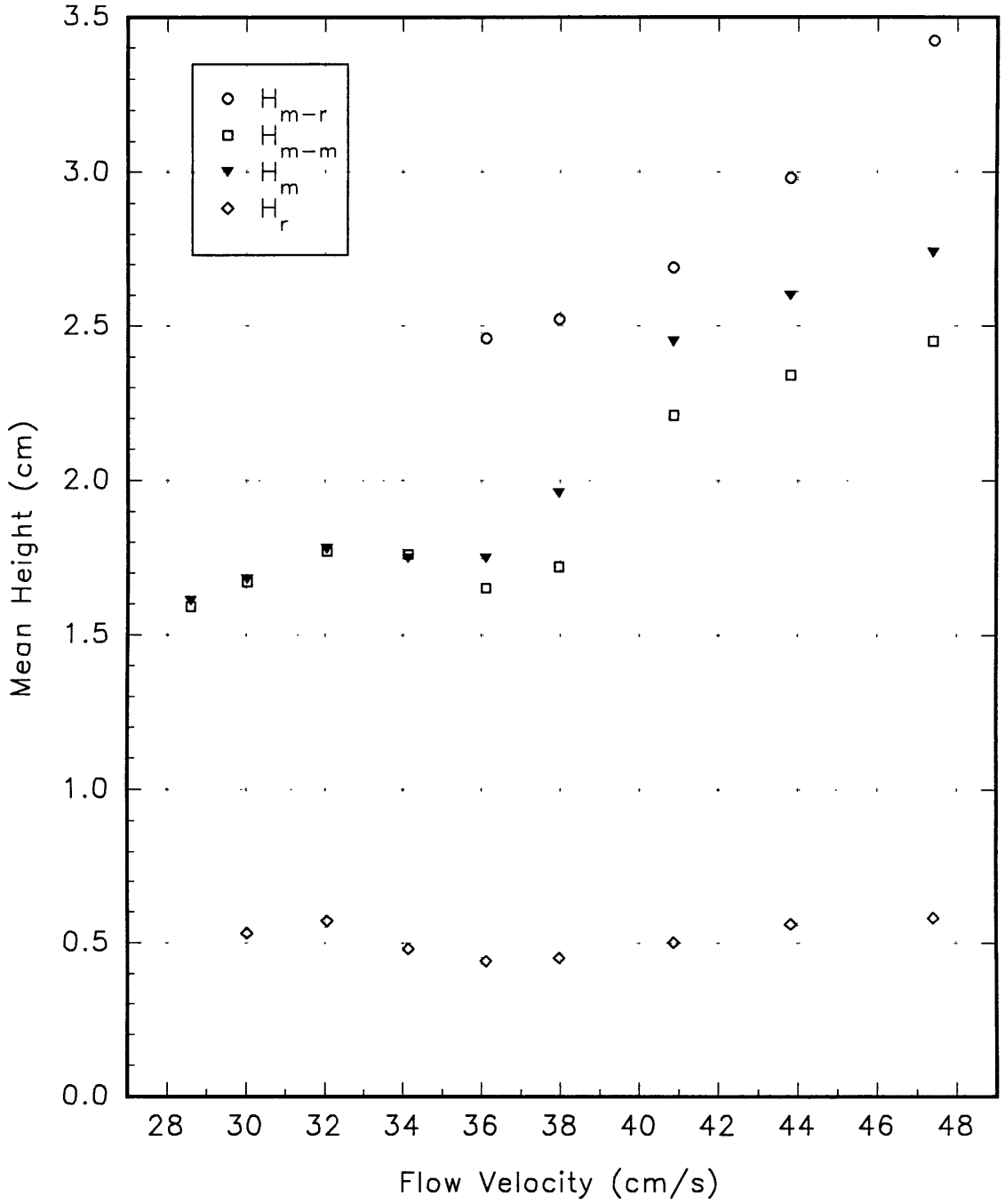

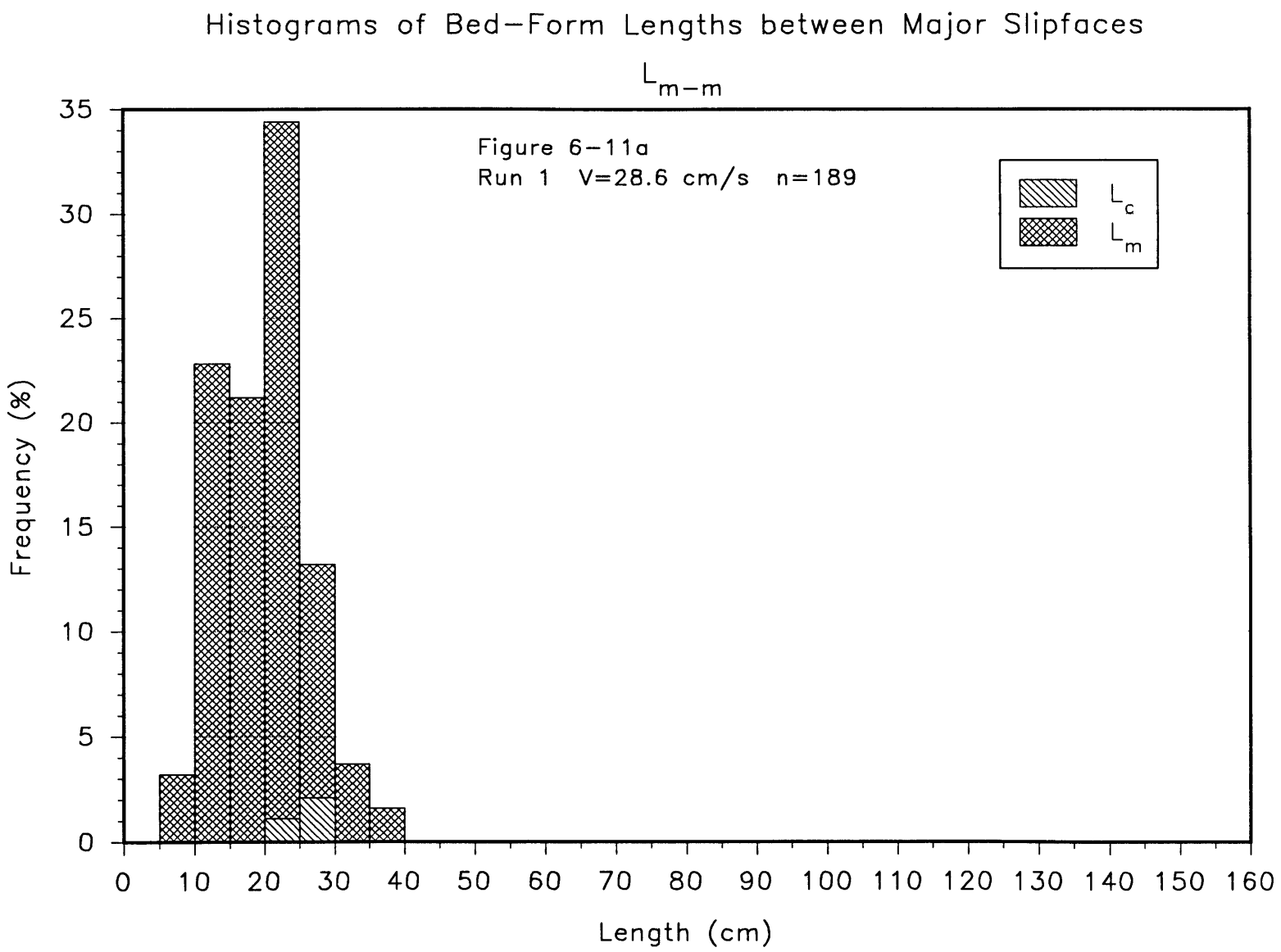
Histograms of Bed-Form Lengths between Major Slipfaces
L_{m-m}
Figure 6-11a
Run 1 V=28.6 cm/s n=189
L_c
L_m
Frequency (%)
0
5
10
15
20
25
30
35
0 10 20 30 40 50 60 70 80 90 100 110 120 130 140 150 160
Length (cm)

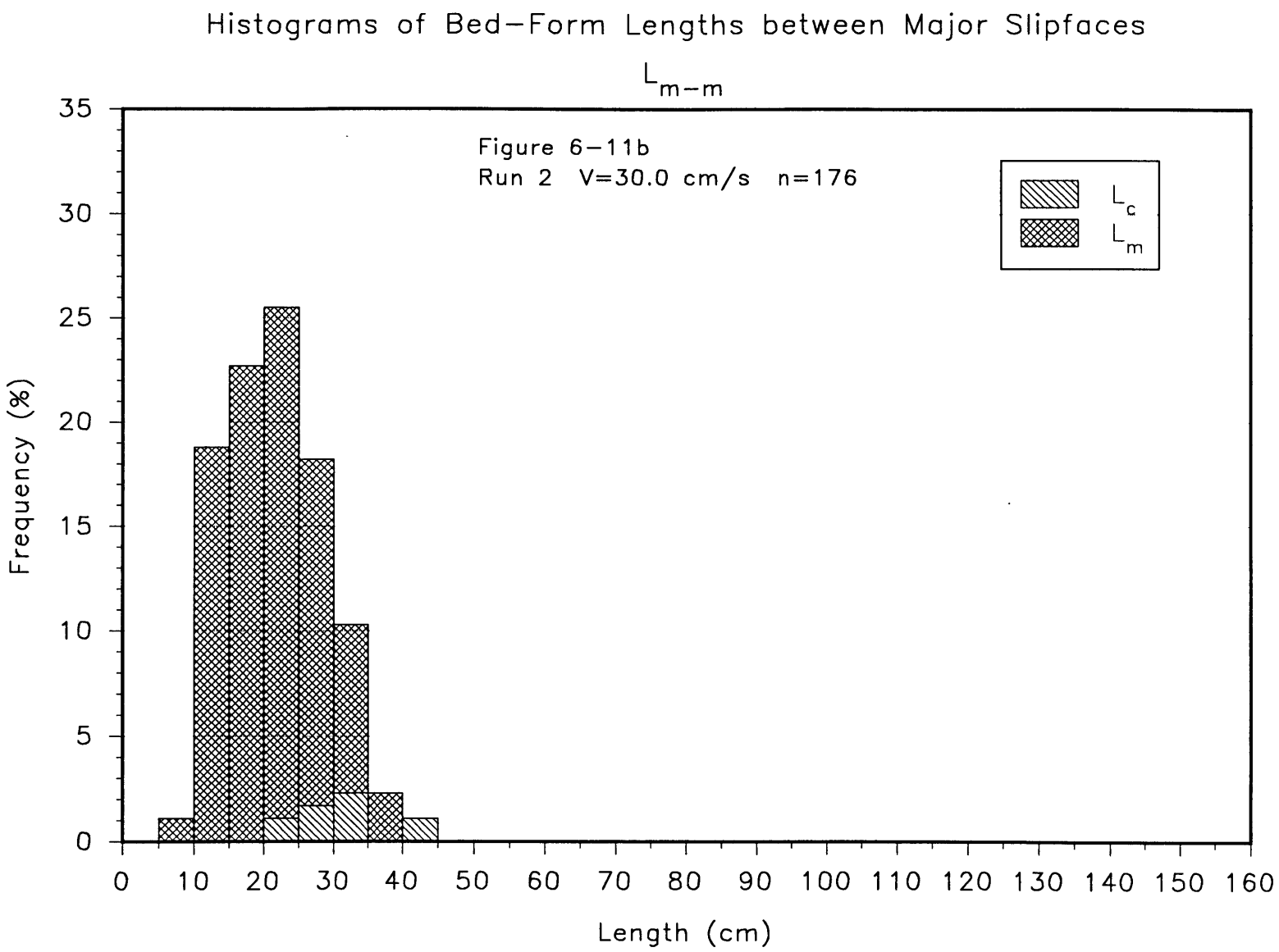
Histograms of Bed-Form Lengths between Major Slipfaces
L_{m-m}
Figure 6-11b
Run 2 V=30.0 cm/s n=176
L_c
L_m
Frequency (%)
0
5
10
15
20
25
30
35
0 10 20 30 40 50 60 70 80 90 100 110 120 130 140 150 160
Length (cm)

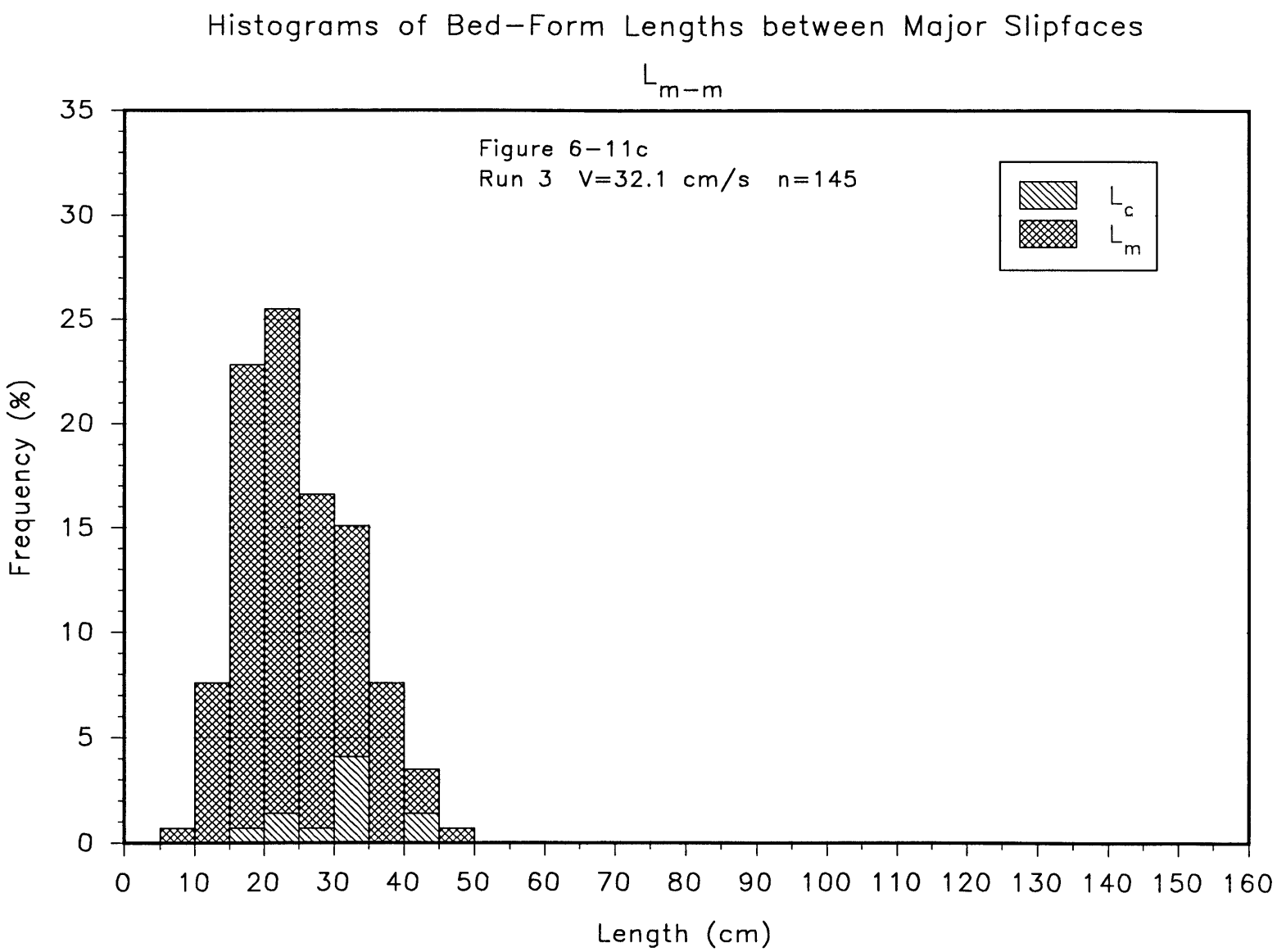
Histograms of Bed-Form Lengths between Major Slipfaces
L_{m-m}
Figure 6-11c
Run 3 V=32.1 cm/s n=145
L_c
L_m
Frequency (%)
0
5
10
15
20
25
30
35
0 10 20 30 40 50 60 70 80 90 100 110 120 130 140 150 160
Length (cm)

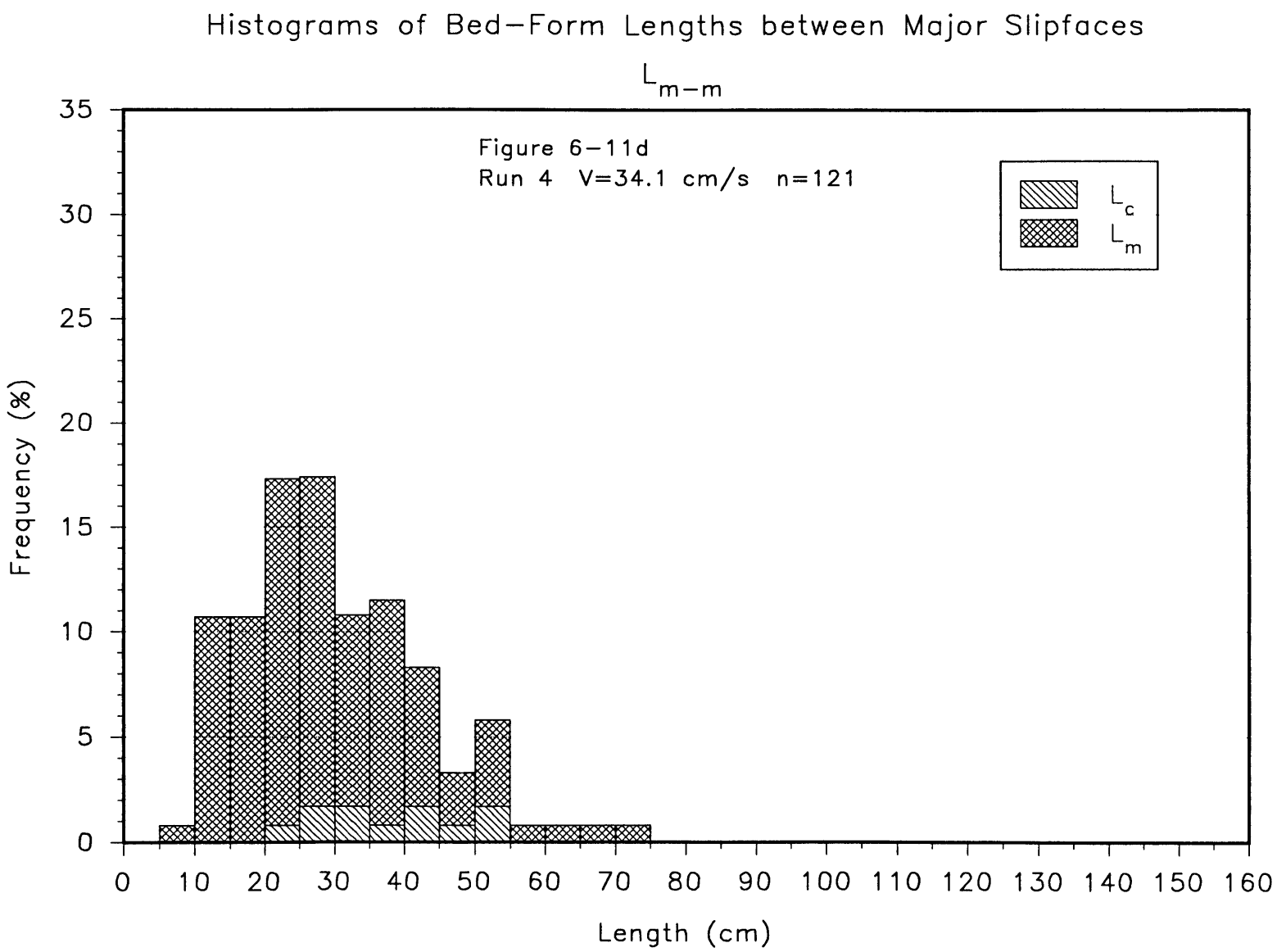
Histograms of Bed-Form Lengths between Major Slipfaces
L_{m-m}
Figure 6-11d
Run 4 V=34.1 cm/s n=121
L_c
L_m
Frequency (%)
0
5
10
15
20
25
30
35
0 10 20 30 40 50 60 70 80 90 100 110 120 130 140 150 160
Length (cm)

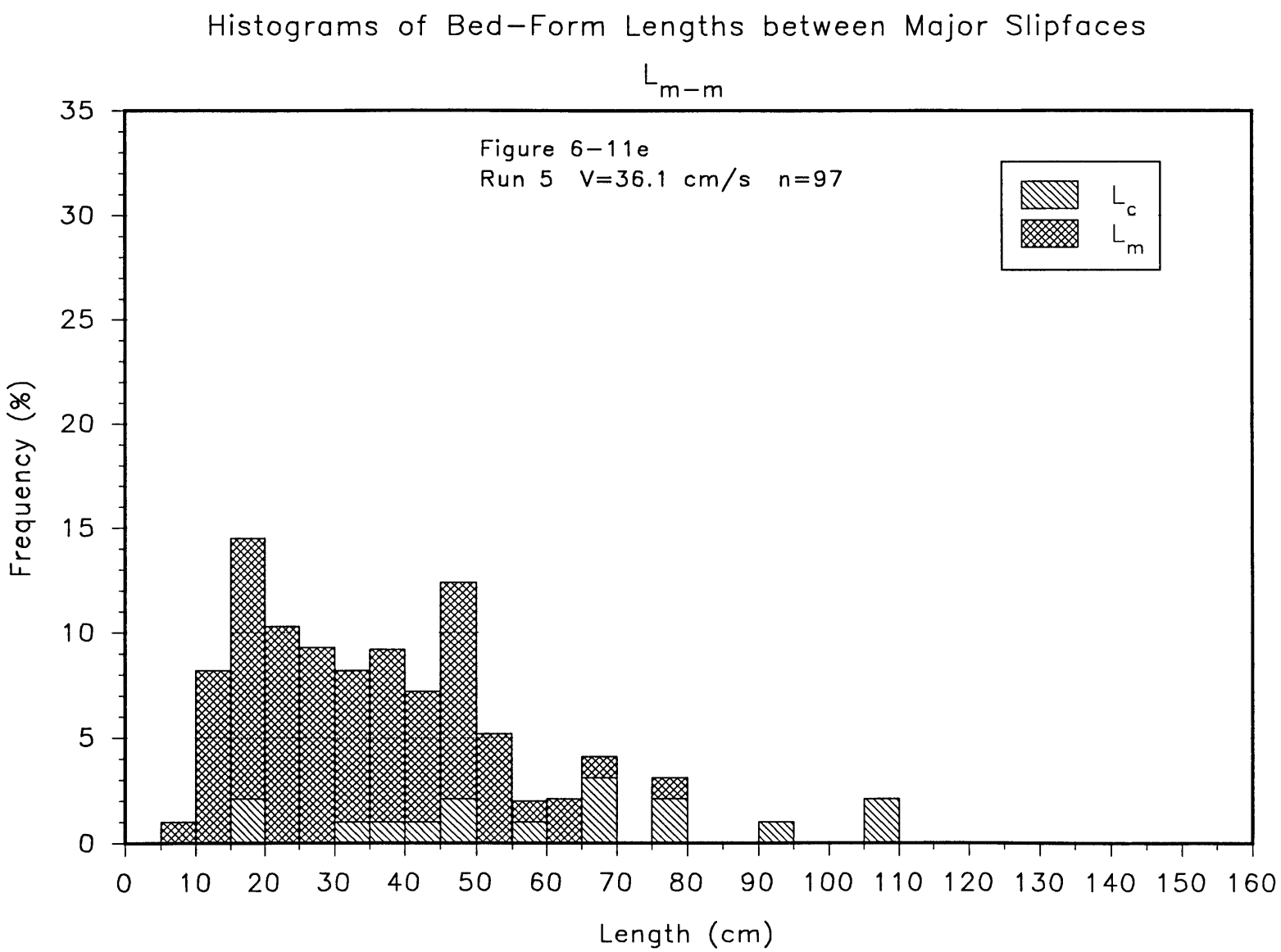
Histograms of Bed-Form Lengths between Major Slipfaces
L_{m-m}
Figure 6-11e
Run 5 V=36.1 cm/s n=97
L_c
L_m
Frequency (%)
0
5
10
15
20
25
30
35
0 10 20 30 40 50 60 70 80 90 100 110 120 130 140 150 160
Length (cm)

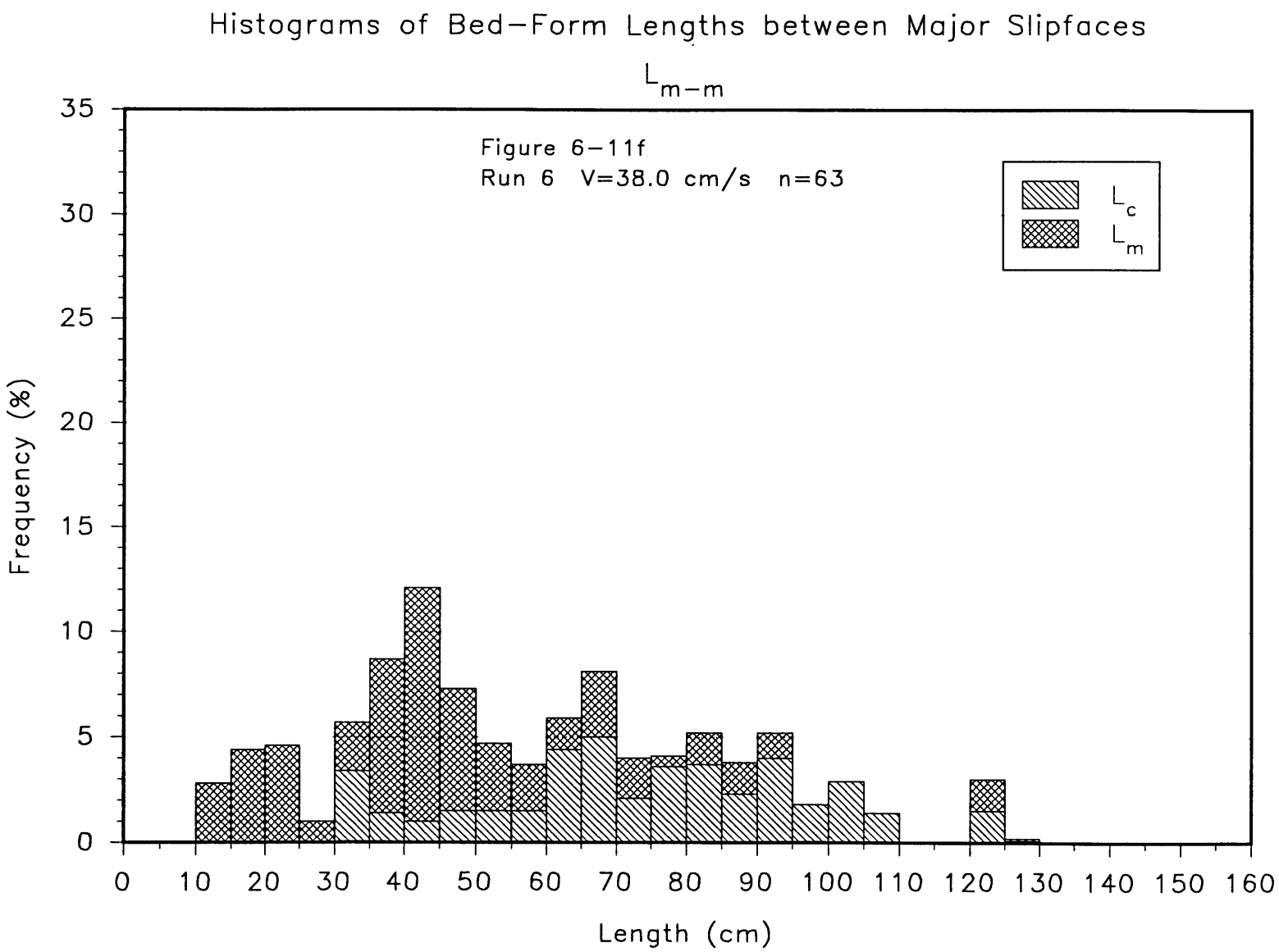
Histograms of Bed-Form Lengths between Major Slipfaces
L_{m-m}
Figure 6-11f
Run 6 V=38.0 cm/s n=63
L_c
L_m
Frequency (%)
0
5
10
15
20
25
30
35
0 10 20 30 40 50 60 70 80 90 100 110 120 130 140 150 160
Length (cm)

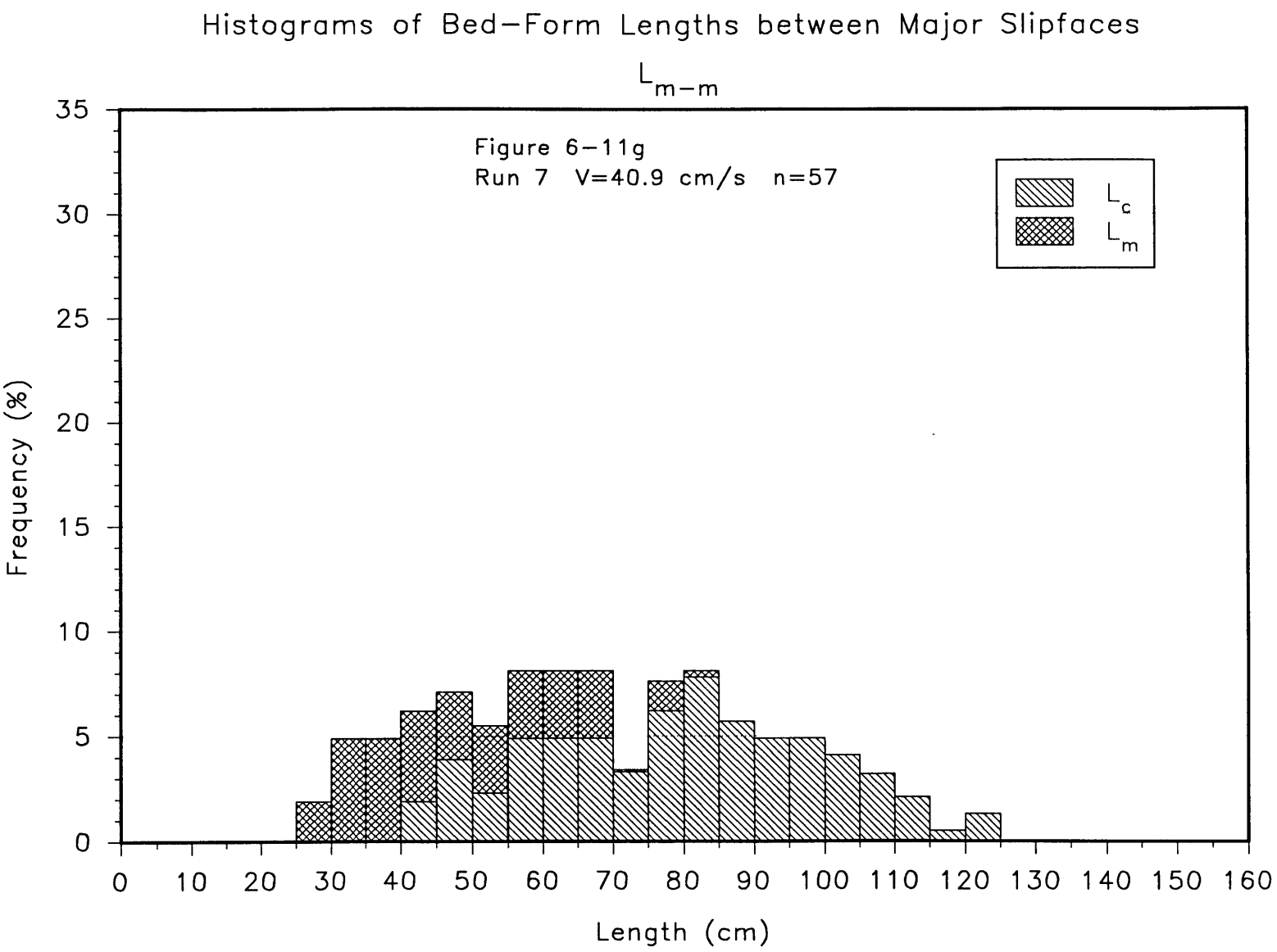
Histograms of Bed-Form Lengths between Major Slipfaces
L_{m-m}
Figure 6-11g
Run 7 V=40.9 cm/s n=57
L_c
L_m
Frequency (%)
0
5
10
15
20
25
30
35
0 10 20 30 40 50 60 70 80 90 100 110 120 130 140 150 160
Length (cm)

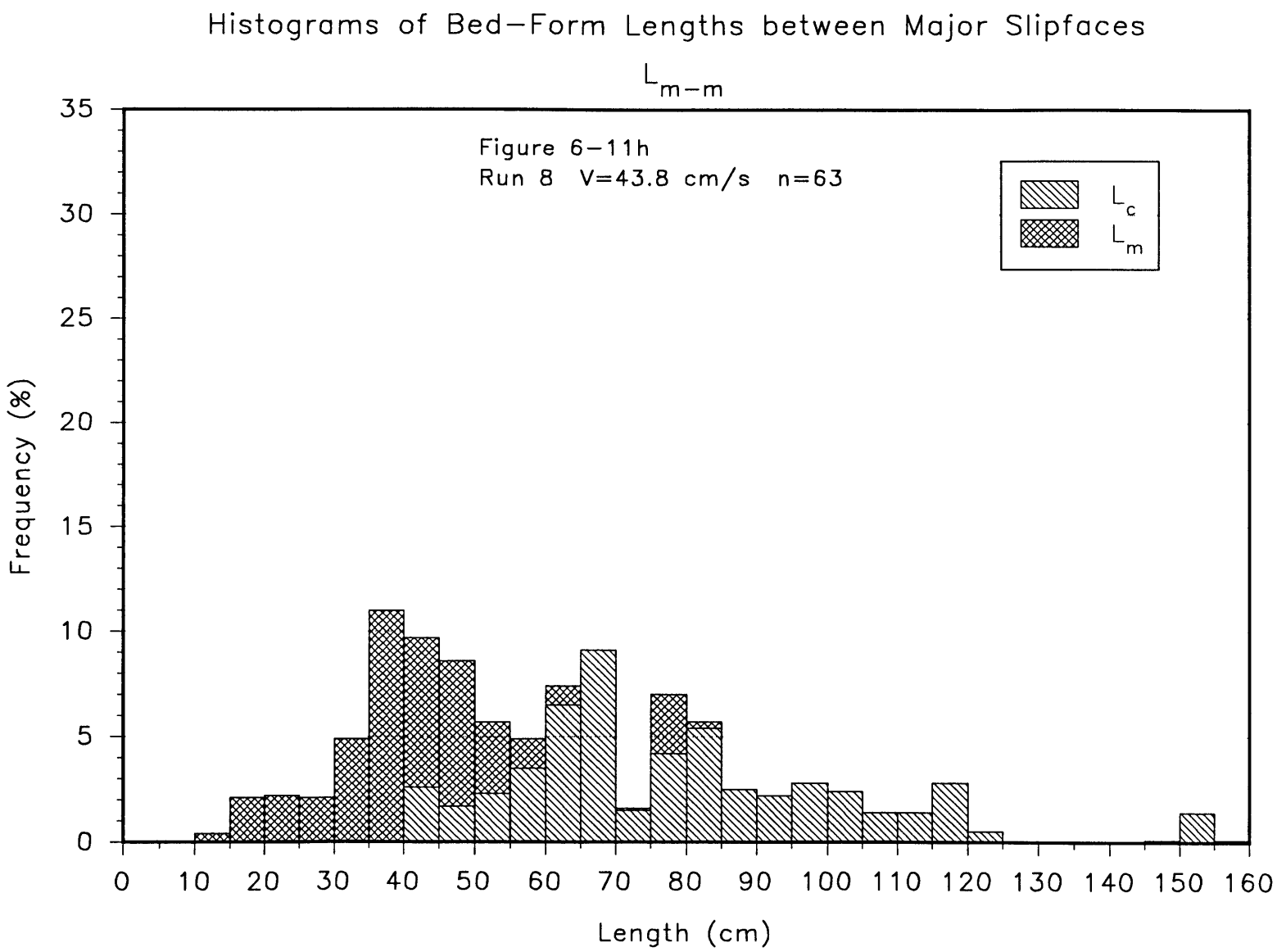
Histograms of Bed-Form Lengths between Major Slipfaces
L_{m-m}
Figure 6-11h
Run 8 V=43.8 cm/s n=63
L_c
L_m
Frequency (%)
0
5
10
15
20
25
30
35
0 10 20 30 40 50 60 70 80 90 100 110 120 130 140 150 160
Length (cm)

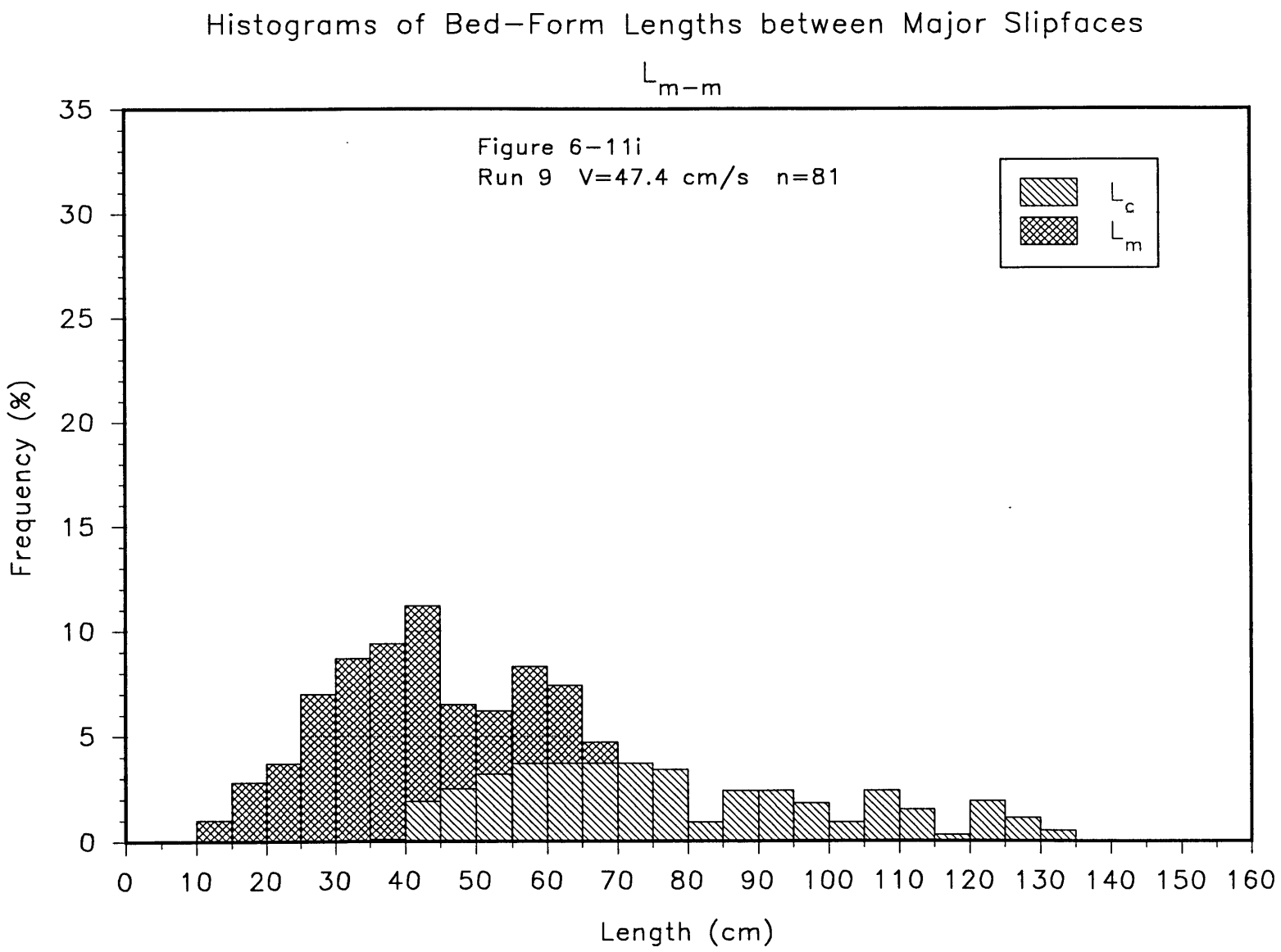
Histograms of Bed-Form Lengths between Major Slipfaces
L_{m-m}
Figure 6-11i
Run 9 V=47.4 cm/s n=81
L_c
L_m
Frequency (%)
0
5
10
15
20
25
30
35
0 10 20 30 40 50 60 70 80 90 100 110 120 130 140 150 160
Length (cm)

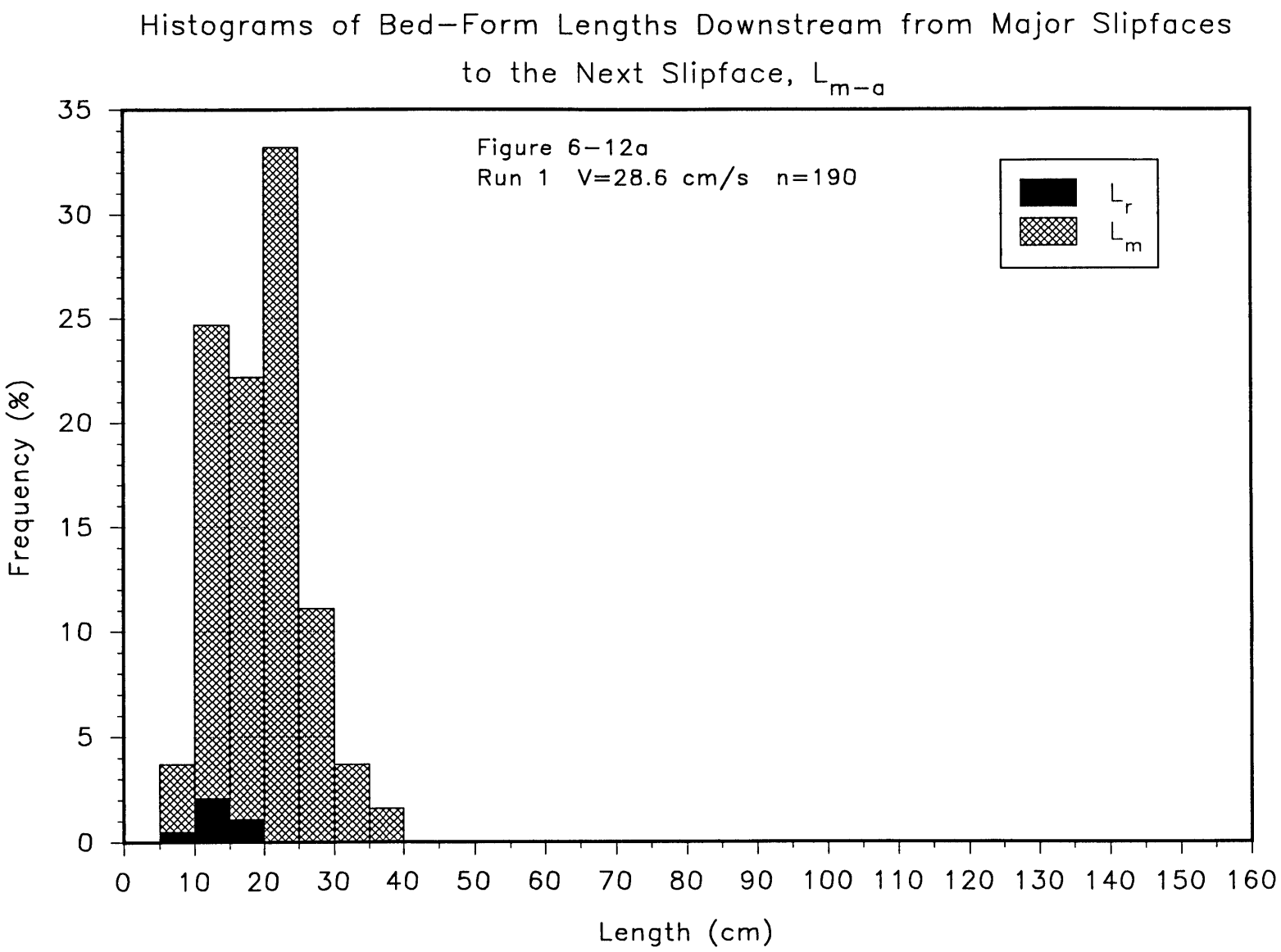
Histograms of Bed-Form Lengths Downstream from Major Slipfaces to the Next Slipface, L_{m-a}
Figure 6-12a
Run 1 V=28.6 cm/s n=190
L_r
L_m
Frequency (%)
0
5
10
15
20
25
30
35
0 10 20 30 40 50 60 70 80 90 100 110 120 130 140 150 160
Length (cm)

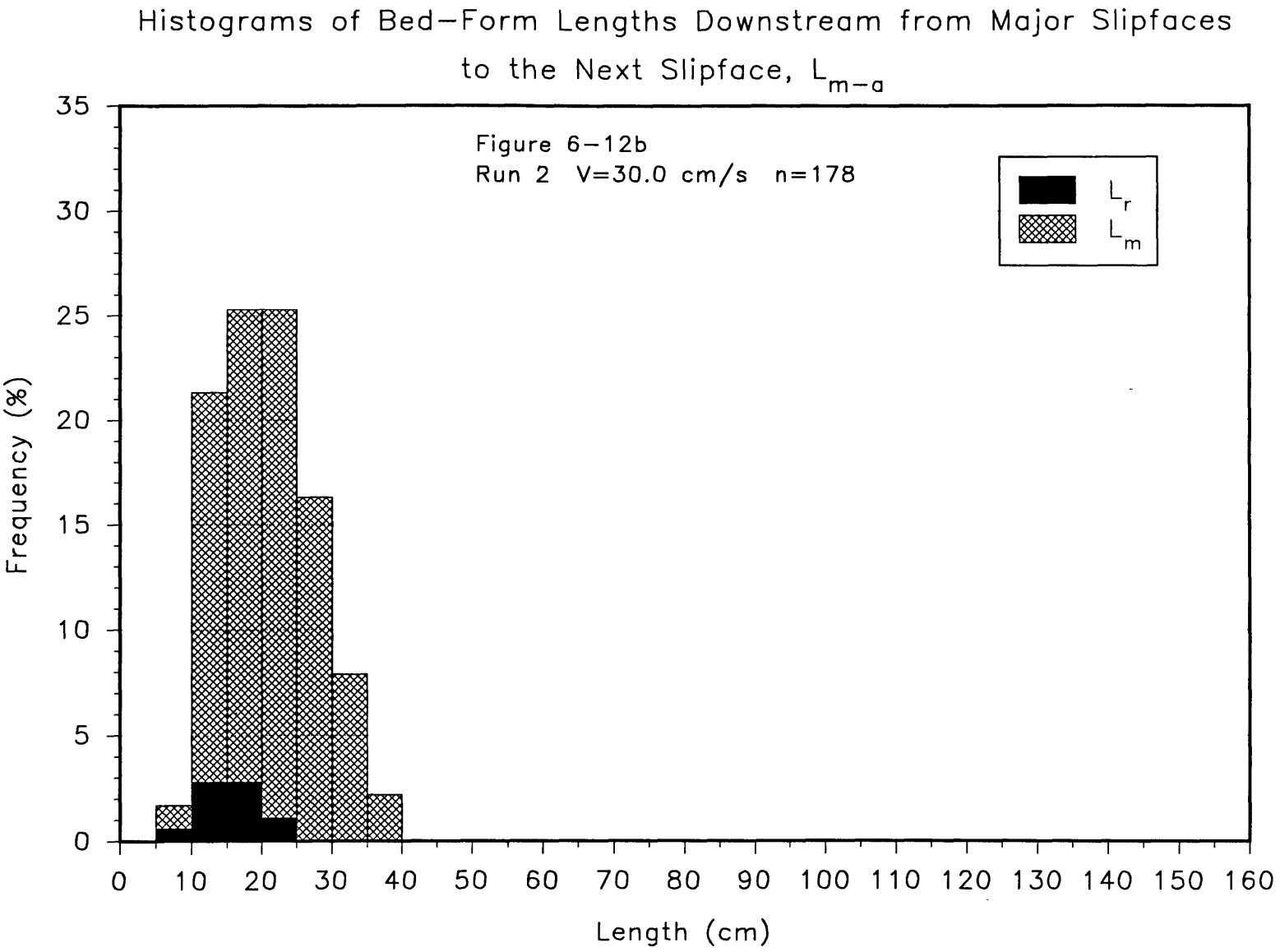
Histograms of Bed-Form Lengths Downstream from Major Slipfaces
to the Next Slipface, L_{m-a}
Figure 6-12b
Run 2 V=30.0 cm/s n=178
L_r
L_m
Frequency (%)
0
5
10
15
20
25
30
35
0 10 20 30 40 50 60 70 80 90 100 110 120 130 140 150 160
Length (cm)

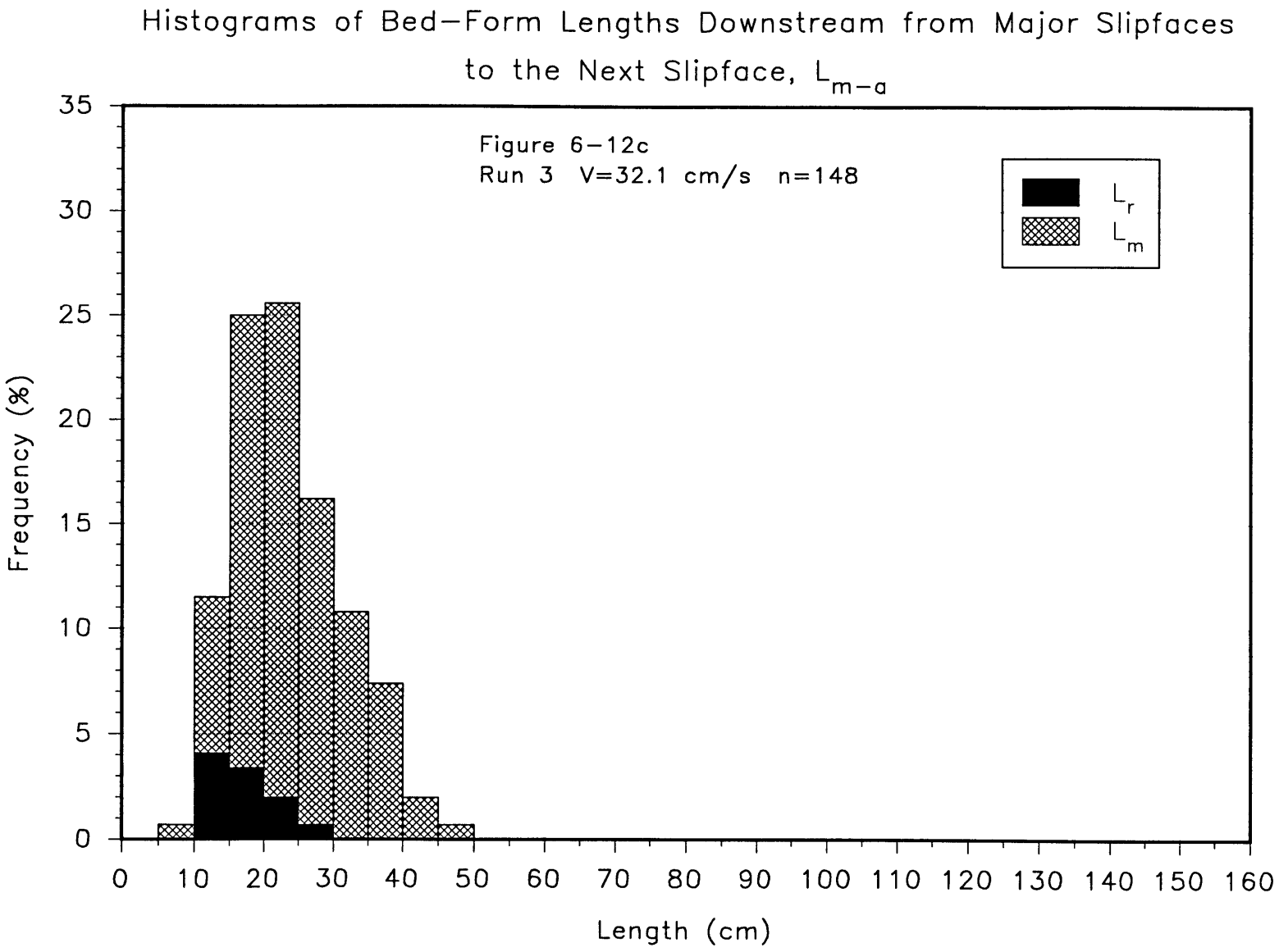
Histograms of Bed-Form Lengths Downstream from Major Slipfaces
to the Next Slipface, L_{m-a}
Figure 6-12c
Run 3 V=32.1 cm/s n=148
L_r
L_m
Frequency (%)
0
5
10
15
20
25
30
35
0 10 20 30 40 50 60 70 80 90 100 110 120 130 140 150 160
Length (cm)

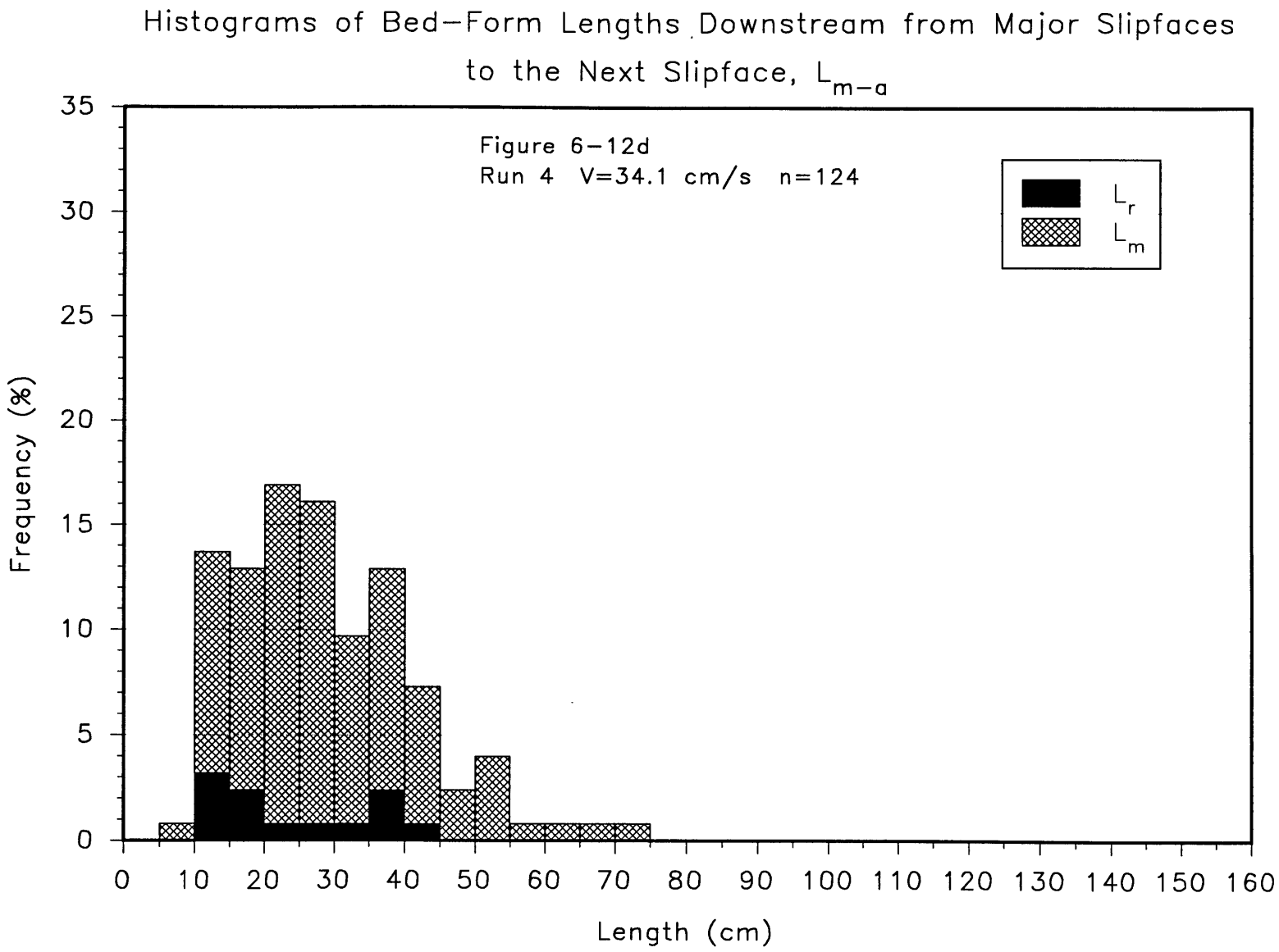
Histograms of Bed–Form Lengths Downstream from Major Slipfaces to the Next Slipface, L_{m-a}
Figure 6–12d
Run 4 V=34.1 cm/s n=124
L_r
L_m
Frequency (%)
0
5
10
15
20
25
30
35
0 10 20 30 40 50 60 70 80 90 100 110 120 130 140 150 160
Length (cm)

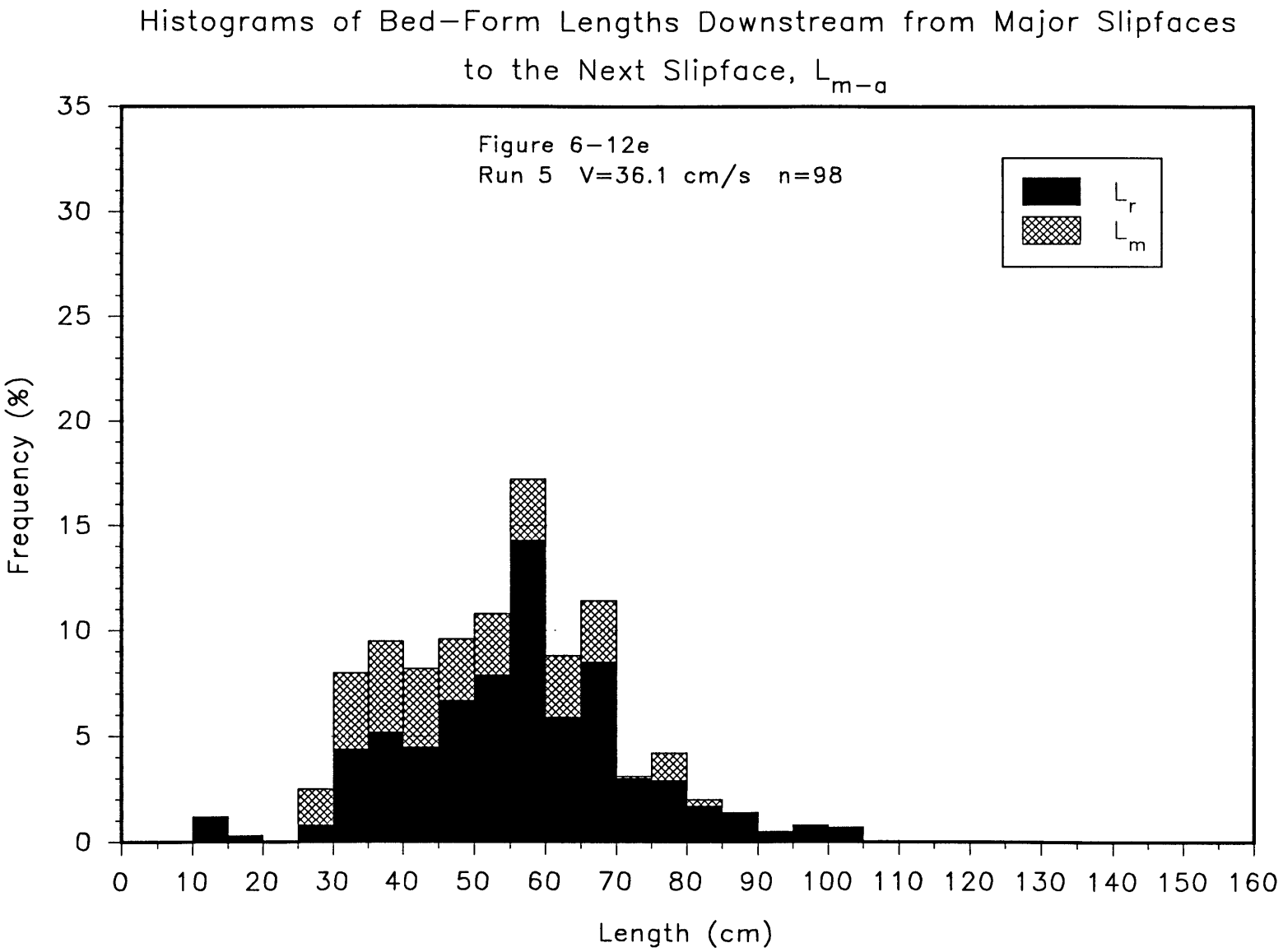
Histograms of Bed-Form Lengths Downstream from Major Slipfaces
to the Next Slipface, L_{m-a}
Figure 6-12e
Run 5 V=36.1 cm/s n=98
L_r
L_m
Frequency (%)
0
5
10
15
20
25
30
35
0 10 20 30 40 50 60 70 80 90 100 110 120 130 140 150 160
Length (cm)

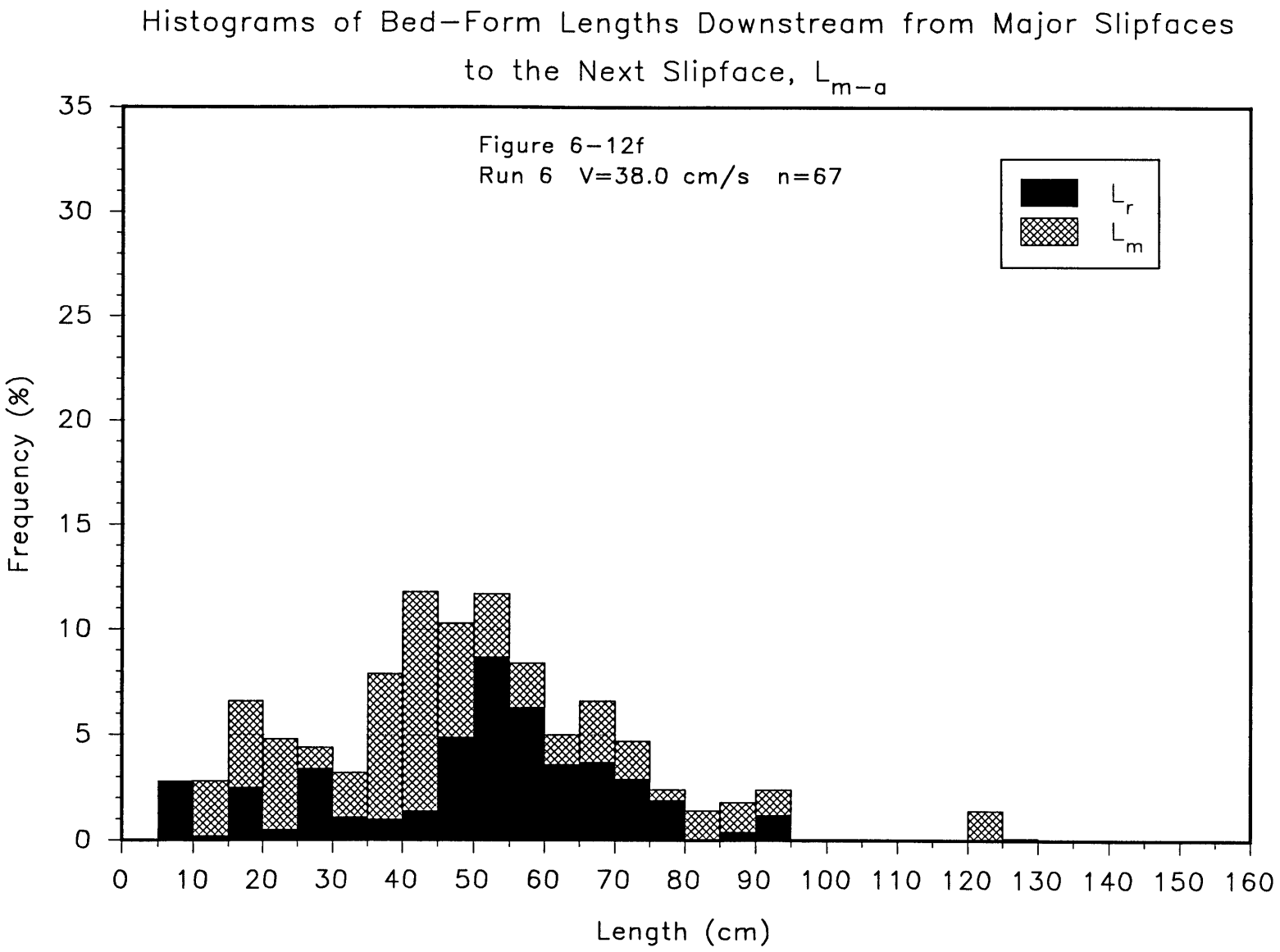
Histograms of Bed-Form Lengths Downstream from Major Slipfaces
to the Next Slipface, L_{m-a}
Figure 6-12f
Run 6 V=38.0 cm/s n=67
L_r
L_m
Frequency (%)
0
5
10
15
20
25
30
35
0 10 20 30 40 50 60 70 80 90 100 110 120 130 140 150 160
Length (cm)

Histograms of Bed–Form Lengths Downstream from Major Slipfaces to the Next Slipface, L_{m-a}

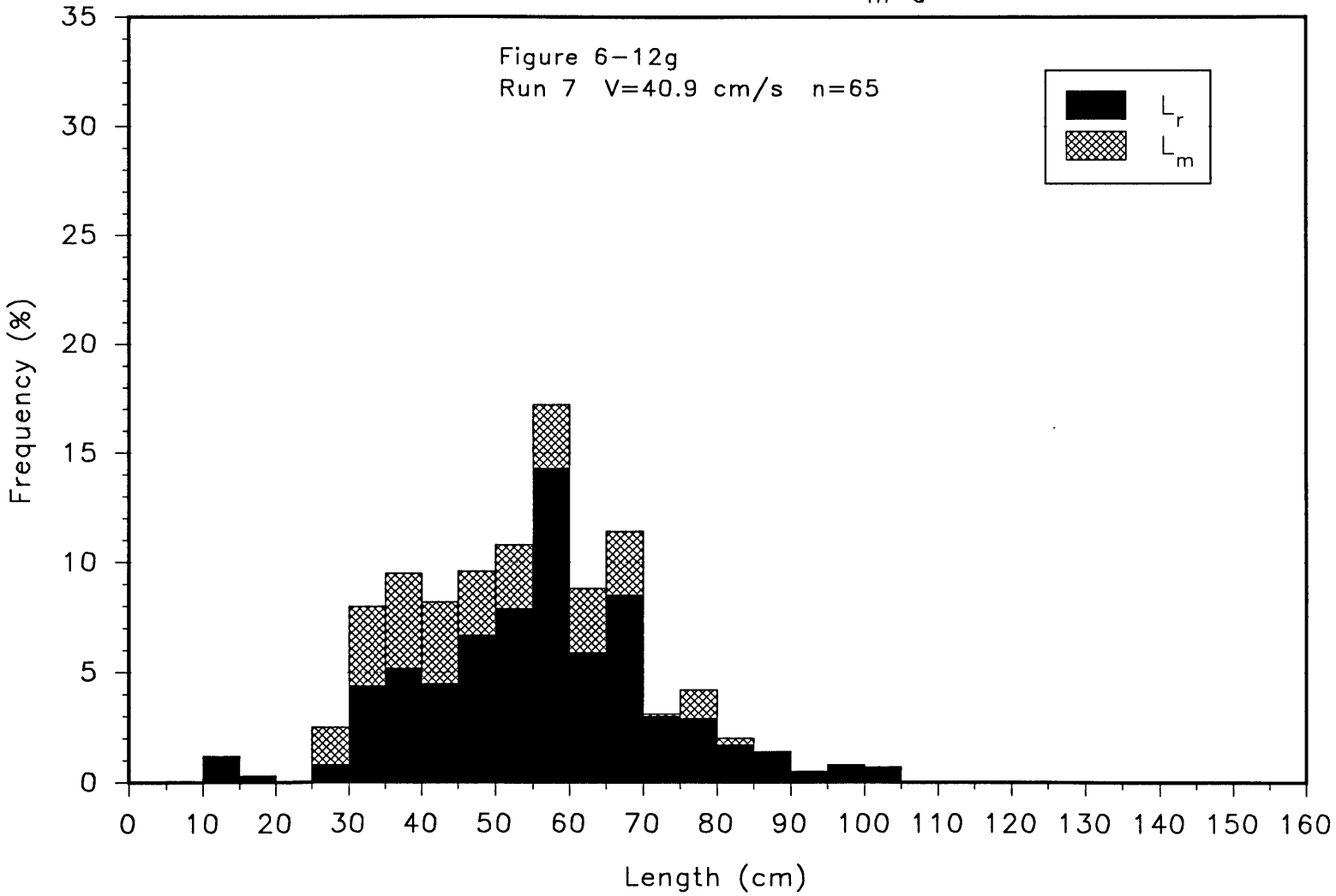

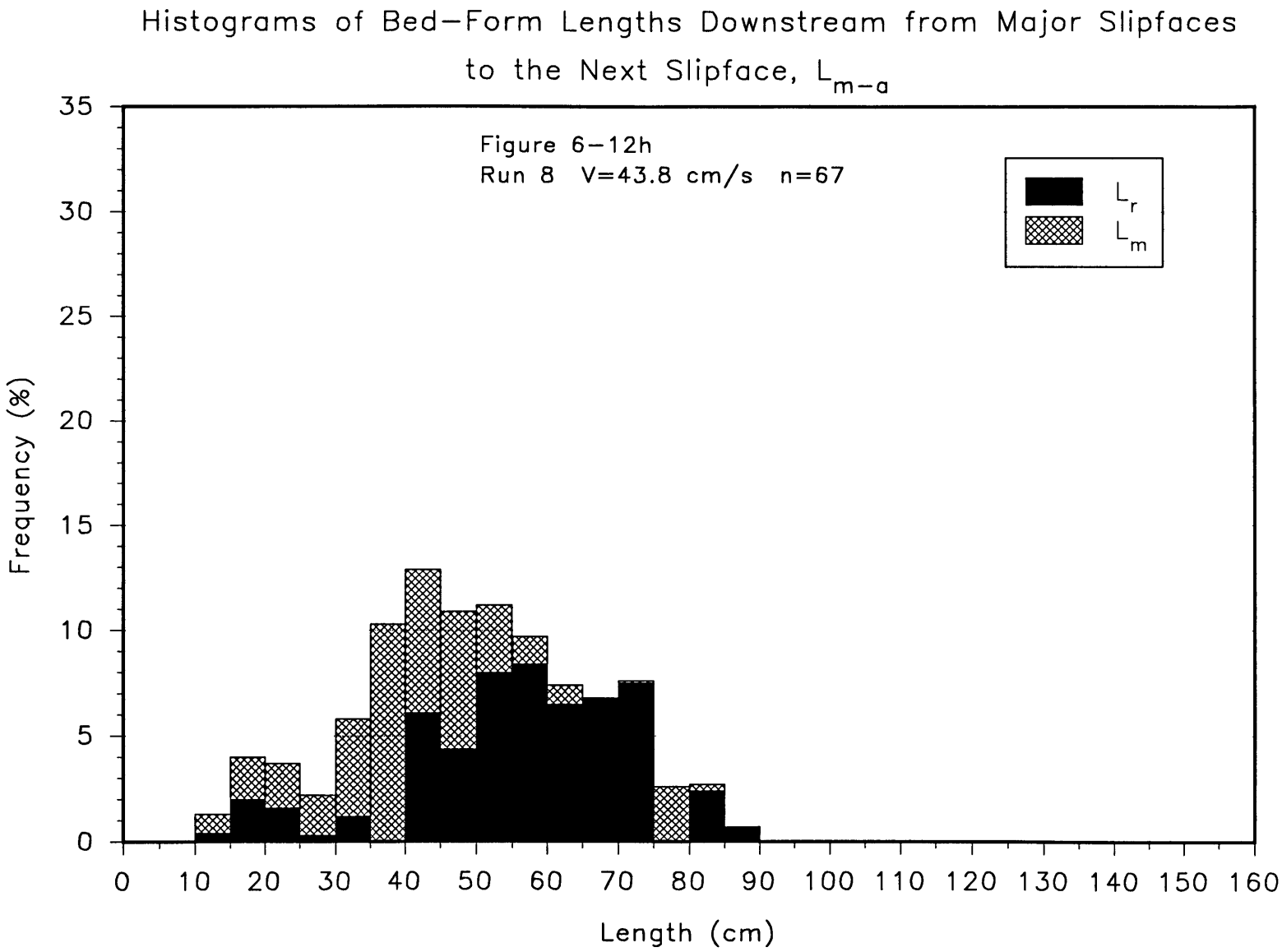
Histograms of Bed–Form Lengths Downstream from Major Slipfaces to the Next Slipface, L_{m-a}
Figure 6–12h
Run 8 V=43.8 cm/s n=67
L_r
L_m
Frequency (%)
0
5
10
15
20
25
30
35
0 10 20 30 40 50 60 70 80 90 100 110 120 130 140 150 160
Length (cm)

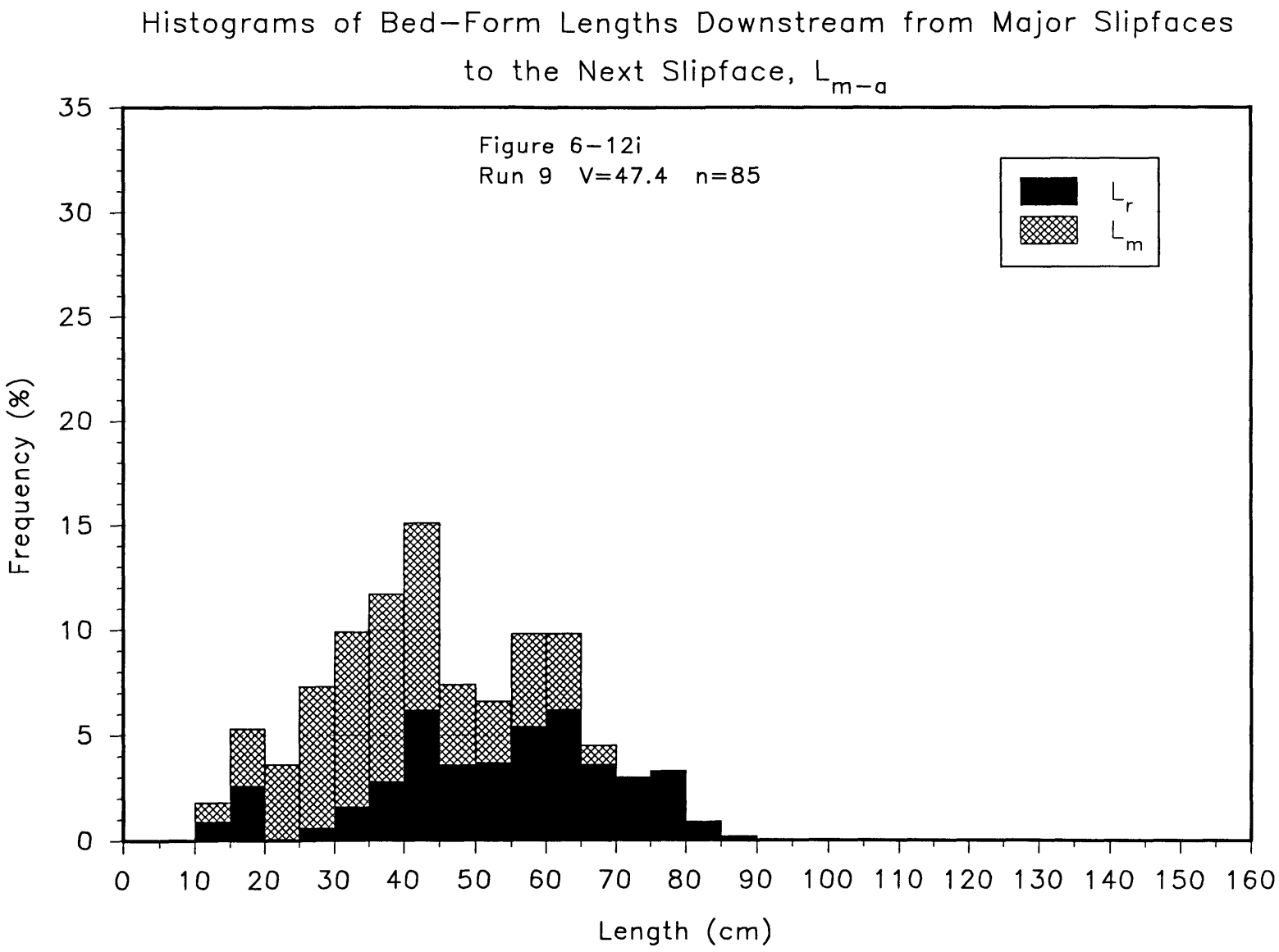
Histograms of Bed-Form Lengths Downstream from Major Slipfaces
to the Next Slipface, L_{m-a}
Figure 6-12i
Run 9 V=47.4 n=85
L_r
L_m
Frequency (%)
0
5
10
15
20
25
30
35
0 10 20 30 40 50 60 70 80 90 100 110 120 130 140 150 160
Length (cm)

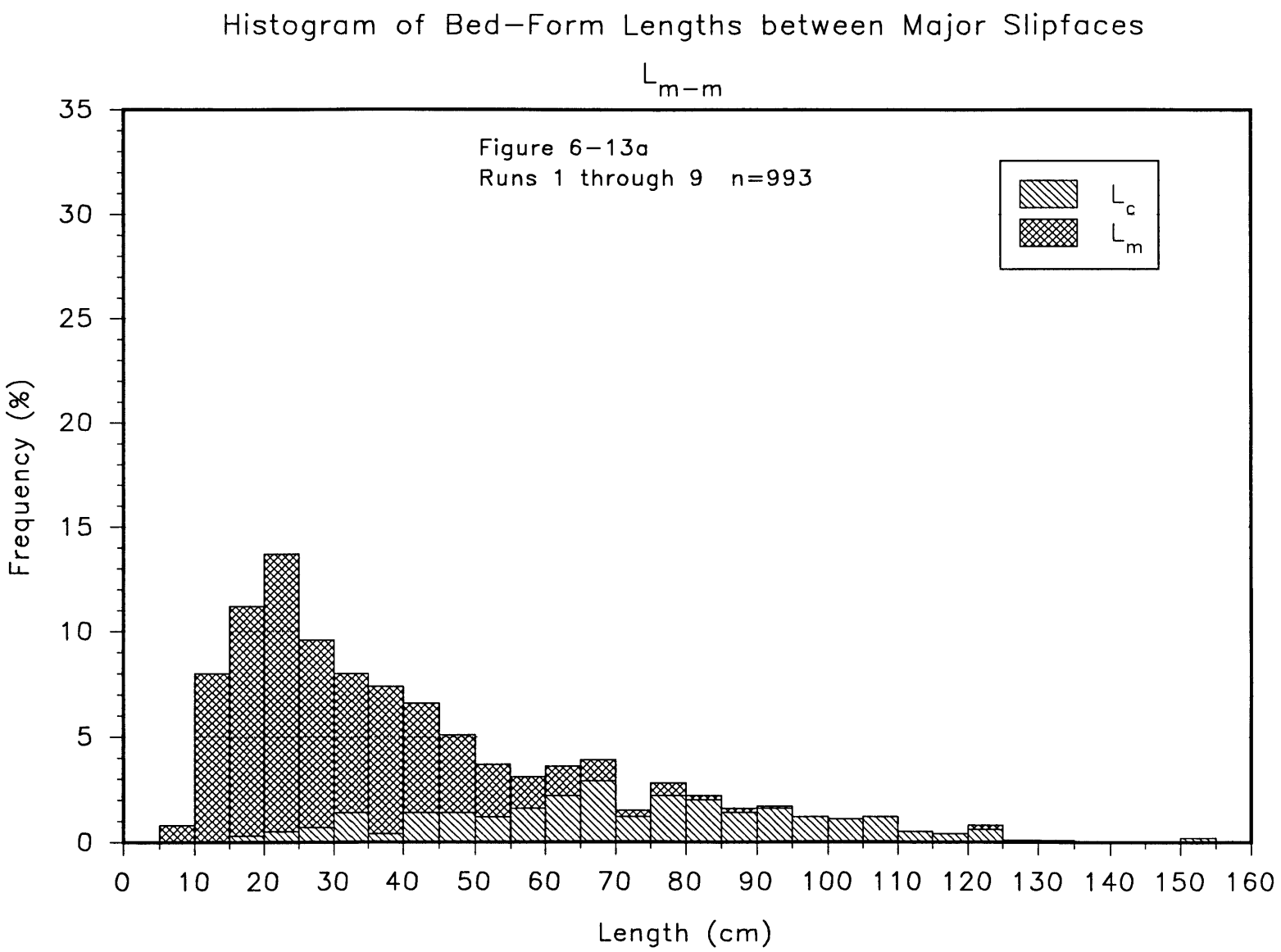
Histogram of Bed–Form Lengths between Major Slipfaces
L_{m-m}
Figure 6–13a
Runs 1 through 9 n=993
L_c
L_m
Frequency (%)
0
5
10
15
20
25
30
35
0 10 20 30 40 50 60 70 80 90 100 110 120 130 140 150 160
Length (cm)

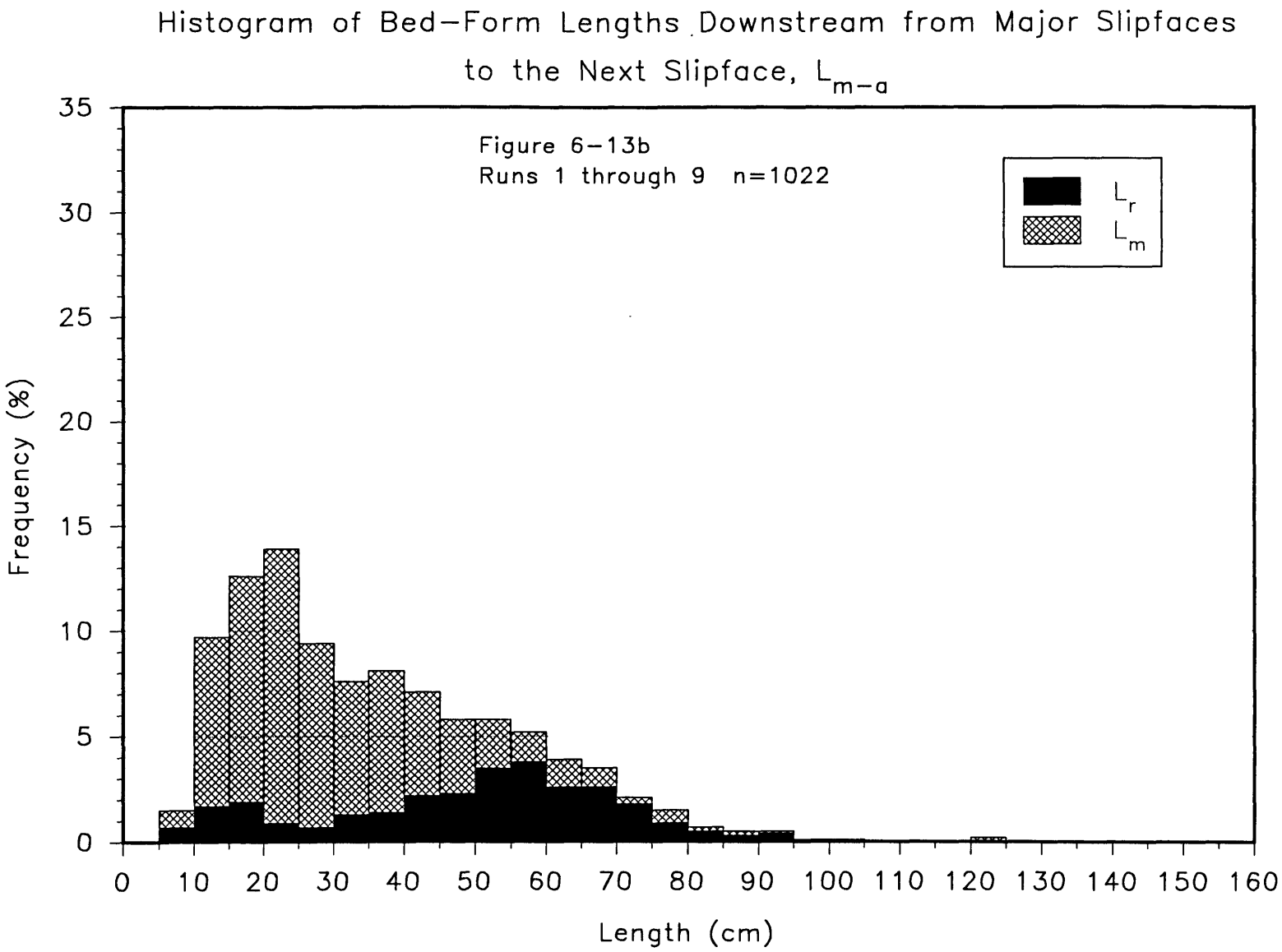
Histogram of Bed-Form Lengths Downstream from Major Slipfaces
to the Next Slipface, L_{m-a}
Figure 6-13b
Runs 1 through 9 n=1022
L_r
L_m
Frequency (%)
0
5
10
15
20
25
30
35
0 10 20 30 40 50 60 70 80 90 100 110 120 130 140 150 160
Length (cm)

Figure 6–14

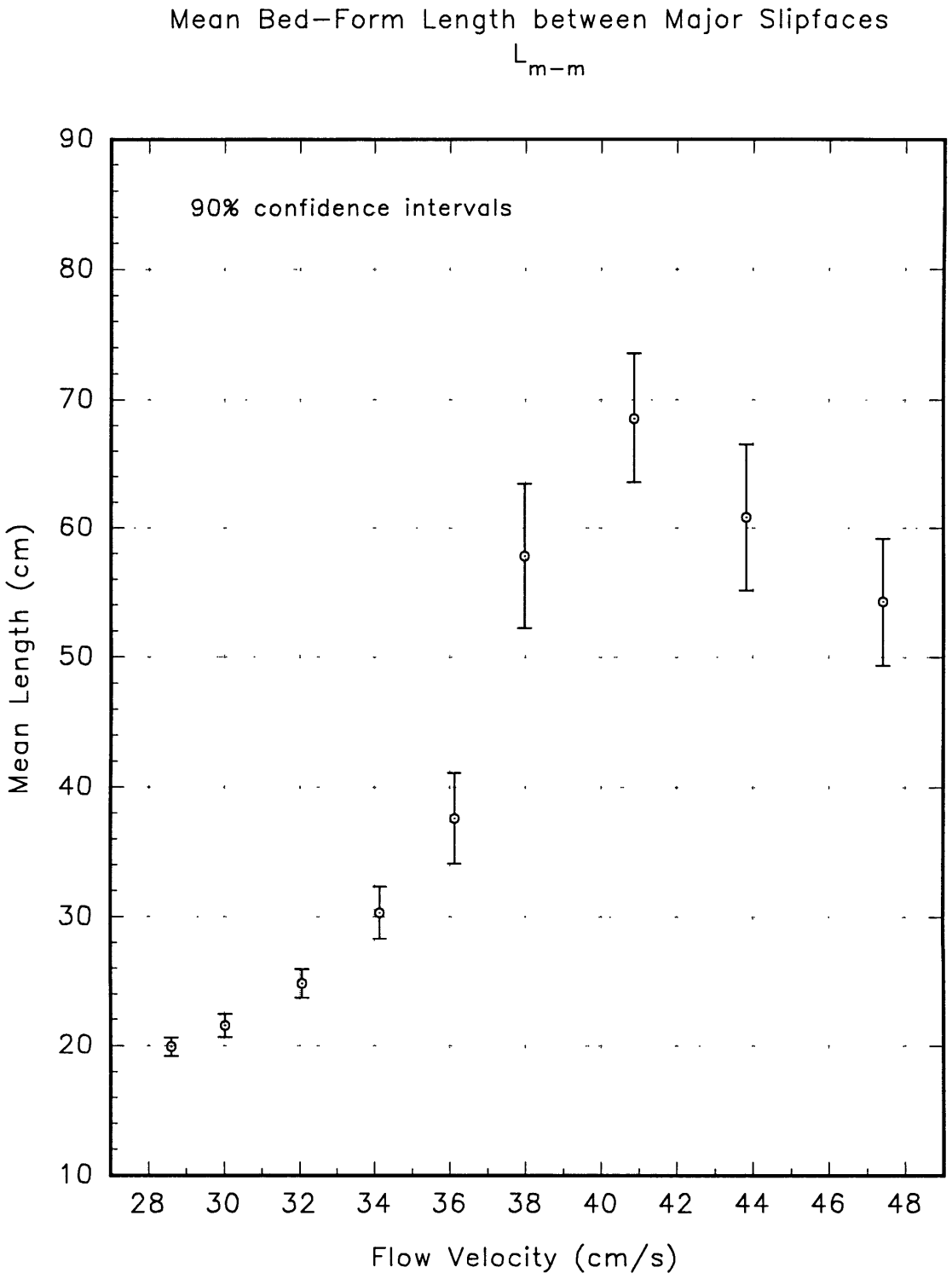
Mean Bed–Form Length between Major Slipfaces
L_{m-m}
90% confidence intervals
Mean Length (cm)
Flow Velocity (cm/s)
90
80
70
60
50
40
30
20
10
28
30
32
34
36
38
40
42
44
46
48

Figure 6–15

Mean Bed–Form Length Downstream from Major Slipfaces to the Next Slipface, L_{m-a}

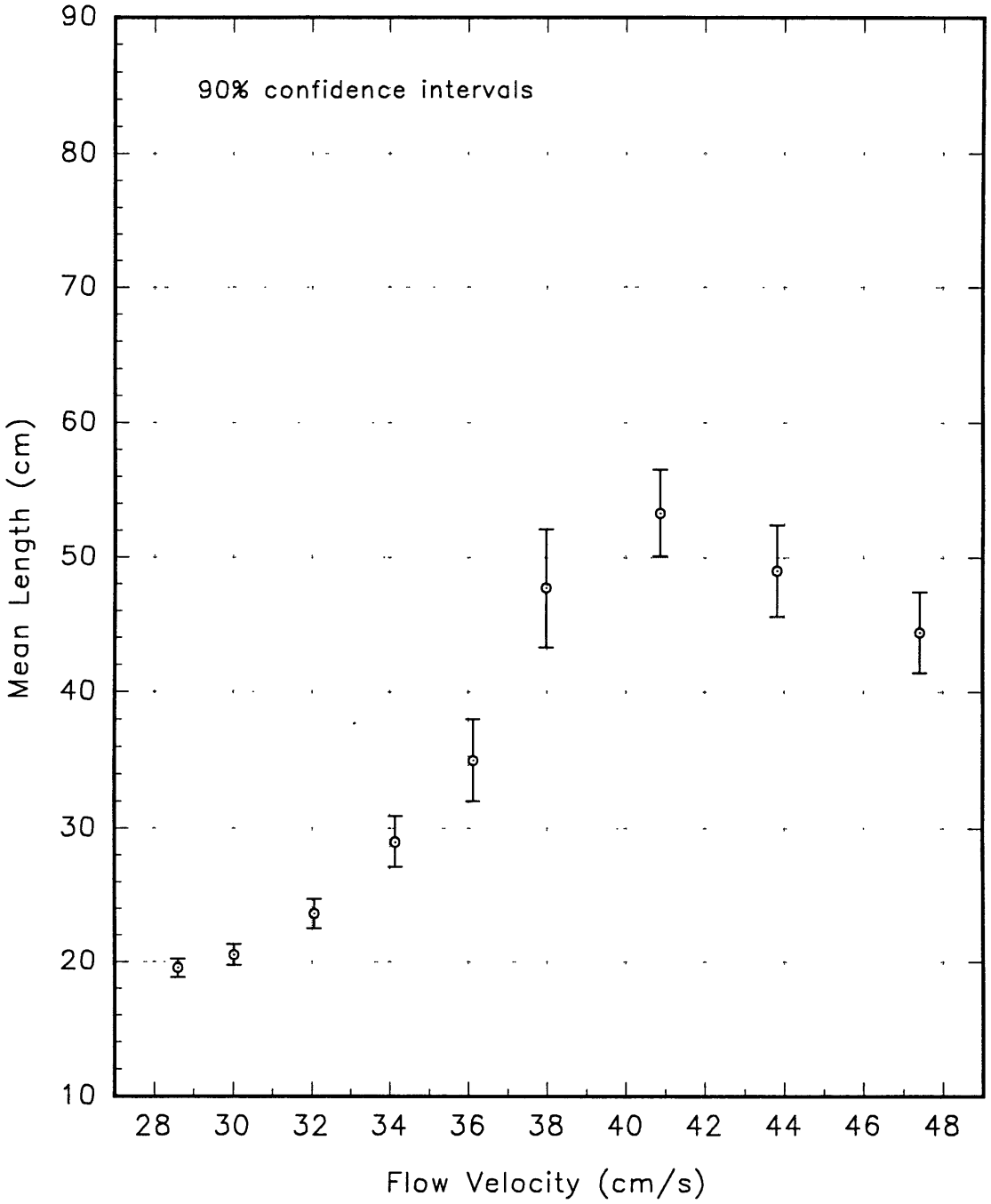

Figure 6–16

Comparison of Bed–Form Lengths

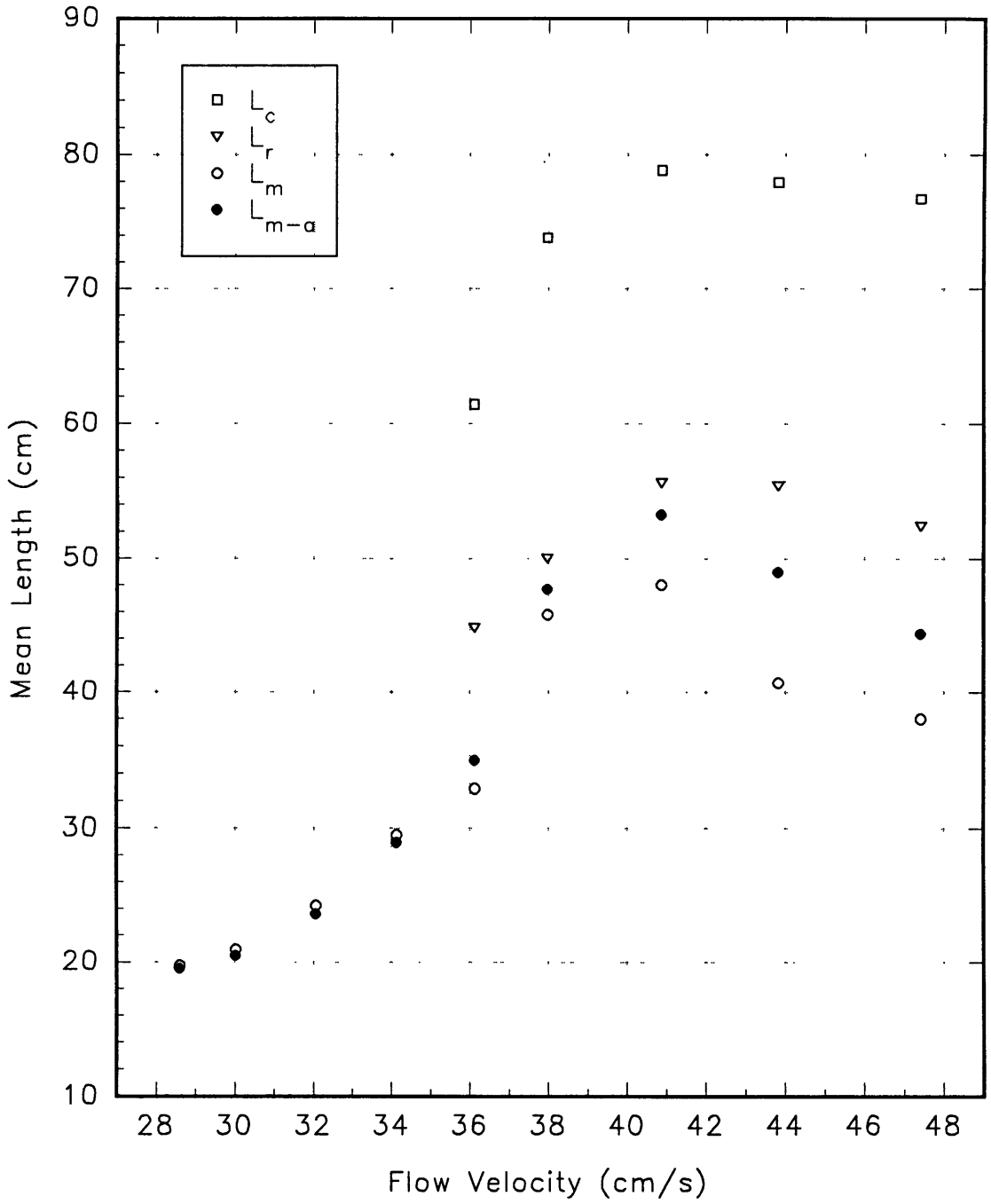

Figure 6–17

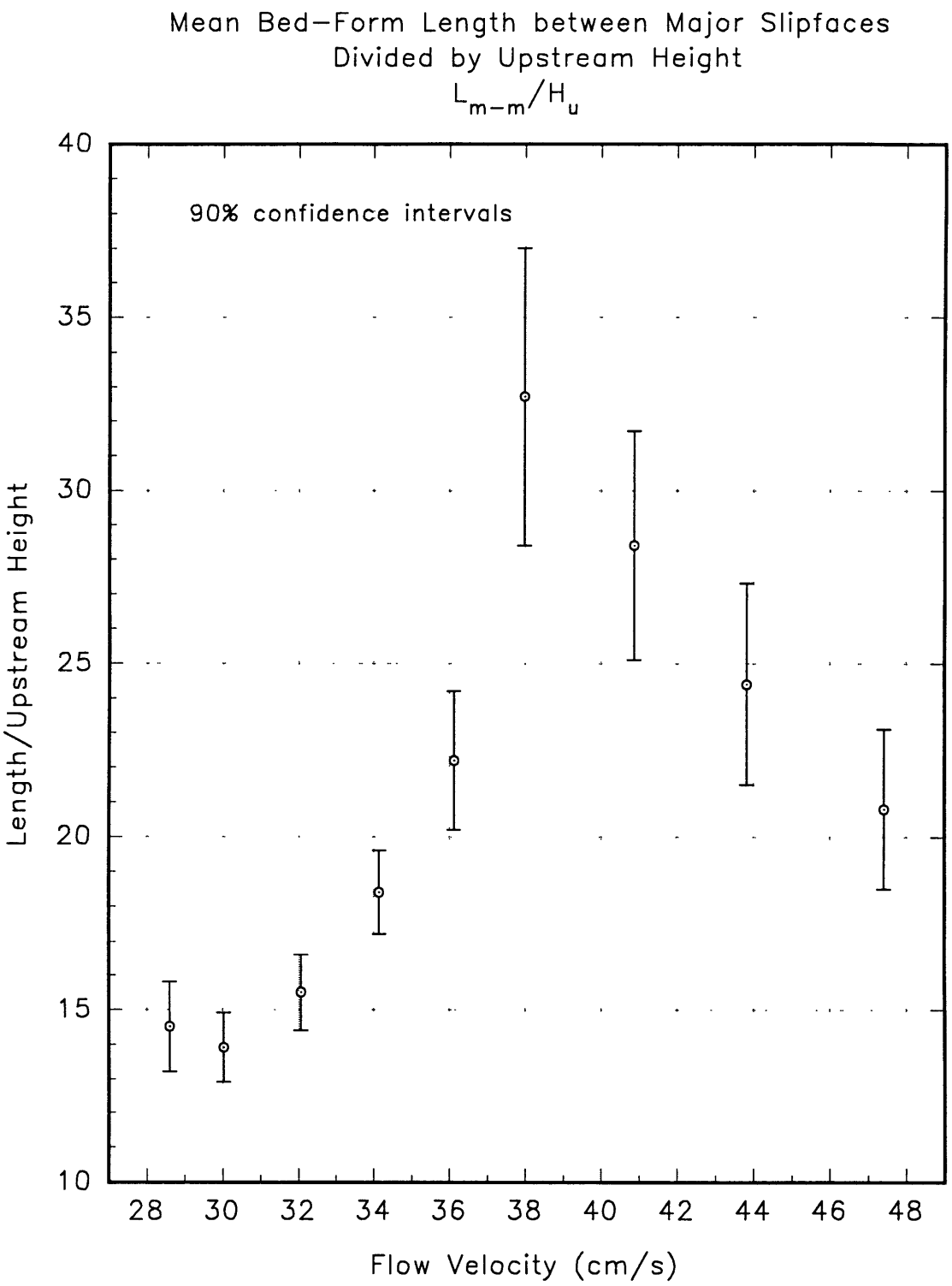
Mean Bed–Form Length between Major Slipfaces
Divided by Upstream Height
L_{m-m}/H_u
90% confidence intervals
Length/Upstream Height
40
35
30
25
20
15
10
28
30
32
34
36
38
40
42
44
46
48
Flow Velocity (cm/s)

Figure 6–18

Mean Bed–Form Length Downstream from Major Slipfaces to the Next Slipface Divided by Upstream Height

L_{m-a}/H_u

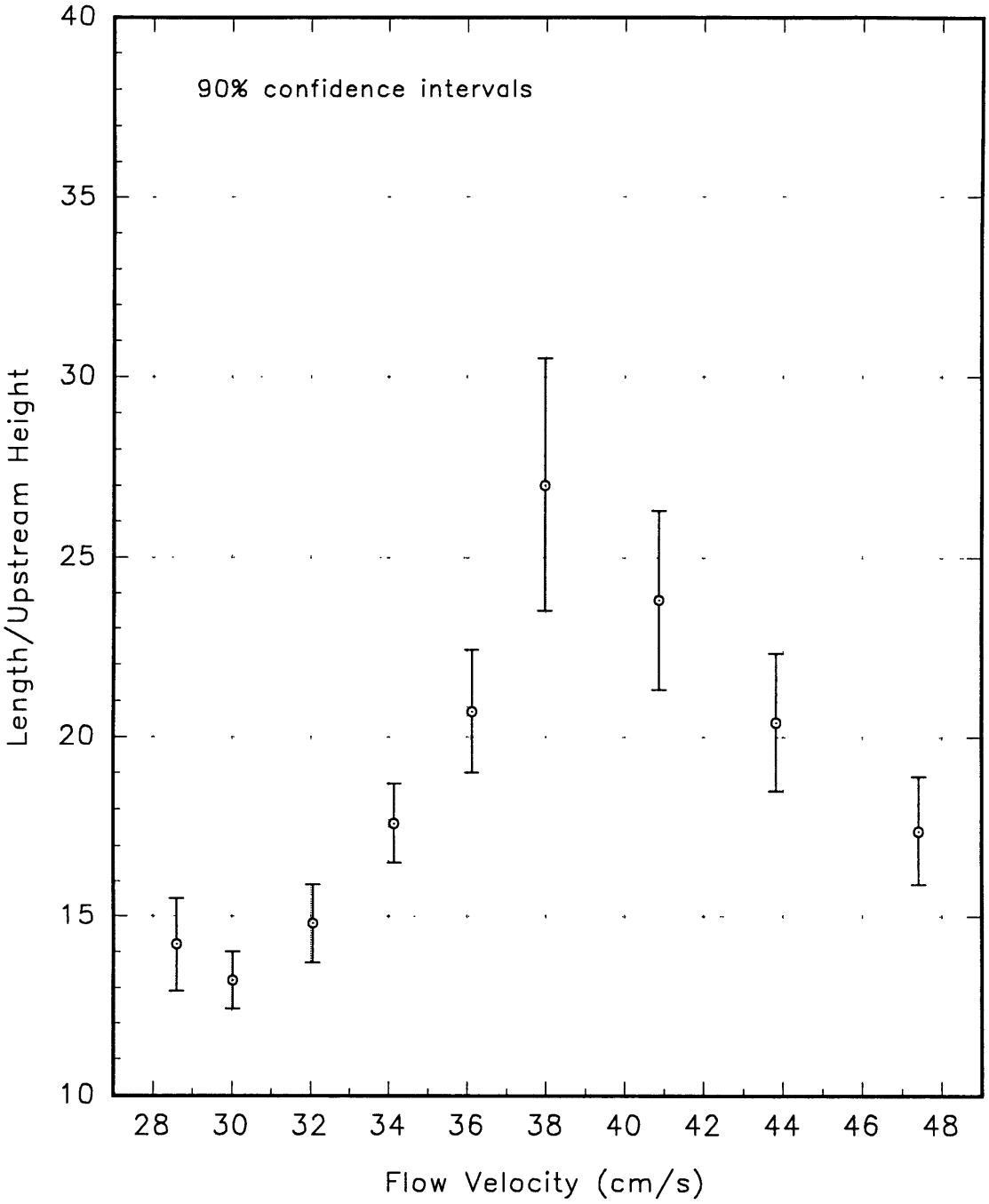

Figure 6–19

Comparison of Bed–Form Length
Divided by Upstream Height